Dynamiques de la composition et de la structure des forêts tropicales

M. Réjou-Méchain

▶ **To cite this version:**

M. Réjou-Méchain. Dynamiques de la composition et de la structure des forêts tropicales. Sciences de l'environnement. Université de Montpellier (UM), FRA, 2023. tel-04154057

HAL Id: tel-04154057
https://hal.inrae.fr/tel-04154057

Submitted on 6 Jul 2023

HAL is a multi-disciplinary open access archive for the deposit and dissemination of scientific research documents, whether they are published or not. The documents may come from teaching and research institutions in France or abroad, or from public or private research centers.

L'archive ouverte pluridisciplinaire **HAL**, est destinée au dépôt et à la diffusion de documents scientifiques de niveau recherche, publiés ou non, émanant des établissements d'enseignement et de recherche français ou étrangers, des laboratoires publics ou privés.

Distributed under a Creative Commons Attribution - NonCommercial - NoDerivatives 4.0 International License

Mémoire pour le Diplôme d'Habilitation à Diriger des Recherches

DYNAMIQUES DE LA COMPOSITION ET DE LA STRUCTURE DES FORÊTS TROPICALES

Un large chablis naturel dû à un "coup de vent" dans une forêt du Nord Congo (© Sylvafrica)

Maxime Réjou-Méchain
UMR AMAP, IRD

Université de Montpellier
2023

Je déclare avoir respecté, dans la conception et la rédaction de ce mémoire d'HDR, les valeurs et principes d'intégrité scientifique destinés à garantir le caractère honnête et scientifiquement rigoureux de tout travail de recherche, visés à l'article L.211-2 du Code de la recherche et énoncés par la Charte nationale de déontologie des métiers de la recherche et la Charte d'intégrité scientifique de l'Université de Montpellier. Je m'engage à les promouvoir dans le cadre de mes activités futures d'encadrement de recherche.

Résumé

Mes travaux se situent à un point de convergence entre plusieurs thématiques visant à comprendre l'organisation spatio-temporelle de la composition et de la structure des forêts tropicales. Mon travail de recherche a notamment visé à comprendre les mécanismes écologiques impliqués dans l'assemblage des communautés d'arbres tropicaux, principalement à partir de données de terrain extensives et à des échelles spatiales larges rarement traitées. J'ai également travaillé en collaboration avec diverses équipes et différents réseaux internationaux sur les stratégies de mesure de la biomasse ligneuse et sur les variations spatio-temporelles de la structure forestière sous les tropiques. En particulier, mes travaux établissent des liens entre divers outils de télédétection et des données de terrain pour suivre la structure et la composition des forêts tropicales dans le temps et dans l'espace. Actuellement, je vise à mobiliser des approches complémentaires d'expérimentation et d'observations à différentes échelles spatio-temporelles pour comprendre les conditions de réversibilité de la déforestation et de la dégradation forestière suite à des perturbations de différentes natures. Je m'intéresse notamment à la dynamique de recolonisation forestière en Thaïlande afin de comprendre les facteurs écologiques responsables d'une résilience plus ou moins rapide et vise à comprendre de manière plus générale comment la composition des communautés et leurs fonctions varie le long des gradients successionnels. Je développe également des projets en Afrique centrale sur des faciès forestiers d'apparences dégradés qui semblent correspondre à des successions dites arrêtées, voir à des états stables alternatifs, dus à l'envahissement du système par des formes de vies autres que les arbres, comme les herbacées géantes ou les lianes. Mes projets futurs s'inscrivent dans cette dynamique avec la volonté de mobiliser des outils complémentaires pour suivre la dynamique et la composition des forêts tropicales suite à des perturbations. L'ensemble de ces travaux se réalise en interaction étroite avec plusieurs instituts des Suds, avec un fort investissement dans le (co-)encadrement d'étudiants.

Remerciements

Dure tâche que de remercier les innombrables personnes ayant alimenté mon parcours de recherches. Je me limiterai donc ici à quelques personnes qui ont joué un rôle majeur dans son développement.

Tout d'abord, j'adresse mes remerciements à Sylvie Gourlet-Fleury, qui m'accompagne dans mes recherches depuis mon Master 2. Sylvie, c'est toujours un grand plaisir d'échanger avec toi, merci pour ta confiance, ton incroyable énergie et ton implication pour la préservation des forêts tropicales.

Je tiens également à remercier Jérôme Chave, avec qui j'ai travaillé durant plus de trois ans lors de mes postdoctorats à Toulouse. C'est une période lors de laquelle j'ai énormément progressé. Merci de m'avoir ouvert tant de portes, y compris celles des Nouragues que je ne désespère pas retrouver un jour!

Je remercie aussi Raphaël Pélissier, avec qui je collabore depuis la rédaction de mon premier article scientifique! Merci pour ta confiance et ton support et merci de nous montrer qu'il est possible de maintenir un pied dans le travail de recherches malgré les lourdes charges de direction qui t'incombent.

Bien sûr, tant d'autres ont participé et continuent de participer à ma construction scientifique, y compris les étudiants que j'ai eu la chance d'encadrer ces dernières années. J'ai notamment le privilège d'évoluer dans un laboratoire qui mise sur le collectif avec une atmosphère de bienveillance. AMAP héberge probablement la plus forte densité d'écologues des forêts tropicales au monde et constitue ainsi un terreau fertile pour l'émergence de collaborations diverses et de projets fascinants!

Je remercie également l'ensemble des membres du comité d'évaluation d'avoir accepté d'évaluer ce travail.

Enfin, naturellement, je remercie Morgane, avec qui j'ai eu la chance d'avoir deux merveilleux enfants, Robin et Malou. Ils me rappellent chaque jour les priorités de la vie...

Table des matières

1 Curriculum Vitae **7**

1.1 Informations générales . . . 7

1.2 Parcours . . . 7

1.3 Financements . . . 7

1.4 Activités d'enseignement ou formation . . . 9

1.5 Encadrement . . . 9

1.6 Evaluation scientifique . . . 9

1.6.1 Activité d'évaluation d'articles . . . 9

1.6.2 Comités de sélection, jury et évaluation . . . 12

1.7 Animation scientifique . . . 12

2 Publications et autres valorisations **13**

2.1 Publications scientifiques (sélection) . . . 13

2.2 Autres valorisations . . . 16

2.3 Vulgarisation scientifique . . . 17

2.4 Communications orales (sélection) . . . 17

3 Activités de recherche passées **18**

3.1 Variations spatio-temporelle de la diversité ligneuse . . . 19

3.1.1 Approche théorique de l'assemblage des communautés . . . 19

3.1.2 Approches empiriques de l'assemblage des communautés en forêts tropicales . . . 20

3.2 Quantification et suivi de la biomasse forestière tropicale . . . 30

3.2.1 Amélioration des équations de biomasse . . . 30

3.2.2 Comprendre la structuration des forêts pour proposer des stratégies d'échantillonnage 31

3.2.3 Approches par télédétection . . . 32

4 Activités de recherches en cours et en projet **36**

4.1 Contexte 36

4.2 Dynamiques de reforestation suite à une déforestation passée 37

4.2.1 Reforestation naturelle 37

4.2.2 Restauration active 42

4.3 Stabilité des systèmes dégradés en forêts tropicales 44

4.3.1 Ecologie des lianes et impacts sur la dynamique des forêts tropicales 44

4.3.2 Les forêts à Marantacées d'Afrique Centrale 50

5 Conclusions **61**

6 Bibliographie **62**

7 ANNEXES (Sélection de 3 articles) **74**

1 Curriculum Vitae

1.1 Informations générales

Maxime Réjou-Méchain
Nationalité française
Né à La Roche sur Yon, Vendée (85) le 18 Décembre 1982
Pacsé, deux enfants (2 et 4 ans)

Adresse professionnelle
UMR 123 botAnique et Modélisation de l'Architecture des Plantes et des Végétations (AMAP)
TA A51/PS2, 34398 Montpellier Cedex 05, France Tel. : +33 (0)4 67 61 65 72
Email : maxime.rejou@ird.fr

1.2 Parcours

- **Sept. 2016 – présent** Chargé de recherche CRCN IRD, UMR AMAP, Montpellier, France.
- **Nov. 2014 – Août 2016** Chargé de recherche MAEDI, responsable du département de géomatique, IFP, Pondichéry, Inde.
- **Nov. 2013 – Nov. 2014** Postdoctorat, UMR AMAP et UR Forêts et Sociétés (CIRAD), Montpellier, France.
- **Avr. 2010 – Oct. 2013** Postdoctorat, laboratoire EDB, Toulouse, France.
- **Oct. 2006 – Dec. 2009** Thèse de doctorat en Ecologie et Biologie de l'Evolution. Université Montpellier II, CEFE/CNRS et CIRAD, Montpellier, France.
- **Sept. 2005 – Juin 2006** Master 2 recherche FENEC (Fonctionnement des Ecosystèmes Naturels Et Cultivés). Montpellier, France.
- **Sept. 2004 – Juin 2005** Master 1 recherche BOPE (Biologie des Organismes, des Populations et des Ecosystèmes). Rennes, France.

1.3 Financements

- **2023-2025** Projet BNP-Paribas - NATURAL FORESTORE: Capture and storage of carbon in natural tropical forests. Collaboration avec le National Biobank of Thailand (NBT), l'Université de Kasetsart et l'UMR ISEM (Montpellier). PI: Emmanuel Paradis (IRD, ISEM). **Rôle:** Responsable d'un work package ; **Organisme contractant: IRD**. (budget TOTAL: 660 k€).

- **2022-2024** Projet JEAI BIMOMS - Biodiversity modeling at multiple scales: from wild ecosystems to regional processes. Collaboration avec le National Biobank of Thailand (NBT) et l'UMR ISEM (Montpellier). PI: Sissades Tongsima (NBT). **Rôle:** Participant ; **Organisme contractant: NBT**. (budget TOTAL: 46 k€).

- **2021-2024** Projet ANR DESSFOR - Degraded stable states in tropical forests. Collaboration avec UR Forêts et Sociétés (CIRAD, Montpellier) et ISEM (Montpellier). PI: Maxime Réjou-Méchain (AMAP).**Rôle:** Porteur ; **Organisme contractant: IRD**. (budget TOTAL: 529 k€).

- **2021-2023** Projet "Use of Machine Learning with Remote Sensing to Predict Forest Biodiversity Metrics across Scale" financé par le Gouvernement Thaïlandais. Collaboration avec le National Biobank of Thailand (Bangkok) et l'Université de Kasetsart (Bangkok). PI: Sissades Tongsima (NBT). **Rôle:** Responsable scientifique AMAP ; **Organisme contractant: NBT**. (budget TOTAL: 148 k€).

- **2020-2022** Projet Labex CEMEB AFRIFIRE - Déterminants et impacts du régime des feux en Afrique tropicale. Collaboration avec ISEM. PI: Charly Favier (ISEM). **Rôle:** Responsable scientifique AMAP ; **Organisme contractant: ISEM**. (budget TOTAL: 20 k€).

- **2018-2020** Projet Forest Observation System (European Space Agency). Collaboration avec IIASA (Autriche), laboratoire EDB (Toulouse), Université de Leeds (UK), Smithsonian Institute (Panama) et UR Forêts et Sociétés (CIRAD, Montpellier). PI: Dmitry Schepaschenko (IIASA). **Rôle:** Responsable scientifique AMAP ; **Organisme contractant: IIASA**. (budget pour AMAP: **20 k€**).

- **2016-2020** Projet LongTime (Labex CEBA). Collaboration avec de nombreux laboratoires dont le LEEISA (Cayenne, Guyane française), laboratoire EDB (Toulouse), UR Forêts et Sociétés (CIRAD, Montpellier) et IRD (Cayenne). PIs: Jean-François Molino (AMAP, Montpellier), Guillaume Odonne (LEEISA). **Rôle:** Responsable d'un Work Package ; **Organisme contractant: CNRS**. (budget total: **240 k€**).

- **2015–2016** Projet Regional Forum on Climate Change (RFCC). **Rôle:** Collaboration avec l'Asian Institute of Technology (AIT, Bangkok), le National Biobank of Thailand (Bangkok) et l'Université de Kasetsart (Bangkok). PIs: Nitin Tripathi (AIT) et Maxime Réjou-Méchain (AMAP). **Organisme contractant: AIT**. (budget TOTAL: 37 k€).

- **2014-2016** Projet Carboshare (programme BioAsia géré par Campus France). Collaboration avec le National Remote Sensing Center d'Hyderabad (Inde), l'UMR CESBIO (Toulouse), l'UMR TETIS (Montpellier), l'Institut Français de Pondichéry (Inde), l'Asian Institute of Technology (AIT, Bangkok), le National Biobank of Thailand (Bangkok) et l'Université de Kasetsart (Bangkok). PI: Raphaël Pélissier (AMAP). **Rôle:** Mise en oeuvre et animation du projet ; **Organisme contractant: IRD**. (budget TOTAL: 32 k€).

1.4 Activités d'enseignement ou formation

- TD Master 1 Université Paul Sabatier, Toulouse (8 h, 2011-2012):
- TP Licence 1 Université Paul Sabatier, Toulouse (24 h, 2012):
- Module Forêt Tropicale Humide AgroParisTech-ENGREF (1 semaine). « Estimation de biomasse en forêt guyanaise : cohérence avec des données radar » 2012.
- Workshop formation logiciel R FAO, Kerala Forest Research Institute, Inde (3 jours, 2014)
- Workshop formation logiciel R Institut Français de Pondichéry, Inde (3 jours, 2015)
- Workshop formation logiciel R Université de Kasetsart, Thaïlande (3 jours, 2019)

1.5 Encadrement

Au total, j'ai réalisé l'encadrement partiel ou total de 21 Ingénieurs, Masters, doctorants et post-doctorants (Table 1). Ces encadrements ont généré à ce jour la publication de 6 articles scientifiques de rang A (voir section 2.1 avec les étudiants encadrés en gras).

1.6 Evaluation scientifique

1.6.1 Activité d'évaluation d'articles

Au cours de la période 2012-2022, j'ai évalué un total de 59 articles ou chapitre de livres pour les journaux suivants (sélection): *Annals of Botany, Basic and Applied Ecology, Biogeosciences, Biological Conservation, BMC Ecology, Ecography, Ecology, Ecosystem, Ecology Letters, Ecosystems, Forest Ecology and Management, Global Change Biology, Global Ecology and Biogeography, Journal of Biogeography, Journal of Ecology, Journal of Tropical Ecology, Journal of Vegetation Science, Methods in Ecology and Evolution, Nature, Nature Communications, Oikos, PLoS ONE, Remote Sensing, Remote Sensing of Environment, Remote Sensing in Ecology and Conservation, Science of the Total Environment et Scientific Reports.*

Table 1: Liste des étudiant(e)s (co-)encadré(e)s jusqu'en Novembre 2022.

Nom	Prénom	Nationalité	Niveau	Période	Sujet	(Co-) Encadrement principal	Articles
BOURGET	Malo	Français	M2	2019	Environmental Drivers of Forest Aboveground Biomass distribution in Central Africa	NON	
DELLA-SIGNORA	Carla	Française	M1 Césure	2021	Impact des lianes sur la croissance des arbres au Nord Congo	OUI	en cours
DESCLOITRE	Justine	Française	M2	2021	Suivi spatio-temporel de l'évolution de l'usage des terres en Afrique	OUI	
JHA	Nidhi	Indienne	Thèse	2017-2020	Modeling forest structure and biomass using LiDAR and satellite data in Khao Yai National Park, Thailand	OUI	2
JOHN	Charles	Indien	M2	2016	Geospatial analysis of natural forest cover dynamics in south India	OUI	
KACAMAK	Begum	Turque	M2 et Thèse	2018-2022	Structure and composition of liana communities in a moist forest of northern Congo	OUI	1 + en cours
LIM	Felix	Singapour	Postdoc	2021-2022	Suivi de la dynamique des forêts à Marantacées dans le Nord Congo	OUI	en cours
MOUA NEDELLEC	Rose-Eva	Française	M1 Césure	2022	Télédetection de la diversité de la canopée dans le parc national de Khao Yai (Thailande)	OUI	
NUNGI-PAMBU	Merveil	Congolais	M2	2021	Répartition et déterminisme des forêts à Marantacées du Nord Congo	OUI	en cours
PARIS	Célia	Française	M2	2021	Réflexions sur la loi de Baker : écologie et évolution du syndrome autogame-colonisateur	OUI	
PERE	Arthur	Français	Ingénieur	2018-2019	Développement d'un package R d'estimation de biomasse forestière	OUI	
PICARD	Juliette	Française	Thèse	2021-2024	Dynamiques et origines des forêts à Marantacées dans le Nord Congo	OUI	en cours
PIMMASARN	Siriruk	Thailandaise	Thèse	2017-2019	Applying Lidar-derived PAI to characterize forest succession in a tropical moist forest, Thailand	NON	en cours
POINAS	Isis	Française	M2	2019	Impacts à long terme des activités amérindiennes précolombiennes sur la composition multi-taxa des forêts de Guyane	OUI	en cours
POUTEAU	Robin	Français	Postdoc	2020	Suivi de la dynamique des forêts à Marantacées dans le Nord Congo	OUI	en cours
RAMBAUD	Fanny	Française	M1	2014	Usages médicinaux des plantes ligneuses d'Afrique centrale: existe t-il un déterminismefonctionnel ?	OUI	
RIEVRS BORGES	Erica	Brésilienne	Postdoc	2021-2022	Relation diversité et biomasse forestière en contexte perturbé	OUI	en cours
SCHMITT	Sylvain	Français	M1 Césure	2016	Déterminisme de la composition fonctionnelle des communautés d'arbres sur le site d'Uppangala, Inde	OUI	1
TANGUY	Ariane	Française	Ingénieur	2015-2016	Développement d'un package R d'estimation de biomasse forestière	OUI	1

Nom	Prénom	Nationalité	Niveau	Période	Sujet	(Co-) Encadrement principal	Articles
TYMEN	Blaise	Français	Thèse	2013-2014	Dynamique des forêts de lianes dans la réserve des Nouragues	NON	2
VALANCE	Anaïs	Française	M2	2016	Assessing the drivers of forest structure and dynamics using airborne LiDAR and field data in an Indian monsoon forest	OUI	
VINCENT	Marion	Française	M1 Césure	2018	Modeling the impact of pre-Columbian civilizations on Amazonian forest dynamic, structure and floristic composition	OUI	

1.6.2 Comités de sélection, jury et évaluation

- Evaluateur thèse de C. Bourgoin : A framework for evaluating forest ecological vulnerability in tropical deforestation fronts from the assessment of forest degradation in a landscape approach: Case studies from Brasil and Vietnam. AgroParisTech, Montpellier, France. 12/2019.
- Evaluateur thèse de M. Decuyper : Combining conventional ground-based and remotely sensed forest measurements. Wageningen University. Pays Bas. 12/2018.
- Evaluation du dossier individuel de recherche d'un chercheur Sud Africain sur demande du National Research Foundation (Afrique du Sud). 09/2017.
- Comité de jury Master 1 BioGET - Biodiversité végétale et Gestion des Ecosysytèmes Tropicaux. 06/2017.
- Comité de sélection d'un Post-Doctorant pour un appel conjoint du labex CeMEB et des Parcs Nationaux de France. 10/2016.
- Comité de jury Master 2 AgroParisTech-ENGREF. 06/2016.
- Comité de sélection d'un Post-Doctorant au sein du labex BcDiv. 11/2015.

1.7 Animation scientifique

Lors de mon poste de chargé de recherche à l'Institut Français de Pondichéry (IFP) de 2014 à 2016, j'étais le responsable du laboratoire de Géomatique, et donc animais une équipe composée d'indiens et de français (10-14 personnes selon la période, Fig. 1).

Sur la période 2021-2025, je co-anime avec Claire Fortunel (IRD) et Isabelle Maréchaux (INRAe) le thème «Dynamique et assemblages des forêts tropicales» au laboratoire AMAP. Ce thème, qui rassemble environ 20 permanents et 10 doctorants/postdoctorants de l'UMR AMAP, vise à animer des discussions sur les activités de recherches liées à la dynamique et les règles d'assemblages des forêts tropicales, avec comme objectif de prévoir le devenir des forêts tropicales sous différents scénarios de changements globaux.

Figure 1: Photo de l'équipe LIAG de l'Institut Français de Pondichéry que j'ai dirigé de 2014 à 2016.

2 Publications et autres valorisations

2.1 Publications scientifiques (sélection)

Nombre total de publications (22/11/2022): 57 (liste complète à consulter ici)
Indices Google Scholar (22/11/2022): > 6900 citations; h=37; i10=53. (Profil ici)

Etudiant(e)s ou ingénieur(e)s (co-)encadrés en gras (voir Tableau 1).

- **Kaçamak, B.**, Barbier, N., Aubry-Kientz, M., Forni, E., Gourlet-Fleury, S., Guibal, D., Loumeto, J.-J., Pollet, S., Rossi, V., Rowe, N.P., Van Hoef, Y., Réjou-Méchain, M. (2022). Linking Drone and Ground-Based Liana Measurements in a Congolese Forest. *Frontiers in Forests and Global Change*, 5. doi: 10.3389/ffgc.2022.803194. Contributions: Concepts, Development, Writing. IF : 4.332.

- **Schmitt, S.**, Raevel, V., Réjou-Méchain, M., Ayyappan, N., Balachandran, N., Barathan, N., Rajashekar, G., Munoz, F. Canopy and understory tree guilds respond differently to the environment

in an Indian rainforest. *Journal of Vegetation Science*, (2021). e13075. doi.org/10.1111/jvs.13075. Contributions: Concepts, Development, Writing. IF : 3.389.

- Thripob, P., Fortunel, C., Réjou-Méchain, M., Nathalang, A., Chanthorn, W. (2022). Size-dependent intraspecific variation in wood traits has little impact on aboveground carbon estimates in a tropical forest landscape. *Functional Ecology*, 36(9), 2303-2316. Contributions: Concepts, Development, Analyses, Writing. IF : 6.282.

- Réjou-Méchain, M., Mortier, F., Bastin, J-F., Cornu, G., Barbier, N., Bayol, N., Bénédet, F., Bry, X., Dauby, G., Deblauwe, V., Doucet, J-L., Doumenge, C., Fayolle, A., Garcia, C., Kibambe, J-P., Loumeto, J-J., Ngomanda, A., Ploton, P., Sonké, B., Trottier, C. , Vimal, R., Yongo, O. , Pélissier, R., Gourlet-Fleury, S (2021). Unveiling African rainforest composition and vulnerability to global change. *Nature*, 593(7857), 90-94. Contributions: Concepts, Development, Analyses, Writing. IF : 69.80.

- **Jha, N.**, Tripathi, N. K., Barbier, N., Virdis, S. G., Chanthorn, W., Viennois, G., Brockelman, W.Y., Nathalang, A., Tongsima, S., Sasaki, N., Pélissier, R., Réjou-Méchain, M. (2020). The real potential of current passive satellite data to map aboveground biomass in tropical forests. *Remote Sensing in Ecology and Conservation*, 7(3), 504-520. Contributions: Concepts, Development, Analyses, Writing. IF : 5.787.

- Vimal, R., Navarro, L. M., Jones, Y., Wolf, F., Le Moguédec, G., Réjou-Méchain, M. (2021). The global distribution of protected areas management strategies and their complementarity for biodiversity conservation. *Biological Conservation*, 256, 109014. Contributions: Analyses, Writing. IF : 7.497.

- Ploton, P., Mortier, F., Réjou-Méchain, M., Barbier, N., Picard, N., Rossi, Dormann, C., Cornu, G., Viennois, G., Bayol, N., Lyapustin, A., Gourlet-Fleury, S., Pélissier, R. (2020). Spatial validation reveals poor predictive performance of large-scale ecological mapping models. *Nature communications*, 11(1), 1-11. Contributions: Concepts. IF : 17.694.

- **Jha, N.**, Tripathi, N. K., Chanthorn, W., Brockelman, W., Nathalang, A., Pélissier, R., **Pimmasarn, S.**, Ploton, P., Sasaki, N., Virdis, S. G. P., Réjou-Méchain, M. (2020). Forest aboveground biomass stock and resilience in a tropical landscape of Thailand. *Biogeosciences*, 17, 121–134. Contributions: Concepts, Development, Analyses, Writing. IF : 5.092.

- Réjou-Méchain, M., Barbier N., Couteron, P., Ploton, P., Vincent, G., Herold, M., Mermoz, S., Saatchi, S. , Chave, J. , de Boissieu, F. , Féret, J.-B. , Momo Takoudjou, S., Pélissier, R. (2019). Upscaling forest biomass from field to satellite measurements: sources of errors and ways to reduce them. Surveys in Geophysics, 1-31. Contributions: Concepts, Development, Analyses, Writing. IF : 7.965.

- Réjou-Méchain, M., **Tanguy, A.**, Piponiot, C., Chave, J., Hérault, B. (2017). BIOMASS: An R Package for estimating above-ground biomass and its uncertainty in tropical forests. *Methods in*

Ecology and Evolution. Contributions: Concepts, Development, Writing. IF : 8.335.

- **Tymen B.**, Réjou-Méchain M., Dalling J.W., Fauset S., Feldpausch T.R., Norden N., Phillips O.L., Turner B.L., Viers J., Chave J. (2016) Evidence for arrested succession in a liana-infested Amazonian forest. *Journal of Ecology*, 104 (1), 149-159. Contributions: Analyses, Concepts, Writing. IF : 6.381.

- Réjou-Méchain M., **Tymen B.**, Blanc L., Fauset S., Feldpausch T., Monteagudo A., Phillips O., Richard H., Chave J. (2015). Using repeated small-footprint LiDAR acquisitions to infer spatial and temporal variations of a high-biomass Neotropical forest. *Remote Sensing of Environment* 169, 93-101. Contributions: Analyses, Concepts, Writing. IF : 13.85.

- Bastin J.-F., Barbier N., Réjou-Méchain M., et al.(2015). Seeing Central African forests through their largest trees. *Scientific Reports*, 5, Article number: 13156, doi:10.1038/srep13156. Contributions: Analyses, Concepts, Writing. IF : 4.996.

- Réjou-Méchain M., Cheptou P.-O. (2015) High incidence of dioecy in young successional tropical forests. *Journal of Ecology*, 103 (3), 725-732. Contributions: Analyses, Concepts, Writing. IF : 6.381.

- Mermoz S., Réjou-Méchain M., Villard L., Le Toan T., Rossi V., Gourlet-Fleury S. (2015) Decrease of L-band SAR backscatter with biomass of dense forests. *Remote Sensing of Environment*, 159, 307-317.Contributions: Analyses, Concepts, Writing. IF : 13.85.

- Réjou-Méchain M., Flores O., Pélissier R., Fayolle F., Fauvet N., Gourlet-Fleury S. (2014). Tropical tree assembly depends on the interactions between successional and soil filtering processes. *Global Ecology and Biogeography*, 23 (12), 1440-1449. Contributions: Analyses, Concepts, Writing. IF : 6.909.

- Chave J, Réjou-Méchain M., et al. (2014). Improved allometric models to estimate the above ground biomass of tropical trees. *Global Change Biology* 20 : 3177–3190. Contributions: Analyses, Concepts. IF : 13.211.

- Réjou-Méchain M., Muller-Landau H. C., Detto M., Thomas S. C., Le Toan T., Saatchi S. S. et al. (2014). Local spatial structure of forest biomass and its consequences for remote sensing of carbon stocks. *Biogeosciences*, 11 : 6827-6840. Contributions: Analyses, Concepts, Writing. IF : 5.092.

- Parmentier I., Réjou-Méchain M., Chave J., Vleminckx J., Thomas D.W., Kenfack D., Chuyong G., Hardy O.J. (2014). Prevalence of phylogenetic clustering at multiple scales in an African rainforest tree community. *Journal of Ecology* 102(4) : 1008-1016. Contributions: Analyses, Concepts, Writing. IF : 6.381.

- Réjou-Méchain M., Flores O., Bourland N., Doucet J-L., Fétéké R., Pasquier A., Hardy O.J. (2011). Spatial aggregation of tropical trees at multiple spatial scales. *Journal of Ecology* 99 : 1373-1381. Contributions: Analyses, Concepts, Writing. IF : 6.381.

- Réjou-Méchain M., Hardy O.J. (2011). Properties of similarity indices under niche-based and dispersal-based processes in communities. *American Naturalist* 177(5): 589-604. Contributions: Analyses, Concepts, Ecriture. IF : 6.381. IF : 4.367.

- Réjou-Méchain M.,Fayolle A., Nasi R., Gourlet-Fleury S., Doucet J-L., Gally M., Hubert D., Pasquier A., Billand A. (2011) Detecting large-scale diversity patterns in tropical trees : can we trust commercial forest inventories? *Forest Ecology and Management* 261 : 187–194. Contributions: Analyses, Concepts, Ecriture. IF : 4.384.

- Réjou-Méchain M., Pélissier R., Gourlet-Fleury S., Couteron P., Nasi R., Thompson J.D. (2008). Regional variation in tropical forest tree species composition in the Central African Republic : an assessment based on inventories by forest companies. *Journal of Tropical Ecology* 24 : 663-674. Contributions: Analyses, Concepts, Ecriture. IF : 1.800.

2.2 Autres valorisations

Depuis 2016, je maintiens un package R visant a faciliter et standardiser les estimations de biomasse forestière tropicale (https://cran.r-project.org/web/packages/BIOMASS/index.html)(Réjou-Méchain et al., 2017). Ce package est désormais couramment utilisé par de grandes institutions telles que la NASA (agence spatiale des Etats-Unis) et l'ESA (agence spatiale européenne) et par de nombreux chercheurs en écologie et télédétection. Je gère donc en continu le package, avec l'aide de Guillaume Cornu (CIRAD). Au 01/11/2022, le package a été téléchargé plus de 47 000 fois (Fig. 2). Je compte poursuivre le développement d'une application simplifiée R Shiny pour les non utilisateurs du logiciel R, initiée à travers l'encadrement d'Arthur Péré (version en développement sur GitHub: https://github.com/umr-amap/BIOMASSapp). Cette application sera librement accessible sur un portail web et sera particulièrement utile pour les pays des Suds, notamment à travers les formations organisées par la FAO (où le package BIOMASS est déjà enseigné).
A travers ce package, j'ai participé activement à un projet financé par l'agence spatiale européenne (Forest Observation System; 2018-2021) qui vise a standardiser des mesures de paramètres structuraux de parcelles forestières permanentes et de les mettre à disposition de la communauté scientifique, en particulier dans les domaines de l'observation de la terre (https://forest-observation-system.net/) (Schepaschenko et al., 2019). Dans le cadre de ce projet, j'ai amélioré les routines du package et participé aux analyses des jeux de données appartenant a des réseaux internationaux comme les réseaux RAINFOR et AFRITRON (Université de Leeds, UK) et le réseau ForestGEO (Smiththonian, Panama).

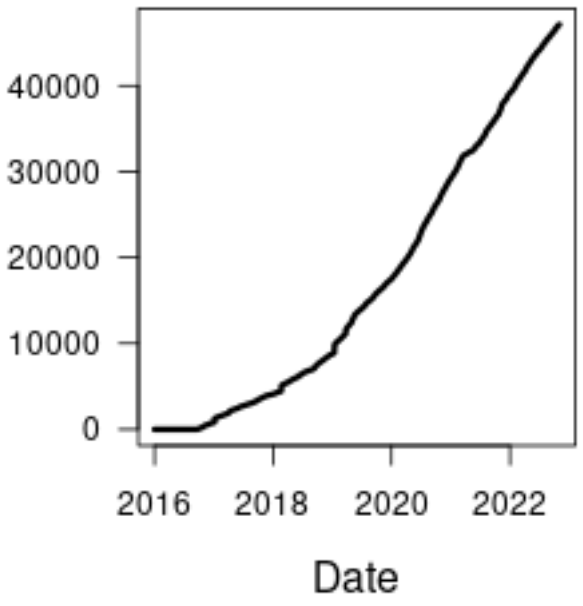

Figure 2: Nombre de téléchargements cumulés du package R BIOMASS sur la période fin 2016 à novembre 2022.

2.3 Vulgarisation scientifique

Les deux publications réalisées dans les journaux Science (Sullivan et al., 2020) et Nature (Réjou-Méchain et al., 2021) ont généré une visibilité importante auprès des médias. J'ai été donc sollicité pour vulgariser mes travaux auprès du grand public ou pour alimenter des articles traitant d'actualité socio-politiques (e.g. zero deforestation importée d'ici 2030, utilisation de bois exotiques pour les JO de Paris; France24). Par exemple, l'article Nature à été relayé/discuté dans 44 médias grand public nationaux et internationaux (dont Le point, Courrier International, Reporterre, RFI et France24) et j'ai réalisé fin Mai 2022 une journée entière de tournage pour un documentaire à venir sur la chaine Ushuaïa où je présente mes recherches sur le stockage de carbone des forêts tropicales. L'ensemble de ces communications est réalisé en concertation avec le service presse de l'IRD.

2.4 Communications orales (sélection)

- Réjou-Méchain, M. The ecology of central African forests: insights from massive commercial datasets. Oxford Centre for Tropical Forests (OCTF) Online Seminar, UK. 2/07/2021.
- Réjou-Méchain, M. Floristic and functional composition of central African forests. Interdisciplinary African forest landscapes conference. Université de Lausanne, Suisse. 10/09/2019.

- Réjou-Méchain, M. Monitoring remotely tropical forests. International Conference on Biodiversity 2019. Bangkok, Thaïlande. 23/05/2019.
- Réjou-Méchain, M. Propagating forest biomass errors from local to regional scales. Workshop at the International Space Science Institute. Bern, Suisse. 7/11/2017.
- Réjou-Méchain, M. Local spatial structure of forest biomass and its consequences for the calibration strategy of BIOMASS. ESA 1st BIOMASS Science Workshop. ESA-ESRIN, Frascati, Italie 27/01/2015.
- Réjou-Méchain, M. Mapping forest carbon at large scale: the need to consider error propagation from smaller scales. Regional Forum on Climate Change (RFCC), Bangkok, Thaïlande 1-3/07/2015.
- Réjou-Méchain M. Calibration and validation of remote sensing methods for global carbon stock mapping in tropical forests. CTFS analytical workshop. University of Washington, Seattle. 26/07/2012.
- Réjou-Méchain M. Dissecting tropical tree assemblage along successional and across soil gradients: Insights from a trait-based approach in Central Africa. Séminaire au sein du projet COBIMFO, Bruxelles, Belgique. 05/01/2012.
- Réjou-Méchain M. Drivers of spatial aggregation of tropical forest tree species at multiple spatial scales. Joint Meeting of Association for Tropical Biology and Conservation and Society for Tropical Ecology (ATBC). Marburg, Germany. 27/07/2009
- Réjou-Méchain M. Peut-on expliquer les patrons d'agrégation spécifiques d'arbres tropicaux à partir de leurs traits ? Une analyse de l'échelle locale à l'échelle régionale. 5ème congrès francophone d'écologie des communautés végétales (ECOVEG 5). Gembloux, Belgique. 8/04/2009
- Réjou-Méchain M. Organisation spatiale des communautés en forêt tropicale : mise en évidence des facteurs écologiques et neutres en forêt dense Centrafricaine. Séminaire à l'Université Libre de Bruxelles. 20/11/2008, Bruxelles, Belgique.

3 Activités de recherche passées

Les forêts tropicales sont les plus grands réservoirs de biodiversité et de carbone de la végétation terrestre. Elles constituent donc un excellent modèle d'étude pour comprendre comment et sous quels processus écologiques la biodiversité et sa biomasse s'organisent dans le temps et l'espace. En utilisant des relevés extensifs de terrain, des simulations théoriques, des données de télédétection et des statistiques spatiales, mes travaux se sont portés sur les mécanismes écologiques sous-tendant les variations spatio-temporelle de la diversité ligneuse, de la structure forestière et des stocks de carbone forestier dans les forêts tropicales d'Amazonie, d'Afrique centrale et d'Asie du Sud et Sud-Est.

3.1 Variations spatio-temporelle de la diversité ligneuse

La structuration spatiale de la biodiversité est régie par des mécanismes écologiques et évolutifs hiérarchisés dans l'espace et dans le temps (Cavender-Bares et al., 2009). Un défi majeur est d'identifier lesquels prévalent à différentes échelles spatio-temporelles et de comprendre leurs potentielles interactions. Ces connaissances sont un prérequis à la mise en place de modes de gestion durables des écosystèmes, notamment dans un contexte de changement global préoccupant. Une partie de mes travaux s'est ainsi focalisée sur l'identification des mécanismes responsables de la structuration spatiale des communautés d'arbres tropicaux à différentes échelles spatiales. A travers une approche théorique, j'ai cherché à comprendre les conséquences de l'interaction des processus de niche et de dispersion limitée sur les patrons d'assemblage de communautés. Puis, en utilisant différent jeux de données floristiques, je me suis intéressé à la structuration des communautés naturelles d'arbres tropicaux à différentes échelles spatiales.

3.1.1 Approche théorique de l'assemblage des communautés

Pendant ma thèse, j'ai développé avec Olivier Hardy (Université Libre de Bruxelles, ULB) un modèle de communauté spatialement explicite au sein duquel l'assemblage des espèces se réalise sous des processus de niche et/ou de dispersion limitée (Réjou-Méchain & Hardy, 2011). Excepté quelques travaux cherchant à unifier la théorie des niches et la théorie neutre (Gravel et al., 2006), ces deux théories était à cette époque largement opposées dans la littérature. Nous avons montré que le déterminisme environnemental dépendait de l'interaction entre les processus de filtrage environnementaux et de dispersion limitée (Fig. 3). En effet, en présence de dispersion limitée, la plupart des descendants se développe dans le même habitat que celui de leurs parents si l'habitat est structuré dans l'espace. Ainsi, les processus de filtrages environnementaux opèrent sur des générations et conduisent à un déterminisme environnemental plus marqué qu'en absence de dispersion limitée. Nous avons donc montré qu'il est très difficile de dissocier les effets du filtrage environnemental et de la dispersion limitée sur l'organisation spatiale des communautés naturelles car ces deux processus interagissent à travers la structure spatiale des habitats. Néanmoins, le partitionnement des sites en intra et inter-habitats permet d'identifier des effets de niches en présence de dispersion limitée. Enfin, en utilisant divers indices de (dis)similarité, nous avons montré que leurs capacités différaient à (i) établir des prédictions en conditions neutres; (ii) être indépendants du niveau global de diversité et (iii) détecter des processus de niches.

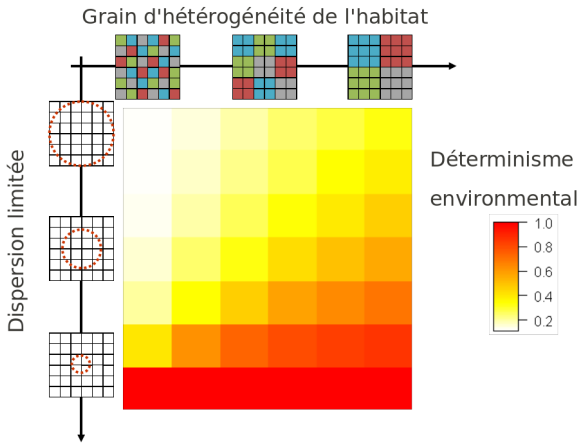

Figure 3: Déterminisme environnemental en fonction de la distance moyenne de dispersion et du grain d'hétérogénéité des habitats sous des processus de filtrage d'habitats constants. Figure adaptée de Réjou-Méchain et Hardy (2011).

3.1.2 Approches empiriques de l'assemblage des communautés en forêts tropicales

Structure phylogénétique des communautés d'arbres

Une partie de mon postdoctorat au sein du laboratoire Evolution et Diversité Biologique (EDB, Toulouse) concernait l'étude de la structuration phylogénétique des communautés d'arbres au sein d'une parcelle de 50 ha au Cameroun, en collaboration étroite avec Ingrid Parmentier et Olivier Hardy de l'université libre de Bruxelles (Parmentier et al., 2014). J'ai construit un arbre phylogénétique contenant 272 espèces de cette parcelle en utilisant des séquences moléculaires générées par l'ULB et par moi-même en Afrique centrale. En combinant cet arbre phylogénétique avec les données d'inventaires botaniques (329 000 arbres $\geq$ 1 cm de diamètre), nous avons révélé une agrégation phylogénétique significative à la plupart des échelles spatiales (20-1000 m): les espèces sœurs tendent à coexister plus souvent que par hasard. Le turnover phylogénétique entre habitats était également plus fort qu'au sein des habitats. Ces résultats suggèrent un conservatisme de niche marqué en forêt tropicale. Toutefois, à très faible échelle spatiale, de l'ordre de quelques mètres, nous avons montré que les espèces sœurs tendaient à s'exclure. Les effets de compétition, ou de densité-dépendance entre voisins, favorisent en effet la coexistence d'espèces éloignées phylogénétiquement à très petite échelle spatiale (zone de Darwin-Hutchinson sensu Vamosi et al. (2009)). Aussi, nous avons montré que la structuration phylogénétique observée était principalement due à des relations d'apparentement anciennes. Un conservatisme phylogénétique ancien imprime donc une signature marquée dans l'assemblage des communautés d'arbres tropicaux. L'originalité de ce travail a résidé dans notre capacité à développer des approches permettant d'identifier les échelles spatiales et les profondeurs phylogénétiques auxquelles différents mécanismes d'assemblages opèrent.

Dans un travail en cours mené par Felix Lim, en postdoctorat sous ma direction, nous étudions la structuration phylogénétique des communautés d'arbres tropicaux mais cette fois à l'échelle de l'Afrique centrale, avec le jeu de données CoFor (voir ci-dessous, Réjou-Méchain et al., 2021). En utilisant une

mégaphylogénie datée que nous avons récemment publié (Janssens et al., 2020), nous visons à tester si certains évènements évolutifs ont disproportionnellement contribués à la structuration actuelle des communautés d'arbres d'Afrique centrale. A travers une décomposition de la diversité β (inter-site) à différentes profondeurs phylogénétiques (Mazel et al., 2017), nos résultats préliminaires montrent que la diversité β actuelle des arbres d'Afrique centrale est disproportionnellement due à des évènements de radiations qui ont eu lieu lors de deux périodes estimées aux alentours de 70 et de 160 millions d'années. Lorsque l'on s'intéresse à la part de la diversité β organisée le long des gradients climatiques, la période la plus ancienne, qui semble correspondre à la radiation des Rosids et des Asterids, semble avoir eu un impact important sur la structuration des communautés actuelles le long d'un gradient contrastant des forêts à nébulosité quasi-permanente (Gabon) à celles ayant de fort taux d'évapotranspiration (marge nord forestière). Nous avions déjà montré que ce gradient climatique était étroitement associé au degré de déciduité des peuplements (voir ci-dessous, Réjou-Méchain et al., 2021) et montrons dans cette nouvelle étude que l'émergence très anciennes (estimée à plus de 150 million d'années par notre phylogénie datée) de groupes taxonomiques dominés par des espèces décidues ou sempervirentes est responsable d'une structuration très marquée des communautés actuelles. A contrario, nous n'avons pas détecté de conservatisme phylogénétique marqué le long des gradients climatiques de saisonnalités et de température maximale, pour lesquels d'importants changements sont prévus dans le siècle à venir. Ce travail est en cours de valorisation et devrait être soumis dans le premier semestre 2023.

Structure floristique et fonctionnelle aux échelles du paysage et régionale

Très peu d'études ont eu l'opportunité d'appréhender la structure des communautés d'arbres tropicaux à larges échelles spatiales. Dans mes travaux, j'ai utilisé des données d'inventaires d'aménagements forestiers couvrant d'immenses surfaces. Des jeux de données initialement réalisés à des fins industrielles avaient déjà été mobilisés dans des travaux portant sur l'écologie des forêts tropicales (Caballé, 1978; Couteron et al., 2003; Feldpausch et al., 2006; Schulze et al., 2008; Van Vliet & Nasi, 2008) mais jamais à ma connaissance avec des taux de sondage aussi élevés sur des superficies aussi grandes. Dans le cadre de ma thèse, nous avons tout d'abord évalué la qualité de ce type de données grâce à des ré-échantillonnages systématiques sur un sous-jeu de plus de 1000 parcelles (Réjou-Méchain, Fayolle, et al., 2011). Cette étude a montré que, malgré la qualité très variables des identifications botaniques réalisées dans les inventaires commerciaux, ce type de données révèlent de manière fiable les patrons de diversité et de variations taxonomiques.

Dans la majorité de mes travaux utilisant les données d'inventaires commerciaux, le filtrage édaphique est apparu comme un facteur majeur de la structuration des communautés d'arbres à large échelle spatiale (Fayolle et al., 2012; Gourlet-Fleury et al., 2011; Réjou-Méchain et al., 2008; Réjou-Méchain, Flores, et al., 2014). Ce résultat avait déjà été mis en évidence à une échelle régionale dans le bassin Amazonien (Tuomisto et al., 2003). A l'aide de traits fonctionnels et/ou démographiques, nous avons montré que les sols sableux, pauvres en nutriments et en eau, filtraient préférentiellement des espèces à stratégies « conservatrices » (i.e. taux de croissance faible, densité de bois importante, faibles surfaces foliaires, tolérance à l'ombrage et caractère sempervirent; (Fayolle et al., 2012; Gourlet-Fleury et al., 2011; Réjou-Méchain, Flores, et al., 2014)). Ces résultats avaient alors suggéré que la composition des forêts tropicales

était dans une certaine mesure prédictible, du moins à large échelle spatiale.

Dans un travail initié lors de mon postdoctorat à l'UMR AMAP et à l'UR Forêts et Sociétés (2013-2014), et poursuivi sur plusieurs années ensuite, nous avons travaillé sur la prédiction des compositions floristiques et fonctionnelles des communautés d'arbres à l'échelle de l'Afrique centrale (Réjou-Méchain et al., 2021, article complet en ANNEXES). Ce travail s'est basé sur un jeu de données exceptionnel de plus de 180 000 parcelles d'inventaires réparties dans cinq pays, nommé CoFor (Fig. 4). Afin d'imager la taille de ce jeu de données, nous avons estimé qu'il aurait fallut non moins de 1000 années de travail de terrain de la part d'une seule personne pour produire un jeu de données similaire. Grace à ce jeu de données, nous avons pu modéliser conjointement la distribution en abondance des taxons d'arbres les plus dominants d'Afrique centrale et produire les premières cartes continues de la composition floristique et fonctionnelle des forêts d'Afrique centrale (Fig. 5). Une des originalités de ce travail repose sur l'utilisation d'une nouvelle méthode de prédiction multivariée qui identifie les dimensions les plus prédictives au sein d'un grand nombre de variables explicatives (Bry et al., 2013; Gibaud et al., 2022). Nos résultats ont montré que l'incertitude dans la distribution individuelle des taxons se moyenne à l'échelle des communautés, révélant des assemblages floristiques et fonctionnels déterministes. Nous avons mis en évidence des compositions floristiques et fonctionnelles contrastées le long des gradients climatiques, entre différents types de sol et le long de gradients anthropiques, avec des convergences fonctionnelles entre types de forêts floristiquement dissemblables (Fig. 5). La combinaison de ces prédictions spatiales avec des scénarios de changements globaux suggère une forte vulnérabilité des marges nord et sud des forêts, des forêts Atlantiques et de la plupart des forêts de la République démocratique du Congo où les menaces climatiques et anthropiques devraient augmenter fortement d'ici 2085 (Fig. 6). Ces résultats constituent des références quantitatives clés pour les scientifiques et les décideurs politiques dans une perspective de développer des stratégies transnationales de conservation et de gestion des forêts d'Afrique centrale.

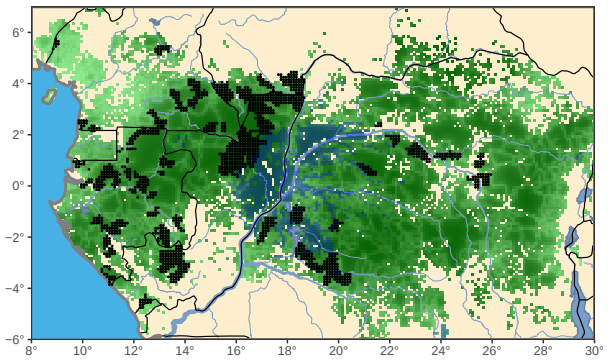

Figure 4: Jeux de données CoFor contenant 180 000 parcelles d'inventaires distribuées sur cinq pays d'Afrique centrale (en noir sur la carte). En vert, la distribution actuelle des forêts tropicales selon [European Space Agency Climate Change Initiative (ESA-CCI) landcover](http://cci.esa.int/) (V.1.6) avec un gradient allant du vert foncé vers le blanc pour représenter la pression anthropique estimées à partir d'un indice spécifiquement développé dans le cadre de Réjou-Méchain et al. (2021). Les zones non forestières sont représentées en beige et les zones indondées en permanence sont représentées en bleu. Figure tirée de Réjou-Méchain et al. (2021).

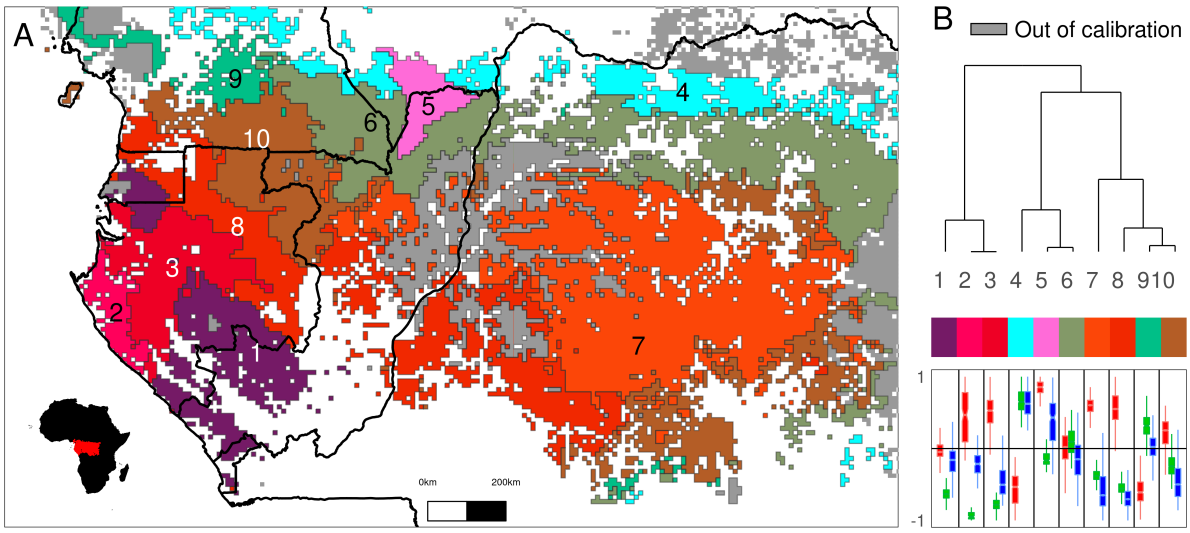

Figure 5: Principaux types de forêts d'Afrique centrale et leur composition fonctionnelle. **A** Classification des types de forêts obtenus par classification hiérarchique des gradients floristiques prédits. Les couleurs représentent un composite rouge vert bleu (RVB) des valeurs moyennes prédites de trois traits fonctionnels par type de forêt, à savoir la densité du bois (rouge), la déciduité (vert) et le diamètre maximal (bleu). Ainsi, des couleurs similaires illustrent des compositions fonctionnelles proches. **B** Relations taxonomiques entre les types de forêts illustrées par un dendrogramme (en haut) et une boîte à moustaches de la composition fonctionnelle prédite standardisée (en bas), avec la densité du bois en rouge, la deciduité en vert et le diamètre maximum en bleu. Noms des types de forêts: (1) Sempervirent des hautes terres de la zone Atlantique, (2) Sempervirent de la côte Atlantique (3) Sempervirent intérieur de la zone Atlantique, (4) Semi-décidue des marges forestières, (5) Sempervirent-semi-décidue sur grès, (6) Semi-décidue, (7) Sempervirent central (8) Sempervirent mixte, (9) Semi-décidue dégradé (10) Transition semi-décidue-sempervirent. Les frontières des pays sont représentées en noir et les zones boisées en dehors du domaine de calibration du modèle en gris. Figure tirée de Réjou-Méchain et al., (2021).

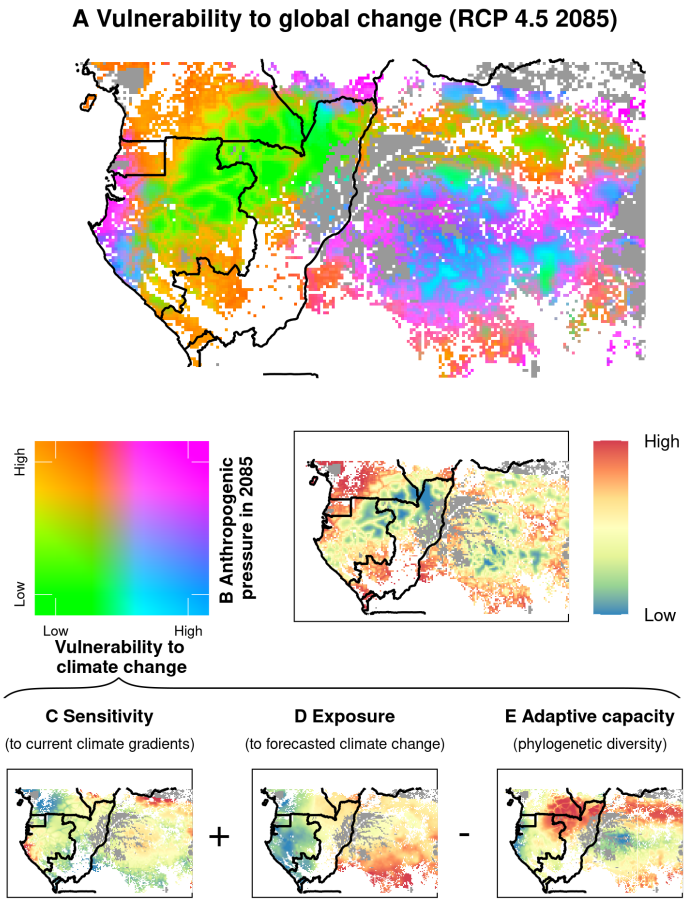

Figure 6: Vulnérabilité prédite des communautés d'arbres d'Afrique centrale aux changements globaux. (**A**) Carte composite de la vulnérabilité aux changements climatiques et de l'intensité des perturbations forestières induites par l'homme d'ici 2085. (**B**) Intensité projetée des perturbations forestières d'origine humaine en 2085. La vulnérabilité au changement climatique a été estimée comme la sensibilité des communautés d'arbres au climat actuel (**C**) plus l'exposition aux changements climatiques prévus d'ici 2085 (**D**) moins la capacité d'adaptation des communautés d'arbres en utilisant leur diversité phylogénétique comme proxy (**E**). Figure tirée de Réjou-Méchain et al. (2021).

Le rôle des successions forestières dans l'assemblage des forêts tropicales

Le stade successionnel d'un peuplement forestier joue un rôle majeur dans la structure floristique et fonctionnelle des communautés d'arbres tropicaux (Chazdon, 2014). Toutefois, les processus impliqués dans les successions végétales sont souvent étudiés indépendamment d'autres processus écologiques, comme le filtrage édaphique. Dans une étude initiée pendant ma thèse, nous avons montré que le filtrage édaphique n'était pas constant le long des gradients successionnels (Réjou-Méchain, Flores, et al., 2014). En début de succession, l'effet du filtrage édaphique est maximal, puis à mesure que les forêts deviennent matures, la composition taxonomique et fonctionnelle des communautés d'arbres situées sur des sols contrastés tend à converger (Fig. 7). Deux principales hypothèses non exclusives peuvent être émises. La première est

que les ressources deviennent de plus en plus uniformes le long des gradients successionnels (Guariguata & Ostertag, 2001; Tilman, 2004), avec une potentielle convergence des conditions édaphiques sur des sols ayant des origines géologiques distinctes. La seconde hypothèse est que les espèces de début de succession sont plus sensibles aux variations édaphiques que les espèces de fin de succession. Ces premières ont en général une stratégie de croissance rapide qui nécessite une exploitation rapide des ressources abiotiques (Bazzaz, 1979; Grime, 1977). Ainsi, elles pourraient souffrir d'une variance démographique inter-sol plus élevée que les espèces de fin de succession à stratégie plus conservatrice.

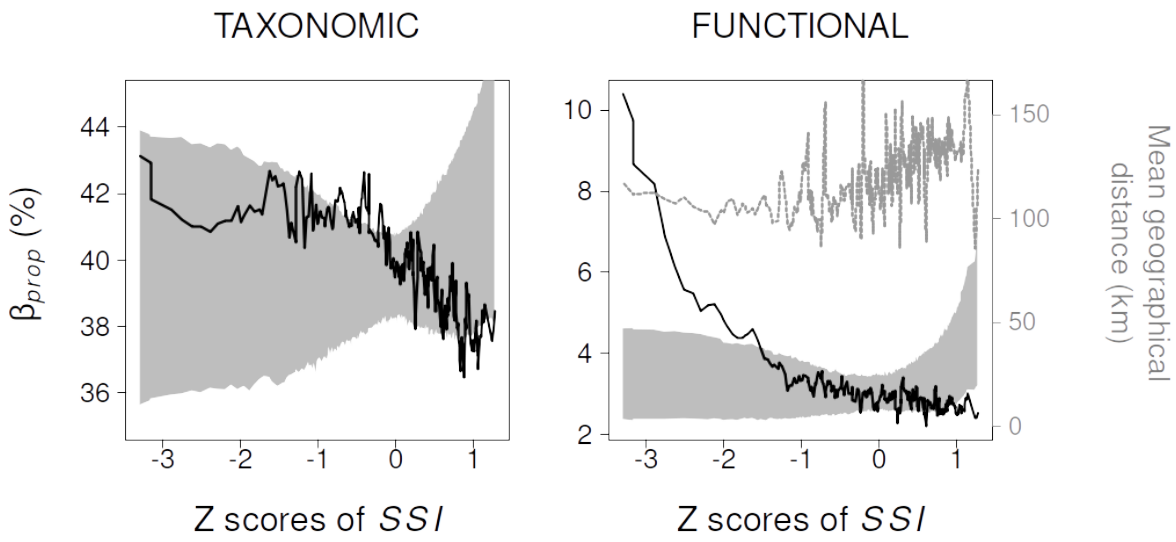

Figure 7: Variations de la diversité β taxonomique et fonctionnelle entre types de sol au cours de la succession forestière. La diversité β proportionnelle moyenne (β_{prop}) a été calculée dans des fenêtres de 200 placettes le long du gradient de succession *SSI* et en ne considérant que des paires de placettes situées dans différents types de sol (ligne noire épaisse). Les enveloppes de confiance obtenues à partir de modèles nuls préservant la structuration spatiale des abondances sont représentées en gris et la distance géographique moyenne entre les parcelles utilisées pour estimer la diversité β taxonomique et fonctionnelle est illustrée par des lignes grises en pointillés (l'axe correspondant est à droite du panneau). Figure tirée de Réjou-Méchain, Flores, et al., (2014).

Dans une étude en collaboration avec Pierre-Olivier Cheptou (CEFE-CNRS, Montpellier), nous avons également montré que les stratégies de reproduction des arbres ont une influence sur l'assemblage des communautés d'arbres le long des gradients successionnels (Réjou-Méchain & Cheptou, 2015, article complet en ANNEXES). En effet, un pourcentage anormalement élevé d'espèces et d'individus dioïques est présent dans les stades de début de succession (Fig. 8). Ce résultat va à l'encontre de la théorie de Baker (1955, 1967) qui prédit une plus forte capacité de colonisation des espèces auto-compatibles car un seul migrant est capable d'initier une population viable à long terme. La théorie de Baker a largement été reprise pour expliquer le succès d'espèces invasives, la limite de distribution des espèces et la composition floristique des îles éloignées (Cheptou, 2012). Nous avons proposé deux hypothèses alternatives permettant d'expliquer la sur-représentation des systèmes dioïques en début de succession. La première est que dans des conditions de stress, telles que celles rencontrées en début de succession,

les individus possédant les deux sexes (i.e., hermaphrodites ou monoïques) ont tendance à diminuer l'importance donnée à la fonction femelle, plus couteuse en énergie que la fonction male (Ashman, 2006). Ainsi, le désavantage démographique des espèces dioïques par rapport aux espèces possédant les deux sexes serait minimisé en condition de stress. La seconde hypothèse est reliée au «seed-shadow handicap» formulé par Heilbuth et al. (2001). Ce handicap résulterait de phénomènes de densité-dépendance plus forts chez les espèces dioïques car, comme seules les femelles produisent des graines, les individus sont plus agrégés dans l'espace. Les espèces dioïques doivent donc compenser ce handicap par une augmentation des capacités de dispersion, et donc de colonisation. A travers le co-encadrement de Célia Paris (Master 2), avec Pierre-Olivier Cheptou, nous avons étendu ces analyses au jeu de données CoFor (Fig. 4). Ce travail à confirmé une association significative entre le pourcentage de dioécie et un indice d'anthropisation mais à surtout révélé un gradient très marqué du pourcentage d'individus dioïques à l'échelle de l'Afrique centrale, le long d'un gradient climatique opposant les forêts à saisons sèches marquées au Nord et celles à nébulosité quasi-permanente au Sud-Ouest (Fig. 9; non publié). Ce résultat est cohérent avec le fait que les individus mâles sont généralement moins sensibles à l'aridité que les individus femelles, menant potentiellement à des sex-ratio très déséquilibrés en faveur des mâles dans des situations de déficit hydrique plus marqué (Hultine et al., 2016). Ces études font partie des rares à avoir étudié l'effet des modes de reproduction sur l'assemblage des communautés d'arbres tropicaux et montrent, comme l'avait pressentit Darwin (1877), leur rôle majeur dans la structuration spatiale des communautés végétales.

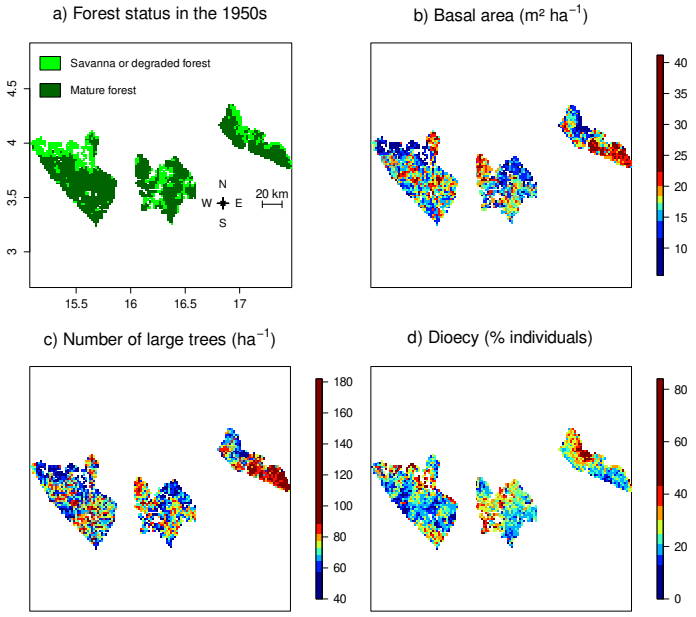

Figure 8: Relation entre le statut successionnel des forêts et la proportion d'individus dioïques au sein d'un paysage de République Centrafricaine. L'état des forêts dans les années 1950 a été obtenu à partir de photographies aériennes anciennes prises par l'Institut Géographique National (voir projet de recherche pour des exemples de photographies). Les pourcentages d'individus dioïques ont été calculés au sein de 17 198 parcelles de 0.5 ha, puis discrétisés en 8 classes avec une classification hiérarchique de Ward. La résolution de ces cartes est de 2 km. Figure tirée de Réjou-Méchain et Cheptou (2015).

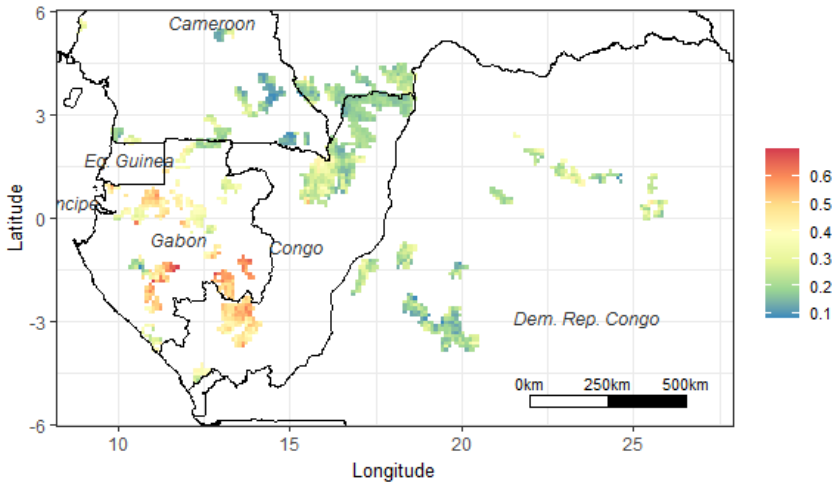

Figure 9: Proportion d'individus dioïques au sein du jeu de données CoFor. La résolution de cette carte est de 10 km. © Célia Paris.

Enfin, en Guyane Française, j'ai étudié l'influence de perturbations pré-Colombiennes sur la composition et la structure des forêts tropicales (projet LongTime; labex CEBA Guyane, co-responsable d'un work package 2017-2019). En effet, depuis quelques années, l'importance des perturbations humaines anciennes sur la composition des forêts tropicales est de plus en plus reconnue (Levis et al., 2017; Odonne et al., 2019; Walters et al., 2019) et certains travaux suggèrent même qu'une large partie des forêts amazoniennes correspondent à des systèmes domestiqués par le passé (Levis et al., 2018; Rostain, 2021). Dans le cadre du projet multidisciplinaire LongTime, j'ai encadré deux étudiantes: i) Marion Vincent (Master 1), en co-encadrement avec Isabelle Maréchaux (AMAP), qui visait a modéliser et évaluer l'importance relative des mécanismes écologiques responsables du maintien des signatures anthropiques anciennes dans les forêts actuelles et ii) Isis Poinas (Master 2) qui a réalisé les analyses statistiques des données collectées dans le cadre du projet LongTime. Le second stage a mené à des résultats originaux sur la réserve naturelle des Nouragues, en Guyane française, toujours en cours de valorisation du fait de l'arrivée tardive de certaines données génomiques. Deux zones de la réserve ont été sélectionnées grâce à des artefacts humains révélés par des données LiDAR (laser aéroporté; Fig. 10). Sur chaque zone, des placettes d'inventaires d'arbres, des prélèvements de sols, des fosses pédologiques et de la récolte opportuniste d'artefacts archéologiques ont été réalisés. Sur base d'analyses de micromorphologie des sols (proportion de microcharbons et sols brulés), d'abondances de charbons et de tessons ou de présence d'autres artefacts humains (fossés) nous avons classé les sites comme ayant expérimenté ou non une anthropisation ancienne. Les résultats préliminaires des analyses conduites sur la composition en arbre (inventaires) et de données génomiques sur les vers de terre, les bactéries et les champignons ont montré que ces activités anthropiques anciennes, estimées à plus de 400 ans par des analyses du ^{14}C, ont laissé une signature marquée dans la composition actuelle des communautés d'arbres et de bactéries mais pas sur la composition des champignons et des vers de terre (Fig. 11). Ce travail est toujours en cours en vue d'une valorisation.

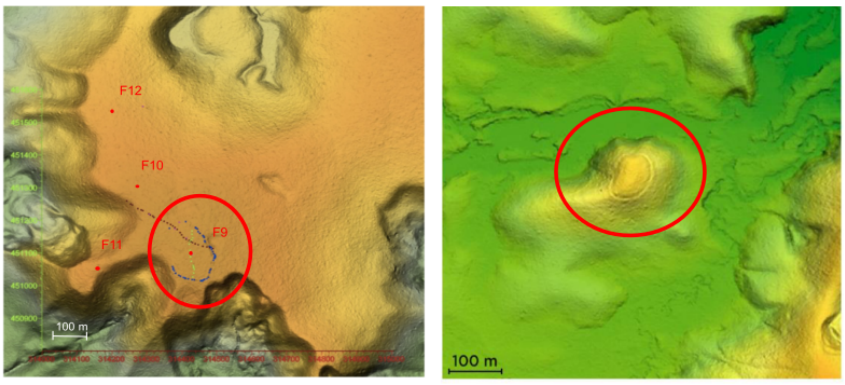

Figure 10: Artefacts humains révélés par un modèle numérique de terrain issus de données LiDAR dans la réserve naturelle des Nouragues, en Guyane française. A gauche, un site situé près de la station Inselberg où un fossé d'origine anthropique à pu être décelé. A droite, proche de la station Pararé, une montagne couronnée, une structure relativement commune sur le plateau des Guyanes dont l'origine reste encore incertaine (probablement lieux de sépulture). © Jean-François Molino.

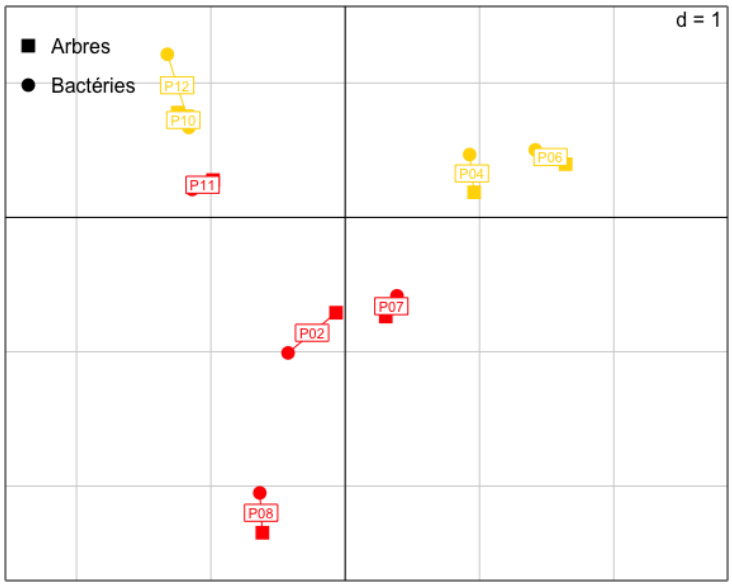

Figure 11: Analyse de co-inertie sur la composition des communautés d'arbres et de bacteries sur 8 sites de la réserve naturelle des Nouragues. L'axe 2 de cette analyse oppose clairement les sites ayant été anciennement anthropisés (en rouge) à ceux n'ayant pas d'artefacts archéologiques majeurs. Ce résultat préliminaire montre que des activités humaines anciennes (> 400 ans) ont laissé une signature marquée dans la composition actuelle des communautés d'arbres et de bactéries. A noté que la structuration spatiale des sites ne semble pas avoir influencé de façon majeure ce patron. © Isis Poinas.

Le rôle de la dispersion limitée dans l'assemblage des arbres tropicaux

J'ai étudié les processus de dispersion limitée en communauté naturelle de deux façons complémentaires: par une approche communauté (non publiée) et par une approche populationnelle (Réjou-Méchain, Flores, et al., 2011). Dans l'approche communauté, j'ai montré qu'au sein d'un environnement globalement homogène, la similarité des communautés d'arbres centrafricains diminuait linéairement en fonction du logarithme de leur distance géographique, un patron caractéristique en présence de dispersion limitée (Chave & Leigh, 2002). Nous avons donc testé l'influence de la capacité de dispersion des espèces sur leur agrégation dans l'espace à différentes échelles spatiales (Réjou-Méchain, Flores, et al., 2011). Les précédentes études ayant testé la relation entre syndromes de dispersion et degré d'agrégation des arbres tropicaux avaient montré des effets significatifs uniquement à des échelles très locales (< 200 m), et principalement sur les arbres les plus jeunes (Flores, 2005; Hubbell, 1979; Seidler & Plotkin, 2006). De notre côté, nous avons montré l'existence d'un effet significatif, bien que faible, du type de diaspores sur l'agrégation spatiale des arbres de canopée à large échelle spatiale (1-100 km) : les espèces dotées d'une faible capacité de dispersion sont effectivement plus agrégées à ces échelles spatiales. A des échelles spatiales plus locales (< 10 km), nous avons montré que des mêmes groupes taxonomiques (espèce, genre et famille) montrait une agrégation similaire dans les 5 sites étudiés et suggère donc que des traits conservés dans la phylogénie, non identifiés dans cette étude, influencent de manière significative les patrons d'agrégation.

3.2 Quantification et suivi de la biomasse forestière tropicale

Les forêts tropicales jouent un rôle majeur dans le cycle du carbone terrestre, à la fois puits et sources de CO_2 atmosphérique à travers la reforestation et la déforestation. On estime que les forêts tropicales contiennent environ 60% du carbone contenu dans la végétation terrestre (Dixon et al., 1994), et que 98% des émissions associées aux changements d'utilisation des terres sont directement liés à la déforestation sous les tropiques (IPCC, 2007). Le suivi des stocks de carbone forestier tropicaux est donc un enjeu majeur dans la réduction des incertitudes associées au bilan global du carbone (Lewis et al., 2009). Une partie de mes recherches s'est concentrée sur l'amélioration des estimations de la biomasse forestière à travers différents niveaux d'approches, incluant les stratégies d'échantillonnage depuis le terrain jusqu'à l'extrapolation de ces mesures à travers de récentes technologies et approches de télédétection. Une publication réalisée en collaboration avec des collègues d'AMAP résume une partie de ces différentes étapes (Réjou-Méchain et al., 2019, article complet en ANNEXES).

3.2.1 Amélioration des équations de biomasse

Les erreurs et biais associés à l'utilisation d'équations allométriques sont parmi les plus importantes sources d'erreurs dans l'estimation de la biomasse ligneuse en forêt tropicale (Chave et al., 2004; Molto et al., 2013). Les variations régionales dans les relations hauteur-diamètre (Feldpausch et al., 2012), dans la densité de bois (T. R. Baker et al., 2004; Phillips et al., 2019) et dans la taille du houppier (Goodman et al., 2014; Loubota Panzou et al., 2021; Ploton et al., 2016) sont des arguments régulièrement invoqués en faveur de la construction d'équations allométriques locales, i.e., spécifiques à chaque site. Un grand nombre d'études réalise donc des mesures destructives (pesées directes suite à un abattage) en forêts tropicales pour calibrer des équations de biomasse locales (Henry et al., 2013). Toutefois, la multitude d'équations allométriques existante limite la capacité des utilisateurs à choisir les équations les plus pertinentes sur des bases objectives. Avec un réseau de collaborateurs d'Amérique du Sud, j'ai participé à l'écriture d'une série de quatre articles pour une édition spéciale visant à: i) recommander des standards pour renseigner les équations de biomasse ou de volume lors de leur publication (Cifuentes Jara et al., 2014); (ii) aider les utilisateurs à choisir des équations pertinentes et à estimer les erreurs associées à ces équations (Henry, Cifuentes Jara, et al., 2015) ; (iii) recommander des pratiques permettant de dépasser les obstacles au partage de données issues des campagnes de pesées directes d'arbres (Cifuentes Jara et al., 2015); et (iv) proposer une synthèse des technologies disponibles pour des suivis de dynamique forestière à l'échelle nationale (Henry, Réjou-Méchain, et al., 2015).

Dans un travail mené par Jérôme Chave (CNRS/EDB), nous avons compilé un grand nombre de pesées directes d'arbres sous les tropiques pour proposer un modèle générique d'estimation de biomasse ligneuse en milieu tropical (Chave et al., 2014). En se basant sur plus de 4000 arbres coupés et pesés dans 58 sites distribués sur l'ensemble des tropiques, nous avons montré qu'un seul et unique modèle intégrant le diamètre, la hauteur et la densité de bois, était capable d'estimer la biomasse épigée dans différents types de forêts tropicales naturelles. La précision et l'erreur de ce modèle étaient similaires à celles des modèles développés localement car près de 80 % de l'erreur résiduelle se situait à l'intérieur des sites, et

non entre les sites. En négligeant la hauteur des arbres, une mesure difficile à réaliser de façon précise en forêt tropicale (Larjavaara & Muller-Landau, 2013), l'erreur d'un modèle générique était bien plus élevée. Nous avons donc proposé un second modèle générique, intégrant des données bioclimatiques, permettant de prendre en compte de façon implicite les variations régionales dans les relations hauteur-diamètre.

3.2.2 Comprendre la structuration des forêts pour proposer des stratégies d'échantillonnage

A l'échelle globale, le suivi des forêts depuis le sol est très inégalement réparti. Par exemple, des centaines de milliers de parcelles d'environ 0.1 ha sont suivies sur l'ensemble du territoire des Etats Unis et de Suède alors que de vastes zones tropicales restent inexplorées. Il est donc important de définir des stratégies d'échantillonnage réalistes et les plus représentatives possible. Dans un travail collaboratif au sein du réseau international CTFS-ForestGEO (Center for Tropical Forest Science - Forest Global Earth Observatory), nous avons quantifié la variabilité spatiale locale de la biomasse forestière dans 30 larges parcelles (8-50 ha) distribuées globalement (Réjou-Méchain, Muller-Landau, et al., 2014). Nous avons montré que la forte variabilité locale de la biomasse forestière induisait des erreurs d'échantillonnage élevées pour des parcelles de petites tailles (e.g. 46 % pour des parcelles de 0.1 ha). Contrairement à une idée reçue, la variabilité relative locale n'était pas plus importante en milieu tropical qu'en milieu tempéré. Elle était aussi indépendante du continent considéré. Par contre, cette variabilité était bien plus forte dans des zones à forte topographie. En utilisant des statistiques spatiales, nous avons confirmé que l'autocorrelation spatiale de la biomasse, une caractéristique fondamentale pour les questions d'erreurs d'échantillonnage, était en effet plus importante dans les zones à topographie complexe. Enfin, à travers un travail de simulations, nous avons montré que les erreurs d'échantillonnage, qui sont par définition aléatoires, pouvaient se transformer en une erreur systématique au sein des produits de télédétection (Fig. 12). En effet, en utilisant des modèles classiques d'inversion basés sur les moindres carrés, les erreurs d'échantillonnage conduisent à une forte sur-estimation (sous-estimation) des valeurs de biomasse dans les zones de faible (forte) biomasse. Ce phénomène de biais statistique de dilution, bien connu dans le domaine de l'épidémiologie (Frost & Thompson, 2000), était jusqu'ici largement ignoré dans les approches de télédétection. C'est un résultat important car de nombreux travaux calibrent des modèles de biomasse avec des parcelles de terrain de très petite taille (< 0.1 ha; Carreiras et al., (2012)). Dans cet article, nous préconisons donc l'utilisation de grandes parcelles pour calibrer les produits de télédétection, comme ceux qui seront issus de la prochaine mission BIOMASS (voir ci-dessous).

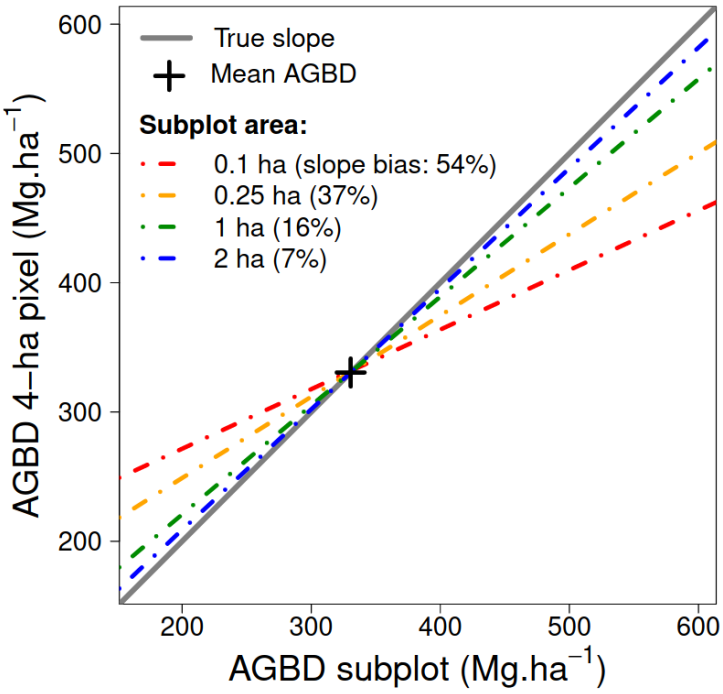

Figure 12: Simulations illustrant le biais de dilution de modèles d'inversion de biomasse lorsque de petites parcelles de calibration sont utilisées. En abscisse: biomasse réelle telle que mesurée sur le terrain. En ordonnée: biomasse estimée à partir de modèles d'inversion utilisant des sous parcelles de calibration (les tailles des parcelles, et les biais de pente associés, sont donnés dans la légende). Figure tirée de Réjou-Méchain, Muller-Landau, et al. (2014).

Etablir de larges parcelles pour minimiser les erreurs d'échantillonnage ferait consensus si les coûts associés aux campagnes de terrain n'étaient pas si élevés. Une piste intéressante pour diminuer les coûts d'échantillonnage est de focaliser sur les grands arbres, qui représentent la plus grande part de la biomasse ligneuse (Slik et al., 2013). J'ai travaillé en collaboration avec un étudiant de l'Université libre de Bruxelles pour mettre en place des modèles de prédiction de biomasse à partir d'un nombre restreint de grands arbres (J.-F. Bastin et al., 2015; Bastin et al., 2018). En utilisant un jeu de données original de 175 parcelles de 1 ha largement réparties en Afrique centrale, nous avons montré que la biomasse ligneuse totale pouvait être précisément estimée en ne mesurant qu'un petit nombre de gros arbres. La relation entre la biomasse des plus gros arbres et la biomasse totale était remarquablement stable à travers les sites, soulignant l'aspect universel de cette relation.

3.2.3 Approches par télédétection

La cartographie du carbone forestier via des outils de télédétection est pressentie comme une pierre angulaire des systèmes MRV (Measuring, Reporting and Verification) promus par le programme UN-REDD (United Nations Collaborative Programme on Reducing of Emissions from Deforestation and For-

est Degradation in Developing Countries). Jusqu'à récemment, les approches par télédétection avaient surtout été utilisées pour caractériser la dynamique de déforestation (premier «D» de REDD) mais la dynamique de dégradation (second «D» de REDD) était largement ignorée par manque d'approches quantitatives sur la structure forestière (DeFries et al., 2007). Ces dernières années, de nouvelles technologies et/ou méthodologies ont permis des avancées majeures pour la cartographie de la biomasse forestière à large échelle, mais aussi à haute résolution spatiale. Ces outils, toujours en développement, ouvrent des perspectives énormes pour mieux caractériser les dynamiques de dégradation des forêts tropicales denses, comme les pertes de biomasse suite à une perturbation anthropique. Une part de mes travaux de recherche s'est porté sur ces approches de télédétection pour caractériser la structure forestière de l'échelle de l'arbre à l'échelle d'une région. Ci-dessous, je présente ces travaux structurés par types de technologie.

Estimation de la structure forestière par LiDAR haute résolution

La technologie LiDAR (Light Detection And Ranging) consiste à envoyer des impulsions laser et à mesurer le temps et l'intensité des retours ayant été réfléchis par un objet. Cette technologie permet de caractériser la structure forestière en trois dimensions avec une résolution extrêmement fine. Le LiDAR aéroporté est notamment un des outils les plus efficace pour cartographier les stocks de carbone forestier sous les tropiques (Mascaro et al., 2014; Zolkos et al., 2013), même si les contraintes logistiques et financières associées à ce type d'acquisition aéroportée limite des approches à très larges échelles (mais voir par exemple: Xu et al., 2017). La capacité de cette technologie à cartographier de très fortes biomasses et à estimer la dynamique temporelle des stocks de biomasse en forêt naturelle restait toutefois peu connue il y a quelques années.

J'ai commencé à utiliser des données LiDAR durant mon postdoctorat au laboratoire EDB. J'ai analysé deux couvertures LiDAR acquises au sein de la station CNRS des Nouragues en Guyane Française, connue pour contenir des forêts à forte biomasse ligneuse au sein du bassin Amazonien (Malhi et al., 2006). J'y ai encadré des équipes sur le terrain, pendant 5 mois cumulés, pour installer et/ou remesurer des parcelles permanentes sur un total de 28 ha (14.500 arbres), en collaboration avec le réseau amazonien RAINFOR (ForestPlots.net et al., 2021) qui m'associe désormais à de nombreux articles utilisant les données que j'ai contribué à collecter (e.g., Esquivel-Muelbert et al., 2019; Fauset et al., 2015; Feldpausch et al., 2016; Sullivan et al., 2017).
J'ai montré que les données LiDAR permettaient de cartographier la biomasse ligneuse avec une erreur de 13% à l'échelle de 1 ha et de 23% à l'échelle de 0.25 ha (Réjou-Méchain et al., 2015). En utilisant deux campagnes LiDAR, réalisées à 4 ans d'interval (2008 et 2012), j'ai montré que la dynamique temporelle de la biomasse pouvait être inférée uniquement à des échelles fines en forêt tropicale mature (<0.25 ha; Fig. 13). En effet, les événements les plus importants en matière de dynamique de biomasse sont les chutes d'arbres, bien captées à fine résolution par le LIDAR mais noyées dans la dynamique globale à une résolution plus grossière. Enfin, j'ai montré qu'a l'échelle du paysage, le facteur le plus déterminant de la variabilité spatiale de la biomasse était l'altitude, avec de fortes biomasses sur les plateaux et de faibles biomasses dans les vallées dans le contexte Guyanais.

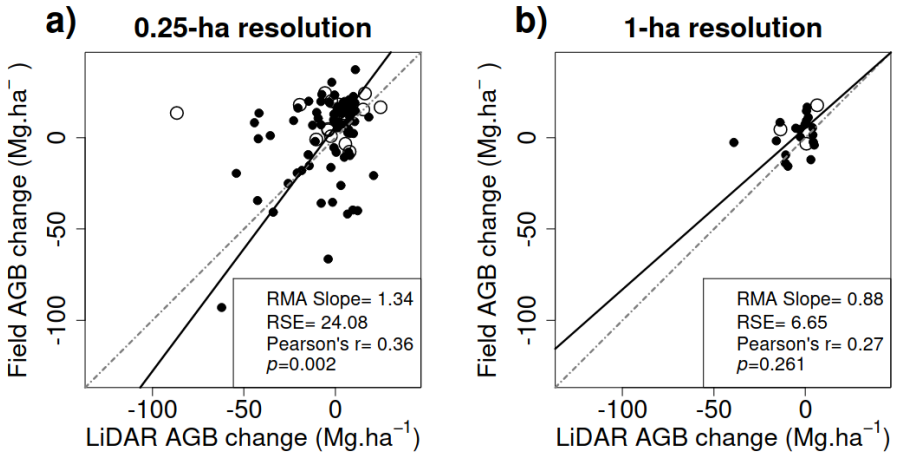

Figure 13: Relation entre le changement de biomasse aérienne estimé à partir du terrain et à partir de campagnes LiDAR répétées. Les lignes noires continues représentent des régressions de type RMA (Residual Major Axis) et la ligne 1:1 est illustrée par des lignes pointillées grises. Figure tirée de Réjou-Méchain et al. (2015).

Comme l'attestent mes travaux en cours (cf ci-dessous), la technologie LiDAR aéroportée tient toujours une place importante dans mes activités de recherches.

Estimation des stocks de biomasse par radar

En milieu forestier, les signaux issus de capteurs radars résultent de l'interaction entre les ondes électromagnétiques et la structure forestière. Ces signaux portent donc une information sur la biomasse forestière mais leur sensibilité à différentes gammes de biomasse dépend de la longueur d'onde utilisée. Plus la longueur d'onde est grande, plus les mesures sont sensibles à des structures forestières grossières, et donc à de fortes biomasses (Le Toan et al., 1992). En collaborant avec des spécialistes du traitement des données radar, mes travaux se sont concentrés sur les instruments ayant les longueurs d'ondes les plus larges: les radars en bande L (λ d'environ 25 cm) et en bande P (λ d'environ 70 cm).
Jusqu'à présent, les radars satellitaires possédant les plus grandes longueurs d'onde sont les instruments en bande L (e.g. ALOS PALSAR). Dans un travail en collaboration avec le laboratoire CESBIO (Toulouse), j'ai travaillé sur le potentiel de cette bande pour cartographier la biomasse forestière dans deux études. Dans la première, nous avons utilisé des données ALOS PALSAR pour estimer la biomasse stockée dans les savanes à l'échelle du Cameroun, avec une résolution de 25 m (Mermoz et al., 2014). Nous n'avons pas cartographié la biomasse des forêts denses humides dans cette étude car, dans un contexte de forte biomasse, la relation entre le signal en bande L et la biomasse faisait débat (Woodhouse et al., 2012). Ce débat opposait principalement deux écoles: ceux qui faisaient l'hypothèse d'une augmentation constante du signal avec la biomasse (Englhart et al., 2011; Shugart et al., 2010), et ceux qui supposaient une saturation du signal pour de fortes biomasses (Imhoff, 1995; Mitchard et al., 2011). Dans une seconde étude, nous avons donc utilisé un jeu de données d'inventaires commerciaux de République centrafricaine (près de 20,000 parcelles de 0.5 ha) et une approche théorique par simulations électromagnétiques pour étudier le comportement du signal en bande L dans des contextes de fortes biomasses. Nous avons mon-

tré que, contrairement aux deux hypothèses classiques, le signal radar en bande L tend à s'atténuer de manière faible mais linéaire avec la biomasse dans des contextes de biomasse élevée (Fig. 14; Mermoz et al., (2015)). En effet, à mesure que la biomasse forestière augmente, l'extinction du signal au sein de la végétation augmente également. Ce résultat à de fortes conséquences car il suggère que pour un même signal radar en bande L, deux valeurs de biomasses forestières sont possibles, une très faible et une très forte. Pour dissocier ces deux valeurs, une source de données indépendante, comme des produits de télédétection optique, est nécessaire. Enfin, ce nouveau résultat suggère que, même si la décroissance est très faible, la bande L contient une information sur la structure, y compris en contexte de forte biomasse.

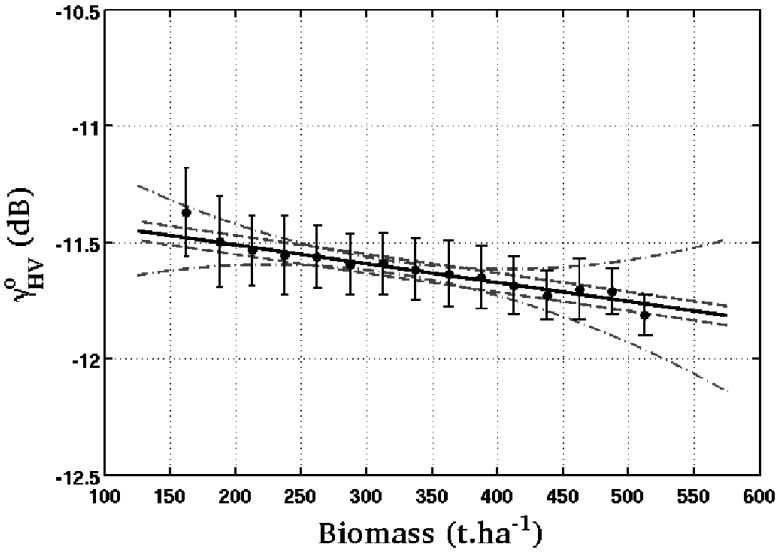

Figure 14: Relation entre le coefficient de rétrodiffusion d'un radar en bande L (ALOS) et la biomasse aérienne (AGB) estimée depuis des données de terrain extensives d'Afrique centrale pour des valeurs d'AGB supérieures à 150 Mg/ha. A des fins d'illustration, les points sont les valeurs moyennes par classe de biomasse de 25 Mg/ha et les barres représentent les écarts types au sein de ces classes. Les régressions linéaires (traits pleins noirs) ont été ajustées sur les données individuelles des parcelles. Ce résultat montre une diminution progressive et linéaire du coefficient de rétrodiffusion avec l'AGB. Figure tirée de Mermoz et al. (2015).

Face à la faible sensibilité de la bande L dans des gammes élevées de biomasse, le radar en bande P est un bon candidat pour cartographier la biomasse stockée en forêt tropicale dense humide car il possède une plus grande longueur d'onde (~ 70 cm). Au début de mon travail au laboratoire EDB de Toulouse (Avril 2010), la mission BIOMASS avait été retenue en phase A comme un des 3 candidats pour la 7ème mission Earth Explorer de l'agence spatiale européenne (ESA). Depuis Mai 2013, BIOMASS a été définitivement sélectionnée: un satellite embarquant un radar en bande P devrait être lancé en 2023 pour mesurer la distribution spatiale et temporelle de la biomasse forestière à l'échelle globale (Le Toan et al., 2011). Plusieurs étapes de validation du concept avaient été effectuées par des expériences aéroportées en milieu boréal et tempéré, mais l'enjeu majeur se situait sous les tropiques. Ainsi, une campagne de mesure aéroportée, TropiSAR, co-financée par l'ESA et le centre national d'études spatiales (CNES), a eu lieu en 2009 en Guyane française. C'est dans ce cadre que j'ai effectué une partie de mes travaux

au laboratoire EDB. J'ai participé activement à la campagne TropiSAR en intervenant sur la stratégie de calibration/validation des produits en bande P sur les sites guyanais de Paracou (station scientifique CIRAD) et des Nouragues (station scientifique CNRS). A travers une collaboration étroite avec Thuy Le Toan (CNRS/CESBIO, Toulouse) et trois de ses post-doctorants (Stéphane Mermoz, Dinh Ho Tong Minh et Ludovic Villard), j'ai participé au développement de ce que pourront être les méthodologies de références de la mission BIOMASS. L'ensemble de ces travaux a été reporté dans le rapport officiel rendu à l'ESA en Février 2011 (Dubois-Fernandez et al., 2011). Aussi, ces travaux ont été valorisés sous forme de nombreuses présentations dans des conférences internationales et d'un article présentant une nouvelle méthode utilisant une approche tomographique (Minh et al., 2016).

4 Activités de recherches en cours et en projet

4.1 Contexte

Alors que de nombreux pays développés voient actuellement leur couvert forestier augmenter, les forêts tropicales subissent toujours de fortes pressions sous les effets des changements globaux (Vancutsem et al., 2021). La déforestation tropicale, et les facteurs qui en sont à l'origine, ont ainsi été largement étudiés ces dernières décennies (Hoang & Kanemoto, 2021). Cependant, les conditions et les vitesses avec lesquelles une reforestation s'opère restent largement incertaines, en particulier en Afrique et en Asie où très peu de dispositifs de suivis existent en comparaison avec l'Amérique latine (Requena Suarez et al., 2019). De plus, la dégradation forestière et ses conséquences ont été beaucoup moins étudiées et quantifiées que la déforestation. Pourtant, la dégradation est omniprésente sous l'ensemble des tropiques et mène a une perte considérable de services écosystémiques, parfois avec des conséquences plus importante que la déforestation (Pearson et al., 2017). Dans de nombreux cas, il est attendu que des processus successionels tendent à ramener le système dans un état similaire à l'état initial suite à une perturbation. Cependant, dans certains cas, le système peut avoir franchi un seuil et le système déforesté ou dégradé peut rester dans une succession dite « arrêtée » ou dans un état stable alternatif (Ghazoul et al., 2015). Par exemple, l'ouverture partielle de la canopée suite à une perturbation peut conduire à la prolifération de certaines forme de vie (e.g. végétation arbustive, herbacée ou lianescente) qui vont rapidement dominer certains étages forestiers pendant des décennies ou plus, bloquant ou retardant la succession (Soto & Puettmann, 2020). Une composante majeure de mon travail actuel et de mes projets vise donc à comprendre les conditions de réversibilité de la déforestation et de la dégradation à travers le suivis de la structure et de la composition forestière suite à des perturbations de différentes natures. Pour ce faire, je travaille sur deux principaux chantiers géographiques: la Thaïlande, où j'étudie les dynamiques de reforestation suite à une déforestation passée, et la République du Congo, où je me focalise sur des systèmes dégradés ayant potentiellement une faible résilience.

4.2 Dynamiques de reforestation suite à une déforestation passée

Plusieurs initiatives internationales, comme le défi de Bonn en 2011 suivis de la Déclaration de New York sur les forêts en 2014, visent à utiliser le reboisement des terres dégradées et déforestées comme une solution naturelle pour limiter le réchauffement climatique. Depuis un peu plus d'une décennie, de nombreux débats scientifiques ont émergés autour de la sélection des lieux ou des écosystèmes devant être reboisés (Bastin et al., 2019; Grainger et al., 2019; Lewis et al., 2019; Skidmore et al., 2019; Veldman et al., 2019) ou sur la manière d'effectuer ce reboisement (Chazdon et al., 2021; Holl & Aide, 2011). Mon travail ne s'inscrit pas dans ces débats mais vise à comprendre les mécanismes écologiques qui se mettent en place lors d'une régénération forestière naturelle ou assistée.

Après une déforestation intense durant le siècle dernier, certains pays d'Asie du Sud-Est, dont la Thaïlande, vivent actuellement une transition forestière avec une augmentation de leur couvert forestier, parfois au détriment d'autres pays voisins (Pendrill et al., 2019). La Thaïlande constitue donc un excellent laboratoire d'étude pour comprendre comment, et sous quelles conditions, les forêts tropicales reconstituent naturellement ou de manière assistée leur structure, composition et les services écosystémiques associés en l'absence de perturbations majeures. J'ai ainsi commencé à travailler en Thaïlande lors de mon poste de directeur du laboratoire de géomatique à l'Institut Français de Pondichéry en Inde (2014-2016). J'ai notamment initié des collaborations avec l'Asian Institute of Technology (AIT, Bangkok), l'Université de Kasetsart (KU, Bangkok) et le National Biobank of Thailande (NBT, Bangkok), le tout en lien avec le Département des Parcs Nationaux (DNP, Bangkok). Mes collaborations se sont récemment étendues à l'Université de Chiang Mai (CMU, Chiang Mai) au sein de laquelle j'ai demandé une affectation IRD à partir de mi 2023. Une excellente dynamique de collaboration est en cours avec des montages de projets nationaux (NSTDA Hyperspectral-LiDAR, 2021-2023), français (JEAI BIMOMS, 2022-2024) et internationaux (Projet Natural Forestore, 2023-2025).

4.2.1 Reforestation naturelle

Mes travaux en Thaïlande se sont jusqu'ici conduits sur le parc National de Khao Yai en Thaïlande (14.43N, 101.37E). Ce parc est le premier parc national de Thaïlande, créé en 1962. Il abrite une forêt dense sempervirente (2200 mm de précipitations par an) où de nombreuses espèces végétales et animales menacées sont présentes (Kitamura et al., 2004). Avant la création du parc, certaines zones ont été utilisées pour des activités agricoles de faible intensité de la fin du 19ème siècle à 1962 (Brockelman et al., 2011), puis reboisées naturellement à différents moments en fonction de la période où les perturbations d'origines anthropiques ont cessé (Chanthorn et al., 2016). Certaines zones sont d'ailleurs encore entretenues par le parc à des fins de gestion ou touristiques. En conséquence, le paysage constitue une mosaïque de forêts matures et secondaires d'âges différents (Chanthorn et al., 2016; Jha et al., 2020) et constitue donc un excellent site d'étude pour comprendre les dynamiques de reforestation, et les processus successionnels associés, en absence de nouvelles perturbations anthropiques.

Mes travaux à Khao Yai ont principalement visé à utiliser des données extensives de terrain couplées à des

données de télédétection (aéroportées et satellitaires) pour caractériser les dynamiques forestières post-perturbations et leur impact sur les services écosystémiques. En particulier, des parcelles forestières permanentes régulièrement suivies par mes collaborateurs du National Biobank of Thailand et de l'Université de Kasetsart ont été installées le long d'un gradient successionnel avec la présence notable d'une parcelle de 30 ha où tous les arbres $\geq$ 1 cm de diamètre sont suivis depuis 2004 dans une forêt mature (parcelle Mo Singto appartenant au réseau de parcelles ForestGEO; https://forestgeo.si.edu/sites/asia/mo-singto). Suite à un travail collaboratif impliquant l'analyse de la parcelle Mo Singto (Réjou-Méchain, Muller-Landau, et al., 2014), j'ai initié l'acquisition de données LiDAR aéroportées en 2017 sur le parc de Khao Yai (projet RFCC). Cette première série de données aéroportées a permit de lancer plusieurs travaux dont certains sont introduits ci-dessous.

Dans le cadre de la thèse de Nidhi Jha (2016-2019), que j'ai encadré, nous avons utilisé les données LiDAR acquises en 2017 pour estimer la distribution spatiale de la biomasse forestière sur un paysage de 60 km^2 (Jha et al., 2020). En utilisant une série temporelle Landsat de 1972 à 2017, nous avons pu assigner un âge aux jeunes forêts secondaires et quantifier l'évolution de la biomasse dans le temps (Fig. 15). Nos résultats montrent que la biomasse s'accumule de manière similaire aux jeunes forêts tropicales Africaines ou Américaines, et invalide la révision des taux d'accumulation de carbone de référence pour l'IPCC qui ont récemment diminué de moitié pour les forêts secondaires d'Asie du Sud-Est (Requena Suarez et al., 2019). Cette dernière étude s'était basé sur un manque flagrant de données sur les jeunes forêts secondaires en Asie du sud, considérant seulement 7 chronosequences dont certaines suivies avec des parcelles de moins de 10 m de diamètre. Il y a en effet aucune raison de penser que ces forêts stockent le carbone moins rapidement que sur les autres continents dans les 20 premières années. Dans le cadre du projet "Natural Forestore" (voir ci-dessous), nous allons répliquer ce travail dans d'autres sites en Thaïlande pour mieux comprendre les déterminants des taux d'accumulation de carbone dans les jeunes forêts.

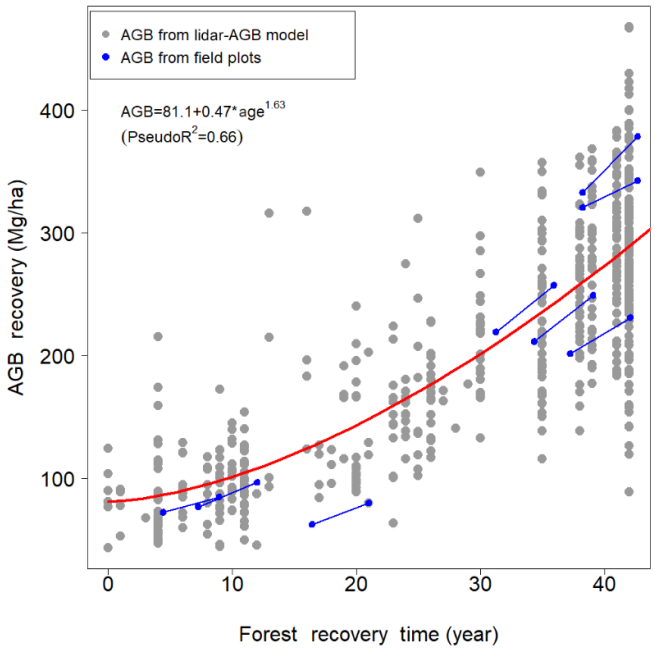

Figure 15: Relation entre la biomasse forestière (AGB) estimée à partir d'un modèle basé sur des données LiDAR et l'âge de la forêt estimé à partir d'une série temporelle d'images Landsat (points gris). Le modèle ajusté est représenté en rouge. Les lignes et les points bleus représentent l'AGB directement estimé à partir de huit parcelles de terrain en 2013 et en 2017/18 et pour lesquelles l'âge a été également déduit des séries Landsat (les mêmes parcelles sont jointes par une ligne). Figure reprise de Jha et al. (2020).

Dans le cadre d'une collaboration avec Dr. Wirong Chanthorn (Université de Kasetsart, Bangkok), initiée lors de la thèse de Siriruk Pimmasarn (2016-2020), nous mobilisons les données LiDAR, les inventaires de terrain et avons conduits de nombreux prélèvements de sols pour des analyses chimiques afin de (i) cartographier les différents types de successions forestières de la zone d'étude en se basant sur seulement trois métriques de structure forestière facilement interprétables et dérivées de données LiDAR (Fig. 16); (ii) relier cette cartographie au suivi de la dynamique au sol pour mieux évaluer le rôle de puits de carbone que joue vraisemblablement le paysage; (iii) comprendre quels facteurs influencent la densité de végétation, estimée à travers les données LiDAR, à un âge de forêt donné (la quantité de phosphore assimilable dans le sol semble être le plus déterminant selon nos résultats préliminaires).

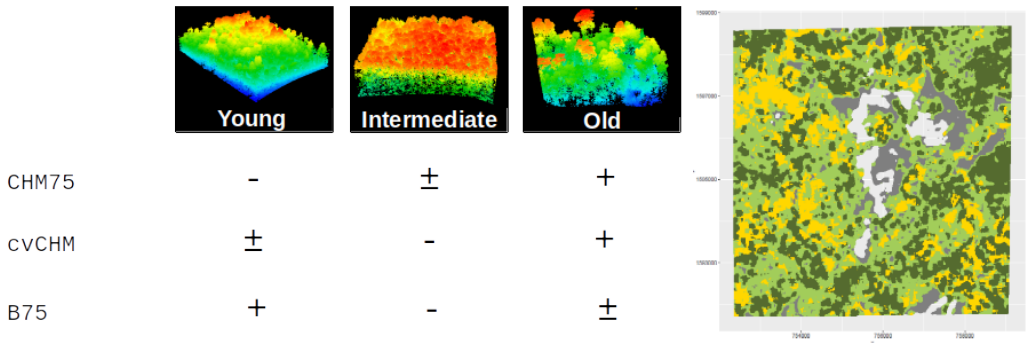

Figure 16: Attendus des valeurs relatives de trois métriques LiDAR complémentaires le long d'un gradient de succession classique (gauche) et classification des types successionels basée sur ces trois métriques à l'échelle du paysage dans le parc National de Khao Yai (droite). CHM75 = 75ème percentile du modèle de canopée (hauteur de la canopée) ; cvCHM = coefficient de variation du modèle de canopée ; B75 = proportion de pixels ayant une valeur inférieure à 75% de la hauteur maximale de canopée. Un nuage de points LiDAR pour chaque stade successionnel est montré pour illustrer les caractéristiques de structure de trois types successionels (l'échelle de couleur n'est pas la même entre les trois images).

Dans un travail collaboratif récent autour du travail de mémoire de master 2 de Patcharapan Thripob (KU), nous avons étudié les déterminants et les conséquences en matière d'estimation des stocks de carbone de la variabilité intraspécifique de l'infradensité et de la concentration en carbone du bois. En combinant des données d'inventaires, un large échantillonnage de carottes de bois des espèces d'arbres dominantes le long d'un gradient de succession et des données LiDAR, nous avons montré que la variabilité intraspécifique des traits du bois étaient faiblement structurés le long de gradients abiotiques et biotiques et dépendaient principalement de la taille des arbres (Thripob et al., 2022). En propageant l'effet de ces variabilités intraspécifiques jusqu'à l'estimation des stocks de carbone à l'échelle des peuplements, nous avons montré que la variabilité intraspécifique de l'infradensité et de la teneur en carbone du bois n'avaient qu'une influence limitée sur l'estimation des stocks de carbone.

Le projet Hyperspectral-LiDAR, co-construit avec mes partenaires de NBT et KU, offre également des perspectives importantes pour comprendre comment la composition floristique et fonctionnelle des communautés d'arbres varie à l'échelle du paysage, notamment le long des gradients de succession. Ce projet génèrera des données aéroportées hyperspectrales et LiDAR sur le site de Khao Yai en Mars 2023. Ces données auront un fort potentiel de valorisation car elles permettront de: (i) mesurer la dynamique temporelle de la structure forestière et du carbone en les couplant avec les données LiDAR acquises en 2017; (ii) cartographier la diversité taxonomique et fonctionnelle des communautés d'arbres et en comprendre les déterminants à l'échelle du paysage, en particulier le long du gradient successionnel. Deux demandes de financements de postdoctorat d'un an chacun ont été demandé à l'agence nationale de la recherche Thaïlandaise par mes collaborateurs de NBT et KU pour travailler sur ces deux points en interaction avec moi. Concernant le point (ii), j'ai encadré un stage de césure (Rose-Eva Moua Nedellec), durant le premier semestre 2022, qui visait à produire des données et des résultats préliminaires sur le lien entre réponses spectrales des arbres, estimées à partir d'une campagne drone multispectrale (Février 2022), et les stratégies fonctionnelles des arbres au sein de la parcelle Mo Singto. Les résultats préliminaires

indiquent des relations significatives entre réponses spectrales et valeurs de certains traits fonctionnels, même si ces relations sont relativement tenues et souffrent d'une très forte variabilité individuelle (Fig. 17). Nous visons désormais à mieux comprendre l'origine de cette forte variabilité en séparant les effets instrumentaux des réels effets biologiques. Ce travail préliminaire nous permets d'anticiper les potentiels problèmes auxquels nous devrons faire face avec les données aéroportées hyperspectrales à venir.

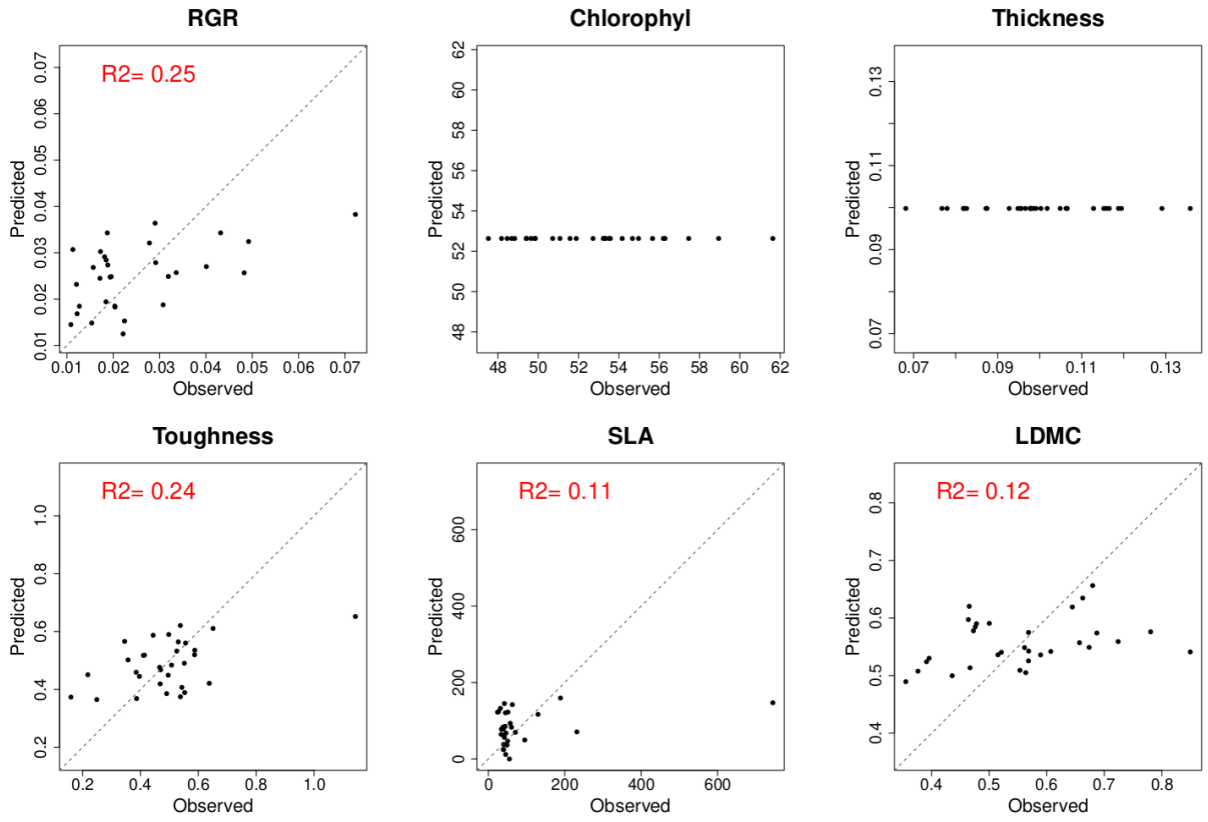

Figure 17: Prédiction des valeurs de traits moyen de 31 espèces pour lesquelles un lien entre réponse spectrale à l'échelle de la couronne et trait fonctionnels à pu être testé avec au moins 5 individus par espèce. Les modèles linéaires montrant une relation significative sont représentés avec leur R^2 en rouge. RGR = Taux de croissance relative moyen à l'échelle des espèces; Chlorophyl = Teneur en chlorophylle; Thickness = Epaisseur du limbe; Toughness = Dureté du limbe; SLA = Surface spécifique foliaire; LDMC = Teneur en matière séche du limbe. © Rose-Eva Moua Nedellec.

Enfin, le projet "Natural Forestore", qui débutera en 2023, vise à prédire les dynamiques de séquestration et de stockage du carbone dans les forêts en régénération d'Asie du Sud-Est. Ce projet multidisciplinaire, porté par Emmanuel Paradis (IRD, UMR ISEM), mobilisera des données de génomique environnementale, de pédologie, de suivis de terrain à long terme et de télédétection dans cinq sites en Thaïlande, dont le site de Khao Yai et un site dans la province de Chiang Mai. Dans un premier work package (WP), mené par Komsit Wisitreassameewong (NBT), nous étudierons la composition des communautés de bactéries et de champignons le long des gradients de succession et viserons à comprendre leurs contributions dans

la dynamique de reconstitution forestière et dans la séquestration du carbone. Dans un second WP que je mènerai, nous réaliserons de nouvelles campagnes LiDAR aéroportées et des acquisitions drones sur les différents sites et viserons à identifier les facteurs qui contribuent à la variation de la biomasse forestière pour un âge de forêt donné, en poursuivant le travail déjà initié sur le site de Khao Yai (cf plus haut). Un financement d'un postdoctorat de deux ans est prévu dans le cadre de ce WP. Dans un troisième WP, mené par Emmanuel Paradis, nous travaillerons à plus large échelle en cartographiant les changements d'utilisation des terres au cours des dernières décennies en Thaïlande et plus largement en Asie du Sud-Est. L'objectif de ce WP est, entre autres, d'identifier les conditions socio-économiques favorables, ou non, à la reforestation naturelle. Enfin, le dernier WP, mené par Anuttara Nathalang (NBT), visera à renforcer un partenariat stratégique avec le Département des Parcs Nationaux (DNP) de Thaïlande dans le but de collaborer avec les gestionnaires des parcs et de participer à la mise en oeuvre des décisions concernant la surveillance de la faune, la gestion des aires protégées et la prévention des conflits pouvant émerger entre les Hommes et la grande faune (e.g., éléphants, gaurs, tigres). Ce projet devrait générer d'importantes connaissances sur la résilience des forêts asiatiques et ses co-bénéfices en termes de séquestration de carbone et de préservation de la biodiversité. En outre, ces connaissances permettront potentiellement d'améliorer les modes de gestions des écosystèmes forestiers en Thaïlande à travers le WP4.

4.2.2 Restauration active

En 1994, l'équipe FORRU de l'Université de Chiang Mai a initié des projets de restauration active de zones complètement déforestées et, depuis, suit la dynamique de ces forêts restaurées au sein de parcelles permanentes (Fig. 18 & 19; https://www.forru.org/) (Elliot et al., 2013). L'objectif principal de leur action est de développer des techniques de restauration les plus efficaces possible à travers le développement d'une chaine opérationnelle complète de la pépinière à la plantation et incluant le choix des espèces natives à planter. A travers une collaboration avec l'équipe FORRU, je vise à comparer la structure et les dynamiques de ces forêts restaurées activement par rapport à des forêts n'ayant pas eu de régénération assistée dans la région. Ces dernières forêts sont en cours de sélection dans le cadre du projet "Natural Forestore" qui intégrera la province de Chiang Mai dans un des cinq sites d'étude du projet. Je viserais en particulier à comparer les capacités de séquestration de carbone et de diversité ligneuse entre les deux modalités (régénération active ou non). La comparaison de systèmes restaurés de manière active ou passive (régénération naturelle) permettra en outre d'évaluer le coût-bénéfice de ces deux approches en Thaïlande. L'ampleur de ce travail comparatif dépendra de mon affectation à l'Université de Chiang Mai en août 2023 (demande en cours à l'IRD).

Figure 18: Exemple de restauration active sur une parcelle ayant été déforestée, cultivée puis brûlée dans la haute vallée de Mae Sa, au nord de la Thaïlande. En 2000, 30 espèces d'arbres ont été plantée sur le site et la végétation a été ensuite régulièrement suivie au sein de parcelles permanentes (illustration empruntée à https://www.forru.org/about/our-mission).

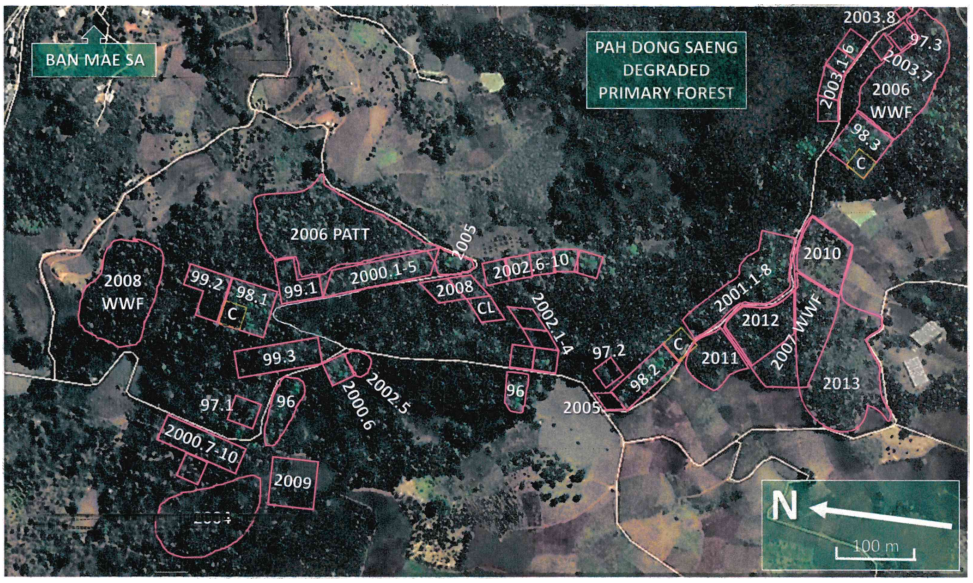

Figure 19: Dispositif de suivis de parcelles reforestées à différentes périodes au sein de parcelles permanentes sur le site de Pah Dong Saeng géré par l'équipe FORRU de Chiang Mai University. L'année de restauration est noté sur la carte (de 1996 à 2013 sur ce site) et illustre les chronoséquences disponibles (carte communiquée par Stephen Elliot, CMU).

4.3 Stabilité des systèmes dégradés en forêts tropicales

Depuis quelques années, j'étudie les mécanismes de stabilité d'états dégradés en forêt tropicale humide en utilisant deux modèles d'étude en Afrique centrale: les forêts infestées de lianes et les forêts à Marantacées (herbacées géantes). Ces deux systèmes, ayant des faciès d'apparence dégradés, sont probablement issus et/ou favorisés par les perturbations et montrent une forte stabilité temporelle ou, à minima, une dynamique de récupération très lente (Cuni-Sanchez et al., 2016; Tymen et al., 2016). En utilisant ces deux systèmes, je vise à renseigner les mécanismes écologiques limitant la résilience des forêts tropicales suite à une perturbation et à en comprendre les conséquences en termes de services écosystémiques et de gestion des écosystèmes.

4.3.1 Ecologie des lianes et impacts sur la dynamique des forêts tropicales

Les lianes sont une composante essentielle des forêts tropicales et semblent répondre de manière très favorable aux perturbations (Schnitzer & Carson, 2010). Elles peuvent représenter jusqu'à 40 % de la densité des tiges (Dalling et al., 2012) et envahir plus de la moitié des couronnes d'arbres de la canopée (Ingwell et al., 2010), limitant l'acquisition de la lumière par les arbres (Visser et al., 2018). Les lianes sont également soupçonnées de mieux explorer et capter les ressources du sol que les arbres (Smith-Martin et al., 2019). Elles sont ainsi en concurrence directe avec ces derniers pour les ressources souterraines et aériennes, réduisant la diversité, la croissance et le stockage du carbone des arbres (Heijden et al., 2015; Schnitzer & Carson, 2010), en particulier suite à des perturbations.

J'ai commencé à travaillé sur le rôle des lianes dans la dynamique forestière à travers le co-encadrement d'un chapitre de la thèse de Blaise Tymen lors de mon postdoctorat à Toulouse. Nous avons étudié une forêt fortement infestée par des lianes (Fig. 20) dans la station des Nouragues en Guyane Française et avons montré que cette forêt montrait une dynamique très rapide avec des taux de mortalité et de recrutement élevés en comparaison avec les forêts non infestées voisines (Tymen et al., 2016). A l'échelle du peuplement, la biomasse et le temps de résidence du carbone était de moitié par rapport aux autres forêts. Nous avons montré que si le sol de cette forêt de lianes était plus riche que ceux des forêts avoisinantes, ce n'était pas du au substrat géologique mais probablement à la libération des nutriments contenus dans une végétation ayant un temps de résidence court. En utilisant des données LiDAR répétées et des archives Landsat nous avons finalement montré que l'étendue de cette forêt infestée de lianes est restée stable ces 25 dernières années suggérant que les forêts infestées de lianes sont stabilisées par des processus de rétroaction positive à travers la dynamique forestière (Fig. 21).

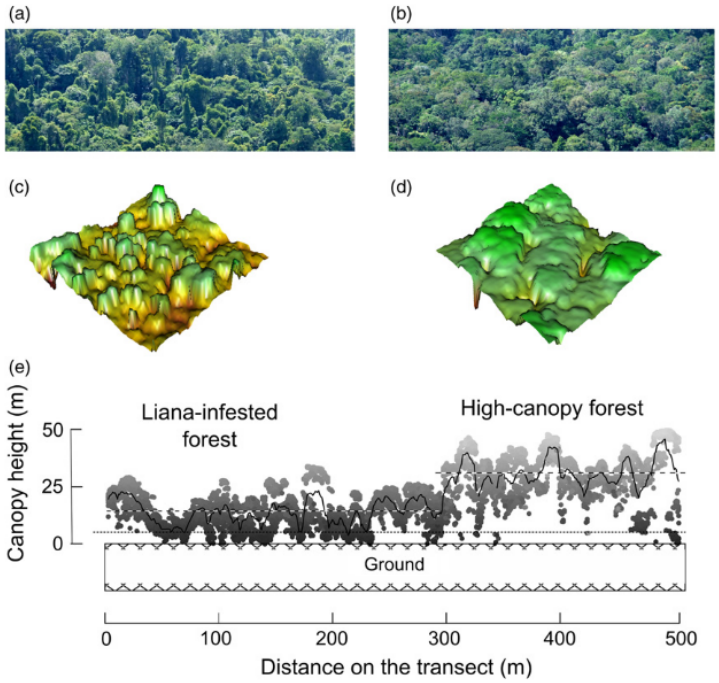

Figure 20: Transition d'une forêt infestée de lianes à une forêt à haute canopée dans la réserve des Nouragues en Guyane française. (a et b) Photographies de la forêt infestée de lianes et d'une forêt non infestée voisine. (c et d) Vues en 3D d'un modèle de canopée (hauteur de la canopée estimée avec des données LiDAR) dans et en dehors de la forêt infestée de lianes, respectivement (64 x 64 m²). (e) hauteur du modèle de canopée le long d'un transect de 20 x 500 m² établit dans la transition entre la forêt infestée de lianes et une forêt non infestée. Figure tirée de Tymen et al. (2016).

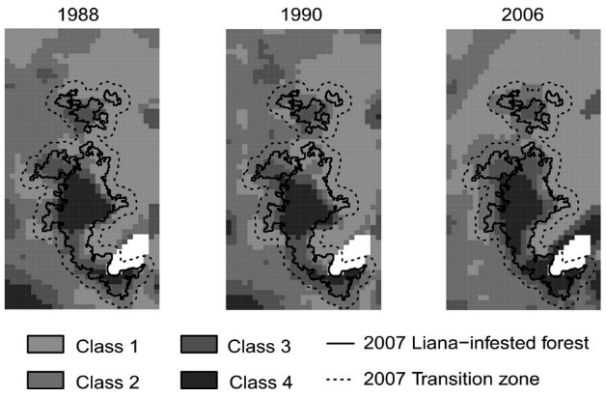

Figure 21: Dynamique spatio-temporelle d"une forêt infestée de lianes dans la réserve des Nouragues en Guyane française. Les classifications de types de végétations sont dérivées de classifications hiérarchiques non supervisées de séries temporelles Landsat. La classe 4 peut être attribuée de manière conservatrice à la forêt infestée de lianes. La ligne pleine représente l'étendue de la forêt infestée de lianes telle que définie à partir du modèle de canopée LiDAR de 2007 (avec la zone de transition représentée par une ligne pointillée). Figure tirée de Tymen et al. (2016).

Afin de poursuivre cette thématique de recherche, j'ai lancé une expérimentation de terrain dans le Nord de la République du Congo en 2017 visant à comprendre la réponse des lianes et des herbacées géantes à l'exploitation forestière, en collaboration avec Sylvie Gourlet-Fleury et Eric Forni (Cirad). L'expérimentation a prit place dans un dispositif permanent installé en 2013 où tous les arbres de plus de 10 cm de diamètre sont suivis annuellement dans 4 parcelles de 9 ha gérées par le Cirad. Fin 2018, deux parcelles ont été soumises à exploitation forestière par la compagnie forestière CIB-OLAM et deux ont été préservées afin de constituer un contrôle. Nous avons installé 144 placettes de 20 $\times$ 20 m^2, nichées dans les 4 parcelles de 9 ha, au sein desquelles toutes les lianes $\geq$ 1 cm de diamètre ont été mesurées et identifiées en 2017 et en 2022 lors de deux inventaires de 6 mois chacun.

Les lianes ont jusqu'ici été principalement étudiées à partir d'inventaires au sol. Dans un récent article mené par Begum Kaçamak, que je co-encadre avec Nick Rowe, Sylvie Gourlet-Fleury et Vivien Rossi, nous avons montré comment les données drones à très haute résolution spatiale constituaient une approche complémentaire aux données sols en permettant de mieux caractériser l'envahissement des lianes dans la canopée (Fig. 22)(Kaçamak et al., 2022). Nous avons montré que si les données de mesures au sol permettaient de prédire le degré d'infestation des houppiers, ce dernier varie considérablement d'un arbre à l'autre pour une même surface terrière de lianes au sol (Fig. 23). Nous avons finalement montré qu'une part de cette variabilité peut être expliquée par la densité de bois moyenne des lianes, les espèces de lianes ayant des tissus moins denses tendent à occuper une surface foliaire plus importante sur les houppiers des arbres pour une même surface terrière. Dans un travail en cours, qui constituera un autre chapitre de la thèse de Begum Kaçamak, nous visons désormais à utiliser la complémentarité des données drones et de terrain pour mieux comprendre l'impact de l'infestation des lianes sur les taux de croissance des arbres dans ce même site d'étude. Pour cela, une étudiante en césure (M1), Carla Della-Signora, co-encadrée avec Begum Kaçamak, a complété le jeu de données disponible en attribuant depuis le terrain plus de 1000 couronnes d'arbres segmentées, à partir de données drones LiDAR, aux arbres mesurés sur le terrain et réalisé la mesure de toutes les lianes ($\geq$ 1 cm de diamètre) infestant ces arbres depuis le sol. Ce travail devrait permettre de mieux comprendre l'impact de l'infestation des lianes sur la croissance des arbres et de tester si cet impact dépend de l'identité fonctionnelle des lianes.

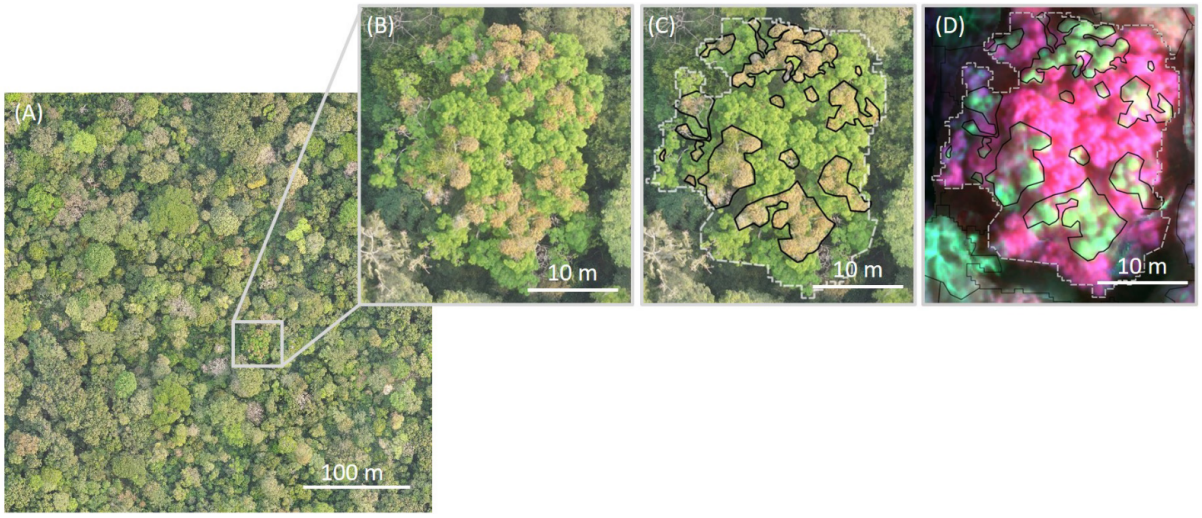

Figure 22: Exemple de délimitation manuelle des feuilles de lianes à l'aide de données RVB et multispectrales. (A) Mosaïque RVB d'une des parcelles de 9 ha du dispositif de Loundoungou au Congo. Une couronne d'arbre infestée de lianes est illustrée avant (B) et après (C-D) la délimitation manuelle des patch de feuilles de lianes (en lignes noires) et la segmentation des couronnes d'arbres issue de données LiDAR (en pointillés blancs) sur une image en RVB (C) et en multispectral (D). Figure tirée de Kaçamak et al. (2022).

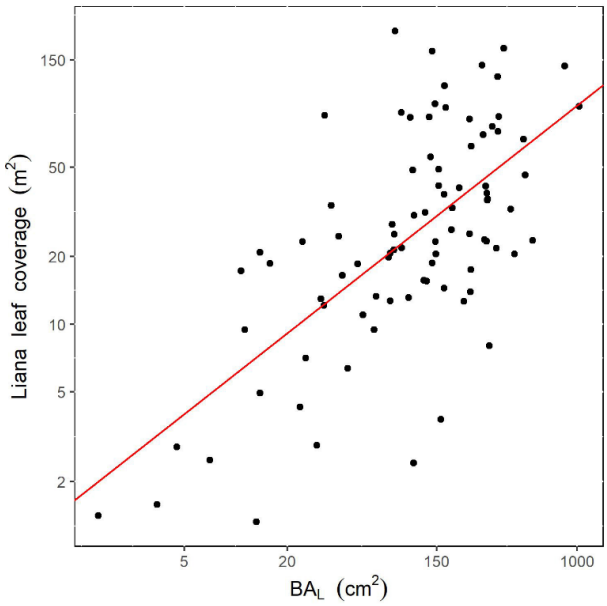

Figure 23: Relation entre la surface terrière totale des lianes mesurée à partir du sol et la couverture foliaire estimée à partir des données de drones pour 87 houppiers d'arbres. La ligne rouge illustre un modèle linéaire log-log (les axes sont affichés en échelle logarithmique). Une partie des résidus de cette relation est expliquée par la densité moyenne des tissus du bois des lianes infestant le houppier. Figure tirée de Kaçamak et al. (2022).

Avant de comprendre l'impact des lianes sur la dynamique naturelle et post-perturbation des forêts tropicales, il est nécessaire de mieux comprendre l'écologie des lianes, très peu connue, en particulier en Afrique. Pour cela, nous générons tout un ensemble de traits fonctionnels foliaires (surface spécifique foliaire, épaisseur du limbe, concentration en azote, phosphore, carbone, et potassium) et de traits liés au bois, comme la densité des tissus du bois et des traits macro-anatomiques en cours d'analyses. Ces données nous ont tout d'abord permis de confirmer que les lianes montraient une forte diversité de stratégies d'acquisitions, comme souligné récemment sur des lianes de Guyane française (Meunier et al., 2020) (Fig. 24). L'abondance des espèces estimée en 2017 (avant exploitation) se répartit de manière hétérogène sur le premier axe (précédemment interprété comme le spectre économique des feuilles (Baraloto et al., 2010; Fortunel et al., 2012)), suggèrant que les espèces ayant des stratégies conservatrices sont plus abondantes que les espèces à stratégies d'acquisition rapide dans une forêt non perturbée. Nous nous attendons à observer un déplacement de ces abondances relatives vers les espèces à stratégies d'acquisition rapide dans l'inventaire post-exploitation de 2022 (données en cours de saisie). A contrario, les abondances sont bien réparties le long de l'axe 2 (précédemment interprété comme le spectre économique du bois (Baraloto et al., 2010; Fortunel et al., 2012), suggérant que de multiples stratégies coexistent en forêts non perturbées le long de ce spectre. Ces données fonctionnelles nous ont également permis de montrer que ces stratégies fonctionnelles jouaient un rôle important dans la structuration des communautés de lianes, principalement en réponse à la structure forestière (travail en cours de valorisation; Fig. 25). En outre, elles nous permettrons de comprendre quelles stratégies fonctionnelles sont sélectionnées suite à des perturbations, en comparant l'évolution des effectifs des différentes espèces de lianes avant (inventaire 2017) et près de 4 ans après exploitation forestière (2022). Ces travaux en cours devrait permettre d'améliorer nos connaissances sur l'écologie des lianes africaines, largement sous étudiées en comparaison aux lianes d'Amérique centrale et du sud, sur leur rôle dans la dynamique naturelle et post-perturbation des forêts tropicales et de tester si l'augmentation de densité des lianes au cours du temps est spécifique aux forêts d'Amérique latine ou bien un phénomène pantropical (Schnitzer & Bongers, 2011).

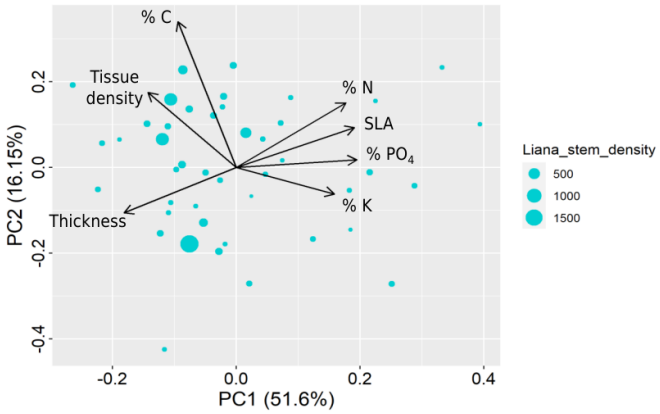

Figure 24: Analyse en composante principale des traits mesurés sur les espèces dominantes de lianes du dispositif expérimental de Loundoungou au Congo. Les deux premiers axes révèlent une structuration des traits le long de deux axes précédemment interprétés comme le spectre économique des feuilles (axe 1) et du bois (axe 2) de manière similaire à ce qui a été montré chez les arbres. La taille des points montre l'abondance des différentes espèces dans l'inventaire de 2017 (avant exploitation). Un des chapitres de la thèse de Begum Kaçamak visera notamment a tester si les traits anatomiques du bois des lianes sont bien représentés le long de ces deux axes où s'ils constituent un autre spectre économique d'intérêt écologique. © Begum Kaçamak.

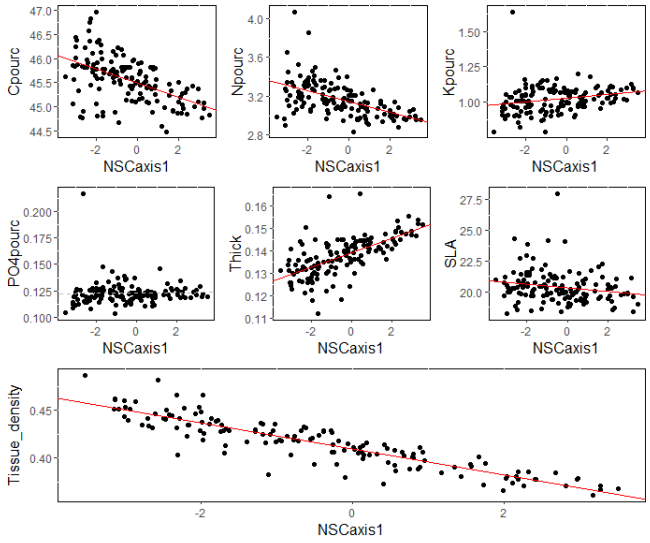

Figure 25: Evolution des traits moyens le long de gradients floristiques des communautés de lianes identifiés à partir d'une analyse non-symmétrique des correspondences (analyse similaire à une analyse factorielle des correspondences symmétrique excepté qu'elle donne plus de poids aux espèces abondantes). Un modèle de permutation des traits au sein des espèces à été utilisé pour tester la significativité des corrélations entre la valeur moyenne des traits et les gradients floristiques (un modèle linéaire à été appliqué lorsque le résultat du test était significatif, illustré avec les lignes rouges). Les résultats montrent que la majorité des gradients floristiques s'accompagnent de changements plus important qu'attendu sous le hasard dans la composition fonctionnelle des communautés de lianes, en particulier le long des gradients de structure forestière (non montré). © Begum Kaçamak.

A travers mes collaborations en Thaïlande, je vise également à poursuivre mes recherches sur le rôle des lianes dans la dynamique forestière, en particulier le long des successions. Des données de mesures de lianes et de leurs traits sont déjà disponibles sur le site de Khao Yai (Sun et al., 2022). De manière similaire à nos observations sur le site de Loundoungou au Congo, nous montrons dans un travail en cours de publication que les communautés de lianes du parc National de Khao Yai montrent une structuration principalement due à la structure forestière et répondent de manière moins prononcée que les communautés d'arbres aux conditions abiotiques (Chanthorn et al. submitted). Je souhaite à terme poursuivre mes travaux sur l'écologie des lianes et leurs impacts sur la dynamique forestière en Afrique centrale et en Asie du Sud-Est où les lianes ont largement été sous-étudiées jusqu'ici.

4.3.2 Les forêts à Marantacées d'Afrique Centrale

Les herbacées de l'ordre des Zingéribales sont une composante importante des forêts africaines et sont parfois abondantes au point de former un sous-type forestier distinct, les forêts à Marantacées (Fig. 26) (Gibert, 1984; Maisels, 1996). Ces forêts sont largement réparties en Afrique centrale (Fig. 27), couvrent des surfaces immenses et présentent une très faible densité d'arbres avec un sous-bois dense composé principalement d'herbacées géantes (Gillet, 2013). Le peu d'études conduites sur les forêts à Marantacées suggère que celles couvrant de grandes surfaces (jusqu'à 2000 km^2) seraient issues de perturbations très anciennes ($>$ 1000 ans), et se seraient maintenues par la suite à travers des mécanismes d'auto-entretien, e.g. inhibition de la régénération des arbres par les herbacées géantes. Ces forêts semblent donc correspondre à un système dégradé stable. De plus, les perturbations anthropiques actuelles, telle que l'exploitation forestière, et les anomalies climatiques, semblent également favoriser l'expansion de ces forêts dégradées (Gillet, 2013), soulevant des enjeux écologiques, sociétaux et économiques majeurs. Pourtant, si l'écologie de ces forêts a souvent été décrite dans la littérature grise, ces forêts ont été jusqu'à présent très peu représentées dans la littérature scientifique internationale (Cuni-Sanchez et al., 2016; White et al., 1995; White, 2001). Dans le cadre de mes recherches, j'utilise ces forêts comme un modèle d'étude permettant de comprendre comment les forçages exogènes associés à des processus de rétroactions positives peuvent conduire à des types alternatifs de forêts coexistants à long terme.

Figure 26: Une forêt à Marantacées dans le Nord Congo. La canopée y est très ouverte, avec une densité relativement faible d'arbres de diamètre moyen à gros, une quasi absence d'arbres de petit diamètre et une forte abondance d'herbacées géantes en sous bois. Sur cette photo, une forme lianescente d'herbacée géante (*Haumania liebrechstiana*) forme des "manchons" sur certains troncs alors que plusieurs espèces non lianescentes se mélangent au premier plan, dont *Aframomum sp.* et *Megaphrynium macrostachyum*. © Juliette Picard.

Figure 27: Emplacements des forêts à Marantacées décrites dans la littérature en Afrique centrale et de l'Ouest (points rouges). © Robin Pouteau.

L'objectif principal du projet ANR DESSFOR (2021-2024), que je dirige, est d'étudier la dynamique spatio-temporelle des forêts à Marantacées en Afrique centrale et de comprendre les mécanismes qui sous-tendent leur origine et leur maintenance. Pour répondre à ces objectifs, nous étudions les mécanismes par lesquels les forêts à Marantacées s'installent et se maintiennent à différentes échelles spatiales et temporelles. Le projet se structure en quatre tâches (WP) complémentaires (Fig. 28): WP0 est consacré à la synthèse de nos connaissances sur les forêts à Marantacées, incluant la littérature grise. Ce travail a été mené par Robin Pouteau, en postdoctorat sous ma direction, et fait l'objet d'une publication de synthèse en cours de finalisation ; WP1 vise à étudier les principaux mécanismes écologiques qui sous-

tendent la dynamique des forêts à Marantacées ; WP2 vise à étudier les dynamiques spatio-temporelles contemporaines (<100 ans) et à long terme (> 500 ans) de ces forêts en se basant sur des données de télédétection et des approches d'écologie historique ; Enfin, WP3 vise à comprendre les conditions de stabilité post-perturbation des forêts à Marantacées et l'importance relative des déterminants de cette stabilité à travers le développement de modèles mathématiques. Nos travaux se conduisent sur deux principales zones d'études au Nord du Congo (Fig. 29).

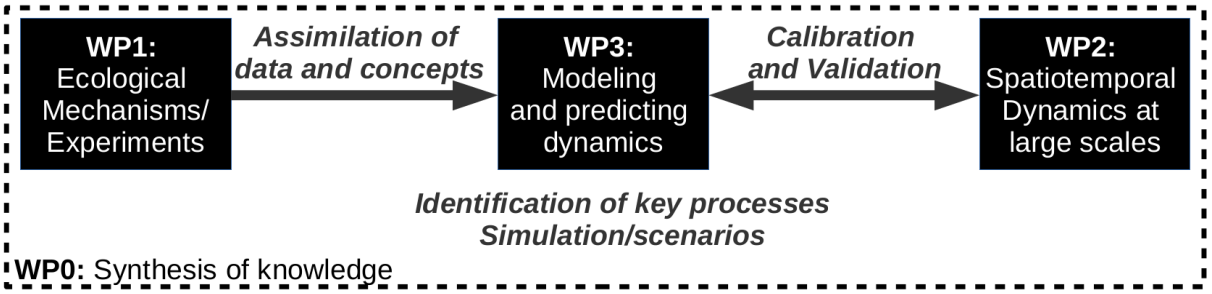

Figure 28: Organisation du projet DESSFOR en 4 principaux Work Packages (WP).

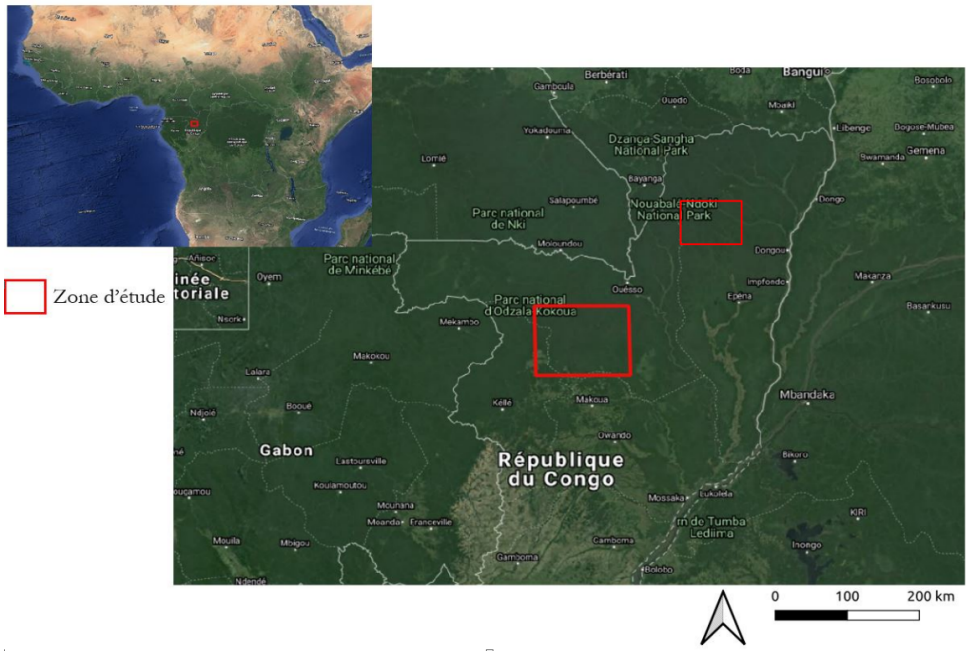

Figure 29: Zones d'études du projet (en rouge). La zone sud correspond à une zone d'étude à cheval sur le parc National d'Odzala et sur la concession forestière gérée par l'entreprise IFO (Industrie Forestière d'Ouesso) et la zone nord correspond au dispositif experimental de Loundoungou, sur la concession forestière gérée par la compagnie CIB-OLAM (Congolaise Industrielle des Bois).

4.3.2.1 WP1 : Mécanismes écologiques qui sous-tendent la dynamique des forêts à Marantacées

Des travaux antérieurs ont montré que les herbacées géantes concurrencent les jeunes arbres de façon aérienne et souterraine (Brncic, 2002), limitant considérablement la régénération des arbres dans les forêts à Marantacées. Toutefois, de nombreuses incertitudes subsistent quant aux conditions dans lesquelles les herbacées géantes colonisent de nouvelles zones puis inhibent le recrutement des arbres, conduisant à une monodominance d'herbacées géantes à long terme. Dans cette tâche, nous menons principalement des travaux de terrain (expérimentations, mesures et enquêtes) afin de comprendre l'origine des forêts à Marantacées et les conditions et mécanismes permettant leur stabilité. Cette tâche est divisée en quatre sous tâches dont l'avancement actuel et les perspectives sont décrits ci-dessous. Juliette Picard, une étudiante en thèse sous ma co-direction (avec Sylvie Gourlet-Fleury et Pierre Couteron), est fortement impliquée dans la majorité des sous tâches décrites ci-dessous.

Quantification de l'envahissement des herbacées géantes suite à exploitation forestière

L'effet positif de l'exploitation forestière sur la prolifération des herbacées géantes à déjà été documenté (e.g., Gillet, 2013; White et al., 1995) et est souvent décrit comme un potentiel problème par les exploitants forestiers eux mêmes. Cependant, cet envahissement a rarement été caractérisé et quantifié de manière contrôlée. Dans cette sous-tâche, nous poursuivons un effort que j'ai initié en 2017, où les herbacées géantes ont été inventoriées dans une maille de 10 m au sein de quatre parcelles de 9-ha du dispositif de Loundoungou (voir section lianes). Un nouvel inventaire, concomitant avec celui des lianes, s'est terminé fin octobre 2022 dans le cadre du projet DESSFOR. En parallèle de cet inventaire, Juliette Picard et une étudiante de Master 2 de l'Université de Marien Ngouabi (Victoire Damba) ont réalisé des prélèvements de sol et de feuilles de Marantacées sur le dispositif au sein de deux modalités: forêt perturbée ou non par l'exploitation forestière de 2019 (Fig. 30). Le but de ces prélèvements est de comprendre les stratégies de colonisation des herbacées géantes, en quantifiant la disponibilité des graines de Marantacées dans la banque de graines du sol (travail en cours de finalisation au sein de la pépinière du SNR de Brazzaville, Congo) et de quantifier le taux de clonalité des herbacées géantes à partir de d'analyses génétiques (microsatelittes développé par Alexandra Ley sur *Haumania danckelmaniana* (Ley & Hardy, 2016)). Ces analyses génétiques sont planifiées début 2023, en collaboration avec Olivier Hardy de Université Libre de Bruxelles. Ce travail fera l'objet d'un des chapitres de la thèse de Juliette Picard et devrait permettre de mieux comprendre les mécanismes de réponses des herbacées géantes à l'exploitation forestière.

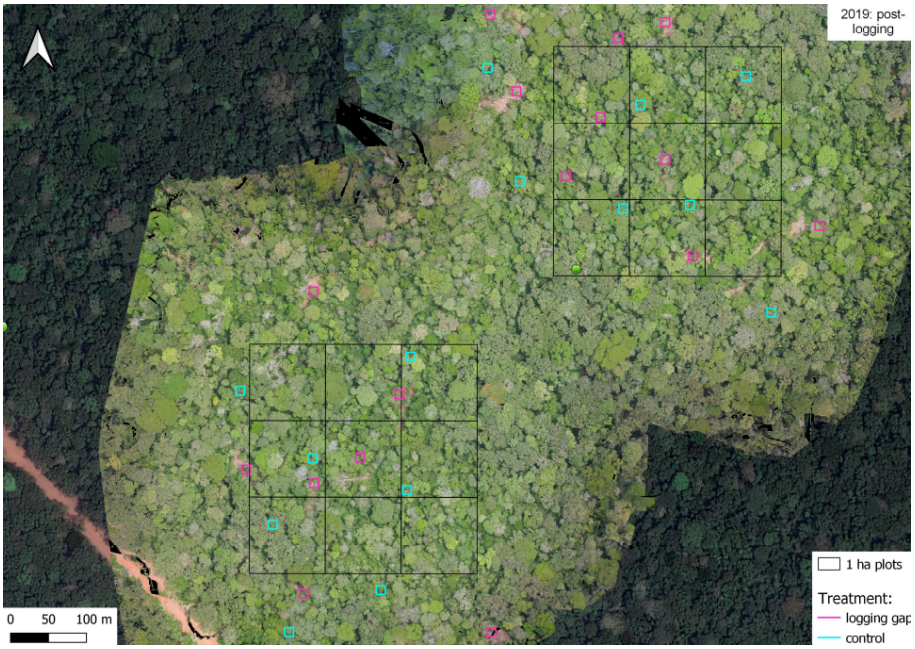

Figure 30: Echantillonage des feuilles et de la banque de graines du sol au sein des deux parcelles exploitées fin 2018 du dispositif de Loundoungou au Congo. Les placettes représentées en rose sont les placettes ayant été perturbées par l'exploitation forestière tandis que les bleues représentent les placettes contrôles. Le fond de carte représente une acquisition drone en RVB acquise juste après exploitation, début 2019, et qui permet d'identifier précisémment les zones impactées par l'exploitation forestière. © Juliette Picard.

Effets des feux sur la dynamique des forêts à Marantacées

Les grands feux sont suspectés d'être un élément moteur de la dynamique des forêts à Marantacées (Brncic, 2002; Gillet, 2013; Tovar et al., 2014). Entre fin janvier et début février 2016, des incendies majeurs se sont produits dans une zone de forêts à Marantaceae (zone IFO/Odzala), couvrant plus de 37 000 ha, suite à un évènement El Niño (Verhegghen et al., 2016). En synergie avec le projet «paysage Nord Congo» (AFD, retenu en 2020 ; PI S. Gourlet-Fleury), nous avons lancé des inventaires d'ampleurs dans la zone touchée par les feux afin de suivre la régénération en ligneux dans des zones brûlées et témoins. Des travaux d'inventaires ont été réalisés entre Février 2022 et Août 2022 par une équipe de terrain qui a mesuré tous les arbres $\geq$ 1 cm de diamètre dans des placettes de 20 $\times$ 20 m réparties dans 4 localités (Fig. 31). En parallèle, nous avons collecté des échantillons de sol et de feuilles de *Megaphrynium macrostachyum* dans l'ensemble des parcelles inventoriées afin de réaliser des analyses physico-chimiques. Ces données en cours d'analyses par un stagiaire du projet, Théau Despeyroux, nous permettrons de mieux comprendre le rôle du feux dans la dynamique des forêts à Marantacées et son impact sur la biodisponibilité en éléments nutritifs.

Figure 31: Mesure du diamètre d'un jeune *Maracaranga sp.* dans une forêt à Marantacées ayant subit un feux en 2016. © Juliette Picard.

Compétition et effets allélopathiques

Si la compétition entre herbacées géantes et plantules d'arbres a déjà été quantifiée (Brncic, 2002), des auteurs soupçonnent que le système racinaire des herbacées géantes peut inhiber la germination des graines et la croissance des plantules par des effets allélopathiques (Brncic, 2002; Brugière et al., 2000). Nous avons donc lancé une expérimentation ex-situ, sur le site de Pokola, où la germination et la croissance de quatre espèces d'arbres est suivi sur une période de 10 mois (Fig. 32, 33). Cette expérimentation est menée par Juliette Picard sous ma supervision. Un stage de Master prévu pour le premier semestre 2023 permettra de réaliser des mesures de traits foliaires et racinaires des plantules d'arbres dans les différents traitements en fin d'expérimentation et donc de tester pour la première fois l'existence de mécanismes allélopathiques dans la famille des Marantacées.

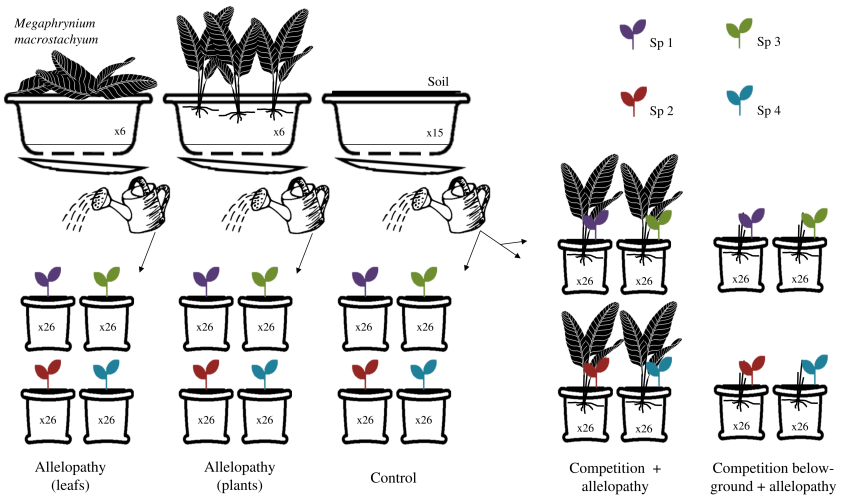

Figure 32: Principe de l'expérimentation visant à quantifier l'importance de la compétition et des potentiels effets allélopathiques sur 4 espèces d'arbres. Les effets allélopathiques sont testés à travers la méthode de donneurs-cibles (à gauche): l'eau de pots contenant des plants vivants ou des feuilles en décomposition d'herbacées géantes est utilisé pour arroser les plantules d'arbres. Le taux de germination, la croissance et les traits foliaires et racinaires des plantules seront ensuite comparés avec un contrôle (plantules arrosés par de l'eau issu de pots ne contenant que de la terre) et avec un dispositif ou les compétitions aérienne et/ou racinaire sont prises en compte (à droite). © Juliette Picard.

Figure 33: Pépinière lancée depuis Avril 2022 sur le site de Pokola. Deux techniciens et 1 ingénieur s'occupent à plein de temps du dispositif. © Juliette Picard.

Perceptions locales des forêts à Marantacées

Des enquêtes éthnobotaniques ont été réalisées dans la région de Ouesso d'Avril à Mai 2022 par Emile Catillon, un étudiant en Master 2 de l'Université de Wageningen (WUR), sous ma co-direction et celles de Solen Le Clech (WUR) et Aida Cuni-Sanchez (Norwegian University of Life Sciences). Au total, 78 personnes vivant dans quatre villages différents ont participé à l'enquête (30 d'origines Bantus et 48 d'origines Baaka; 52 hommes et 26 femmes). Ces enquêtes sont en cours d'analyses et devraient permettre de mieux comprendre les services écosystémiques rendus par les forêts à Marantacées mais aussi d'appréhender la perception de différents groupes éthniques sur la dynamique contemporaine des forêts à Marantacées. Le stage devrait se terminer en Décembre 2022.

4.3.2.2 WP2 : Dynamiques spatio-temporelles des forêts à Marantacées

L'étude de la dynamique spatio-temporelle des forêts à Marantacées est essentielle pour comprendre si ces systèmes sont stables dans le temps et/ou s'ils sont en expansion avec les changements globaux en cours. Une meilleure compréhension de la dynamique de ces forêts peut, en outre, valider ou invalider certaines hypothèses sur l'origine des forêts à Marantacées (par exemple, si ce sont des stades de succession intermédiaires entre les savanes et les forêts à couvert fermé (White, 2001) ou si ces forêts sont en expansion sous l'effet de perturbations humaines ou naturelles (Gillet, 2013)). Dans cette tâche WP2, nous combinons des approches de télédétection et des approches d'écologie historique pour appréhender la dynamique spatio-temporelle des forêts à Marantacées à différentes échelles spatiales. Cette tâche est divisée en trois sous tâches complémentaires.

Distribution et déterminants des forêts à Marantacées

La répartition des forêts à Marantacacées et les déterminants écologiques de celles-ci sont très peu connus. Dans cette sous tâche, nous utilisons une combinaison de données de télédétection (Sentinel, Planet et Pleiades) afin de cartographier la répartition des forêts à Marantacées dans la zone d'IFO/Odzala, et d'en inférer les potentiels déterminants écologiques, notamment topographiques (Fig. 34). En combinant ces cartes avec des données d'inventaires botaniques conduits par la société IFO et des données d'inventaires de la mégafaune conduits par African Parks dans le parc d'Odzala, nous visons à caractériser les spécificités faunistiques, floristiques et fonctionnelles de ces forêts et de mesurer leur contribution au stockage du carbone en comparaison avec les forêts denses. Ce travail a été initié dans le cadre du stage de master 2 de Maïalicah Nungi-Pambu sous ma co-direction et celles de Gaëlle Viennois (AMAP) et Robin Pouteau (AMAP). Les résultats préliminaires montrent une forte association entre les forêts à Marantacées et les zones situées en hauteur par rapport au niveau de drainage le plus proche (Fig. 34). Ce travail est en cours de finalisation dans le cadre de la thèse de Juliette Picard.

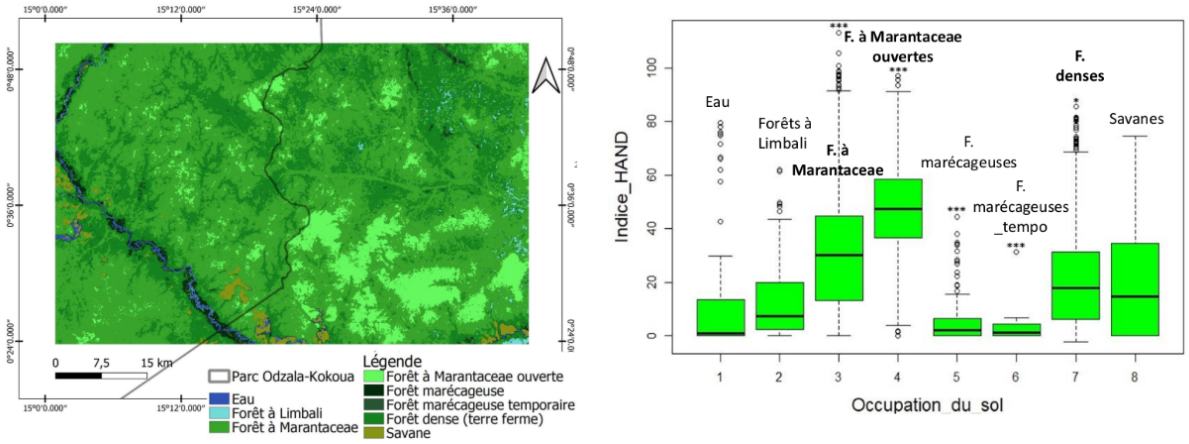

Figure 34: Carte préliminaire de la répartition des forêts à Marantacées dans la zone d'Odzala/IFO et lien des différents types de végétation avec la hauteur au dessus du niveau de drainage le plus proche (indice HAND). © Maïalicah Nungi-Pambu.

Dynamique spatio-temporelle des forêts à Marantacées des années 1950 à aujourd'hui

Des informations sur la distribution passée des forêts à Marantacées peuvent être extraites de photographies aériennes prises par l'institut géographique national (IGN) français dans les années 1950 et 1960 sur l'ensemble du territoire de la République du Congo. Ces photographies argentiques panchromatiques ou en infrarouge ont été acquises avec un chevauchement suffisant pour faire de la stéréophotogrammétrie (i.e. reconstruire les surfaces en 3D car elles sont vues de différents angles). Ces rares données historiques ont été peu exploitées jusqu'à présent pour des analyses à grande échelle (Hufkens et al., 2020), bien qu'elles représentent une source unique d'informations sur l'état des forêts tropicales à des échelles temporelles rarement accessibles en télédétection. A travers une collaboration avec l'IGN-Congo de Brazzaville (anciennement CERGEC), nous avons construit une base de données unique de la structure en 3D de la végétation en 1959 sur plus de 4000 km^2 à cheval sur le parc d'Odzala et la concession forestière de la compagnie IFO. En utilisant des données satellitaires Pléiades acquises en 2022 en mode stéréo, nous visons à comparer la dynamique de la structure forestière sur 63 ans (Fig. 35, 36). Ce travail à été mené par Felix Lim, en postdoctorat sous ma direction, et est actuellement en cours de valorisation pour décrire la méthode. Cette dernière peut désormais être transférées sur d'autres sites, comme en Guyane, à la Réunion, en Asie du Sud-Est (e.g. Laos et Vietnam) et sur d'autres zones d'Afrique centrale où des images similaires ont été acquises par le passé par l'IGN. L'intérêt majeur de passer par une analyse de ces modèles de surface 3D (DSM) plutôt que par une analyse directe des orthomosaiques est double: premièrement cela permet d'accéder à la dynamique de la structure forestière en 3D et donc potentiellement de mieux quantifier les conséquences des changements en termes de stockage de carbone et, secondement, ces DSMs permettent de dépasser les problèmes souvent rencontrés lors de l'analyse d'images à très haute résolution, comme les effets BRDF qui impactent significativement la texture de ces images obtenues depuis différents angles d'acquisitions (Barbier et al., 2011).

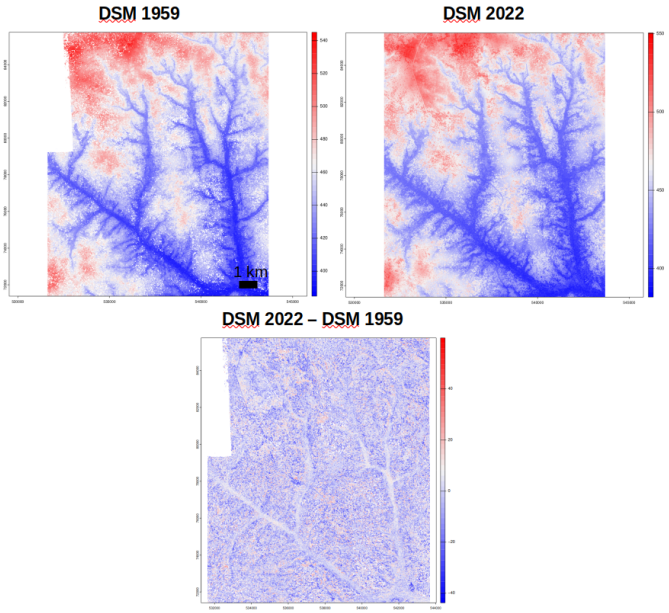

Figure 35: Evolution de la structure 3D forestière de 1959 à 2022 estimée à partir d'approches stéréophotogramétriques. Les modèles digitaux de surface (DSM; hauteur au dessus du niveau de la mer) estimés en 1959 et 2022 sont représentés en haut à gauche et droite, respectivement. La différence entre les deux DSMs est représentée en bas et indique, malgré un fort bruit lié aux problèmes de co-alignement des images et de fenêtre temporelle large, des zones ayant perdu de la hauteur de végétation (en bleu) et des zones ayant gagné en hauteur de végétation (en rouge). © Felix Lim.

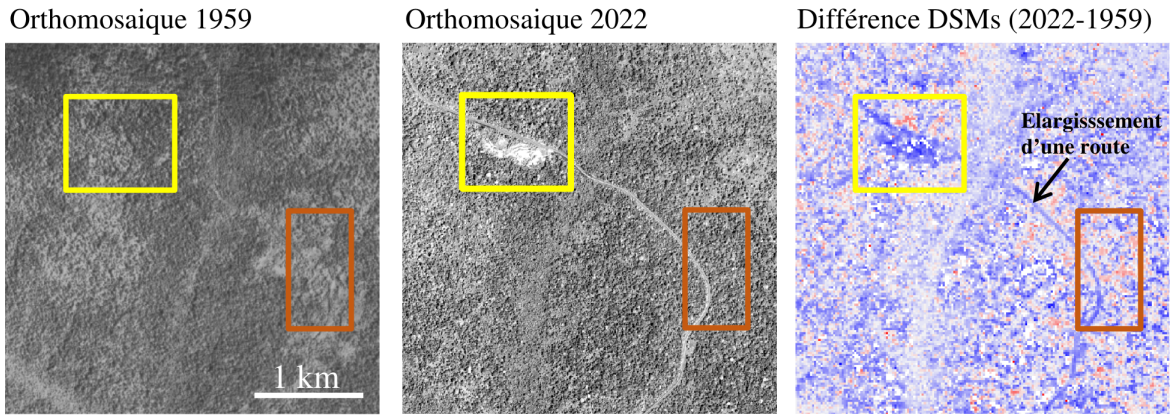

Figure 36: Exemples de changements de structures forestières observés depuis 1959 sur une zone du Nord Congo. Les orthomosaïques des photographies aériennes de 1959 (gauche) et des images satellitaires pléiades acquises en 2022 (milieu) illustrent que des changements de végétation ont eu lieu sur cette zone et qu'ils impriment bien une signature dans la différence des DSMs issus des deux dates (droite; voir Fig. 35). L'apparition et l'élargissement d'une route apparait en bleu sur la carte de droite, le carré jaune indique une carrière (sol nu) apparue entre les deux dates (perte de hauteur de végétation en bleu) et le carré rouge illustre une forêt très ouvertes en 1959 qui s'est refermé depuis (gain en hauteur de végétation en rouge). © Felix Lim

Dans un second temps, je viserai à extrapoler ces mesures 3D à de plus grandes zones et à comprendre les déterminants des changements de hauteur de la végétation. Les analyses préliminaires suggèrent notamment que l'effet du feu sur les forêts à Marantacées peut être double: il peut soit maintenir le système encore plus ouvert qu'il ne l'était avant le feu, soit ré-initier une succession à canopée fermée. Les conditions de bifurcation vers un état ou l'autre suite à un feux restent toutefois encore incertaines et pourront bénéficier des connaissances générées sur l'effet des feux de 2016 sur la régénération forestière (WP1).

Enfin, à travers une collaboration avec un postdoctorant d'AMAP, Paul Tresson, nous testons des approches de Deep Learning (sous-ensemble de l'intelligence artificielle) pour extraire des informations pertinentes des orthomosaïques à très hautes résolutions spatiales anciennes (IGN) et récentes (Pléiades). Nos résultats préliminaires montrent que des réseaux de neurones récemment développés (Transformers), utilisés en apprentissage non supervisés dans un premier temps pour réduire le volume de données de calibration nécessaire à ce type d'approche, permettent de révéler des patrons de structure forestière en minimisant les effets de conditions d'acquisition, notamment les effets de BRDF qui ont jusqu'ici limité considérablement le potentiel d'utilisation automatisée des images à très haute résolution en contexte forestier. Ce travail devrait faire l'objet d'une valorisation dans le courant du premier semestre 2023.

Dynamiques spatio-temporelles anciennes des forêts à Marantacées

Certaines forêts à Marantacées semblent être nées de perturbations humaines très anciennes (> 1000 ans; (Brncic, 2002; Gillet, 2013; Tovar et al., 2014)). Cette hypothèse s'appuie sur les fortes abondances de charbons et de poteries trouvées dans les forêts à Marantacées de la République Centrafricaine et de la République du Congo. Ces approches ne donnent cependant pas d'informations directes sur la présence/absence ou l'abondance d'herbacées géantes dans le temps et ne fournissent donc pas de preuves directes de la stabilité à long terme des forêts à Marantacées.

A travers une collaboration avec Laurent Brémond (UMR ISEM, Montpellier), responsable de cette partie du projet, nous visons à utiliser des approches d'écologie historique pour reconstruire le passé des forêts à Marantacées et environnantes. En pratique, Amandine Cartier, en CDD dans le cadre du projet DESSFOR, a prélevé des échantillons de sol sur l'ensemble des 23 parcelles que nous suivons dans la concession d'IFO (voir WP1 *Effets des feux sur la dynamique des forêts à Marantacées*) afin de réaliser d'une part des analyses sur les charbons présents (identifications et datations carbone), l'abondance en charbon de bois dans les sols tropicaux étant souvent considérée comme un bon indicateur des perturbations anciennes (Hubau et al., 2013; McMichael et al., 2012), et sur la composition en phytolithes du sol (concrétion de silice présentes dans les plantes qui se conserve bien dans le sol et dont la forme peut constituer une signature propre à un groupe taxonomique). En particulier, les phytolithes d'herbacées géantes peuvent souvent être identifiés au niveau du genre, et parfois au niveau de l'espèce (Piperno, 2006), comme le montrent nos analyses préliminaires. Nous prévoyons d'analyser plusieurs niveaux de sol par carotte et de quantifier les rapports entre les phytolithes produits par les herbacées géantes et les arbres afin de suivre dans le temps de potentiels changements dans l'abondance relative de ces deux groupes. Alors que l'abondance de charbon de bois peut valider l'occurrence plus élevée d'incendies historiques dans les

forêts à Marantacées par rapport aux forêts à couvert fermé, les analyses de phytolithes combinées aux datations carbone permettront de quantifier l'abondance relative d'herbacées géantes dans le temps. Nous visons donc ici à tester la stabilité à long terme de certaines forêts à Marantacées et à évaluer si les forêts à canopée fermée ont été couvertes d'herbacées géantes dans le passé (cela indiquerait, contrairement à notre hypothèse, une possible transition des forêts à Marantacées vers des forêts à canopées fermées).

4.3.2.3 WP3 : Modélisation des intéractions arbres-herbacées géantes

La dynamique des forêts à Marantacées s'opère vraisemblablement sur de longues périodes de temps. Les observations et expérimentations réalisées à l'échelle locale (WP1), combinée aux observations réalisées à larges échelles spatio-temporelles (WP2), sont nécessaires pour appréhender cette dynamique complexe, mais des modèles doivent être mobilisés pour établir un pont entre ces différents niveaux d'échelles (e.g., comment les processus locaux se propagent à des échelles spatio-temporelles plus larges). L'objectif de ce WP est donc de développer un modèle théorique, calibré avec des paramètres dérivés empiriquement, pour comprendre et simuler la dynamique spatio-temporelle des forêts à Marantacées en modélisant les interactions entre herbacées géantes et arbres (l'unité considérée étant leur biomasse respectives). En particulier, nous visons à adapter un modèle développé en partie au sein d'AMAP, initialement construit pour étudier les dynamiques forêts-savanes (Yatat et al., 2018). A travers des analyses de sensibilité et des simulations, ce modèle permettra de tester (i) les conditions sous lesquelles les forêts à Marantacées peuvent être considérées comme des états stables (ou transitoires), et (ii) quels sont les rôles individuels et conjoints de l'exploitation forestière et du feu dans la dynamique des forêts à Marantacées. Ce WP, encore peu avancé à ce stade du projet, est mené sous la co-direction de Charly Favier (ISEM) et de Pierre Couteron (AMAP).

5 Conclusions

Dans l'ensemble de mon parcours, j'ai étudié la dynamique spatio-temporelle de la structure et de la composition des forêts tropicales à différentes échelles spatio-temporelles. Pour celà, j'ai mobilisé des outils et des thématiques diverses, parfois à travers la mise en place de collaborations avec des spécialistes d'autres domaines (e.g. écologie historique, statistiques, télédétection, éthnologie). En particulier, j'ai orienté mon profil de chercheur à l'interface entre deux domaines qui communiquaient relativement peu jusqu'ici : l'écologie forestière et la télédétection. Aujourd'hui et à l'avenir, je vise à rester à cet interface en construisant des projets multidisciplinaires basés sur un triptyque expérimentation, observation et modélisation, comme illustré par le projet DESSFOR. Une part importante de mes travaux se réalise à travers l'encadrement actif d'étudiants qui me permettent de me démultiplier sur divers axes de recherches simultanément. En retour, ces étudiants évoluent souvent dans un cadre multidisciplinaire et collaboratif qui, je l'espère, leur donnera un large éventail de possibilités pour développer leur carrière dans le domaine de recherche de leur choix. A l'avenir, je poursuivrai mes travaux sur la résilience des forêts tropicales

suite à des perturbations pour produire des connaissances sur les mécanismes écologiques facilitant ou bloquant cette résilience. A termes, j'aimerai que ces connaissances fondamentales puissent alimenter des réflexions sur les modes de gestion des forêts tropicales en vue de leur envisager un avenir viable.

6 Bibliographie

Ashman, T.-L. (2006). The evolution of separate sexes: A focus on the ecological context. *Ecology and Evolution of Flowers*, 204–222. http://www.pitt.edu/ biology/Dept/pdf/1829.pdf

Baker, H. G. (1955). Self Compatibility and Establishment after Long Distance Dispersal. *Evolution*, *9*(3), 347–349. <Go to ISI>://WOS:A1955XE36500011

Baker, H. G. (1967). Support for Bakers law-as a rule. *Evolution*, *21*(4), 853–856. <Go to ISI>://WOS:A1967A449000020

Baker, T. R., Phillips, O. L., Malhi, Y., Almeida, S., Arroyo, L., Di Fiore, A., Erwin, T., Killeen, T. J., Laurance, S. G., Laurance, W. F., Lewis, S. L., Lloyd, J., Monteagudo, A., Neill, D. A., Patino, S., Pitman, N. C. A., Silva, J. N. M., & Martinez, R. V. (2004). Variation in wood density determines spatial patterns in Amazonian forest biomass. *Global Change Biology*, *10*(5), 545–562. <Go to ISI>://WOS:000221421600003

Baraloto, C., Timothy Paine, C. E., Poorter, L., Beauchene, J., Bonal, D., Domenach, A., Hérault, B., Patiño, S., Roggy, J., & Chave, J. (2010). Decoupled leaf and stem economics in rain forest trees. *Ecology Letters*, *13*(11), 1338–1347. https://doi.org/10.1111/j.1461-0248.2010.01517.x

Barbier, N., Proisy, C., Véga, C., Sabatier, D., & Couteron, P. (2011). Bidirectional texture function of high resolution optical images of tropical forest: An approach using LiDAR hillshade simulations. *Remote Sensing of Environment*, *115*(1), 167–179.

Bastin, J.-F., Barbier, N., Réjou-Méchain, M., Fayolle, A., Gourlet-Fleury, S., Maniatis, D., Haulleville, T. de, Baya, F., Beeckman, H., Beina, D., Couteron, P., Chuyong, G., Dauby, G., Doucet, J.-L., Droissart, V., Dufrêne, M., Ewango, C., Gillet, J. F., Gonmadje, C. H., … Bogaert, J. (2015). Seeing Central African forests through their largest trees. *Scientific Reports*, *5*, 13156. http://dx.doi.org/10.1038/srep13156

Bastin, J.-F., Finegold, Y., Garcia, C., Mollicone, D., Rezende, M., Routh, D., Zohner, C. M., & Crowther, T. W. (2019). The global tree restoration potential. *Science*, *365*(6448), 76–79.

Bastin, J.-F., Rutishauser, E., Kellner, J. R., Saatchi, S., Pélissier, R., Herault, B., Slik, F., Bogaert, J., De Cannière, C., & Marshall, A. R. (2018). Pan-tropical prediction of forest structure from the largest trees. *Global Ecology and Biogeography*, *27*(11), 1366–1383.

Bazzaz, F. A. (1979). Physiological ecology of plant succession. *Annual Review of Ecology and Systematics*, *10*, 351–371. <Go to ISI>://WOS:A1979HU59600014

Brncic, T. (2002). *Ecology and patch dynamics of Megaphrynium macrostachyum (Benth.) Milne-Redh.(Marantaceae) in the south-west Central African Republic* [PhD thesis, University of Oxford]. http://ethos.bl.uk/OrderDetails.do?uin=uk.bl.ethos.270242

Brockelman, W. Y., Nathalang, A., & Gale, G. A. (2011). The Mo Singto forest dynamics plot, Khao

Yai National Park, Thailand. *Natural History Bulletin of the Siam Society*, *57*, 35–55.

Brugière, D., Bougras, S., & Gautier-Hion, A. (2000). *Dynamique forestière et processus de colonisation-extinction: Relations faune-flore dans les forêts a Marantacées d'Odzala* (p. 43). Projet ECOFAC - Composante Congolaise.

Bry, X., Trottier, C., Verron, T., & Mortier, F. (2013). Supervised component generalized linear regression using a pls-extension of the fisher scoring algorithm. *Journal of Multivariate Analysis*, *119*, 47–60. http://www.sciencedirect.com/science/article/pii/S0047259X13000407

Caballé, G. (1978). Essai sur la géographie forestière du Gabon. *Adansonia*, *17*(4), 425–440.

Carreiras, J. M. B., Vasconcelos, M. J., & Lucas, R. M. (2012). Understanding the relationship between aboveground biomass and ALOS PALSAR data in the forests of Guinea-Bissau (West Africa). *Remote Sensing of Environment*, *121*, 426–442. https://doi.org/10.1016/j.rse.2012.02.012

Cavender-Bares, J., Kozak, K. H., Fine, P. V. A., & Kembel, S. W. (2009). The merging of community ecology and phylogenetic biology. *Ecology Letters*, *12*(7), 693–715. <Go to ISI>://WOS:000266699000013

Chanthorn, W., Ratanapongsai, Y., Brockelman, W. Y., Allen, M. A., Favier, C., & Dubois, M. A. (2016). Viewing tropical forest succession as a three-dimensional dynamical system. *Theoretical Ecology*, *9*(2), 163–172.

Chave, J., Condit, R., Aguilar, S., Hernandez, A., Lao, S., & Perez, R. (2004). Error propagation and scaling for tropical forest biomass estimates. *Philosophical Transactions of the Royal Society of London Series B-Biological Sciences*, *359*(1443), 409–420. <Go to ISI>://WOS:000220545100008

Chave, J., & Leigh, E. G. (2002). A spatially explicit neutral model of beta-diversity in tropical forests. *Theoretical Population Biology*, *62*(2), 153–168. <Go to ISI>://WOS:000177739700005

Chave, J., Réjou-Méchain, M., Búrquez, A., Chidumayo, E., Colgan, M. S., Delitti, W. B. C., Duque, A., Eid, T., Fearnside, P. M., Goodman, R. C., Henry, M., Martínez-Yrízar, A., Mugasha, W. A., Muller-Landau, H. C., Mencuccini, M., Nelson, B. W., Ngomanda, A., Nogueira, E. M., Ortiz-Malavassi, E., … Vieilledent, G. (2014). Improved allometric models to estimate the aboveground biomass of tropical trees. *Global Change Biology*, *20*(10), 3177–3190. https://doi.org/10.1111/gcb.12629

Chazdon, R. L. (2014). *Second Growth: The Promise of Tropical Forest Regeneration in an Age of Deforestation*. University of Chicago Press.

Chazdon, R. L., Falk, D. A., Banin, L. F., Wagner, M., J Wilson, S., Grabowski, R. C., & Suding, K. N. (2021). The intervention continuum in restoration ecology: Rethinking the active–passive dichotomy. *Restoration Ecology*, e13535.

Cheptou, P.-O. (2012). Clarifying Baker's law. *Annals of Botany*, *109*(3), 633–641. http://aob.oxfordjournals.org/content/109/3/633.short

Cifuentes Jara, M., Henry, M., Réjou Méchain, M., Lopez, O. R., Wayson, C., Michel Fuentes, J. M., Castellanos, E., Zapata-Cuartas, M., Piotto, D., & Alice Guier, F. (2015). Overcoming obstacles to sharing data on tree allometric equations. *Annals of Forest Science*, *72*(6), 789–794.

Cifuentes Jara, M., Henry, M., Réjou-Méchain, M., Wayson, C., Zapata-Cuartas, M., Piotto, D., Guier, F. A., Lombis, H. C., López, E. C., Lara, R. C., Rojas, K. C., Pasquel, J. D. Á., Montoya, Á. D., Vega, J. F., Galo, A. J., López, O. R., Marklund, L. G., Fuentes, J. M. M., Milla, F., … Westfall, J.

(2014). Guidelines for documenting and reporting tree allometric equations. *Annals of Forest Science*, 1–6. https://doi.org/10.1007/s13595-014-0415-z

Couteron, P., Pelissier, R., Mapaga, D., Molino, J. F., & Teillier, L. (2003). Drawing ecological insights from a management-oriented forest inventory in French Guiana. *Forest Ecology and Management*, *172*(1), 89–108. <Go to ISI>://000180439000007

Cuni-Sanchez, A., White, L. J., Calders, K., Jeffery, K. J., Abernethy, K., Burt, A., Disney, M., Gilpin, M., Gomez-Dans, J. L., & Lewis, S. L. (2016). African savanna-forest boundary dynamics: A 20-year study. *PLoS One*, *11*(6), e0156934. http://journals.plos.org/plosone/article?id=10.1371/journal.pone.0156934

Dalling, J. W., Schnitzer, S. A., Baldeck, C., Harms, K. E., John, R., Mangan, S. A., Lobo, E., Yavitt, J. B., & Hubbell, S. P. (2012). Resource-based habitat associations in a neotropical liana community. *Journal of Ecology*, *100*(5), 1174–1182.

Darwin, C. (1877). *The different forms of flowers on plants of the same species*. John Murray.

DeFries, R., Achard, F., Brown, S., Herold, M., Murdiyarso, D., Schlamadinger, B., et al. (2007). Earth observations for estimating greenhouse gas emissions from deforestation in developing countries. *Environmental Science & Policy*, *10*(4), 385–394. http://www.sciencedirect.com/science/article/pii/S146290110700024X

Dixon, R. K., Solomon, A. M., Brown, S., Houghton, R. A., Trexier, M. C., & Wisniewski, J. (1994). Carbon Pools and Flux of Global Forest Ecosystems. *Science*, *263*(5144), 185–190. https://doi.org/10.1126/science.263.5144.185

Dubois-Fernandez, P., Le Toan, T., Chave, J., Blanc, L., Daniel, S., Oriot, H., Arnaubec, A., Réjou-Méchain, M., Villard, L., Lasne, Y., et al. (2011). TropiSAR. Technical assistance for the development of airborne SAR and geophysical measurements during the TropiSAR 2009 experiment: Final report. *Eur. Space Agency, Paris, France*.

Elliot, S. D., Blakesley, D., & Hardwick, K. (2013). *Restoring tropical forests: A practical guide*. BioOne.

Englhart, S., Keuck, V., & Siegert, F. (2011). Aboveground biomass retrieval in tropical forests—The potential of combined X-and L-band SAR data use. *Remote Sensing of Environment*, *115*(5), 1260–1271. http://www.sciencedirect.com/science/article/pii/S0034425711000216

Esquivel-Muelbert, A., Baker, T. R., Dexter, K. G., Lewis, S. L., Brienen, R. J., Feldpausch, T. R., Lloyd, J., Monteagudo-Mendoza, A., Arroyo, L., & Álvarez-Dávila, E. (2019). Compositional response of Amazon forests to climate change. *Global Change Biology*, *25*(1), 39–56.

Fauset, S., Johnson, M. O., Gloor, M., Baker, T. R., Monteagudo M, A., Brienen, R. J., Feldpausch, T. R., Lopez-Gonzalez, G., Malhi, Y., & Ter Steege, H. (2015). Hyperdominance in Amazonian forest carbon cycling. *Nature Communications*, *6*(1), 1–9.

Fayolle, A., Engelbrecht, B., Freycon, V., Mortier, F., Swaine, M., Réjou-Méchain, M., Doucet, J.-L., Fauvet, N., Cornu, G., & Gourlet-Fleury, S. (2012). Geological substrates shape tree species and trait distributions in african moist forests. *PLoS ONE*, *7*(8), e42381. https://doi.org/10.1371/journal.pone.0042381

Feldpausch, T. R., Lloyd, J., Lewis, S. L., Brienen, R. J. W., Gloor, M., Monteagudo Mendoza, A., Lopez-Gonzalez, G., Banin, L., Abu Salim, K., Affum-Baffoe, K., Alexiades, M., Almeida, S., Amaral, I.,

Andrade, A., Aragão, L. E. O. C., Araujo Murakami, A., Arets, E. J. M. M., Arroyo, L., Aymard C., G. A., ... Phillips, O. L. (2012). Tree height integrated into pantropical forest biomass estimates. *Biogeosciences*, *9*(8), 3381–3403. https://doi.org/10.5194/bg-9-3381-2012

Feldpausch, T. R., McDonald, A. J., Passos, C. A. M., Lehmann, J., & Riha, S. J. (2006). Biomass, harvestable area, and forest structure estimated from commercial timber inventories and remotely sensed imagery in southern Amazonia. *Forest Ecology and Management*, *233*(1), 121–132. ://WOS:000240409800014

Feldpausch, T. R., Phillips, O. L., Brienen, R. J. W., Gloor, E., Lloyd, J., Lopez-Gonzalez, G., Monteagudo-Mendoza, A., Malhi, Y., Alarcón, A., & Dávila, E. Á. (2016). Amazon forest response to repeated droughts. *Global Biogeochemical Cycles*, *30*(7), 964–982.

Flores, O. (2005). *Déterminisme de la régénération chez quinze espèces d'arbres tropicaux en forêt guyanaise: Les effets de l'environnement et de la limitation par la dispersion.* [PhD thesis]. Université Montpellier II,.

ForestPlots.net, Blundo, C., Carilla, J., Grau, R., Malizia, A., Malizia, L., Osinaga-Acosta, O., Bird, M., Bradford, M., Catchpole, D., Ford, A., Graham, A., Hilbert, D., Kemp, J., Laurance, S., Laurance, W., Ishida, F. Y., Marshall, A., Waite, C., ... Tran, H. D. (2021). Taking the pulse of Earth's tropical forests using networks of highly distributed plots. *Biological Conservation*, *260*, 108849. https://doi.org/https://doi.org/10.1016/j.biocon.2020.108849

Fortunel, C., Fine, P. V. A., & Baraloto, C. (2012). Leaf, stem and root tissue strategies across 758 Neotropical tree species. *Functional Ecology*, *26*(5), 1153–1161. https://doi.org/10.1111/j.1365-2435.2012.02020.x

Frost, C., & Thompson, S. G. (2000). Correcting for regression dilution bias: Comparison of methods for a single predictor variable. *Journal of the Royal Statistical Society: Series A (Statistics in Society)*, *163*(2), 173–189.

Ghazoul, J., Burivalova, Z., Garcia-Ulloa, J., & King, L. A. (2015). Conceptualizing forest degradation. *Trends in Ecology & Evolution*, *30*(10), 622–632. http://www.sciencedirect.com/science/article/pii/S0169534715001913

Gibaud, J., Bry, X., Trottier, C., Mortier, F., & Réjou-Méchain, M. (2022). Response mixture models based on supervised components: Clustering floristic taxa. *Statistical Modelling*, 1471082X221115525. https://doi.org/10.1177/1471082X221115525

Gibert, G. (1984). La masse forestière congolaise: Son implantation, ses divers faciès. *Bois Et Forêts Des Tropiques*, *204*, 3–19. http://cat.inist.fr/?aModele=afficheN&cpsidt=8744567

Gillet, J.-F. (2013). *Les forêts à Marantaceae au sein de la mosaïque forestière du Nord de la République du Congo: Origines et modalités de gestion* [PhD thesis, Université de Liège-Gembloux Agro-bio Tech]. http://orbi.ulg.ac.be/handle/2268/155570

Goodman, R. C., Phillips, O. L., & Baker, T. R. (2014). The importance of crown dimensions to improve tropical tree biomass estimates. *Ecological Applications*, *24*(4), 680–698. https://doi.org/10.1890/13-0070.1

Gourlet-Fleury, S., Rossi, V., Rejou-Mechain, M., Freycon, V., Fayolle, A., Saint-André, L., Cornu, G., Gérard, J., Sarrailh, J., Flores, O., Baya, F., Billand, A., Fauvet, N., Gally, M., Henry, M.,

Hubert, D., Pasquier, A., & Picard, N. (2011). Environmental filtering of dense-wooded species controls above-ground biomass stored in African moist forests. *Journal of Ecology*, *99*(4), 981–990. https://doi.org/10.1111/j.1365-2745.2011.01829.x

Grainger, A., Iverson, L. R., Marland, G. H., & Prasad, A. (2019). Comment on "The global tree restoration potential." *Science*, *366*(6463), eaay8334. https://doi.org/10.1126/science.aay8334

Gravel, D., Canham, C. D., Beaudet, M., & Messier, C. (2006). Reconciling niche and neutrality: The continuum hypothesis. *Ecology Letters*, *9*(4), 399–409. ://WOS:000236384100004

Grime, J. P. (1977). Evidence for Existence of 3 Primary Strategies in Plants and Its Relevance to Ecological and Evolutionary Theory. *American Naturalist*, *111*(982), 1169–1194. ://WOS:A1977EF94400009

Guariguata, M. R., & Ostertag, R. (2001). Neotropical secondary forest succession: Changes in structural and functional characteristics. *Forest Ecology and Management*, *148*(1–3), 185–206. https://doi.org/10.1016/S0378-1127(00)00535-1

Heijden, G. M. F. van der, Powers, J. S., & Schnitzer, S. A. (2015). Lianas reduce carbon accumulation and storage in tropical forests. *Proceedings of the National Academy of Sciences*, *112*(43), 13267–13271. https://doi.org/10.1073/pnas.1504869112

Heilbuth, J. C., Ilves, K. L., & Otto, S. P. (2001). The consequences of dioecy for seed dispersal: Modeling the seed-shadow handicap. *Evolution*, *55*(5), 880–888. http://onlinelibrary.wiley.com/doi/10.1111/j.0014-3820.2001.tb00605.x/abstract

Henry, M., Bombelli, A., Trotta, C., Alessandrini, A., Birigazzi, L., Sola, G., Vieilledent, G., Santenoise, P., Longuetaud, F., & Valentini, R. (2013). GlobAllomeTree: International platform for tree allometric equations to support volume, biomass and carbon assessment. *Iforest-Biogeosciences and Forestry*, *6*(6), 326.

Henry, M., Cifuentes Jara, M., Réjou-Méchain, M., Piotto, D., Michel Fuentes, J. M., Wayson, C., Alice Guier, F., Castañeda Lombis, H., Castellanos López, E., & Cuenca Lara, R. (2015). Recommendations for the use of tree models to estimate national forest biomass and assess their uncertainty. *Annals of Forest Science*, *72*(6), 769–777.

Henry, M., Réjou-Méchain, M., Jara, M. C., Wayson, C., Piotto, D., Westfall, J., Fuentes, J. M. M., Guier, F. A., Lombis, H. C., López, E. C., et al. (2015). An overview of existing and promising technologies for national forest monitoring. *Annals of Forest Science*, *72*(6), 779–788. http://link.springer.com/article/10.1007/s13595-015-0463-z

Hoang, N. T., & Kanemoto, K. (2021). Mapping the deforestation footprint of nations reveals growing threat to tropical forests. *Nature Ecology & Evolution*, *5*(6), 845–853.

Holl, K. D., & Aide, T. M. (2011). When and where to actively restore ecosystems? *Forest Ecology and Management*, *261*(10), 1558–1563. https://doi.org/10.1016/j.foreco.2010.07.004

Hubau, W., Van den Bulcke, J., Kitin, P., Mees, F., Baert, G., Verschuren, D., Nsenga, L., Van Acker, J., & Beeckman, H. (2013). Ancient charcoal as a natural archive for paleofire regime and vegetation change in the Mayumbe, Democratic Republic of the Congo. *Quaternary Research*, *80*(2), 326–340.

Hubbell, S. P. (1979). Tree Dispersion, Abundance, and Diversity in a Tropical Dry Forest. *Science*, *203*(4387), 1299–1309. ://WOS:A1979GN50300010

Hufkens, K., Haulleville, T. de, Kearsley, E., Jacobsen, K., Beeckman, H., Stoffelen, P., Vandelook, F.,

Meeus, S., Amara, M., Van Hirtum, L., Van den Bulcke, J., Verbeeck, H., & Wingate, L. (2020). Historical Aerial Surveys Map Long-Term Changes of Forest Cover and Structure in the Central Congo Basin. *Remote Sensing*, *12*(4), 638. https://doi.org/10.3390/rs12040638

Hultine, K. R., Grady, K. C., Wood, T. E., Shuster, S. M., Stella, J. C., & Whitham, T. G. (2016). Climate change perils for dioecious plant species. *Nature Plants*, *2*(8), 1–8. https://doi.org/10.1038/nplants.2016.109

Imhoff, M. L. (1995). A theoretical analysis of the effect of forest structure on synthetic aperture radar backscatter and the remote sensing of biomass. *IEEE Transactions on Geoscience and Remote Sensing*, *33*(2), 341–352. https://doi.org/10.1109/36.377934

Ingwell, L. L., Joseph Wright, S., Becklund, K. K., Hubbell, S. P., & Schnitzer, S. A. (2010). The impact of lianas on 10 years of tree growth and mortality on Barro Colorado Island, Panama. *Journal of Ecology*, *98*(4), 879–887. http://onlinelibrary.wiley.com/doi/10.1111/j.1365-2745.2010.01676.x/full

IPCC. (2007). *Climate Change 2007: The physical basis. Working group I contribution to the fourth assessment report of the intergovernmental panel on climate change* (p. 996). S. Solomon, D. Qin, M. Marquis, K. B. Averyt, & M. Tignor.

Janssens, S. B., Couvreur, T. L., Mertens, A., Dauby, G., Dagallier, L.-P. M., Vanden Abeele, S., Vandelook, F., Mascarello, M., Beeckman, H., Sosef, M., Droissart, V., Bank, M. van der, Maurin, O., Hawthorne, W., Marshall, C., Réjou-Méchain, M., Beina, D., Baya, F., Merckx, V., & Hardy, O. J. (2020). A large-scale species level dated angiosperm phylogeny for evolutionary and ecological analyses. *Biodiversity Data Journal*, *8*.

Jha, N., Tripathi, N. K., Chanthorn, W., Brockelman, W., Nathalang, A., Pélissier, R., Pimmasarn, S., Ploton, P., Sasaki, N., Virdis, S. G. P., & Réjou-Méchain, M. (2020). Forest aboveground biomass stock and resilience in a tropical landscape of Thailand. *Biogeosciences*, *17*(1), 121–134. https://doi.org/https://doi.org/10.5194/bg-17-121-2020

Kaçamak, B., Barbier, N., Aubry-Kientz, M., Forni, E., Gourlet-Fleury, S., Guibal, D., Loumeto, J.-J., Pollet, S., Rossi, V., & Rowe, N. P. (2022). Linking drone and ground-based liana measurements in a Congolese forest. *Frontiers in Forests and Global Change*, *5*.

Kitamura, S., Yumoto, T., Poonswad, P., Chuailua, P., & Plongmai, K. (2004). Characteristics of hornbill-dispersed fruits in a tropical seasonal forest in Thailand. *Bird Conservation International*, *14*(S1), S81–S88. https://doi.org/10.1017/S0959270905000250

Larjavaara, M., & Muller-Landau, H. C. (2013). Measuring Tree Height: A Quantitative Comparison of Two Common Field Methods in a Moist Tropical Forest. *Methods in Ecology and Evolution*, *4*(9), 793–801. https://doi.org/10.1111/2041-210X.12071

Le Toan, T., Beaudoin, A., Riom, J., & Guyon, D. (1992). Relating forest biomass to SAR data. *IEEE Transactions on Geoscience and Remote Sensing*, *30*(2), 403–411. https://doi.org/10.1109/36.134089

Le Toan, T., Quegan, S., Davidson, M. W. J., Balzter, H., Paillou, P., Papathanassiou, K., Plummer, S., Rocca, F., Saatchi, S., Shugart, H., & Ulander, L. (2011). The BIOMASS mission: Mapping global forest biomass to better understand the terrestrial carbon cycle. *Remote Sensing of Environment*, *115*(11), 2850–2860. https://doi.org/10.1016/j.rse.2011.03.020

Levis, C., Costa, F. R. C., Bongers, F., Peña-Claros, M., Clement, C. R., Junqueira, A. B., Neves, E. G.,

Tamanaha, E. K., Figueiredo, F. O. G., Salomão, R. P., Castilho, C. V., Magnusson, W. E., Phillips, O. L., Guevara, J. E., Sabatier, D., Molino, J.-F., López, D. C., Mendoza, A. M., Pitman, N. C. A., ... Steege, H. ter. (2017). Persistent effects of pre-Columbian plant domestication on Amazonian forest composition. *Science*, *355*(6328), 925–931. https://doi.org/10.1126/science.aal0157

Levis, C., Flores, B. M., Moreira, P. A., Luize, B. G., Alves, R. P., Franco-Moraes, J., Lins, J., Konings, E., Peña-Claros, M., & Bongers, F. (2018). How people domesticated Amazonian forests. *Frontiers in Ecology and Evolution*, *5*, 171.

Lewis, S. L., Lloyd, J., Sitch, S., Mitchard, E. T. A., & Laurance, W. F. (2009). Changing ecology of tropical forests: Evidence and drivers. *Annual Review of Ecology, Evolution, and Systematics*, *40*(1), 529–549. https://doi.org/10.1146/annurev.ecolsys.39.110707.173345

Lewis, S. L., Mitchard, E. T. A., Prentice, C., Maslin, M., & Poulter, B. (2019). Comment on "The global tree restoration potential." *Science*, *366*(6463), eaaz0388. https://doi.org/10.1126/science.aaz0388

Ley, A. C., & Hardy, O. J. (2016). Spatially limited clonality and pollen and seed dispersal in a characteristic climber of Central African rain forests: Haumania danckelmaniana (Marantaceae). *Biotropica*, *48*(5), 618–627. http://onlinelibrary.wiley.com/doi/10.1111/btp.12341/full

Loubota Panzou, G. J., Fayolle, A., Jucker, T., Phillips, O. L., Bohlman, S., Banin, L. F., Lewis, S. L., Affum-Baffoe, K., Alves, L. F., & Antin, C. (2021). Pantropical variability in tree crown allometry. *Global Ecology and Biogeography*, *30*(2), 459–475.

Maisels, F. (1996). Synthesis of information concerning the Park National d'Odzala, Congo. *Brazzaville, ECOFAC*, *97*.

Malhi, Y., Wood, D., Baker, T. R., Wright, J., Phillips, O. L., Cochrane, T., Meir, P., Chave, J., Almeida, S., Arroyo, L., Higuchi, N., Killeen, T. J., Laurance, S. G., Laurance, W. F., Lewis, S. L., Monteagudo, A., Neill, D. A., Vargas, P. N., Pitman, N. C. A., ... Vinceti, B. (2006). The regional variation of aboveground live biomass in old-growth Amazonian forests. *Global Change Biology*, *12*(7), 1107–1138. https://doi.org/10.1111/j.1365-2486.2006.01120.x

Mascaro, J., Asner, G. P., Davies, S., Dehgan, A., & Saatchi, S. (2014). These are the days of lasers in the jungle. *Carbon Balance and Management*, *9*(1), 7. https://doi.org/10.1186/s13021-014-0007-0

Mazel, F., Wüest, R. O., Lessard, J.-P., Renaud, J., Ficetola, G. F., Lavergne, S., & Thuiller, W. (2017). Global patterns of Beta-diversity along the phylogenetic time-scale: The role of climate and plate tectonics. *Global Ecology and Biogeography*, *26*(10), 1211–1221.

McMichael, C. H., Piperno, D. R., Bush, M. B., Silman, M. R., Zimmerman, A. R., Raczka, M. F., & Lobato, L. C. (2012). Sparse pre-Columbian human habitation in western Amazonia. *Science*, *336*(6087), 1429–1431.

Mermoz, S., Le Toan, T., Villard, L., Réjou-Méchain, M., & Seifert-Granzin, J. (2014). Biomass assessment in the Cameroon savanna using ALOS PALSAR data. *Remote Sensing of Environment*, *155*, 109–119. https://doi.org/10.1016/j.rse.2014.01.029

Mermoz, S., Réjou-Méchain, M., Villard, L., Le Toan, T., Rossi, V., & Gourlet-Fleury, S. (2015). Decrease of L-band SAR backscatter with biomass of dense forests. *Remote Sensing of Environment*, *15*, 307–317. https://doi.org/10.1016/j.rse.2014.12.019

Meunier, F., Krishna Moorthy, S. M., De Deurwaerder, H. P., Kreus, R., Van den Bulcke, J., Lehnebach,

R., & Verbeeck, H. (2020). Within-site variability of liana wood anatomical traits: A case study in Laussat, French Guiana. *Forests*, *11*(5), 523.

Minh, D. H. T., Le Toan, T., Rocca, F., Tebaldini, S., Villard, L., Réjou-Méchain, M., Phillips, O. L., Feldpausch, T. R., Dubois-Fernandez, P., & Scipal, K. (2016). SAR tomography for the retrieval of forest biomass and height: Cross-validation at two tropical forest sites in French Guiana. *Remote Sensing of Environment*, *175*, 138–147.

Mitchard, E. T. A., Saatchi, S. S., Lewis, S. L., Feldpausch, T. R., Woodhouse, I. H., Sonké, B., Rowland, C., & Meir, P. (2011). Measuring biomass changes due to woody encroachment and deforestation/degradation in a forest–savanna boundary region of central Africa using multi-temporal L-band radar backscatter. *Remote Sensing of Environment*, *115*(11), 2861–2873. https://doi.org/10.1016/j.rse.2010.02.022

Molto, Q., Rossi, V., & Blanc, L. (2013). Error propagation in biomass estimation in tropical forests. *Methods in Ecology and Evolution*, *4*(2), 175–183. https://doi.org/10.1111/j.2041-210x.2012.00266.x

Odonne, G., Van den Bel, M., Burst, M., Brunaux, O., Bruno, M., Dambrine, E., Davy, D., Desprez, M., Engel, J., & Ferry, B. (2019). Long-term influence of early human occupations on current forests of the Guiana Shield. *Ecology*, *100*(10), e02806.

Parmentier, I., Réjou-Méchain, M., Chave, J., Vleminckx, J., Thomas, D. W., Kenfack, D., Chuyong, G. B., & Hardy, O. J. (2014). Prevalence of phylogenetic clustering at multiple scales in an African rain forest tree community. *Journal of Ecology*, *102*(4), 1008–1016. https://doi.org/10.1111/1365-2745.12254

Pearson, T. R., Brown, S., Murray, L., & Sidman, G. (2017). Greenhouse gas emissions from tropical forest degradation: An underestimated source. *Carbon Balance and Management*, *12*(1), 3. http://cbmjournal.springeropen.com/articles/10.1186/s13021-017-0072-2

Pendrill, F., Persson, U. M., Godar, J., & Kastner, T. (2019). Deforestation displaced: Trade in forest-risk commodities and the prospects for a global forest transition. *Environmental Research Letters*, *14*(5), 055003. https://doi.org/10.1088/1748-9326/ab0d41

Phillips, O. L., Sullivan, M. J., Baker, T. R., Mendoza, A. M., Vargas, P. N., & Vásquez, R. (2019). Species matter: Wood density influences tropical forest biomass at multiple scales. *Surveys in Geophysics*, *40*(4), 913–935.

Piperno, D. R. (2006). *Phytoliths: A comprehensive guide for archaeologists and paleoecologists*. Rowman Altamira.

Ploton, P., Barbier, N., Takoudjou Momo, S., Réjou-Méchain, M., Boyemba Bosela, F., Chuyong, G., Dauby, G., Droissart, V., Fayolle, A., Goodman, R. C., Henry, M., Kamdem, N. G., Mukirania, J. K., Kenfack, D., Libalah, M., Ngomanda, A., Rossi, V., Sonké, B., Texier, N., ... Pélissier, R. (2016). Closing a gap in tropical forest biomass estimation: Taking crown mass variation into account in pantropical allometries. *Biogeosciences*, *13*(5), 1571–1585. https://doi.org/10.5194/bg-13-1571-2016

Réjou-Méchain, M., Barbier, N., Couteron, P., Ploton, P., Vincent, G., Herold, M., Mermoz, S., Saatchi, S. S., Chave, J., Boissieu, F. de, Féret, J.-B., Takoudjou, M. S., & Pélissier, R. (2019). Upscaling forest biomass from field to satellite measurements: Sources of errors and ways to reduce them. *Surveys in Geophysics*.

Réjou-Méchain, M., & Cheptou, P.-O. (2015). High incidence of dioecy in young successional tropical forests. *Journal of Ecology*, n/a–n/a. https://doi.org/10.1111/1365-2745.12393

Réjou-Méchain, M., Fayolle, A., Nasi, R., Gourlet-Fleury, S., Doucet, J.-L., Gally, M., Hubert, D., Pasquier, A., & Billand, A. (2011). Detecting large-scale diversity patterns in tropical trees: Can we trust commercial forest inventories? *Forest Ecology and Management*, *261*(2), 187–194. https://doi.org/10.1016/j.foreco.2010.10.003

Réjou-Méchain, M., Flores, O., Bourland, N., Doucet, J., Fétéké, R. F., Pasquier, A., & Hardy, O. J. (2011). Spatial aggregation of tropical trees at multiple spatial scales. *Journal of Ecology*, *99*(6), 1373–1381. https://doi.org/10.1111/j.1365-2745.2011.01873.x

Réjou-Méchain, M., Flores, O., Pélissier, R., Fayolle, A., Fauvet, N., & Gourlet-Fleury, S. (2014). Tropical tree assembly depends on the interactions between successional and soil filtering processes. *Global Ecology and Biogeography*, *23*(12), 1440–1449. https://doi.org/10.1111/geb.12222

Réjou-Méchain, M., & Hardy, O. J. (2011). Properties of similarity indices under niche-based and dispersal-based processes in communities. *The American Naturalist*, *177*(5), 589–604. http://cat.inist.fr/?aModele=afficheN&cpsidt=24132738

Réjou-Méchain, M., Mortier, F., Bastin, J.-F., Cornu, G., Barbier, N., Bayol, N., Bénédet, F., Bry, X., Dauby, G., & Deblauwe, V. (2021). Unveiling African rainforest composition and vulnerability to global change. *Nature*, *593*(7857), 90–94.

Réjou-Méchain, M., Muller-Landau, H. C., Detto, M., Thomas, S. C., Le Toan, T., Saatchi, S. S., Barreto-Silva, J. S., Bourg, N. A., Bunyavejchewin, S., Butt, N., Brockelman, W. Y., Cao, M., Cárdenas, D., Chiang, J.-M., Chuyong, G. B., Clay, K., Condit, R., Dattaraja, H. S., Davies, S. J., … Chave, J. (2014). Local spatial structure of forest biomass and its consequences for remote sensing of carbon stocks. *Biogeosciences*, *11*, 6827–6840. http://www.biogeosciences-discuss.net/11/5711/2014/bgd-11-5711-2014-relations.html

Réjou-Méchain, M., Pélissier, R., Gourlet-Fleury, S., Couteron, P., Nasi, R., & Thompson, J. D. (2008). Regional variation in tropical forest tree species composition in the Central African Republic: An assessment based on inventories by forest companies. *Journal of Tropical Ecology*, *24*, 663–674.

Réjou-Méchain, M., Tanguy, A., Piponiot, C., Chave, J., & Hérault, B. (2017). BIOMASS: An r package for estimating above-ground biomass and its uncertainty in tropical forests. *Methods in Ecology and Evolution*, *8*(9), 1163–1167.

Réjou-Méchain, M., Tymen, B., Blanc, L., Fauset, S., Feldpausch, T. R., Monteagudo, A., Phillips, O. L., Richard, H., & Chave, J. (2015). Using repeated small-footprint LiDAR acquisitions to infer spatial and temporal variations of a high-biomass Neotropical forest. *Remote Sensing of Environment*, *169*, 93–101.

Requena Suarez, D., Rozendaal, D. M., De Sy, V., Phillips, O. L., Alvarez-Dávila, E., Anderson-Teixeira, K., Araujo-Murakami, A., Arroyo, L., Baker, T. R., & Bongers, F. (2019). Estimating aboveground net biomass change for tropical and subtropical forests: Refinement of IPCC default rates using forest plot data. *Global Change Biology*, *25*(11), 3609–3624.

Rostain, S. (2021). *Amazonie: Un jardin naturel ou une forêt domestiquée*. Éditions Errance.

Schepaschenko, D., Chave, J., Phillips, O. L., Lewis, S. L., Davies, S. J., Réjou-Méchain, M., Sist, P.,

Scipal, K., Perger, C., & Herault, B. (2019). The Forest Observation System, building a global reference dataset for remote sensing of forest biomass. *Scientific Data*, *6*(1), 1–11.

Schnitzer, S. A., & Bongers, F. (2011). Increasing liana abundance and biomass in tropical forests: Emerging patterns and putative mechanisms. *Ecology Letters*, *14*(4), 397–406. http://onlinelibrary.wiley.com/doi/10.1111/j.1461-0248.2011.01590.x/full

Schnitzer, S. A., & Carson, W. P. (2010). Lianas suppress tree regeneration and diversity in treefall gaps. *Ecology Letters*, *13*(7), 849–857. https://doi.org/10.1111/j.1461-0248.2010.01480.x

Schulze, M., Grogan, J., Landis, R. M., & Vidal, E. (2008). How rare is too rare to harvest? Management challenges posed by timber species occurring at low densities in the Brazilian Amazon. *Forest Ecology and Management*, *256*(7), 1443–1457. ://WOS:000259837300004

Seidler, T. G., & Plotkin, J. B. (2006). Seed Dispersal and Spatial Pattern in Tropical Trees. *PLoS BIOLOGY*, *4*(11), 2132–2137.

Shugart, H. H., Saatchi, S., & Hall, F. G. (2010). Importance of structure and its measurement in quantifying function of forest ecosystems. *Journal of Geophysical Research: Biogeosciences (2005–2012)*, *115*(G2). http://onlinelibrary.wiley.com/doi/10.1029/2009JG000993/full

Skidmore, A. K., Wang, T., Bie, K. de, & Pilesjö, P. (2019). Comment on "The global tree restoration potential." *Science*, *366*(6469), eaaz0111. https://doi.org/10.1126/science.aaz0111

Slik, J. W. F., Paoli, G., McGuire, K., Amaral, I., Barroso, J., Bastian, M., Blanc, L., Bongers, F., Boundja, P., Clark, C., Collins, M., Dauby, G., Ding, Y., Doucet, J.-L., Eler, E., Ferreira, L., Forshed, O., Fredriksson, G., Gillet, J.-F., … Zweifel, N. (2013). Large trees drive forest aboveground biomass variation in moist lowland forests across the tropics. *Global Ecology and Biogeography*, n/a–n/a. https://doi.org/10.1111/geb.12092

Smith-Martin, C. M., Bastos, C. L., Lopez, O. R., Powers, J. S., & Schnitzer, S. A. (2019). Effects of dry-season irrigation on leaf physiology and biomass allocation in tropical lianas and trees. *Ecology*, *100*(11), e02827.

Soto, D. P., & Puettmann, K. J. (2020). Merging Multiple Equilibrium Models and Adaptive Cycle Theory in Forest Ecosystems: Implications for Managing Succession. *Current Forestry Reports*, *6*(4), 282–293.

Sullivan, M. J. P., Lewis, S. L., Affum-Baffoe, K., Castilho, C., Costa, F., Sanchez, A. C., Ewango, C. E. N., Hubau, W., Marimon, B., Monteagudo-Mendoza, A., Qie, L., Sonké, B., Martinez, R. V., Baker, T. R., Brienen, R. J. W., Feldpausch, T. R., Galbraith, D., Gloor, M., Malhi, Y., … Phillips, O. L. (2020). Long-term thermal sensitivity of Earth's tropical forests. *Science*, *368*(6493), 869–874. https://doi.org/10.1126/science.aaw7578

Sullivan, M. J. P., Talbot, J., Lewis, S. L., Phillips, O. L., Qie, L., Begne, S. K., Chave, J., Cuni-Sanchez, A., Hubau, W., Lopez-Gonzalez, G., Miles, L., Monteagudo-Mendoza, A., Sonké, B., Sunderland, T., Steege, H. ter, White, L. J. T., Affum-Baffoe, K., Aiba, S., Almeida, E. C. de, … Zemagho, L. (2017). Diversity and carbon storage across the tropical forest biome. *Scientific Reports*, *7*, 39102. https://doi.org/10.1038/srep39102

Sun, Z., Prachanun, N., Sonsuthi, A., Chanthorn, W., Brockelman, W. Y., Nathalang, A., Lin, L., & Bongers, F. (2022). Whole-Plant Seedling Functional Traits Suggest Lianas Also Support "Fast-Slow"

Plant Economics Spectrum. *Forests*, *13*(7), 990. https://doi.org/10.3390/f13070990

Thripob, P., Fortunel, C., Réjou-Méchain, M., Nathalang, A., & Chanthorn, W. (2022). Size-dependent intraspecific variation in wood traits has little impact on aboveground carbon estimates in a tropical forest landscape. *Functional Ecology*, *36*(9), 2303–2316.

Tilman, D. (2004). Niche tradeoffs, neutrality, and community structure: A stochastic theory of ressource competition, and community assembly. *Proceedings of the National Academy of Sciences of the United States of America*, *101*, 10854–10861.

Tovar, C., Breman, E., Brncic, T., Harris, D. J., Bailey, R., & Willis, K. J. (2014). Influence of 1100 years of burning on the central African rainforest. *Ecography*, *37*(11), 1139–1148. https://doi.org/10.1111/ecog.00697

Tuomisto, H., Ruokolainen, K., & Yli-Halla, M. (2003). Dispersal, environment, and floristic variation of western Amazonian forests. *Science*, *299*(5604), 241–244. ://000180284000036

Tymen, B., Réjou-Méchain, M., Dalling, J. W., Fauset, S., Feldpausch, T. R., Norden, N., Phillips, O. L., Turner, B. L., Viers, J., & Chave, J. (2016). Liana-infested forest as an alternative stable state. *Journal of Ecology*, *104*(1), 149–159.

Vamosi, S. M., Heard, S. B., Vamosi, J. C., & Webb, C. O. (2009). Emerging patterns in the comparative analysis of phylogenetic community structure. *Molecular Ecology*, *18*(4), 572–592. ://000262782400002

Van Vliet, N., & Nasi, R. (2008). Mammal distribution in a Central African logging concession area. *Biodiversity and Conservation*, *17*(5), 1241–1249.

Vancutsem, C., Achard, F., Pekel, J.-F., Vieilledent, G., Carboni, S., Simonetti, D., Gallego, J., Aragao, L. E., & Nasi, R. (2021). Long-term (1990–2019) monitoring of forest cover changes in the humid tropics. *Science Advances*, *7*(10), eabe1603.

Veldman, J. W., Aleman, J. C., Alvarado, S. T., Anderson, T. M., Archibald, S., Bond, W. J., Boutton, T. W., Buchmann, N., Buisson, E., Canadell, J. G., Dechoum, M. de S., Diaz-Toribio, M. H., Durigan, G., Ewel, J. J., Fernandes, G. W., Fidelis, A., Fleischman, F., Good, S. P., Griffith, D. M., ... Zaloumis, N. P. (2019). Comment on "The global tree restoration potential." *Science*, *366*(6463), eaay7976. https://doi.org/10.1126/science.aay7976

Verhegghen, A., Eva, H., Ceccherini, G., Achard, F., Gond, V., Gourlet-Fleury, S., & Cerutti, P. O. (2016). The Potential of Sentinel Satellites for Burnt Area Mapping and Monitoring in the Congo Basin Forests. *Remote Sensing*, *8*(12), 986. https://doi.org/10.3390/rs8120986

Visser, M. D., Schnitzer, S. A., Muller-Landau, H. C., Jongejans, E., Kroon, H. de, Comita, L. S., Hubbell, S. P., & Wright, S. J. (2018). Tree species vary widely in their tolerance for liana infestation: A case study of differential host response to generalist parasites. *Journal of Ecology*, *106*(2), 781–794.

Walters, G., Fraser, J. A., Picard, N., Hymas, O., & Fairhead, J. (2019). Deciphering African tropical forest dynamics in the Anthropocene: How social and historical sciences can elucidate forest cover change and inform forest management. *Anthropocene*, *27*, 100214.

White, L. J. (2001). Forest-savanna dynamics and the origins of Marantaceae forest in central Gabon. *African Rain Forest Ecology and Conservation: An Interdisciplinary Perspective*, 165–182. https://books.google.fr/books?hl=fr&lr=&id=iNwfN5ASigUC&oi=fnd&pg=PA165&dq=

%22marantaceae+forest%22&ots=O1Av6quiOT&sig=utBTP4StpfTUqjOgBWSY-5YCe40

White, L. J., Rogers, M. E., Tutin, C. E., Williamson, E. A., & Fernandez, M. (1995). Herbaceous vegetation in different forest types in the Lopé Reserve, Gabon: Implications for keystone food availability. *African Journal of Ecology*, *33*(2), 124–141. http://onlinelibrary.wiley.com/doi/10.1111/j.1365-2028.1995.tb00788.x/abstract

Woodhouse, I. H., Mitchard, E. T. A., Brolly, M., Maniatis, D., & Ryan, C. M. (2012). Radar backscatter is not a 'direct measure' of forest biomass. *Nature Climate Change*, *2*(8), 556–557. https://doi.org/10.1038/nclimate1601

Xu, L., Saatchi, S. S., Shapiro, A., Meyer, V., Ferraz, A., Yang, Y., Bastin, J.-F., Banks, N., Boeckx, P., & Verbeeck, H. (2017). Spatial Distribution of Carbon Stored in Forests of the Democratic Republic of Congo. *Scientific Reports*, *7*(1), 15030.

Yatat, V., Couteron, P., & Dumont, Y. (2018). Spatially explicit modelling of tree–grass interactions in fire-prone savannas: A partial differential equations framework. *Ecological Complexity*, *36*, 290–313. https://doi.org/10.1016/j.ecocom.2017.06.004

Zolkos, S. G., Goetz, S. J., & Dubayah, R. (2013). A meta-analysis of terrestrial aboveground biomass estimation using lidar remote sensing. *Remote Sensing of Environment*, *128*, 289–298. https://doi.org/10.1016/j.rse.2012.10.017

7 ANNEXES (Sélection de 3 articles)

100 YEARS Journal of Ecology

British Ecological Society

Journal of Ecology 2015, **103**, 725–732 doi: 10.1111/1365-2745.12393

High incidence of dioecy in young successional tropical forests

Maxime Réjou-Méchain[1,2,3,4]* and Pierre-Olivier Cheptou[1]

[1]UMR 5175 Centre d'Ecologie Fonctionnelle et Evolutive (CEFE), CNRS, 1919 Route de Mende, Montpellier 34293, France; [2]UPR BSEF, Centre de Coopération Internationale en Recherche Agronomique pour le Développement (CIRAD), Campus International de Baillarguet, Montpellier F-34398, France; [3]Laboratoire Evolution et Diversité Biologique (EDB) UMR 5174 CNRS, Université Paul Sabatier, Toulouse 31062, France; and [4]UMR botAnique et bioinforMatique de l'Architecture des Plantes (AMAP), Montpellier F-34000, France

Summary

1. The role of plant sexual systems in community assembly has been little studied. Classical assumptions predict an association between self-fertilization and colonizing ability, a pattern not systematically supported by observations.

2. Here, using a data set of 626 462 trees sampled throughout 8300 km^2 in central Africa and historical information collected 60 years ago on forest successional status, we compare sexual system assemblages between young successional and mature communities.

3. We use two multivariate approaches to assess the variation in community dioecism between successional status, while controlling for covariation between dioecy and six other traits usually considered as good proxies for important functions in forest successional dynamics.

4. We show that dioecious trees are significantly overrepresented in young successional areas, contrary to classical expectations. This robust pattern is unlikely to be driven by soil conditions, by the other associated traits or by species-specific abundance. Strikingly, dioecy was one of the traits most correlated with young successional areas.

5. These results show that sexual systems play an important role in community assembly. The higher occurrence of dioecy in young successional areas is likely due to a higher relative seed fitness of dioecious species in more stressful conditions or by an evolutionary-driven association between dioecy and colonization ability, as predicted by theoretical studies.

6. *Synthesis.* Our study emphasizes an overlooked association between sexual system and community assembly and emphasizes the need to revisit classical assumptions regarding that relationship.

Key-words: Baker's law, community assembly, community composition, determinants of plant community diversity and structure, forest succession, functional traits, sexual system, tropical forest

Introduction

A diverse array of sexual systems has been described in plants, with two extreme cases: gender monomorphism (e.g. hermaphroditism and monoecy), where individual plants may contribute as male and female to the next generation, and gender dimorphism (e.g. dioecy), where individuals may only contribute as male or female (Darwin 1877). The evolution of these sexual systems has been studied for a long time in biology, both empirically and theoretically (Bawa 1980; Thomson & Brunet 1990; Ashman 2006). It has been shown that hermaphroditism is by far the dominant system in flowering plants in all biomes, but a substantial variation of this relative dominance has been reported among ecosystems (Renner & Ricklefs 1995) or along environmental gradients (Matallana *et al.* 2005; Vamosi & Queenborough 2010).

Thus far, the selective advantage of one sexual system over another one has been mostly studied at the population or metapopulation level (Charnov, Bull & Smith 1976; Pannell 1997). Some studies have shown that sexual system strategies depend on the ecological context of the plant individuals (Freeman, Harper & Ostler 1980; Lloyd 1980; Barrett, Dorken & Case 2001; Litrico, Pailler & Thompson 2005). For example, harsh or stressful conditions are known to favour the evolution and maintenance of separate sexes from combined sexes (Barrett, Dorken & Case 2001; Ashman 2006). However, the importance of sexual systems in the context of

© 2015 The Authors. Journal of Ecology © 2015 British Ecological Society

13652745, 2015, 3, Downloaded from https://besjournals.onlinelibrary.wiley.com/doi/10.1111/1365-2745.12393 by Cochrane France, Wiley Online Library on [22/11/2022]. See the Terms and Conditions (https://onlinelibrary.wiley.com/terms-and-conditions) on Wiley Online Library for rules of use; OA articles are governed by the applicable Creative Commons License

community assembly has been rarely assessed. In the 1960s, the verbal model 'Baker's law' proposed an explicit link between colonization propensity and sexual systems in plant communities. Because a single self-compatible immigrant can initiate a sexually reproducing colony without the aid of an external agent for pollination, Baker (1955, 1967) stated that selfers should constitute better colonizers than full outcrossers (self-incompatible species or dioecious species). If Baker's arguments hold, we should expect outcrossers to be underrepresented in recently colonized areas compared to mature communities. Baker's model is at the heart of the classical arguments for the association between self-fertilization and colonizing ability. It has been proposed as an explanatory model of the drivers of invasion success, weediness, species range limits and island flora composition [see Cheptou (2012) for a review]. Although Baker's prediction is intuitive and clear cut, it has not been systematically validated by empirical data (Rambuda & Johnson 2004; Cheptou 2012; Shirk & Hamrick 2014).

Several island floras have been used as experimental systems for testing Baker's law. Baker's rule implies that selfing plant species will be favoured in establishment following long-distance dispersal to islands. If true, this should generate floras with relatively few outcrossers on remote islands, compared to the continental flora. Consistently, empirical data showed that the proportion of self-incompatible taxa was lower than that of the continental flora on some islands (Barrett, Emerson & Mallet 1996). Nevertheless, several remote islands, such as Hawaii (Bawa 1980), New Zealand (cited in Barrett, Emerson & Mallet 1996), La Réunion (cited in Humeau, Pailler & Thompson 1999), New Caledonia (Schlessman *et al.* 2014) and the Ogasawara (Bonin) Islands (Abe 2006), exhibit higher incidences of dioecy compared to continental flora. Even if the strength of pollinator or mate limitation is low during colonization (Pannell & Barrett 1998), dioecy incidence should, at minimum, be equivalent, but not higher, compared to that on the continent, as was observed. Whether the patterns observed result from higher colonization propensity of dioecious species from the continent [ecological interpretation of Bawa (1982)] or from post-colonization evolution towards dioecy on islands (Barrett, Emerson & Mallet 1996) remains unclear. A way to disentangle these two competitive hypotheses is to compare recently colonized communities vs. mature communities (i.e. different successional stages) but in the same regional context. In that case, if sexual systems are sorted by ecological filters, the local sexual system assemblages should constitute non-random subsets of the sexual systems found in the regional species pool (Diaz, Cabido & Casanoves 1998). Because suitable empirical data sets are infrequent, sexual system variation in community assembly across ecological or successional gradients has been rarely assessed (Chazdon 2003; Vamosi & Queenborough 2010; Sinclair, Korte & Freeman 2013).

In this study, we analysed the association between the forest successional status and the frequency of dioecy within tropical tree communities in a central African landscape. We used a large data set of 626 462 individual trees (223 taxa) sampled in 17 198 plots of 0.5 ha throughout 8300 km^2. Aerial photographs taken in the 1950s allowed us to locate current young successional forests and mature forests throughout the entire studied area. Consistent with Baker's law, we expect dioecy to be underrepresented in young successional areas.

Materials and methods

SITES

The sites were located in the south-western Central African Republic, in a humid tropical climate with annual rainfall ranging from 1300–1600 mm $year^{-1}$, according to the WorldClim model (Hijmans *et al.* 2005). A 3-month dry season (<100 mm) occurs from December-February. The vegetation corresponds to the mixed moist semi-evergreen forests of the Guineo-Congolian region characterized by a dominance of Ulmaceae [i.e. Cannabaceae in the Angiosperm Phylogeny Group (APG) III classification], Sterculiaceae (i.e. Malvaceae), Sapotaceae and Meliaceae families (Boulvert 1986). The region is also characterized by forest–savanna transitions typical of the regions north of the Congo basin and forest-enclosed savannas. The climate of the area has a low spatial variability and has only a slight effect on the community composition in the area (Réjou-Méchain *et al.* 2008; Fayolle *et al.* 2012).

FLORISTIC DATA

Data came from forest inventories conducted by four logging companies: the Industrie Forestière de Batalimo (IFB) during 1993–1996 and the Société CentrAfricaine Forestière (SCAF), Société Forestière de la Kadéi (SOFOKAD) and Thanry CentrAfrique (TCA) during 2005–2006. The systematic sampling design, fully described in Réjou-Méchain *et al.* (2011a), was composed of 0.5-ha plots established along 25-m wide transects (i.e. 200 × 25 m plots) in forested areas. All forest trees with a diameter at breast height (dbh) ≥30 cm were floristically identified, when possible, by trained local tree-spotters, and their diameters were recorded into 10-cm dbh-wide diameter classes. In the original data set, 319 taxa were identified throughout the entire area. We removed palms, taxa known to be at least partially cultivated and taxa for which we failed to find information on the sexual system. The resulting data set contained 223 taxa representing 99% of the total number of individuals measured in the original data set. Because floristic determination of tropical trees could be problematic, especially when inventories are conducted by forest companies, previous studies working on diversity patterns only focused on a subset of species deemed reliably identified (Réjou-Méchain *et al.* 2011b; Fayolle *et al.* 2012). Here, because most floristic identification errors are expected to have no impact on the inferred sexual system, which was highly taxonomically conserved in our data set (Table S1 in the Supporting Information), we decided to retain all possible inventoried taxa. However, the same conclusions were reached when analyses were based on a subset of 90 reliably identified species (results not shown; 70.9% of the individuals). A total of 19 197 plots were inventoried, but only the 17 198 plots that had at least 20 individual trees were included in the analyses (this resulted in 73 trees ha^{-1}, on average).

SEXUAL SYSTEMS AND FUNCTIONAL TRAITS

Sexual systems of tree taxa were compiled from a large survey of regional flora and data bases (Appendix S1 and Table S1). Reliable

13652745, 2015, 3, Downloaded from https://besjournals.onlinelibrary.wiley.com/doi/10.1111/1365-2745.12393 by Cochrane France, Wiley Online Library on [22/11/2022]. See the Terms and Conditions (https://onlinelibrary.wiley.com/terms-and-conditions) on Wiley Online Library for rules of use; OA articles are governed by the applicable Creative Commons License

sexual system information was available for 223 taxa of interest (99% of the total individuals with dbh ≥30 cm). Taxa were classified as hermaphrodites (n = 149) when bisexual flowers were present, monoecious (n = 12) when separate male and female flowers (unisexual) were present on the same individual and dioecious (n = 56) when female and male flowers were present on different individuals. For a few taxa (n = 4), the different flora exhibited inconsistent information or revealed labile sexual systems (e.g. 'monoecious, sometimes dioecious'). Considering these taxa as dioecious or not did not affect our conclusions (results not shown).

We also compiled six functional traits from local floras, pre-existing data bases and field measurements consisting of the following: the dispersal syndromes (wind, animal or unassisted), the wood density (WD), nitrogen (N) fixation, the foliage phenology (deciduous vs. evergreen), the leaf area classes and the maximum potential diameter (Table S2). Dispersal syndromes were inferred from the diaspore morphology; species with plumed or winged diasporas were considered wind-dispersed and those with arils or pulp as animal-dispersed. Unassisted dispersal was attributed to the remaining species. Wood density data were extracted from both published values of Gourlet-Fleury *et al.* (2011) and the Global Wood Density Database (Chave *et al.* 2009; Zanne *et al.* 2009). Average values at the species (n = 103) and genus (n = 23) levels were calculated. When WD was not available at the species or genus levels, the mean inferred WD value of the other taxa was assigned to give a null weight in the analysis (n = 25 taxa; i.e. 9.2% of the individuals). Nitrogen-fixing species were identified from the data base of the Germplasm Resources Information Network (http://www.ars-grin.gov/~sbmljw/cgi-bin/taxnodul.pl?language). Fifteen of 22 of the studied Fabaceae species were found in that data base, and the seven remaining were considered non-N-fixing (3% of the individuals). The foliage phenology was obtained from local flora and expert knowledge. The leaf area classes (<2 cm²; 2–20 cm²; 20–40 cm²; 40–200 cm²; and >200 cm²) were extracted from Senterre (2005) and completed with local flora. Finally, the maximum potential diameter for each species was estimated as the 98th percentile of its diameter distribution (≥30 cm) in a large data set that included the present floristic data set and additional data from two other forest concessions [SCAD and SEFCA in Réjou-Méchain *et al.* (2008)]. A more detailed description of these functional traits is given in Réjou-Méchain *et al.* (2014). An exhaustive list of sexual systems and functional traits has been possible for only 151 taxa but accounted for 89.6% of all individuals of the original data set.

CHARACTERIZATION OF FOREST STATUS

The most likely large-scale types of disturbances occurring in the central African forest area are logging, cultivation and fire events. Fires can be natural in forest–savanna transitions or anthropogenic due to burning before cultivation. Aerial photographs were taken in the 1950s over the entire studied area by the French National Geographic Institute ['Institut Géographique National' (IGN)]. In the early 1960s, the IGN made 1:200 000-scale topographic maps where savannas, mature forests and degraded forests were identified based on aerial photograph interpretations of vegetation [for details, see Appendix S1 in Réjou-Méchain *et al.* (2014)]. We therefore identified the vegetation status from five topographic maps covering our study area: NB-33-V GADZI, NA-33-XXIII NOLA, NB-33-VI BODA, NA-33-XXIV MBAIKI and NA-33-XXII YOKADOUMA. All forest plots located within a 1-km buffer zone around each savanna or degraded forest identified in the 1960s maps were considered to belong to a young successional forest area (representing 3440 plots out of 17 198; Fig. 2a). These young successional areas are characterized by a significantly higher proportion of pioneer species (i.e. species that require full light conditions for establishment) (Réjou-Méchain *et al.* 2014). It is worth noting that African rain forests have been largely affected by past climatic fluctuations, especially during the Quaternary Period, leading to successive forest contraction and expansion (Maley 1991). Due to favourable climate conditions and lower human population densities, many forests of central Africa are currently in natural expansion, with a progressive reforestation of savannas since at least 500 years before present (BP) (Vincens *et al.* 1999).

Because subsequent large-scale disturbances may have occurred since the 1950s, we additionally calculated the number of trees ≥30 cm dbh and the basal area of all individuals ≥ 30 cm dbh. Both variables are expected to be positively correlated with forest maturity, at least during the first stages of succession (Fig. 2b,c), and thus were additionally used as quantitative proxies of successional stages. Diameter data were grouped into classes of 10 cm widths during the inventories; the basal areas were calculated with the mid-points of diameter classes.

SOIL TYPES

The study area is characterized by contrasting soil types known to have a strong impact on tree species composition (Réjou-Méchain *et al.* 2008, 2014). We used the soil map developed by Boulvert (1983) at 1:1 000 000 scale to assign inventory plots to three main soil types (Fig. S1 in Supporting Information): (i) deep clay and clay loam, hereafter referred to as 'clay soils'; (ii) deep sandy loam, hereafter referred to as 'sandy soils'; and (iii) shallow clay loam (Skeletic Acrisols, Petroplinthic Acrisols) and Stagnosols, hereafter referred to as 'physically constrained soils'. Details on the soil properties are given in Gourlet-Fleury *et al.* (2011).

STATISTICAL ANALYSIS

The relationships between dioecy and the three forest status variables (i.e. status inferred from historical maps, the basal area and the number of large trees), or the soil type, were assessed by a fourth-corner analysis (Dray & Legendre 2008). This analysis estimates independently the links between dioecy and forest status variables through either floristic abundances or presence–absence. Links were quantified either by the analysis of variance (ANOVA)-like pseudo-F statistics for quantitative variables (basal area and number of large trees) or by the chi-square statistic for qualitative variables (status inferred from historical maps and soil type) (Dray & Legendre 2008). Link significance was assessed by a combination of two permutation tests (n = 9999), as recommended by ter Braak, Cormont & Dray (2012). The first model permuted the rows (sites) of the 'site × taxa' matrix, destroying the link between the site and forest status or soil type [model 2 sensu Dray & Legendre (2008)]. The second model permuted the columns (taxa) of the 'site × taxa' matrix, destroying the link between the taxa and their sexual systems [model 4 sensu Dray & Legendre (2008)]. Importantly, this second model maintains the spatial correlation in taxa abundances and, thus, accounts for any bias that would have been raised by dispersal limitation or biogeographical processes. Significance is obtained if the largest of the two P values (from the two models) is lower than $\alpha = 0.05$. This procedure is known to control the type-I error (ter Braak, Cormont & Dray 2012).

To check that the observed spatial pattern in community dioecy was not driven by correlated traits, we performed two analyses. First,

13652745, 2015, 3, Downloaded from https://besjournals.onlinelibrary.wiley.com/doi/10.1111/1365-2745.12393 by Cochrane France, Wiley Online Library on [22/11/2022]. See the Terms and Conditions (https://onlinelibrary.wiley.com/terms-and-conditions) on Wiley Online Library for rules of use; OA articles are governed by the applicable Creative Commons License

we conducted a Hill and Smith analysis (Hill & Smith 1976) on the 'taxa × trait' matrix to assess the multivariate correlations among traits (including dioecy), independent of community composition. This analysis is a multivariate ordination similar to a principal component analysis (PCA) that can be used with a mixture of continuous and categorical variables. Secondly, we conducted an RLQ analysis (Doledec *et al.* 1996), a three-table ordination method that relates the forest status (matrix R) and the taxa traits (matrix Q) through the taxa composition (matrix L). The plots and taxon scores obtained from a correspondence analysis performed on L are used to link the plot scores obtained from a Hill and Smith analysis of R and the taxa scores from a Hill and Smith analysis of Q (this is possible because plots are shared by R and L, and species are shared by Q and L). Hence, unlike the Hill and Smith analysis, the RLQ analysis relates the traits of trees to the characteristics of the environment in which they live (here the forest status).

All statistical analyses and mapping were performed with R statistical software (R Development Core Team 2013). The fourth-corner, Hill and Smith and, RLQ routines are implemented in the ade4 library (Dray, Dufour & Chessel 2007).

Results

ASSOCIATION BETWEEN DIOECY, COLONIZED AREAS AND SOIL TYPES

The percentage of dioecious individuals within tree communities strongly varied among the field plots, ranging from 0% to 96%, with a mean of 23%, a standard deviation of 12% and a median of 21% (Fig. 1). Throughout the study area, community dioecism was strikingly concordant to the underlying forest status (Fig. 2). Fourth-corner analyses revealed a significantly higher frequency of dioecy in younger successional areas (mean of 28.0%, $n = 3440$ plots) compared to older ones (mean of 21.8%, $n = 13\,758$ plots; $\chi^2 = 2008$, $P = 0.02$). Consistently, the structural variables (basal area and number of large trees) were significantly negatively correlated with the frequency of dioecy in communities ($F = 3433$ and $P = 0.002$ for the basal area; $F = 1543$ and $P = 0.03$ for the number of large trees) (Fig. S2). The same trends were obtained with a presence–absence matrix showing that the association between dioecy and forest status throughout our study area was a robust pattern independent from species-specific abundance ($\chi^2 = 498$ and $P = 0.007$ for the status inferred from historical maps; $F = 406$ and $P = 0.008$ for the basal area but $F = 115$ and $P = 0.14$ for the number of large trees). The fourth-corner analyses also revealed no effect of soil type on the frequency of dioecy ($\chi^2 = 5.3$ and $P = 0.66$).

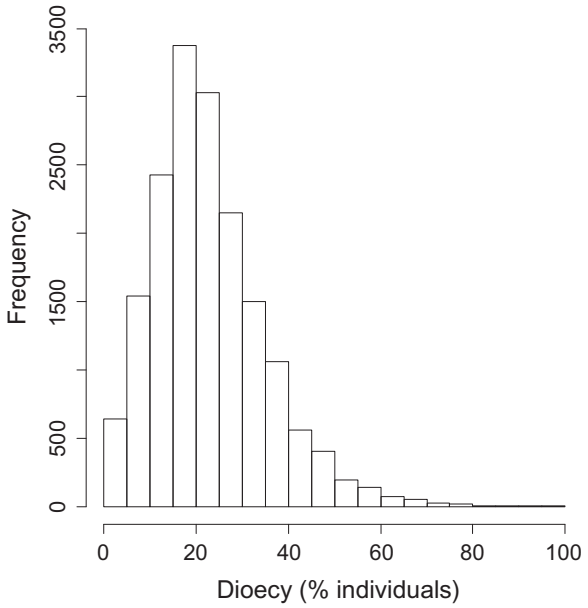

Fig. 1. Histogram of the percentage of dioecy (% of individuals) within the 17 198 0.5-ha field plots.

POTENTIAL CONFOUNDING EFFECT OF TRAIT ASSOCIATION

The Hill and Smith analysis revealed that, among the 151 species for which exhaustive trait information was available, dioecy tends to preferentially occur within animal-dispersed species, characterized by large leaves and having non-N-fixing strategies (Fig. 3a). In contrast, wind-dispersed and deciduous species, often having a large maximum potential diameter, tend to be non-dioecious (Fig. 3a). Wood density was only slightly negatively correlated with dioecy. The RLQ analysis, which shows the association between traits and forest status, confirms that young successional communities, characterized by a low basal area and a low number of large trees, are composed of a higher proportion of dioecious species than old successional ones (Fig. 3b). Critically, most of the functional traits that tend to be associated with young successional areas, such as N-fixing, correspond to traits that are not associated with dioecy within species (Fig. 3a). Hence, the high frequency of dioecy in young successional areas is unlikely to be driven by an association with the traits additionally considered here. Further, the first axis of the RLQ analysis explained 76.1% of the variance, indicating that most of the association between traits and the forest status is held on this axis. Interestingly, dioecy seems to be one of the most correlated traits with young successional areas.

Discussion

Our study reveals a robust association between dioecy incidence and forest successional status over a large area (thousands of square kilometres). Although the overall proportion of dioecy (23% in our study) is similar to the proportions found in other tropical areas (Matallana *et al.* 2005; Queenborough *et al.* 2009; Vamosi & Queenborough 2010), our major finding is that dioecy is more frequent in young successional forests than in mature forests, contrary to classical expectations. Below, we discuss the significance of such results.

ARE DIOECIOUS SPECIES BETTER COLONIZERS?

Because we focused on forest successions within a single region (i.e. at the ecological time-scale), post-colonization

13652745, 2015, 3, Downloaded from https://besjournals.onlinelibrary.wiley.com/doi/10.1111/1365-2745.12393 by Cochrane France, Wiley Online Library on [22/11/2022]. See the Terms and Conditions (https://onlinelibrary.wiley.com/terms-and-conditions) on Wiley Online Library for rules of use; OA articles are governed by the applicable Creative Commons License

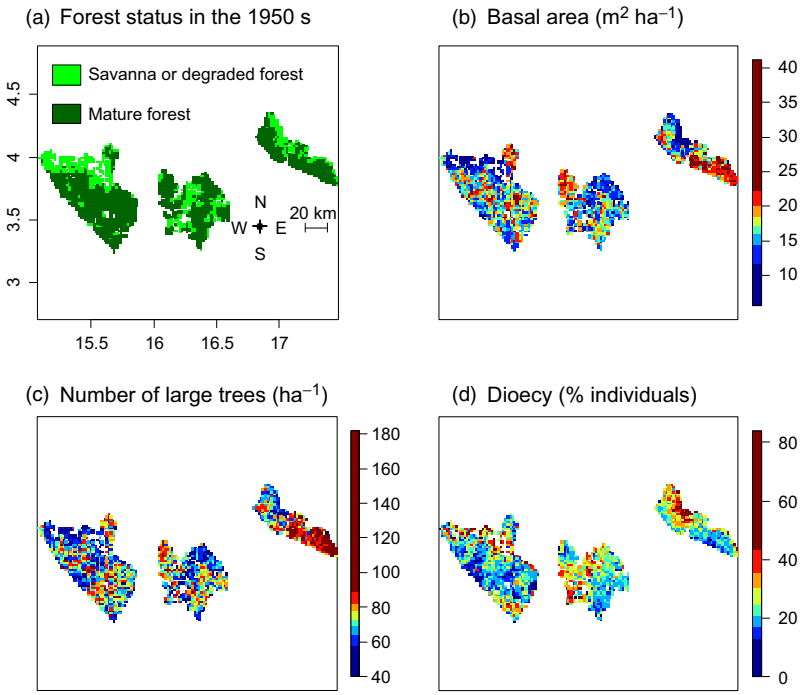

Fig. 2. Comparison of the spatial patterns of forest successional status and their correlates with the spatial pattern of the percentage of dioecious individuals in communities. (a) Forest status in the 1950s, inferred from aerial photographs made in the 1950s, with latitude and longitude coordinates labelled on the axes. (b) Plot-based basal area calculated from individuals ≥ 30 cm dbh. (c) Number of trees ≥ 30 cm dbh. (d) Percentage of dioecious individuals in the tree community. For illustration purposes, the resolution of these maps has been set to 2000 m. In b–d, colours distinguish the eight groups identified with a hierarchical clustering approach using the Ward procedure (i.e. minimization of the within-group sum of squares). Soil type distribution over the study area is shown in Fig. S1.

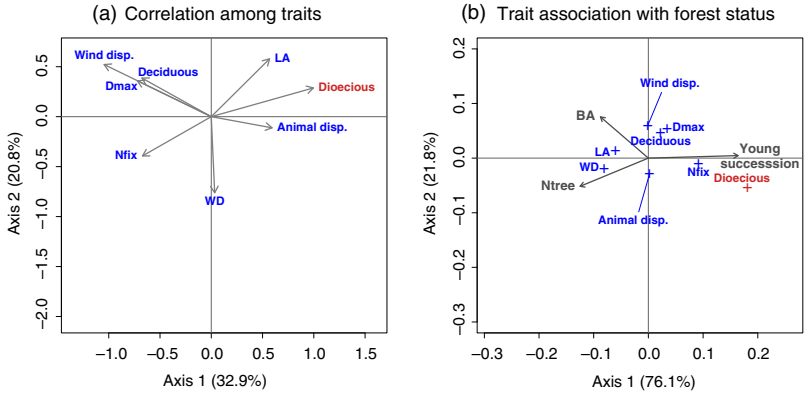

Fig. 3. Multivariate covariation between traits within the flora and between traits and the forest successional status. (a) First two axes of a Hill and Smith analysis showing the multivariate correlations among the six functional traits and the dioecy within 151 taxa, independent from community composition and forest status. (b) First two axes of an RLQ analysis showing the association between the traits and the forest successional status and its correlates. Abbreviations: WD = wood density; Nfix = nitrogen fixation; Dmax = maximum diameter; LA = leaf area; Deciduous = deciduousness; Wind disp. = wind dispersal; Animal disp. = animal dispersal; BA = basal area; Ntree = number of large trees (≥30 cm dbh). Variances explained by the axes are given in brackets, and eigenvalues are shown at the bottom left of the panels.

evolution of reproductive systems cannot be invoked as an explanation for our pattern. The reasons why a high incidence of dioecy is found on islands have been debated and interpreted as either the result of a higher frequency of dioecy among initial colonists or of post-colonization evolution towards dioecy on islands (Bawa 1982; Sakai *et al.* 1995a,b; Barrett, Emerson & Mallet 1996). In a recent contribution, Schlessman *et al.* (2014) showed, for example, that successful dispersal of already dioecious colonists and post-colonization evolution both explain the high incidence of dioecy on New Caledonia. Our data show unambiguously that dioecious plants have, in general, a higher propensity to colonize new or disturbed areas in tropical communities. Interestingly, the same trend (though non-significant) has been reported in North America (Sinclair, Korte & Freeman 2013). Because analyses based on presence–absence data revealed the same patterns, our conclusions cannot be due only to a few highly abundant dioecious taxa. However, some dioecious species, such as *Musanga cecropioides* R. Br., *Pycnanthus angolensis* (Welw) Warb., *Uapaca guineensis* Müll. Arg., *Ricinodendron heudelotii* (Baill) Pierre ex Heckel, *Myrianthus arboreus* P. Beauv. and *Hymenocardia heudelotii* Müll. Arg., strongly contributed to the observed pattern (Table S1). These species are often viewed as pioneers in central Africa. In other tropical regions, the most emblematic pioneer species, such as *Cecropia* spp. Loefl. or *Pourouma* spp. Aublet in the

13652745, 2015, 3, Downloaded from https://besjournals.onlinelibrary.wiley.com/doi/10.1111/1365-2745.12393 by Cochrane France, Wiley Online Library on [22/11/2022]. See the Terms and Conditions (https://onlinelibrary.wiley.com/terms-and-conditions) on Wiley Online Library for rules of use; OA articles are governed by the applicable Creative Commons License

neotropics and *Macaranga* spp. Thouars in Asia, are also dioecious, suggesting that similar patterns could be observed in other regions.

The robustness of our results lies in the fact that they are obtained from a very large data set, covering a large geographical scale, compared to previous studies (Chazdon 2003; Queenborough *et al.* 2009; Vamosi & Queenborough 2010; Sinclair, Korte & Freeman 2013). In a recent contribution, we showed that the two different soil types occurring in the study area (clay vs. sandy soils; Fig. S1) have a strong influence on the floristic and functional compositions, especially for young successional communities (Réjou-Méchain *et al.* 2014). In this study, the data show that soil type has no direct influence on community dioecy. The association between dioecy and young successional areas was thus observed within different soil types and, thus, with at least two contrasted species pools.

DIOECY AS AN INDICATOR OF COLONIZED AREAS

Dioecy is known to correlate with several other traits (Renner & Ricklefs 1995; Matallana *et al.* 2005). Notably, dioecy is positively associated with fleshy fruit and animal dispersal (Bawa 1980; Sakai *et al.* 1995a,b), which led Bawa to argue that the higher incidence of dioecy on islands results from long-distance dispersal by birds. Our results consistently show that dioecy tends to be associated with animal dispersal. However, this dispersal syndrome cannot account for the pattern observed, because our analysis revealed that animal dispersal tends not to be associated with young successional areas (see also Réjou-Méchain *et al.* 2014). We also found that traits associated with young successional areas (e.g. N-fixing, maximum diameter or deciduousness) are not associated with dioecy in the study flora. Hence, the positive association between dioecy and young successional areas is unlikely to be driven by other associated traits. Of interest, the RLQ analysis revealed that dioecy was one of the most correlated traits with young successional areas. While sexual systems were considered to play a limited role in community assembly in tropical forests (Queenborough *et al.* 2009), our study suggests that, in contrast, sexual systems play a significantrole in successional processes.

WHY ARE DIOECIOUS SPECIES BETTER COLONIZERS?

Our results are not consistent with Baker's arguments stating that full outcrossing, such as dioecy, should be at a disadvantage in colonizing areas because of the dioecious species' dependence on pollinators and mates. Indeed, Baker (1974) stated that the 'ideal coloniser' should be able to self-fertilize (be self-compatible), even if it is not completely autogamous. Furthermore, outcrossers avoid inbreeding depression, which may confer good competitive abilities. Because competition is often assumed to increase along the successional pathway, Sinclair, Korte & Freeman (2013) expected a higher incidence of dioecy in older successional communities. The pattern observed in our data set supports the opposite trend.

The advantage of dioecy in young successional areas may be due to either a better ability of dioecious species to reach bare or disturbed areas or a better ability of their seedlings to develop in open areas. Regarding the latter, a possible explanation lies in the demographic advantage of females over hermaphrodites in stressful conditions (Costich 1995; Litrico, Pailler & Thompson 2005). Ashman (2006) argued that, under stressful conditions, hermaphrodites decrease the emphasis on seed production because female function is much more costly than male function. Under such stressful conditions, hermaphrodite seed production may thus be more impeded than the female seed production of dioecious populations, leading to a demographic advantage of females over hermaphrodites. This hypothesis has been often validated in gynodioecious populations (Ashman 2006), but the same logic may hold at the community level: under stressful conditions, monomorphic species may invest more in the male function, thus reducing their demographic advantage over dioecious species. It may explain why we found a larger proportion of dioecious species in previously bare or disturbed areas, which are typically characterized by stressful conditions in tropical forests. Soil organic matter, which favours water and nutrient storage in soil, is indeed dramatically affected by deforestation and associated burning (Guariguata & Ostertag 2001). In particular, tree growth is strongly limited by N availability during the younger successional stages (Lambers *et al.* 2008), as suggested by the higher occurrence of N-fixing species in colonized areas [this study and Réjou-Méchain *et al.* (2014)]. Furthermore, open areas, characterized by low basal areas and a low numbers of large trees, are prone to atmospheric dryness, another source of stress.

Regarding dispersal strategies, two recent theoretical models predict the pattern we observed. The 'seed-shadow handicap' model predicts that negative density-dependent recruitment of seedlings is more intense in dioecious species because only females produce seeds; they are more spatially clumped (Heilbuth, Ilves & Otto 2001). The maintenance of dioecy is, therefore, possible only if dioecious species compensate such density-dependent processes with an increase in relative fitness (e.g. the previously mentioned 'Ashman's hypothesis') or dispersal ability (Heilbuth, Ilves & Otto 2001). The second theoretical model, developed by Cheptou & Massol (2009), shows that as the probability of pollination decreases, evolution leads to a positive association between dispersal ability and full outcrossing (in particular dioecy). High dispersal is indeed favoured in spatio-temporal heterogeneous landscapes (Comins, Hamilton & May 1980). Pollination uncertainty has been shown to be high in tropical forests (Vamosi *et al.* 2006). Although we have no quantitative measure of such pollination fluctuations, we expect the performances of dioecious or full-outcrossing species to be more affected by such fluctuations than the performances of selfers are.

Conclusion

Our results show that plant sexual systems are not neutral with respect to successional dynamics. The higher incidence

13652745, 2015, 3, Downloaded from https://besjournals.onlinelibrary.wiley.com/doi/10.1111/1365-2745.12393 by Cochrane France, Wiley Online Library on [22/11/2022]. See the Terms and Conditions (https://onlinelibrary.wiley.com/terms-and-conditions) on Wiley Online Library for rules of use; OA articles are governed by the applicable Creative Commons License

of dioecy in young successional areas is not consistent with a disadvantage of dioecy in colonizing areas. In this study, we provide two hypotheses that may both explain why classical evolutionary theories failed to predict the robust pattern observed in our study area. First, under stressful conditions, such as those encountered in bare or disturbed forest areas, the demographic advantage of monomorphic species over dioecious species may be reduced by a lower investment of hermaphroditic individuals in the female function. Secondly, because of the seed-shadow handicap and/or pollen limitation, evolution is expected to lead to a positive association between dioecy and dispersal ability. Our study demonstrates a key role of sexual systems in community assembly that should be further considered in future works.

Acknowledgements

We sincerely thank S. Gourlet-Fleury, C. Fortunel, J. C. Vamosi and two anonymous referees for their helpful and constructive comments on the manuscript. We also thank M.D. Swaine and J.-L. Doucet for reviewing the trait data base and B. Senterre for providing leaf area data. We are grateful to the PARPAF project, the leading consortium CIRAD and Forêt Ressources Management (FRM). We also address special thanks to the Ministère des Eaux, Forêts, Chasses et Pêches of the Central African Republic and to the four forest companies: IFB, SCAF, SOFOKAD and TCA that provided access, albeit restricted, to their inventory data for research purposes. Author M.R.-M. was supported by a grant from the French ministry, the Centre National d'Etudes Spatiales (CNES), the 'Laboratoire d'Excellence' (LABEX) entitled 'Towards a unified theory of biotic interactions' (TULIP; ANR -10-LABX-41), the 'Centre d'Etude de la Biodiversité Amazonienne' (CEBA; ANR-10-LABX-0025) and the CoForTips project (ANR-12-EBID-0002).

Data accessibility

The whole floristic data set is archived in the CIRAD institute (http://www.cirad.fr/en). Due to the highly sensitive nature of the data set, it should be used solely for research purposes, with the understanding that researchers use the data with discretion. Researchers interested in using the floristic data set are thus invited to contact Fabrice Bénédet (fabrice.benedet@cirad.fr) with a short description of the project. This is in order to establish a formal convention for use of the data. Species traits are listed in supplementary information.

References

Abe, T. (2006) Threatened pollination systems in native flora of the Ogasawara (Bonin) Islands. *Annals of Botany*, **98**, 317–334.

Ashman, T.L. (2006) The evolution of separate sexes: a focus on the ecological context. *Ecology and Evolution of Flower* (eds L. D. Harder & S. C. H Barrett), pp. 204–222. Oxford University Press, NY, USA.

Baker, H.G. (1955) Self compatibility and establishment after long distance dispersal. *Evolution*, **9**, 347–349.

Baker, H.G. (1967) Support for Bakers law as a rule. *Evolution*, **21**, 853–856.

Baker, H.G. (1974) The evolution of weeds. *Annual Review of Ecology and Systematics*, **5**, 1–24.

Barrett, S.C.H., Dorken, M.E. & Case, A.L. (2001) A geographical context for the evolution of plant reproductive systems. *Integrating Ecology and Evolution in a Spatial Context* (eds J. Silvertown & J. Antonovics), pp. 341–364. Blackwell, Oxford.

Barrett, S.C., Emerson, B. & Mallet, J. (1996) The reproductive biology and genetics of island plants (and discussion). *Philosophical Transactions of the Royal Society of London Series B: Biological Sciences*, **351**, 725–733.

Bawa, K.S. (1980) Evolution of dioecy in flowering plants. *Annual Review of Ecology and Systematics*, **11**, 15–39.

Bawa, K.S. (1982) Outcrossing and the incidence of dioecism in island floras. *American Naturalist*, **119**, 866–871.

Boulvert, Y. (1986) *Carte Phytogéographique de La République Centrafricaine (Feuille OUEST - Feuille EST) À 1: 1 000 000*. Editions de l'ORSTOM, Paris.

Boulvert, Y. (1983) *Carte Pédologique de la République Centrafricaine à 1 : 1 000 000*. Editions de l'ORSTOM, Paris. 133 pp.

ter Braak, C.J., Cormont, A. & Dray, S. (2012) Improved testing of species traits-environment relationships in the fourth-corner problem. *Ecology*, **93**, 1525–1526.

Charnov, E.L., Bull, J.J. & Smith, J.M. (1976) Why be an hermaphrodite? *Nature*, **263**, 125–126.

Chave, J., Coomes, D., Jansen, S., Lewis, S.L., Swenson, N.G. & Zanne, A.E. (2009) Towards a worldwide wood economics spectrum. *Ecology Letters*, **12**, 351–366.

Chazdon, R.L. (2003) Tropical forest recovery: legacies of human impact and natural disturbances. *Perspectives in Plant Ecology, Evolution and Systematics*, **6**, 51–71.

Cheptou, P.-O. (2012) Clarifying Baker's law. *Annals of Botany*, **109**, 633–641.

Cheptou, P.-O. & Massol, F. (2009) Pollination fluctuations drive evolutionary syndromes linking dispersal and mating system. *American Naturalist*, **174**, 46–55.

Comins, H.N., Hamilton, W.D. & May, R.M. (1980) Evolutionarily stable dispersal strategies. *Journal of Theoretical Biology*, **82**, 205–230.

Costich, D.E. (1995) Gender specialization across a climatic gradient: experimental comparison of monoecious and dioecious ecballium. *Ecology*, **76**, 1036.

Darwin, C. (1877) *The Different Forms of Flowers on Plants of the Same Species*. John Murray, London.

Diaz, S., Cabido, M. & Casanoves, F. (1998) Plant functional traits and environmental filters at a regional scale. *Journal of Vegetation Science*, **9**, 113–122.

Doledec, S., Chessel, D., terBraak, C.J.F. & Champely, S. (1996) Matching species traits to environmental variables: a new three-table ordination method. *Environmental and Ecological Statistics*, **3**, 143–166.

Dray, S., Dufour, A.B. & Chessel, D. (2007) The ade4 Package–II: two-table and K-table methods. *R News*, **7**, 47–52.

Dray, S. & Legendre, P. (2008) Testing the species traits-environment relationships: the fourth-corner problem revisited. *Ecology*, **89**, 3400–3412.

Fayolle, A., Engelbrecht, B., Freycon, V., Mortier, F., Swaine, M., Réjou-Méchain, M., Doucet, J.-L., Fauvet, N., Cornu, G. & Gourlet-Fleury, S. (2012) Geological substrates shape tree species and trait distributions in African moist forests. *PLoS ONE*, **7**, e42381.

Freeman, D.C., Harper, K.T. & Ostler, W.K. (1980) Ecology of plant dioecy in the intermountain region of western North America and California. *Oecologia*, **44**, 410–417.

Gourlet-Fleury, S., Rossi, V., Rejou-Mechain, M., Freycon, V., Fayolle, A., Saint-André, L. *et al.* (2011) Environmental filtering of dense-wooded species controls above-ground biomass stored in African moist forests. *Journal of Ecology*, **99**, 981–990.

Guariguata, M.R. & Ostertag, R. (2001) Neotropical secondary forest succession: changes in structural and functional characteristics. *Forest Ecology and Management*, **148**, 185–206.

Heilbuth, J.C., Ilves, K.L. & Otto, S.P. (2001) The consequences of dioecy for seed dispersal: modeling the seed-shadow handicap. *Evolution*, **55**, 880–888.

Hijmans, R.J., Cameron, S.E., Parra, J.L., Jones, P.G. & Jarvis, A. (2005) Very high-resolution interpolated climate surface for global land areas. *International Journal of Climatology*, **25**, 1965–1978.

Hill, M.O. & Smith, A.J.E. (1976) Principal component analysis of taxonomic data with multi-state discrete characters. *Taxon*, **25**, 249–255.

Humeau, L., Pailler, T. & Thompson, J.D. (1999) Cryptic dioecy and leaky dioecy in endemic species of *Dombeya* (Sterculiaceae) on La Réunion. *American Journal of Botany*, **86**, 1437–1447.

Lambers, H., Raven, J.A., Shaver, G.R. & Smith, S.E. (2008) Plant nutrient-acquisition strategies change with soil age. *Trends in Ecology and Evolution*, **23**, 95–103.

Litrico, I., Pailler, T. & Thompson, J.D. (2005) Gender variation and primary succession in a tropical woody plant, *Antirhea borbonica* (Rubiaceae). *Journal of Ecology*, **93**, 705–715.

Lloyd, D.G. (1980) Demographic factors and mating patterns in angiosperms. *Demography and Evolution in Plant Populations* (ed. T. Solbrig), pp. 67–88. Univ. California Press, Berkeley.

Maley, J. (1991) The African rain forest vegetation and palaeoenvironments during late Quaternary. *Climatic Change*, **19**, 79–98.

Matallana, G., Wendt, T., Araujo, D.S.D. & Scarano, F.R. (2005) High abundance of dioecious plants in a tropical coastal vegetation. *American Journal of Botany*, **92**, 1513–1519.

Pannell, J. (1997) The maintenance of gynodioecy and androdioecy in a metapopulation. *Evolution*, **51**, 10–20.

13652745, 2015, 3, Downloaded from https://besjournals.onlinelibrary.wiley.com/doi/10.1111/1365-2745.12393 by Cochrane France, Wiley Online Library on [22/11/2022]. See the Terms and Conditions (https://onlinelibrary.wiley.com/terms-and-conditions) on Wiley Online Library for rules of use; OA articles are governed by the applicable Creative Commons License

Pannell, J.R. & Barrett, S.C. (1998) Baker's law revisited: reproductive assurance in a metapopulation. *Evolution*, **52**, 657–668.

Queenborough, S.A., Mazer, S.J., Vamosi, S.M., Garwood, N.C., Valencia, R. & Freckleton, R.P. (2009) Seed mass, abundance, and breeding systems among tropical forest species: do dioecious species exhibit compensatory reproduction or abundances? *Journal of Ecology*, **97**, 555–566.

R Development Core Team. (2013) *R: A Language and Environment for Statistical Computing*. R Foundation for Statistical Computing, Austria, Vienna.

Rambuda, T.D. & Johnson, S.D. (2004) Breeding systems of invasive alien plants in South Africa: does Baker's rule apply? *Diversity and Distributions*, **10**, 409–416.

Réjou-Méchain, M., Pélissier, R., Gourlet-Fleury, S., Couteron, P., Nasi, R. & Thompson, J.D. (2008) Regional variation in tropical forest tree species composition in the Central African Republic: an assessment based on inventories by forest companies. *Journal of Tropical Ecology*, **24**, 663–674.

Réjou-Méchain, M., Fayolle, A., Nasi, R., Gourlet-Fleury, S., Doucet, J.-L., Gally, M., Hubert, D., Pasquier, A. & Billand, A. (2011a) Detecting large-scale diversity patterns in tropical trees: can we trust commercial forest inventories? *Forest Ecology and Management*, **261**, 187–194.

Réjou-Méchain, M., Flores, O., Bourland, N., Doucet, J., Fétéké, R.F., Pasquier, A. & Hardy, O.J. (2011b) Spatial aggregation of tropical trees at multiple spatial scales. *Journal of Ecology*, **99**, 1373–1381.

Réjou-Méchain, M., Flores, O., Pélissier, R., Fayolle, A., Fauvet, N. & Gourlet-Fleury, S. (2014) Tropical tree assembly depends on the interactions between successional and soil-filtering processes. *Global Ecology and Biogeography*, **23**, 1440–1449.

Renner, S.S. & Ricklefs, R.E. (1995) Dioecy and its correlates in the flowering plants. *American Journal of Botany*, **82**, 596–606.

Sakai, A.K., Wagner, W.L., Ferguson, D.M. & Herbst, D.R. (1995a) Origins of dioecy in the Hawaiian flora. *Ecology*, **76**, 2517–2529.

Sakai, A.K., Wagner, W.L., Ferguson, D.M. & Herbst, D.R. (1995b) Biogeographical and ecological correlates of dioecy in the Hawaiian flora. *Ecology*, **76**, 2530–2543.

Schlessman, M.A., Vary, L.B., Munzinger, J. & Lowry, P.P. II (2014) Incidence, correlates, and origins of dioecy in the island flora of New Caledonia. *International Journal of Plant Sciences*, **175**, 271–286.

Senterre, B. (2005) Recherches méthodologiques pour la typologie de la végétation et la phytogéographie des forêts denses d'Afrique tropicale. *Acta Botanica Gallica*, **152**, 409–419.

Shirk, R.Y. & Hamrick, J.L. (2014) High but variable outcrossing rates in the invasive *Geranium carolinianum* (Geraniaceae). *American Journal of Botany*, **101**, 1200–1206.

Sinclair, J.P., Korte, J.L. & Freeman, D.C. (2013) The pattern of dioecy in terrestrial, temperate plant succession. *Evolutionary Ecology Research*, **15**, 545–556.

Thomson, J.D. & Brunet, J. (1990) Hypotheses for the evolution of dioecy in seed plants. *Trends in Ecology and Evolution*, **5**, 11–16.

Vamosi, S.M. & Queenborough, S.A. (2010) Breeding systems and phylogenetic diversity of seed plants along a large-scale elevational gradient. *Journal of Biogeography*, **37**, 465–476.

Vamosi, J.C., Knight, T.M., Steets, J.A., Mazer, S.J., Burd, M. & Ashman, T.-L. (2006) Pollination decays in biodiversity hotspots. *Proceedings of the National Academy of Sciences of the United States of America*, **103**, 956–961.

Vincens, A., Schwartz, D., Elenga, H., Reynaud-Farrera, I., Alexandre, A., Bertaux, J. *et al.* (1999) Forest response to climate changes in Atlantic equatorial Africa during the last 4000 years BP and inherence on the modern landscapes. *Journal of Biogeography*, **26**, 879–885.

Zanne, A.E., Lopez-Gonzalez, G., Coomes, D.A., Ilic, J., Jansen, S., Lewis, S.L., Miller, R.B., Swenson, N.G., Wiemann, M.C. & Chave, J. (2009) Global wood density database. Dryad. Identifier: http://hdl.handle.net/10255/dryad.235.

Received 18 July 2014; accepted 2 March 2015
Handling Editor: Jason Fridley

Supporting Information

Additional Supporting Information may be found in the online version of this article:

Appendix S1. References used to compile sexual systems of tree taxa.

Table S1. List of the 223 tree taxa studied and their sexual systems

Table S2. List of the 151 tree taxa considered in the trait-based analyses and their functional traits

Figure S1. Soil type distribution over the study area.

Figure S2. Relation between community dioecism and (a) basal area and (b) the number of large trees.

13652745, 2015, 3, Downloaded from https://besjournals.onlinelibrary.wiley.com/doi/10.1111/1365-2745.12393 by Cochrane France, Wiley Online Library on [22/11/2022]. See the Terms and Conditions (https://onlinelibrary.wiley.com/terms-and-conditions) on Wiley Online Library for rules of use; OA articles are governed by the applicable Creative Commons License

Surveys in Geophysics
https://doi.org/10.1007/s10712-019-09532-0

Upscaling Forest Biomass from Field to Satellite Measurements: Sources of Errors and Ways to Reduce Them

Maxime Réjou-Méchain[1] · Nicolas Barbier[1] · Pierre Couteron[1] · Pierre Ploton[1] · Grégoire Vincent[1] · Martin Herold[2] · Stéphane Mermoz[3,8] · Sassan Saatchi[4] · Jérôme Chave[5] · Florian de Boissieu[6] · Jean-Baptiste Féret[6] · Stéphane Momo Takoudjou[1,7] · Raphaël Pélissier[1]

Received: 16 October 2018 / Accepted: 12 April 2019
© Springer Nature B.V. 2019

Abstract
Forest biomass monitoring is at the core of the research agenda due to the critical importance of forest dynamics in the carbon cycle. However, forest biomass is never directly measured; thus, upscaling it from trees to stand or larger scales (e.g., countries, regions) relies on a series of statistical models that may propagate large errors. Here, we review the main steps usually adopted in forest aboveground biomass mapping, highlighting the major challenges and perspectives. We show that there is room for improvement along the scaling-up chain from field data collection to satellite-based large-scale mapping, which should lead to the adoption of effective practices to better control the propagation of errors. We specifically illustrate how the increasing use of emerging technologies to collect massive amounts of high-quality data may significantly improve the accuracy of forest carbon maps. Furthermore, we discuss how sources of spatially structured biases that directly propagate into remote sensing models need to be better identified and accounted for when extrapolating forest carbon estimates, e.g., through a stratification design. We finally discuss the increasing realism of 3D simulated stands, which, through radiative transfer modelling, may contribute to a better understanding of remote sensing signals and open avenues for the direct calibration of large-scale products, thereby circumventing several current difficulties.

Keywords Biomass · Calibration · Carbon · Error propagation · Field data · Modelling

1 Introduction

The large uncertainty associated with the global spatio-temporal dynamics of forest carbon (C) is a major obstacle to the projection of future atmospheric CO_2 concentrations and the implementation of mitigation strategies. Satellite observations of land-use changes are currently reliable enough to provide robust information on deforestation dynamics (Hansen

✉ Maxime Réjou-Méchain
maxime.rejou@ird.fr

Extended author information available on the last page of the article

Published online: 30 May 2019

et al. 2013). However, the associated C release remains uncertain because broad-scale C mapping applications from satellite data still convey large uncertainty (Mitchard et al. 2013; Huang et al. 2015; Rodriguez-Veiga et al. 2017). Even higher uncertainty is associated with C fluxes related to forest degradation and regrowth because small changes in the C stocks in closed-canopy forests are challenging to detect remotely (Bustamante et al. 2016), resulting in an underestimation of forest degradation globally (Pearson et al. 2017).

Forest aboveground biomass (AGB), the main proxy for forest C stock, is rarely directly measured, either in the field or via remote sensing (RS) (Clark and Kellner 2012). AGB estimations are thus derived from statistical models with their own underlying assumptions that can generate random and/or systematic errors when violated. The way the errors that are associated with these models propagate up to the final AGB estimate is, however, generally poorly understood and accounted for. A simple illustration of how RS–AGB models may produce inaccurate AGB density maps is shown in Fig. 1. First, the propagation of a uniform bias over calibration data (e.g., field plot AGB estimates) conveys a systematic over- or underestimation, which may be straightforward to correct in the final density map provided that the bias can be quantified (Fig. 1b). A more overlooked but common effect is the propagation of a non-uniform bias, leading the RS model to overestimate small AGB values and underestimate large AGB values, resulting in density maps flattened around the mean (Fig. 1c; Avitabile et al. 2016; Xu et al. 2016). Such bias may originate from three sources: (1) a non-uniform bias exists in the calibration dataset, such as an AGB over- or underestimation in young versus old successional forests, which can be corrected if the non-uniform pattern of errors is well identified a priori; (2) the low sensitivity of RS signals to high AGB values generally results in an AGB underestimation (i.e. signal saturation), while in low AGB open areas, non-forest land surfaces (i.e. surface roughness, non-woody vegetation) also contribute to the remotely sensed signal, leading to an overestimation of forest AGB; (3) in regression models, violation of the assumption of low/non-existent error in the independent variable (the "observed" AGB) results in a systematic underestimation of the model slope (Fuller 1987; Réjou-Méchain et al. 2014). Finally, the major source of

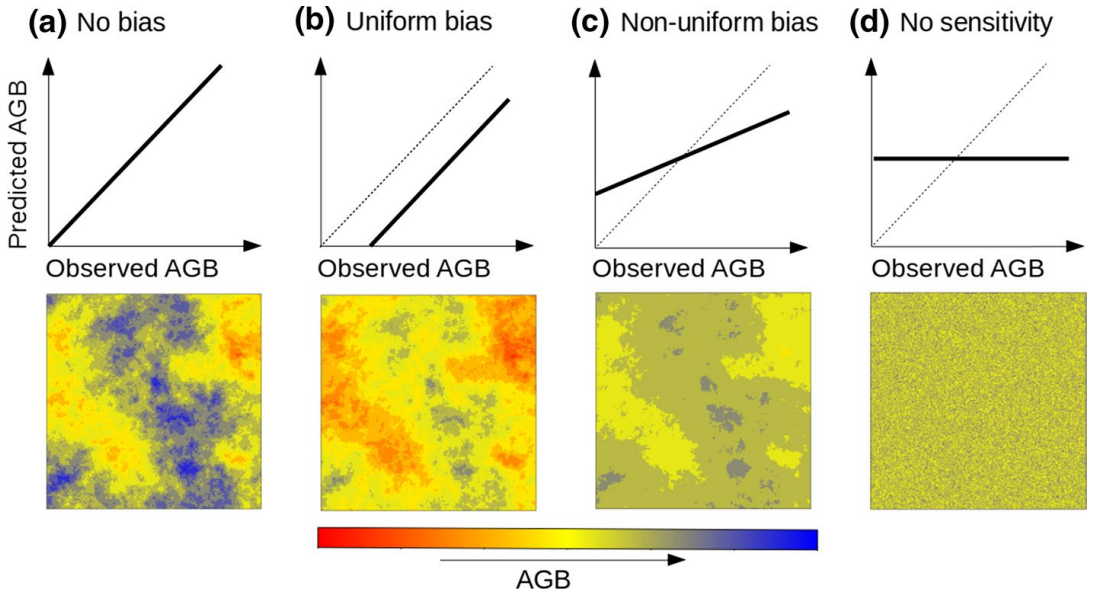

Fig. 1 Conceptual representation of common bias patterns found in remote sensing AGB models

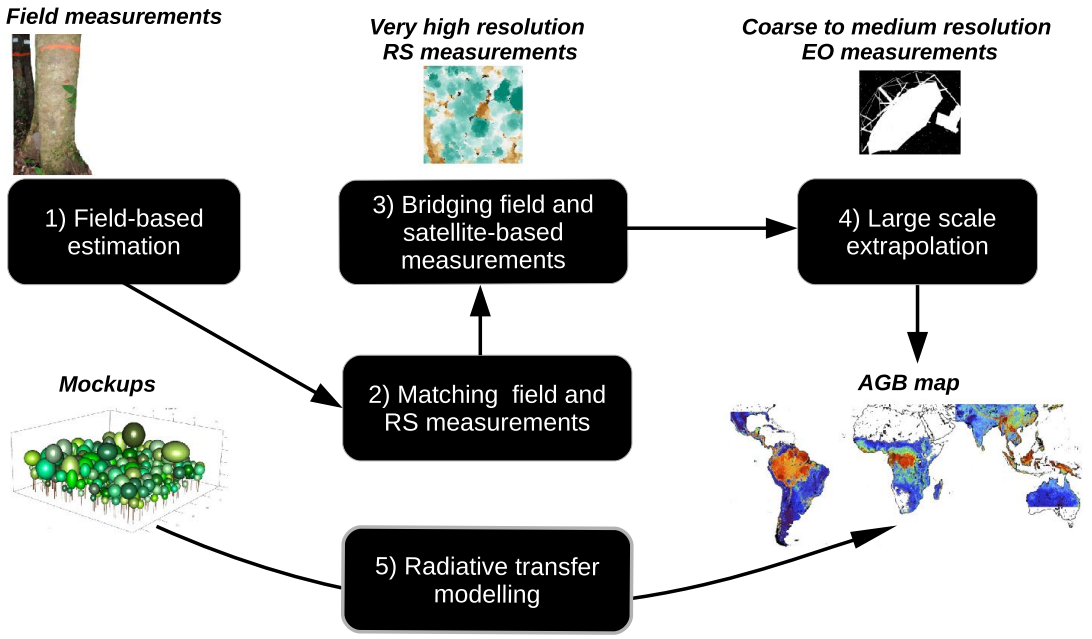

Fig. 2 Flowchart illustrating the main sections of this paper

uncertainty in RS-based models is obviously the poor signal sensitivity to AGB variations, which makes the post-correction of density maps impossible (Fig. 1d).

In this paper, we review the sources of errors that may occur during the process of upscaling AGB estimates from ground to RS data and provide suggestions for reducing these errors (Fig. 2). Section 2 illustrates that field-based estimates—often improperly seen as "ground truth"—most likely convey more important errors than generally assumed. Section 3 discusses the issues associated with mismatching field-based AGB estimates to RS data. Section 4 presents a multi-step calibration strategy aimed at bridging field and satellite measurements through airborne or spaceborne very high-resolution RS products. This section also highlights the pitfalls and promises of such a strategy. Section 5 discusses the common problems associated with broad-scale AGB extrapolations for regional mapping through inexpensive satellite imagery. Finally, Sect. 6 reviews physical modelling approaches and discusses how they may improve our ability to map AGB. These sections mostly focus on tropical forest examples, where uncertainty in C dynamics is the highest globally (Mitchard 2018), although most of the issues that are discussed are also concerns in other forest biomes.

2 Improving Field-Based AGB Estimation

Uncertainty in field-based AGB estimation has recently become a matter of concern for the RS community (e.g., Mermoz et al. 2014, 2015; Longo et al. 2016; Xu et al. 2017; Bouvet et al. 2018; Jucker et al. 2018a). For instance, Chen et al. (2015) developed an analytical framework to track the sources of errors from field measurements in airborne LiDAR-AGB predictions. The authors estimated that field-based uncertainty contributed only 10% of the total pixel-level uncertainty at a 0.16-ha resolution (see also Longo et al. 2016). However, the statistical framework developed by these authors rested upon the assumption that tree-level AGB estimation errors are independent within and between field plots; thus,

they average out in RS models. While this assumption is common (e.g., Chave et al. 2004; McRoberts and Westfall 2013; Longo et al. 2016), it is often violated, generating overlooked biases in AGB maps.

Field-based AGB estimates at the plot level are obtained by summing individual AGB values for all trees within the plot. At the tree level, AGB is generally estimated using an allometric model that combines key tree features, typically the stem diameter (D), total tree height (H) and wood density (WD; Chave et al. 2005, 2014). While D may suffer from important measurement errors (Clark 2002), significant efforts have been made towards protocol standardization (Phillips et al. 2009; Condit et al. 2014) to warrant negligible errors, at least in scientific plots (Chave et al. 2004; Molto et al. 2013). However, as shown below, the two other predictors, as well as the AGB model itself, may convey systematic error components within and between plots that may directly propagate into RS models.

2.1 Uncertainty in Wood Density

Individual tree AGB is directly proportional to WD, which varies by as much as tenfold among tree species (Chave et al. 2009). However, WD is rarely measured on individual trees in forest inventories, and in most cases, a mean specific value is assigned from independent databases to all trees of a given taxonomic category, often higher than the species level. This approximation is very crude beyond the genus level (Flores and Coomes 2011); however, it is common in the tropics because of inaccurate botanical identifications (Gomes et al. 2013) or the limited availability of WD data (Chave et al. 2009). For example, in the well-known pantropical forest inventory dataset generated by Al Gentry, which includes 43,000 trees (> 8000 taxa), more than one-third of the trees could not be assigned a WD value at the species or genus level from the Global Wood Density Database (Chave et al. 2009; Zanne et al. 2009). Given that most tropical tree taxa are spatially aggregated at various scales (Condit et al. 2000), uncertainty in WD estimates is expected to cause spatially structured errors, potentially generating biases in plot-level AGB estimates (Baker et al. 2004). One way to mitigate this error source is to rely on permanent scientific sites for model calibration. For instance, in the 50-ha Center for Tropical Forest Science (CTFS) permanent plot at Barro Colorado Island, Panama (Condit 1998), less than 2% of the trees have WD values assigned at a coarser taxonomic resolution than the genus level. In addition, repeated censuses also strongly minimize field measurement or encoding errors and reduce the number of missing trees (Lopez-Gonzalez et al. 2011), providing high-quality calibration data for RS applications (Chave et al. this issue).

The assignment of a WD value to an individual tree at the species level does not, however, ensure bias-free estimates. WD is known to vary widely between individuals of the same species and even within individual trees (Tarelkin et al. 2019; Swenson and Enquist 2008; Bastin et al. 2015a; Wassenberg et al. 2015). For example, species having at least 10 observations in the Global Wood Density Database ($n = 109$) exhibit a mean WD variation of 9% around the mean. Given that two-thirds of the taxa in that dataset are documented with a single measure, the effects of intra-specific variations in WD on AGB estimates are currently difficult to quantify. Intra-individual variations may also have a strong impact on field AGB estimations, e.g., when converting volume estimations (e.g., from terrestrial LiDAR, see below) into biomass. A recent study conducted in Cameroon showed a significant decrease in WD with height for most species; thus, the use of WD at the trunk base to convert volume into biomass led to an AGB overestimation of approximately 10% at

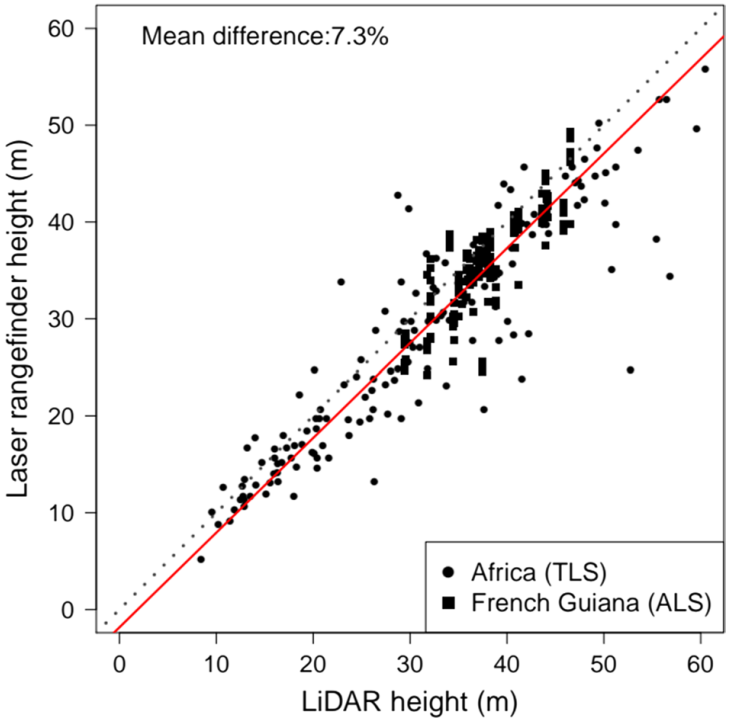

Fig. 3 Comparison between height measurements inferred from airborne or terrestrial LiDAR acquisitions and measured in the field using a laser hypsometer (TruPulse 360R for the 151 trees from Cameroon and Haglöf Laser Vertex for the 306 French Guiana trees). The relationship suggests that tree height measurements from laser rangefinders underestimate the tree height by 7.3%. The red line illustrates the output of a standard major axis regression (i.e. minimizing errors in both X and Y), and the dotted line represents the 1:1 line

the plot level (Sagang et al. 2018). The authors, however, demonstrated that vertical variations could be predicted from basal WD; thus, these variations could be controlled for in biomass estimations, which was recently confirmed in a large dataset from 6 different countries in central Africa (Momo Takoujdou et al. in preparation).

A lesson learned from this short review is that more efforts are needed to collect WD data for tropical taxa using standardized protocols (Williamson and Wiemann 2010) while accounting for all major sources of variation. Given the time and cost of wood core analyses, non-destructive and rapid WD measurement techniques are appealing, such as torsiometers, Pilodyns, nail withdrawal tools or emerging electronic devices to measure drilling resistance (reviewed in Gao et al. 2017). For instance, the use of an empirical model developed from Pilodyn measurements led to a predicted WD error of 15% for 1427 trees from four continents.

2.2 Uncertainty in Tree Height

As for WD, tree height is not systematically available from field plot inventories, and *H*–*D* models are often used to estimate the height (*H*) of individual trees from stem diameter (*D*) measurements. These models are built from *H* measurements that are subjected to errors, especially in dense forest canopies. Indeed, in addition to a strong operator effect, Larjavaara and Muller-Landau (2013) showed that the two most common *H* measurement methods (the so-called tangent method, which combines horizontal distance to the trunk and the angle to the treetop, and the "sine" method, which combines the angle and distance measurements to the treetop) led to significantly contrasting results, with an underestimation of ca. 20% with the "sine" method. Based on an original dataset of *H* measurements of 457 trees using both a laser hypsometer in the field and LiDAR systems (airborne or terrestrial), we confirm that the "sine" method results in a systematic bias of −7% in the *H*

estimations (Fig. 3). The way this bias propagates into AGB estimates through direct measurements or *H–D* models depends on whether a similar bias occurred in the destructive reference dataset used to build the AGB allometric model.

Beyond measurement errors, *H–D* allometric models represent a major source of uncertainty in field-based AGB estimates because this allometry exhibits large spatially structured variations at local, regional and continental scales (Ketterings et al. 2001; Feldpausch et al. 2011; Vieilledent et al. 2012; Vincent et al. 2012b; Réjou-Méchain et al. 2015). To account for broad-scale variations, both regionally averaged *H–D* relationships (Feldpausch et al. 2012) and bioclimatic proxies (Eq. 6 in Chave et al. 2014) have been proposed. These approaches significantly reduce AGB model errors in tropical regions, but certain local deviations may remain quite large. For instance, in the central Congo Basin, forest AGB was overestimated by 24% when the Feldpausch et al. (2012) regional *H–D* relationship was used instead of a local relationship (Kearsley et al. 2013). In the Khao Yai Forest Reserve in Thailand, we found that the bioclimatic proxy proposed by Chave et al. (2014) underestimated *H* by 26% (Jha, Chanthorn, Réjou-Méchain, unpublished). Finally, both approaches resulted in an AGB underestimation > 20% in a Brazilian forest (Hunter et al. 2013). Considering such uncertainty in only *H* estimations, any RS–AGB model calibrated in these regions would result in a systematic bias > ± 20% in AGB estimations (case B in Fig. 1), i.e. an error margin larger than the commonly admitted accuracy.

H–D relationships may also strongly vary between plots within landscapes. Average differences in *H* of approximately 10% for a given *D* were found between plots within areas < 10 km^2 in French Guiana (Vincent et al. 2012a, 2014; Réjou-Méchain et al. 2015). More specifically, the *H–D* relationship was found to strongly vary along a successional gradient in Thailand (Chanthorn et al. 2017); hence, this relationship varied concomitantly with forest AGB, potentially leading to a non-uniform bias in RS models (case of Fig. 1c). Various strategies may be adopted to better account for these inter-plot variations. The most straightforward strategy is to acquire *H* data for at least a subsample of trees to calibrate plot-specific *H–D* allometries (Vieilledent et al. 2012; Hunter et al. 2013), even though care must be taken with respect to the *H* measurement method and sampling strategy (see above and Sullivan et al. 2018). Another way to better account for systematic variations in *H–D* allometry between plots would consist of finding local covariates. Forest structural metrics that reflect stand competition intensity or soil fertility were found to explain some variation, but to a relatively small extent (Feldpausch et al. 2011; Banin et al. 2012). In contrast, mean canopy height has been found to correlate well with tree slenderness (a higher *H* for a given *D*), both within species and at the community level (Vincent et al. 2012a). Hence, when a high-resolution canopy height map is available, the accuracy of individual *H* estimations from *D* measurements can be significantly improved by adding local canopy height metrics to the *H–D* model (e.g., median of the canopy height model in a 50-m window centred on each tree). Using this approach, the individual *H* error was reduced by 14%, leading to a threefold decrease in the plot-level AGB bias at the Paracou site, French Guiana ($n = 2141$ trees; Vincent et al. unpublished). This result adequately illustrates that if field-based estimates generally feed into RS models, they may also themselves be improved by RS measurements. With the recent advances in our ability to extract individual trees from dense LiDAR point clouds (Ferraz et al. 2016), *H* measurements may be directly assigned to individual canopy trees that account for a large share of the stand AGB (Bastin et al. 2015b). In conclusion, better integration of LiDAR technologies and field measurements has the potential to substantially reduce the uncertainties associated with tree height variations.

2.3 Uncertainty in AGB Allometric Equations

The allometric conversion of individual tree attributes into AGB is a major source of uncertainty in tree and plot AGB estimates (Chave et al. 2004; Molto et al. 2013). At the tree level, the predictive error associated with the pantropical allometric model of Chave et al. (2014) reaches almost 40% (the total error is slightly above 50%), but if considered random, this error rapidly averages out as the number of trees increases in the predicted population (Réjou-Méchain et al. 2017). A cross-validation assessment of this model indeed revealed a mean bias across sites of only 5% but exceeded 30% in 8 out of 58 sites (Chave et al. 2014). Models that assume universal allometry may thus be liable to strong and uncontrolled local bias, which is generally ignored in error propagation schemes. This site effect may reflect differences in species composition or biotic (e.g., competition intensity) or abiotic (e.g., soil fertility) conditions. For instance, the use of biome-specific rather than species-specific allometries resulted in an AGB prediction bias between −18% and +14% for a Brazilian mangrove forest (de Souza Pereira et al. 2018).

Crown allometry variations among sites have also been identified as a major source of uncertainty in pantropical allometric models (Goodman et al. 2014). The proportion of the crown to the total tree AGB is indeed highly variable among trees (3–88%) and tends to increase with the increase in tree AGB beyond 10 Mg, reaching 50% on average for trees > 45 Mg and 34% for trees < 10 Mg (Ploton et al. 2016). This systematic change in tree shape with total tree AGB explained 20% of the underestimation of the AGB of large trees reported by Chave et al. (2014). Using simulations, Ploton et al. (2016) showed that, for 1-ha plots, this bias led to systematic errors ranging from −26% to +16% that depended on the frequency of large trees, thus introducing a non-uniform bias in AGB maps (Fig. 1c). Integrating crown dimensions in allometric models strongly reduces this allometric uncertainty. Jucker et al. (2017b) even proposed an AGB allometry using crown size and tree height, i.e. tree dimensions potentially directly measurable by means of RS (e.g., Ferraz et al. 2016).

Another potential source of uncertainty in the allometric conversion of tree attributes into AGB is the existence of hollow parts in the trunks or branches. Hollow parts are implicitly accounted for in AGB estimates when allometric equations are built on directly weighed trees. However, direct weighing is rarely possible for large trees, which are also more prone to hollows (Fig. 4). As a consequence, volume estimation is usually preferred for large trees (Henry et al. 2010; Fayolle et al. 2013; Chave et al. 2014), which results in potential estimation bias (Moundounga Mavouroulou et al. 2014). For instance, Nogueira et al. (2006) found that hollows occurred in ca. 10% of the trees > 5 cm in diameter in Brazil, but hollows occurred in up to 50% of trees > 80 cm in diameter (but $n = 4$ in that study). This condition, however, resulted in a bias ≤ 1% in the AGB in a 1-ha plot, which is consistent with the results of Clark and Clark (2000) in Costa Rica (hollow parts accounted for only 1.7% of the outer volume). Conversely, other studies reported much higher errors in other sites (Rodrigues and Valle 1964 cited in Nogueira et al. 2006; Dickinson and Tanner 1978), suggesting that the frequency of hollow trees may vary between sites and may also be a source of uncertainty in AGB maps. For instance, in over 523 forested sites in south-eastern Australia, the number of hollow trees strongly varied between sites with a skewed distribution, i.e. many study sites contained few or no hollow trees, but some sites contained up to 13 hollow trees per ha (Lindenmayer et al. 1991). Interestingly, the occurrence of hollow trees was well predicted by topography, stand age, region, logging history and the dominant species. Similarly, in a subtropical forest in China, the density of hollow

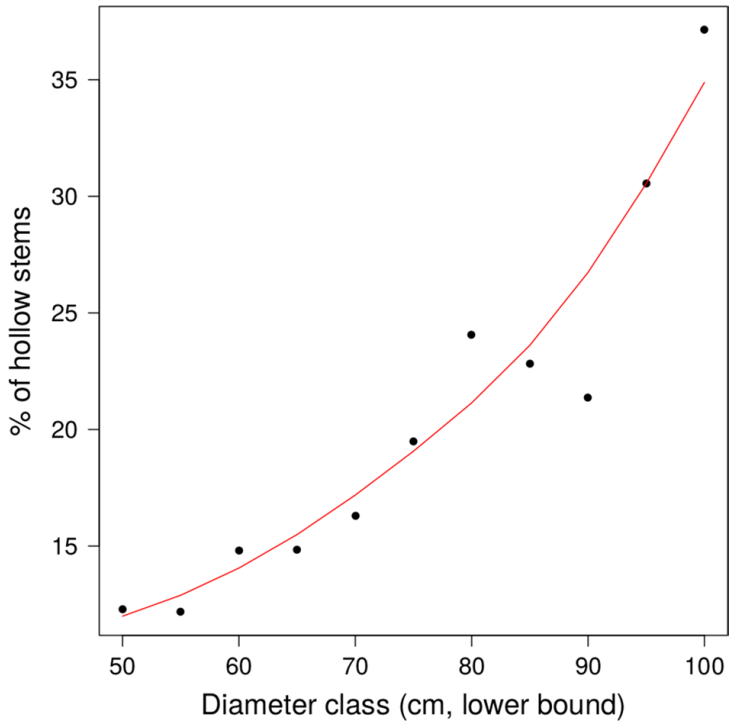

Fig. 4 Increase in hollow occurrence with tree diameter in a French Guiana dataset. In total, 17% of a sample of 3746 stems with DBH > 50 cm in French Guiana were found to be hollow. This proportion appeared to be strongly positively related to tree size. Courtesy of L. Descroix, unpublished

trees was approximately 90 trees per ha, which is much higher than that in temperate forests, and hollow occurrence varied significantly with species, crown position and topographical context (Liu et al. 2018). However, more studies are needed to better quantify the impact of hollows or simply wood decay on stand AGB estimates, using, for instance, non-destructive wood imaging techniques (Arciniegas et al. 2014). Marra et al. (2018) used sonic and electrical resistance tomography to identify internal wood decay without apparent cavities that resulted in C loss in the trunk ranging from 0.1 to 24% (5–37% with an apparent cavity).

2.4 Perspective on Field-Based AGB Estimation

The use of terrestrial laser scanners (TLS) has recently emerged as a credible alternative to destructive approaches for the estimation of tree AGB (Calders et al. 2014; Disney 2018; Gonzalez de Tanago et al. 2018; Lau et al. 2018; Momo Takoudjou et al. 2018). This technology and the associated processing methods are rapidly progressing but still face a number of challenges in tropical moist forests, such as the high degree of occlusion, the difficulty in segmenting individual trees in intricate vegetation (Trochta et al. 2017; Calders et al. 2018) and in filtering out leaves (Béland et al. 2014; Ma et al. 2016; Calders et al. 2018), which is a required step prior to tree structure reconstruction from the point cloud (Momo Takoudjou et al. 2018). Overcoming these issues would take us one step closer to an automated routine for reconstructing entire forest stands, thereby producing large amounts of data to feed allometric models (Raumonen et al. 2013). However, the above-mentioned problems associated with poor WD estimates and the presence of hollow trees remain a serious difficulty for TLS to overcome, which inherently measures the outer volume.

Another perspective from the advent of LiDAR technology is the possibility of directly estimating stand-level AGB instead of summing the AGBs of individual trees. For instance, Vincent et al. (2014) analytically derived a stand-level AGB equation based on stand volume-weighted WD, tree density, mean quadratic diameter and mean canopy height, which, as discussed above, controls the local *H–D* allometry. Stand density and mean quadratic diameter can both be extracted from TLS data (e.g., Bauwens et al. 2016) more accurately and more easily than individual tree volumes, while a canopy height model within a scanned plot can be derived from the same TLS data. Once such a relationship is calibrated, airborne laser scanners (ALS, including those on unmanned aerial vehicles (UAVs)) suffice to derive AGB estimates from standard stem diameter measurements and WD estimates. However, the calibration step is challenging because it would ideally rely on destructive stand-level measurements. Such an approach would probably limit the propagation of individual errors, especially when neither tree height measurements nor a reliable local *H–D* allometry is available.

3 Matching Field and RS Measurements

When an RS signal is related to a field-based estimate of forest AGB, the basic assumption is that they both measure the same area and objects. This assumption is often violated in practice, leading to large uncertainty in the final AGB density maps (Gobakken and Naesset 2009; Frazer et al. 2011; Mascaro et al. 2011; Réjou-Méchain et al. 2014; Saatchi et al. 2015). Here, we review important sources of mismatch between field and RS measurements and identify ways to overcome them.

3.1 Geolocation Uncertainty

Geolocation mismatch between RS and field measurements is an obvious source of uncertainty (Frazer et al. 2011). Ground measurements are generally geolocated using a global navigation satellite system (GNSS) receiver, whose accuracy is known to vary with receiver quality or topographical and vegetation conditions by up to 2 orders of magnitude (Johnson and Barton 2004). In particular, GNSS accuracy decreases exponentially with the increase in canopy cover (Sigrist et al. 1999). From simultaneous acquisitions, Johnson and Barton (2004) found that 20% of the measurements had geolocation errors > 10 m under forest cover (due to multipathing effects), but only 2% in a nearby open area. Under unfavourable satellite conditions, the error even exceeded 200 m under forest cover. Under a dense forest cover in Gabon, a recent high-grade GNSS resulted in a mean measurement error of 5 m with 2.5% of extremes greater than 70 m (Fig. 5; Réjou-Méchain and Barbier, unpublished). Differential GNSS corrections did not reduce this uncertainty because vegetation cover prevents the use of phase-shift information. However, geolocation errors rapidly averaged out as the number of measurement points increased in either space (over a few tens of metres) or time (over several hours or days), stabilizing below 5 m with 20 measurement points and below 3 m with 50 measurement points. This result confirms the recommendation of Segrist et al. (1999) to collect at least 20 GNSS measurement points at different locations or times to accurately geolocate a field plot in dense forest conditions.

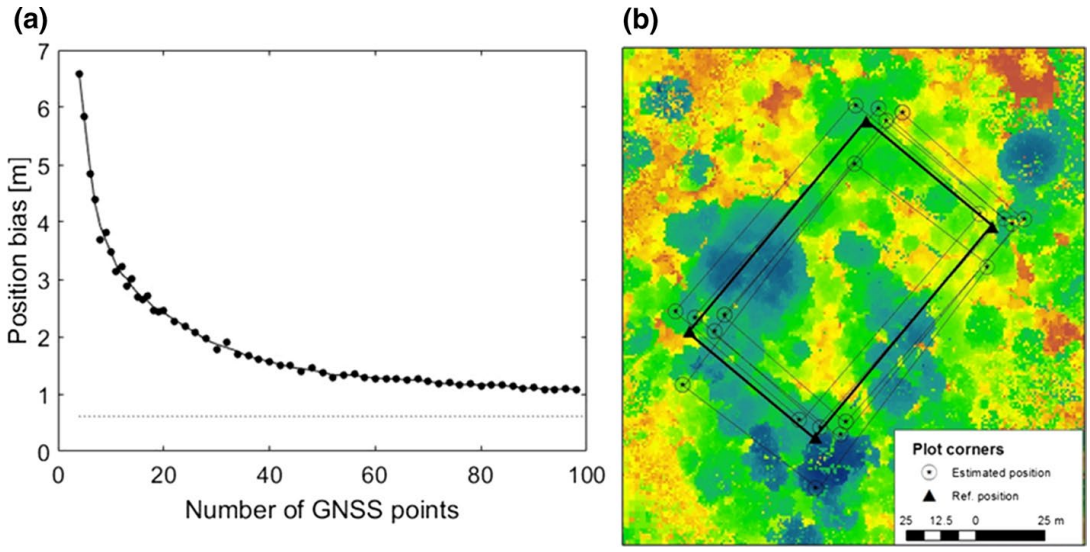

Fig. 5 Plot positioning error in a dense forest from Gabon. **a** The 75th percentile of mean position bias as a function of the number of GNSS points taken along plot limits from random point sets taken among 207 GNSS points (using a Trimble L1/L2 GEOXT 7000 rover GNSS device). The dotted line represents the background error level (e.g., due to imperfections in the relative positions of field marks). **b** An example of plot position bias for a 60 × 100 m plot at the 75th percentile of the error distribution using random sets of 4 GNSS points to estimate the transformation from local to UTM coordinates. Reference positions were provided by a professional topography consultant using a total station. Background colours show maximum canopy height (from brown to blue) from terrestrial laser scanning data

3.2 Acquisition Angle

Satellite-borne instruments do not always measure forests vertically (i.e. in nadir mode). When an active penetrating signal (e.g., RADAR or LiDAR) is sent with a large (pluri-metric) footprint size and a significant incidence angle (typically > 30° for RADAR sensors; Saatchi et al. 2011a; Robinson et al. 2013), the forest volume measured in field plots and intercepted by the satellite sensor does not correspond to the same physical objects, especially for small plots or in topographically complex areas (Villard and Le Toan 2015). Using theoretical simulations, Réjou-Méchain and Barbier (unpublished) found that an incidence angle of 30° may lead to volume differences of ca. 55, 20 and 10% for plot and pixel sizes of 20, 50 and 100 m, respectively, even if existing surrounding trees partly compensate for this mismatch. Thus, any RS signal acquired with a significant incidence angle should not be calibrated and validated with small field plots or in small patches of heterogeneous vegetation.

3.3 Mismatch in Tree Representation

The mismatch between the RS and field measurements may also be due to differences in tree representation. Conventional field measurements for AGB estimations are "trunk-based", i.e. a tree is considered to belong to a given field plot when half its trunk base section is within the plot limits, irrespective of the proportion of its vertical crown projection falling outside the plot. With RS approaches, AGB is measured from an area-based perspective, i.e. only the plant material with a ground projection within the area of interest is considered. Using LiDAR data, Mascaro et al. (2011) showed that

accounting for this edge effect reduces the LiDAR-AGB model error by 55, 21 and 4% at 20-, 50- and 100-m resolution, respectively, i.e. with a decrease in the perimeter-to-area ratio, the associated edge effects logically vanish because the proportion of trees with crowns crossing the plot edge decreases with the increase in plot size.

Differences in tree representation may also impact the estimates of forest C dynamics. Réjou-Méchain et al. (2015) compared the 4-year AGB dynamics inferred from repeated field plot censuses and LiDAR acquisitions and found relatively poor agreement between the two estimates; these authors concluded that different components of forest dynamics are measured by the two approaches. Natural canopy dynamics is dominated by many small-scale events that are captured by LiDAR data but not by field measurements (Kellner and Asner 2009; Leitold et al. 2018). Similarly, leaf density, which influences LiDAR estimates but not field estimates, regenerates faster than woody biomass after a disturbance (Asner et al. 2006). Thus, any dynamics inferred from RS measurements should be interpreted differently from the dynamics inferred from the ground.

3.4 Temporal Mismatch

The temporal difference between RS and field measurements is a common problem in RS studies. The impact of such temporal mismatches is difficult to predict in natural forests due to the high stochasticity of tree mortality. This stochasticity, however, decreases with the increase in plot size (Chambers et al. 2013); hence, the error associated with the temporal difference between measurements is likely to decrease with increasing plot size in the absence of major climate anomalies (e.g., El Niño events) or major disturbances, such as hurricanes or fires, which may be detected with Landsat (Kennedy et al. 2010) or MODIS (Justice et al. 2002) time series data. (MODIS is the Moderate Resolution Imaging Spectroradiometer aboard the NASA Terra and Aqua satellites.) In this case, estimated growth rates may be used to compensate for the time lag in AGB estimates from field and RS data (Avitabile and Camia 2018).

3.5 Scale Mismatch

The issue of scale mismatch between calibration field plots and RS data pixels is challenging, particularly when coarse-resolution RS products are calibrated with numerous small field plots such as national forest inventory data collected in sampling units less than 0.1 ha in size. For instance, the pantropical 1-ha resolution AGB map of Saatchi et al. (2011b) was calibrated using field plots that were typically ≤ 1 ha in size, hence representing a local sampling rate of 1% at best. For instance, Réjou-Méchain et al. (2014) showed that the use of calibration plots smaller than the RS pixels generates large sampling errors, producing significantly biased AGB maps (case Fig. 1c). For a given pixel-to-plot size ratio, the error due to local AGB variability is larger for small plots and pixels than for large plots and pixels (Réjou-Méchain et al. 2014). Thus, studies aiming at building coarse-resolution maps face the challenge of minimizing this sampling error. A common practice is to spatially aggregate field estimates to better match the RS pixel resolution; however, this approach results in large uncertainty in the associated sampling error (Avitabile and Camia 2018). A more reliable approach consists of using intermediate-resolution RS data, such as very high-resolution images, to bridge the gap.

4 Bridging Field and Satellite-Based Measurements

Field plots are generally too costly and time-consuming to establish to be densely and evenly distributed within landscapes. Consequently, RS models are often calibrated with field plots that are not representative of the area of interest (Marvin et al. 2014). Furthermore, field plot size rarely approaches the size of coarse-resolution RS pixels (e.g., MODIS, ca. 250 m), which are the current basis of the wall-to-wall biome or global mapping. This problem generates the mismatch issues discussed in the previous section. To overcome these problems, a multi-step upscaling approach involving RS data of very high spatial resolution (VHSR) can provide intermediate-scale biophysical maps to be then used as reference to calibrate wall-to-wall RS data of coarse resolution and broad swaths (Asner et al. 2013; Baccini and Asner 2013; Xu et al. 2017). In this section, we first review the VHSR RS products that may be used in such an approach and then discuss the caveats and perspectives associated with such a multi-step upscaling strategy.

4.1 Airborne LiDAR

Airborne LiDAR (ALS), with its ability to penetrate the canopy, provides a fine 3D description of the forest structure and represents an excellent option for linking field plots to broad-scale RS data. Over the last decade, a large number of studies have aimed at retrieving forest AGB from LiDAR-derived metrics, usually with good accuracy at the 1-ha scale (i.e. with a model prediction error typically below 15%; Zolkos et al. 2013). ALS allows for the computation of a variety of metrics related to the vertical or horizontal forest profile (Lefsky et al. 2002). Many studies have relied on statistical fittings (e.g., stepwise linear models) to identify the most predictive metrics in a given context, resulting in site-specific ALS–AGB model forms with limited transferability across sites (Vincent et al. 2012b; Zolkos et al. 2013). For this reason, some studies aimed at designing generic ALS–AGB models that were expected to perform consistently across sites. For instance, Bouvier et al. (2015) identified predefined metrics of strong complementarity and interpretability to build a generic model transferable across temperate forest types. In the tropics, another attempt used a single ALS metric, the mean top-of-canopy height (TCH), combined with minimal field data to predict forest AGB. Asner and Mascaro (2014) used data from 14 tropical areas to calibrate a model of the form $\mathrm{AGB} = a\mathrm{TCH}^{b1}\mathrm{BA}^{b2}\ \mathrm{WD}^{b3}$, where the basal area (BA) was locally predicted from TCH, and where WD relied on regional estimates. However, the fitted equation, which was presented as universal, led to underestimations of 7% (Jucker et al. 2017a) and 16% (Réjou-Méchain et al. 2015) in two independent sites compared with locally adjusted models. A modification of the model form was suggested by Vincent et al. (2014), where the scaling of AGB estimates from tree to plot used the stem number (N) and average stem cross-sectional area (or quadratic diameter) instead of BA to avoid unwarranted errors in the scaling process. A universal predictive equation that relates ALS metrics and AGB should continue to be sought to maximize the benefits from the increasing availability of ALS data (Labriere et al. 2018). However, as long as *H–D* variability is not accounted for, a single predictive equation would remain elusive. Furthermore, airborne data acquisition remains costly (ca. 200–500€ km^{-2}) and is subjected to flight authorization, which hampers ALS acquisitions in certain countries.

4.2 Unmanned Aerial Vehicle (UAV) Systems

UAVs may reduce the cost of airborne acquisitions and are thus increasingly utilized. UAV systems can generate 3D point clouds through the acquisition of very high-resolution passive imagery. The overlap between UAV acquisitions enables stereoscopic image processing with potentially very high spatial resolution and low cost compared to LiDAR systems (Puliti et al. 2015). Under the generic appellation of structure-from-motion approaches, the automation of traditional photogrammetry by the detection of invariant features in 2D images allows for the derivation of dense point clouds (Fig. 6). However, such systems mostly capture variation in the top of the canopy and have a rather low ability to penetrate dense forests, limiting the computation of forest height metrics (Roşca et al. 2018). UAV-borne LiDAR systems are rapidly developing but are still relatively new (Brede et al. 2017). With an optimized sampling strategy, these systems are able to generate a large number of points (thousands of pts m^{-2}), opening the door for individual tree volume reconstruction using toolboxes developed for TLS (Morsdorf et al. 2017), even if UAV-specific methods would be preferable due to an inverted vertical distribution of point density. However, flight authorization remains an issue in some countries, and even where authorized, maximum legal UAV piloting distances limit the acquisitions to rather small areas (e.g., ca. 300 ha in France).

4.3 VHSR Spaceborne Systems

Spaceborne data may be mobilized to complement ALS or UAV data and move beyond the relatively small extents of ALS and UAV campaigns, notably because these data can be acquired at a low cost and with few issues regarding authorizations. For instance, VHSR satellite optical images ($\leq$2 m resolution) are able to characterize canopy texture, which informs the size distribution of canopy crowns and inter-crown gaps (Couteron et al. 2005; Frazer et al. 2005), thus indirectly informing stand structure and AGB. Texture has historically been widely used in forest science for visual interpretation of aerial photographs. Similar interpretations from automated processing can be carried out from VHSR images via canopy texture analysis whenever images have sufficient effective resolution (the maximum acceptable seems to be approximately 2 m; Proisy et al. 2007). For instance, the Fourier-based textural ordination (FOTO) method aims to ordinate canopy image windows along texture gradients based on Fourier spectra (Couteron et al. 2005), and this method successfully retrieved the AGB gradients in several case studies across the tropics with an accuracy only slightly lower than that of ALS approaches (relative prediction error $\leq$20%; Proisy et al. 2007; Ploton et al. 2012; Bastin et al. 2014; Singh et al. 2014; Pargal et al. 2017) but at 50–100 times lower cost (2–10€ km^{-2} for optical images). Hence, the trade-off between data interpretability versus affordability should suggest designing scaling-up strategies based on nested sampling of field, airborne and VHSR satellite data. Satellite-borne optical sensors offering VHSR may thus be part of an effective chain for mapping AGB at landscape-regional scales. However, there are also situations in which texture analyses fail to properly retrieve certain AGB gradients (Ploton et al. 2013; Blanchard et al. 2015) because the way in which texture features relate to AGB strongly varies across forest types (Ploton et al. 2017). Due to the limited number of field plots available for calibration and validation, biophysical drivers of canopy texture have not been fully identified in previous studies. The increasing availability of ALS data will help to better evaluate such texture-based approaches and ultimately allow for the calibration and validation of texture indices in sufficiently diverse forest types. However, canopy texture,

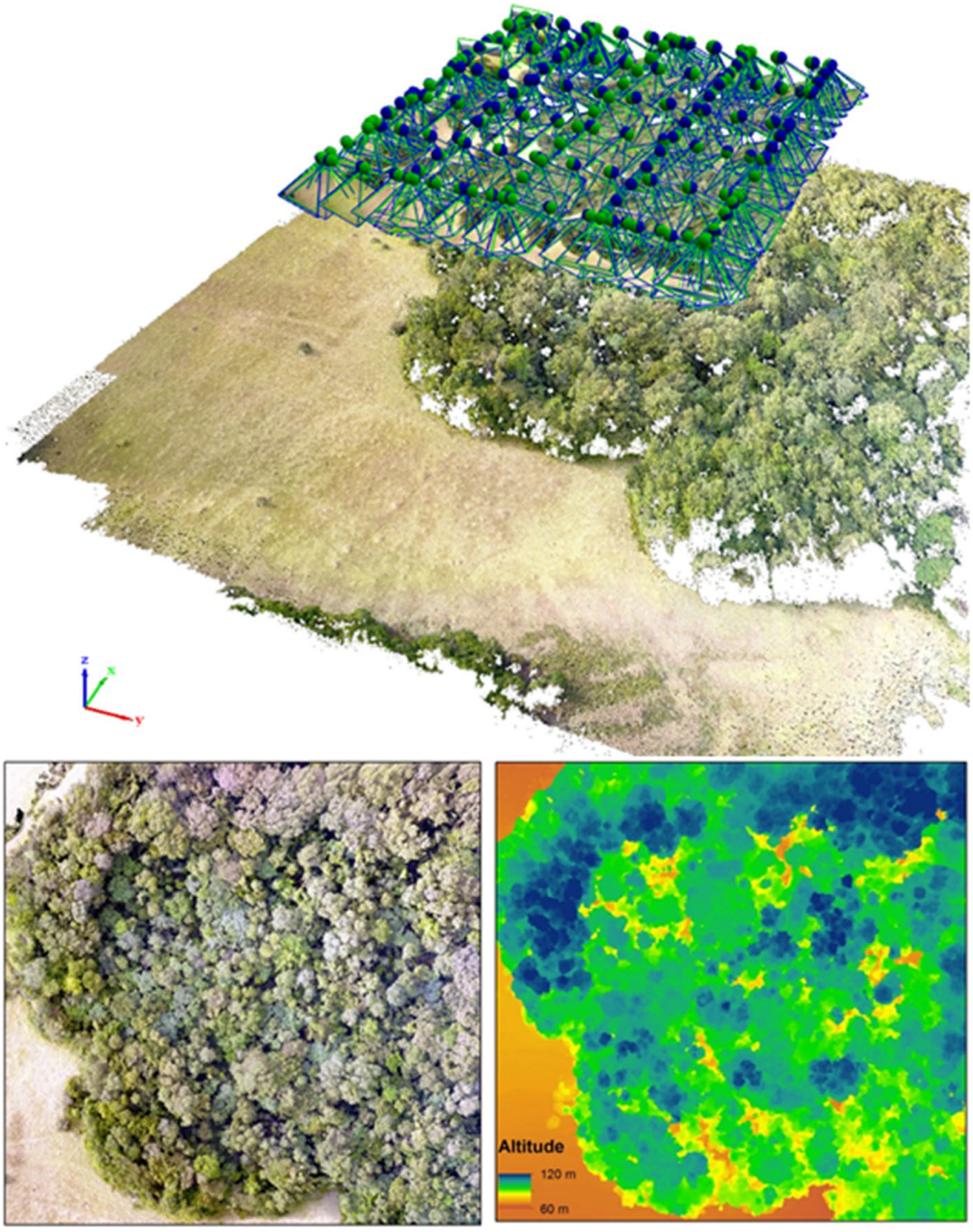

Fig. 6 Illustration of the structure-from-motion approach allowing for the derivation of an orthomosaic (lower left) and a surface model (lower right) by automated stereophotogrammetry from drone imagery (upper panel) in a forest-savanna mosaic from central Cameroon

such as reflectance, is strongly impacted by the Sun–scene–sensor geometry, although correction techniques have been proposed (Barbier et al. 2011; Barbier and Couteron 2015). The number of textural descriptors, therefore, needs to be kept to a minimum to control these effects in large collections of images acquired in diverse geometrical configurations.

Apart from texture indices, stereophotogrammetric approaches from VHSR satellite images allow for the retrieval of canopy surface models that may then be used to predict

AGB. This retrieval implies more cloud-free images and a higher budget for data acquisition and, contrary to LiDAR, stereophotogrammetric approaches do not provide information on fine-scale topographical variation, which is detrimental for building canopy height models. Thus, such approaches remain very scarce in the literature (St-Onge et al. 2008; Lagomasino et al. 2015). Finally, non-penetrating X-band RADAR satellite images used in stereo mode (Tandem-X) have also shown to have the potential to predict AGB gradients linked to logging and forest degradation and to assess AGB losses through diachronic comparisons (Schlund et al. 2015; Solberg et al. 2018).

4.4 Limits and Perspectives on Bridging Field and Satellites

Regardless of the VHSR product or model structure used for bridging field plots and large-scale RS data, there are several caveats. First, both the number of calibration field plots and their size remain important for restricting VHSR-based AGB prediction errors to acceptable limits. For instance, in a meta-analysis of LiDAR-based AGB estimations, Zolkos et al. (2013) showed an asymptotic decrease in the prediction error with the increase in the size of the calibration plots, with a slow decay on average above a plot size of 0.2 ha, corresponding to a prediction error of ca. 20%. However, highly contrasted results can be found across case studies, suggesting that prediction errors vary with forest structure at a given plot size. For instance, in tropical forests of Ghana, Chen et al. (2015) found a LiDAR-based prediction error on AGB of ca. 42% at a spatial resolution of 0.16 ha. Thus, AGB estimates derived from VHSR data and used for calibrating broad-scale products should be performed at a rather coarse resolution, with 1 ha being a conservative resolution to ensure an acceptable accuracy.

Another major problem that may arise during the plot to VHSR step is that significant biases may occur during the extrapolation of plot AGB estimates through the VHSR products. For instance, the prediction of AGB from local stand height or related RS metrics relies on knowledge of local WD and height–diameter allometry. As discussed in Sect. 2, both measures are known to vary, sometimes abruptly, within landscapes, and there is thus no guarantee against biases when extrapolating AGB estimates over areas where these variations are unknown. Stratifying the landscape by forest types prior to AGB model calibration thus appears essential to guarantee model robustness, although there are not many accounts of thorough pre-stratification processes in the literature (Gregoire et al. 2016). However, sources of complementary data are developing. Notably, hyperspectral sensors now appear to able be to provide information on canopy species composition and help infer WD (Jucker et al. 2018b). Moreover, some LiDAR metrics (e.g., canopy gap fractions) can help assess the disturbance or successional status of the forest with relevance for the explicit estimation of WD (Guitet et al. 2018).

5 Global Wall-to-Wall Extrapolation

Earth system models and international policy initiatives both require wall-to-wall data (Sitch et al. 2008; Romijn et al. 2018; Herold et al. 2019). Thus, there is a strong need for going beyond local to regional AGB estimates to produce unified AGB density maps at the biome or global scale. Pantropical, temperate, boreal and global AGB maps have been proposed in the last decade, most often by extrapolating field-based and/or LiDAR-based AGB

estimations through the use of global optical, RADAR and environmental datasets. In this section, we discuss the issues associated with large-scale AGB mapping and the promise of new methods and upcoming spaceborne missions.

5.1 The Problem of Interpolation

None of the RS systems available to date that display fair to good correlation with AGB (with no signal saturation) offers wall-to-wall coverage at very broad scales (i.e. regions, countries, continents). At best, these systems provide a fairly systematic sampling of the earth surface under the form of belt transects (e.g., ICESat/GLAS or the upcoming GEDI and MOLI missions). This condition implies that an interpolation step is necessary to produce a continuous AGB map from this discrete sampling. To that end, all published approaches have used or combined statistical interpolation (e.g., kriging or co-kriging with environmental drivers) and predictions from high- to medium-resolution spaceborne RS data to produce wall-to-wall coverage (e.g., Landsat, MODIS, QuickScat, ALOS PALSAR). For instance, Saatchi et al. (2011b) and Baccini et al. (2012) mapped AGB over the tropics by spatially interpolating discrete AGB estimates using Quick Scatterometer and/or MODIS data. Avitabile et al. (2016) then combined these two maps and used additional reference data (field plots and locally calibrated maps) in an attempt to generate an improved AGB map. Finally, the map from Santoro et al. (2018) was derived at 100-m resolution using a combination of maps based on ALOS PALSAR, ASAR data, Landsat data and ICESat GLAS transects, without any calibration from in situ data.

The use of these RS data for estimating AGB at a large scale raises two problems, which remain largely unsolved. First, most current satellite-based data relate to signals for which relationships to AGB are saturating and/or highly context-dependent (Steininger 2000), due to either varying relationships between AGB and RS signals or signal artefacts. Optical images are affected by geometrical and atmospheric effects that may produce significant spatial and/or seasonal artefacts in surface reflectance (Morton et al. 2014). For instance, the high degree of cloudiness in western Gabon and Cameroon is known to strongly impact MODIS reflectance data and is likely the reason why Baccini et al. (2012) underestimated the AGB values in this region (Fig. 7). Similarly, RADAR data are affected by factors related to forest structure and the environment (e.g., soil and vegetation moisture, topography) and the uncertainties associated with RADAR data acquisition (Villard and Le Toan 2015). Second, in natural tropical forests, stand structure variables often strongly vary over short distances. Variograms computed on field plot networks reported spatial correlation in AGB or BA that barely reached 5 km (Guitet et al. 2015; Hajj et al. 2017). This result means that locations that are more than 4–5 km apart are virtually independent; thus, any reliable AGB estimate conveys no useful information for interpolation beyond this distance.

Thus, it is not surprising that strong inconsistencies have been reported among broad-scale AGB maps (Mitchard et al. 2013; Huang et al. 2015; Rodriguez-Veiga et al. 2017). For example, Mitchard et al. (2013) compared two widely used pantropical maps (Saatchi et al. 2011b, Baccini et al. 2012) and found fairly consistent estimates at the continental scale but large regional differences ($>100\%$) within continents. In Amazonia, a comparison with field estimates suggested that both pantropical maps failed to capture the AGB gradient across regions with some regions over- or underestimated by $>25\%$ (Mitchard et al. 2014). However, without a systematic field sampling of AGB at a large scale, as done

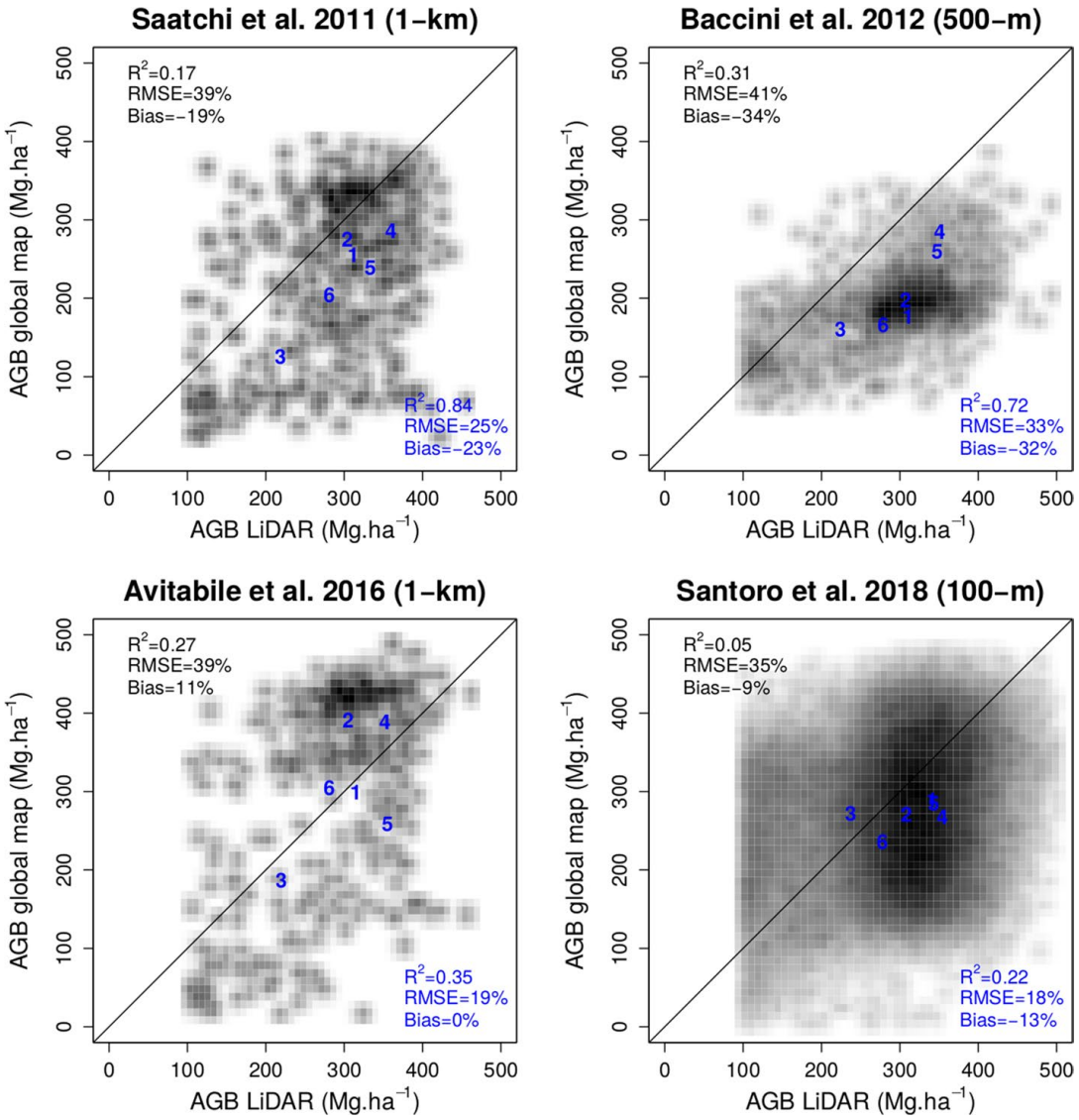

Fig. 7 Validation of global and pantropical maps using independent AGB estimates from six airborne LiDAR (ALS) campaigns in French Guiana and Gabon in forests > 100 Mg ha^{-1}. The results are reported at both the pixel (black) and mean AGB site (blue) level (1: Lope; 2: Mabounie; 3: Mondah; 4: Nouragues; 5: Paracou; 6: Rabi). ALS–AGB density maps at 50 m resolution were first resampled to the resolution of the pantropical and global maps using the Geospatial Data Abstraction Library (GDAL) *gdalwarp* routine in average mode. ALS- and global AGB density maps were then superimposed using bicubic interpolation (Inglada and Vadon 2005) through the *otbcli_Superimpose* routine of the Orfeo ToolBox (https://www.orfeo-toolbox.org/). Spatial correlations using fast Fourier transforms in moving windows confirmed that the spatial match between both AGB estimates was high (uncertainty was below the pixel resolution)

in national forest inventories (Kleinn 2017), it is difficult to validate whether a map captures the regional AGB gradients.

In Fig. 7, we report the result of a comparison of five existing pantropical/global AGB maps with six LiDAR-based AGB maps from Africa and French Guiana (Labriere et al. 2018). The results confirm that in dense forests (> 100 Mg ha^{-1}), broad-scale maps display relatively weak ($R^2 \leq 0.3$) if any correlation at the pixel level with independent AGB data of improved quality. However, some maps exhibit much higher correlations than others considering the very coarse-resolution gradients (here the mean AGB per LiDAR site),

with the R^2 value for the map of Saatchi et al. (2011b) exceeding 0.8. Although this result is based on six observations and should be confirmed with more sites, it could suggest that broad-scale AGB variations may be successfully captured with such maps. These comparisons shed some light on the uncertainty associated with these AGB map estimates, but they also convey their own errors for validation or accuracy assessments for at least two reasons. First, the maps are all produced for different time periods, e.g., the Saatchi et al. (2011b) map is for ca. 2000, the Baccini et al. (2012) map is for ca. 2008 and Avitabile et al. (2016) combined these two maps using ground- and LiDAR-estimated AGB at different spatial scales and time periods. Second, the definition of forest and AGB may be different for each map. In Saatchi et al. (2011b), the biomass estimate at 1 km referred to the biomass of remaining forest in each 1 km grid cell, whereas in all other maps, the estimates referred to the mean biomass at the grid cell of the map (average of forest and non-forest biomass).

5.2 The Use of Environmental Proxies

One possible way to mitigate the aforementioned difficulties that hinder interpolation is to rely on spatialized environmental proxies to enhance the mapping. In the central Amazon, Saatchi et al. (2007) used a multivariate decision tree approach featuring both environmental variables (e.g., elevation, climate) and saturating RS metrics (e.g., Qscat_SV, NDVI) and found that AGB classes referring to values above 250 Mg ha^{-1} were mainly located in areas below 190 m elevation and of limited ruggedness (both assessed from SRTM). AGB is indeed known to covary with topography globally (Réjou-Méchain et al. 2014), but the strength and direction of the relationship strongly vary across sites (de Castilho et al. 2006; McEwan et al. 2011; Detto et al. 2013; Réjou-Méchain et al. 2015). Some studies successfully relied on spatialized climatic variables (Simard et al. 2011; Fayad et al. 2016) or geomorphological units (Guitet et al. 2015) to predict AGB or forest height in particular regional contexts. Thus, the ongoing development and improvement of global databases of environmental variables open avenues for geographically enlarging such approaches bearing in mind that relationships between AGB and the environment are intrinsically context-dependent. Indeed, AGB is largely driven by complex edaphic processes, such as soil structure (Gourlet-Fleury et al. 2011; Jucker et al. 2018b) or water table and bedrock depth (Emilio et al. 2013), which often vary at a relatively fine scale and for which continuous information is lacking. Furthermore, past and present anthropogenic activities, which are not randomly distributed according to abiotic conditions, may largely blur such environmental determinism at large scales. Therefore, calibration and prediction should be designed according to a relevant pre-stratification of the territory, accounting for anthropogenic activities, with sufficient reference data in each stratum.

5.3 Perspectives on Extrapolation

Upcoming RADAR satellite missions, such as NISAR in 2021 (Rosen et al. 2017) and BIOMASS in 2022 (Le Toan et al. 2011), should be pivotal in global-scale AGB mapping by providing wall-to-wall active measurements. While NISAR will be relevant for low AGB areas due to the use of an L-band saturating signal, BIOMASS will operate with a 50-m resolution P-band signal that is sensitive to large AGB values. (AGB products will, however, be delivered at 200-m resolution.) Preliminary analyses from P-band airborne missions revealed that polarimetric intensities (PolSAR) and polarimetric RADAR

interferometry (PolInSAR) correlated well with AGB values up to 300 Mg ha^{-1} in temperate and tropical areas (ESA 2012). Above 300 Mg ha^{-1}, such approaches failed to detect AGB variations, but tomographic approaches may significantly improve the retrieval of AGB up to 500 Mg ha^{-1} with no obvious saturation and a prediction error of only ca. 10% at a 1.5-ha resolution (Minh et al. 2014). A cross-validation performed between two sites of tropical forests in French Guiana suggested that tomographic models are transferable with an error within 20% at 1-ha resolution (Minh et al. 2016). However, these approaches rely on multiple acquisitions with different geometries over the same site, constituting a challenge for a spaceborne sensor and limiting the areas that may be covered in such a way. As a consequence, tomography will be implemented in only the first year of the mission; the three subsequent years will instead correspond to an interferometry phase. Beyond AGB mapping, the upcoming missions, including GEDI and MOLI, also constitute a unique opportunity to better understand the relationship between forest AGB, productivity and spatialized environmental proxies in tropical dense forests.

Finally, if future missions will considerably improve our ability to monitor AGB in space and time, the full potential of current RS products has not yet been completely assessed. For instance, using multi-angle MODIS observations to characterize the anisotropy of forests, de Moura et al. (2016) were able to generate metrics that displayed a good correlation ($r^2 > 0.5$) with ALS-derived metrics in high AGB forests in the Brazilian Amazon, with no apparent saturation. This result adequately illustrates that there is also room for progress through the development of new methodologies to be used with the current RS products.

6 Radiative Transfer Modelling for Understanding Error Sources

A prerequisite to controlling the sources of errors in satellite-based assessments of forest AGB is to understand how the electromagnetic signal of interest interacts with forest components. Contrary to sea surface temperature, for instance, there is not yet any sensor that directly measures woody AGB per se. We thus use the variations in proximal measurements or indices to infer the AGB variations; however, these measures may be prone to interferences and artefacts that sometimes blur the true response of the forest AGB. Thus, radiative transfer (RT) modelling has become a standard approach in RS to analyse sensor sensitivity, and inverse modelling is used to measure the extent at which specific forest information is recoverable from the recorded signals. Some recent prominent examples can be found in studies that investigated the seasonal variation in leaf area in tropical forests (Morton et al. 2014; Wu et al. 2018) or texture retrieval of forest AGB from VHSR optical images (Ploton et al. 2017). Even crude modelling approaches may prove useful to untangle complex interactions in the sensor–atmosphere–scene–light source system (Barbier et al. 2011; Barbier and Couteron 2015), but a key point in such simulation studies is the way in which the complex 3D organization of tropical forest components can be represented. We will focus here on examples involving passive and active optical signals, but similar progress can be observed in RADAR studies (Villard 2009), which were historically pioneering (Ishimaru 1978).

6.1 An Increase in Model Realism

In the early days, geometric-optic models were used to understand the variation in directional reflectance within large pixels comprising a number of objects (e.g., trees) (Egbert 1977; Li and Strahler 1992; Roujean et al. 1992; Ni et al. 1999). Scene reflectance was computed as the sum of nominal reflectance of the components (e.g., shaded and lit surfaces) of a projection of simple, generally opaque, geometrical shapes within a scene. These efforts allowed for the derivation of analytical functions (kernels) that proved useful to fit actual directional reflectance variations with a small number of parameters (e.g., Lyapustin et al. 2011).

As computing power increased, it became possible to increase scene complexity, as well as to improve the level of detail in the descriptions of light–matter interactions. Discrete ray-tracing models based on Monte Carlo simulations of photon behaviour and (multiple) scattering within the scene have now become standard. This phenomenon is, for instance, evidenced by the periodic RAMI (RAdiation transfer Model Intercomparison) experiment, which aims at benchmarking and testing a number of existing models (Widlowski et al. 2013). Initially, scenes represented homogeneous parallel layers (Verhoef 1985; Myneni et al. 1989) of a turbid medium, in which the macroscopic transfer equation was statistically deduced from the microscopic distribution of elements, such as leaves or aerosols, within the cell. These elements were characterized by a density and angle distribution, as well as optical properties, which imply a probability of intercepting light rays depending on the incoming and outgoing directions. In addition to turbid elements, solid surfaces can be added in the form of triangle meshes to represent scene elements other than leaves (woody parts, roads, ground, building or water bodies). Triangles can be translucid and display Lambertian, specular or other optical properties. Progressively, spatial heterogeneity was introduced in the turbid medium distribution (Myneni 1991; Gastellu-Etchegorry et al. 1996; North 1996). Indeed, as opposed to most annual crops, crown shading is fundamental to understanding scene reflectance in forests. This fundamental need is even more pronounced when the spatial resolution of a sensor increases to a point where the pixels are smaller than the tree crowns, as biophysical descriptors can then be found in the texture features, and describing the spatial arrangement of reflectance values is crucial (Couteron et al. 2005; Barbier et al. 2011; Barbier and Couteron 2015). The degree of realism of a 3D description has evolved from sets of floating spheres or ellipsoids to more complex envelopes describing tree crown contours (Cescatti 1997; Widlowski et al. 2013). The dimensions and spatial distributions of these envelopes can generally be inferred from standard forestry measurements or allometric equations (Barbier et al. 2011).

To further improve the realism of the forest scenes, LiDAR data constitute a giant leap forward, as they provide both access to a detailed description of the geometry and topology of solid surfaces (trunks and branches) and a statistical sampling of foliage directly compatible with the turbid representation via voxelization procedures accounting for spatial sampling variations (Grau et al. 2017; Tymen et al. 2017; Vincent et al. 2017). In a temperate montane forest, a voxel-based approach performed better at simulating hyperspectral data than an approximation of individual tree envelopes (Schneider et al. 2014). Given the importance of LiDAR technology in detailed measurements of vegetation from space, air or ground stations, simulating the transfer of this active signal in vegetation is now itself an active field of study (Sun and Ranson 2000; Gastellu-Etchegorry et al. 2015). Figure 8 illustrates the current possibilities and challenges for the realistic simulation of dense tropical forests. On the one hand, the integration of the structure derived from airborne LiDAR

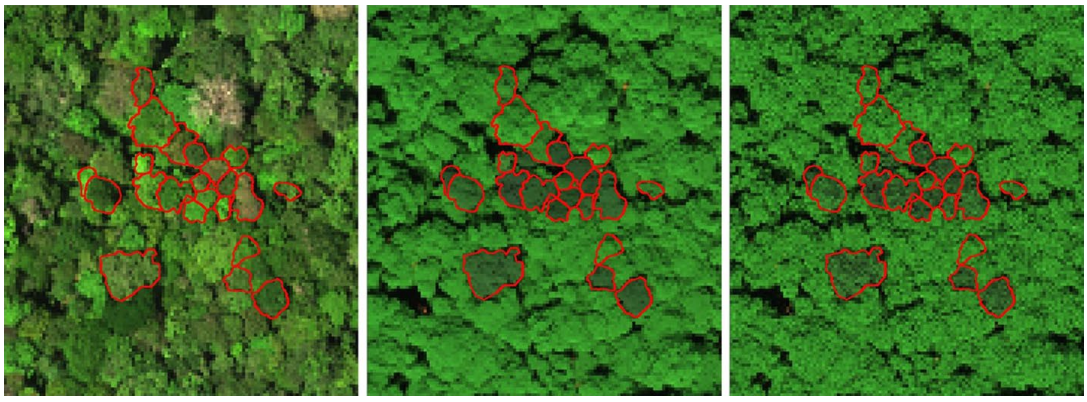

Fig. 8 Simulation of airborne optical imaging in a tropical forest from French Guiana (Paracou). The simulation is based on the integration of airborne LiDAR and field spectroscopy in the DART 3D radiative transfer model (Gastellu-Etchegorry et al. 2015). The 3D mock-ups were computed from airborne LiDAR point clouds using AMAPvox (Vincent et al. 2017), and leaf optical properties corresponding to sampled trees (delineated in red) were measured with a field spectroradiometer and assigned to leaf elements from all voxels on the vertical column of the mock-up. A generic set of leaf optical properties was applied to all trees with undocumented leaf optical properties using the PROSPECT leaf model (Féret et al. 2017). Left: original image (red = 640 nm; green = 549 nm; blue = 458 nm); centre: simulation using a turbid representation for leaf elements; right: simulation using triangle approach for leaf elements

acquisitions allows accurate simulation of canopy grain and gaps with metric resolution. On the other hand, the lack of information about the proportion of leaf versus woody elements (Malenovskỳ et al. 2008) and the difficulty in accurately characterizing the diversity of leaf optical properties at the canopy scale contribute to the relatively low radiometric agreement. Better accounting for the differences in radiometric properties among species or individuals and possibly within individuals would require a better understanding of the spatial heterogeneity of spectral properties (Féret and Asner 2014; Rocchini et al. 2018).

6.2 Limits and Perspectives on RT Modelling

The current difficulties that need to be overcome to effectively derive forest mock-ups from TLS data are the same as those mentioned above for deriving AGB estimates from TLS. For instance, individual tree segmentation is required to allocate species-specific radiometric properties to individual trees. In addition, accurate segmentation of leaves from wood and proper estimation of leaf angle distribution are required to accurately simulate light–vegetation interactions (Antin et al. 2015). These steps become more difficult in the upper canopy as the density of the TLS point cloud decreases dramatically due to occlusion and increasing distance from the laser source. This difficulty may, however, be minimized through the fusion of TLS and UAV data. Finally, a better understanding of leaf demography and its integration into advanced modelling of leaf optical properties, combined with the improved description of non-photosynthetic tissues in LiDAR-derived 3D mockups, will increase the realism of simulations derived from physical modelling.

An alternative to producing a forest scene with a turbid description of leaves is to use an architectural model to simulate the tree branching structure and individual leaf distribution (De Reffye et al. 1995; Dauzat et al. 2001; Côté et al. 2011; Widlowski et al. 2013; Calders et al. 2018). Independently of the biological realism of such detailed scene descriptions, these models provide a means to assess the degradation of the transfer modelling outcome

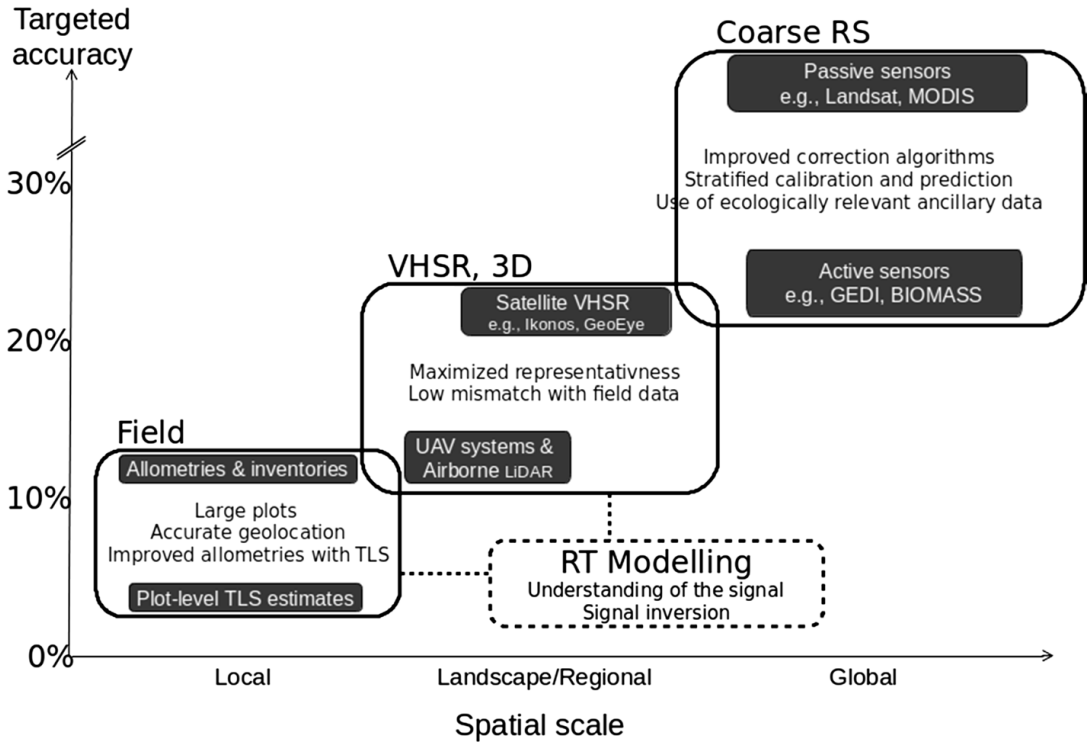

Fig. 9 Best-practice guidelines to upscale AGB estimates from local to global scales. The targeted accuracy (*Y* axis) refers to a 1-ha scale

as the scene is progressively simplified in terms of representation (Jonckheere et al. 2006; Widlowski et al. 2013; Antin et al. 2015).

7 Conclusions and Perspectives

By reviewing the advances and limitations in biomass estimation at each level of the processing chain, we propose a logical workflow that combines what could be considered as best practices given the current state of knowledge (Fig. 9).

Because almost all steps of the processing chain rely on statistical models, the quality of calibration/validation data is crucial, yet often neglected. In this review, we first discussed common-sense procedures to drastically reduce the error levels at the field plot scale, such as improving georeferencing, increasing field plot size (1 ha or more) or developing allometric equations that better account for local ecological variations in plant composition and/or architecture. Terrestrial LiDAR scanning appears to be a promising avenue for individual-level and plot-level measurements of aboveground volumes. Combined with representative WD estimates that account for the intra- and inter-individual patterns of WD variations, robust predictions of AGB may be achievable. Furthermore, the combination of TLS and airborne LiDAR measurements in the upscaling scheme may significantly reduce the source of mismatches described in Sect. 3, allowing for the easy-to-perform control of coregistration and ensuring a continuum in the measured objects (Kükenbrink et al. 2017).

The extrapolation of local estimates to global scales should ideally be performed in successive steps, relying on intermediate, high-resolution data, such as VHSR spaceborne

optical imagery, airborne or UAV-based LiDAR and (UAV-based) stereophotogrammetry. These data can be used to estimate AGB with an accuracy close to the accuracy of ground estimates, but they dramatically increase the representativeness of calibration data when earth observation data of decreased sensitivity (but also decreased cost) are to be used for regional to global predictions. The recent and rapid development of UAV systems, which currently fill the gap between terrestrial and airborne laser scanning systems, is particularly promising because these systems have the potential to bridge different spatial scales, from within-individual-tree to Earth observation pixels of medium resolution (e.g., MODIS).

In parallel, efforts should be expanded to better understand the interactions between different types of electromagnetic signals in varying contexts, e.g., RADAR, LiDAR and passive optical systems, to fully assess the potential of multisensor data fusion. These interactions may be largely blurred by numerous sources of noise and bias—instrumental, atmospheric, geometric, etc. Radiative Transfer (RT) modelling and the prospect to attain a high degree of realism in 3D stand modelling have made this approach a central tool for performing sensitivity analysis and designing signal correction algorithms. Assuming that 3D simulated stands will soon closely reflect reality, they may even be used to directly calibrate inversion models, bypassing many issues such as plot geolocation problems.

The last promise comes from the launch of new space missions (BIOMASS, GEDI, Icesat-2, MOLI, NISAR), which will improve our extrapolation capacities by providing both global coverage and signals of increased relevance. However, whether used individually or in fusion, the calibration of these products should rely on a pre-stratification of forested lands, with enough reference data in each stratum, as it is unlikely that a single universal model can be transferable across forest types and regions without biases.

To conclude, even high-quality Earth observation data currently do not meet the requirements of international environmental policies (e.g., IPCC GPG, REDD+, SDGs, see Herold et al. 2019). Understanding the sources of error and pathways to improve biomass estimation at all levels (as explained in this paper) is fundamental to implementing the best possible practices at each step, resulting in high-quality, consistent biomass estimates with uncertainties quantified to serve the various applications and users.

Acknowledgements We gratefully thank the organizers of the Workshop held at ISSI Bern in November 2017 that was at the origin of this Special Issue. This review has been conducted under the project 3DForMod funded by ERA-GAS (ANR-17-EGAS-0002-01, NWO-3DForMod-5160957540) and has also benefited from the "Investissement d'Avenir" programs managed by Agence Nationale de la Recherche (CEBA, ref. ANR-10-LABX-25-01).

References

Antin C, Grau E, Vincent G et al (2015) From leave scale to tree scale: which structural parameters influence a simulated full-waveform large-footprint LiDAR signal? SilviLaser 2015:110–112

Arciniegas A, Prieto F, Brancheriau L, Lasaygues P (2014) Literature review of acoustic and ultrasonic tomography in standing trees. Trees 28:1559–1567

Asner GP, Mascaro J (2014) Mapping tropical forest carbon: calibrating plot estimates to a simple LiDAR metric. Remote Sens Environ 140:614–624

Asner GP, Broadbent EN, Oliveira PJC et al (2006) Condition and fate of logged forests in the Brazilian Amazon. Proc Natl Acad Sci 103:12947–12950. https://doi.org/10.1073/pnas.0604093103

Asner GP, Mascaro J, Anderson C et al (2013) High-fidelity national carbon mapping for resource management and REDD+. Carbon Balance Manag 8:1–14. https://doi.org/10.1186/1750-0680-8-7

Avitabile V, Camia A (2018) An assessment of forest biomass maps in Europe using harmonized national statistics and inventory plots. For Ecol Manag 409:489–498. https://doi.org/10.1016/j.foreco.2017.11.047

Avitabile V, Herold M, Heuvelink GBM et al (2016) An integrated pan-tropical biomass map using multiple reference datasets. Glob Change Biol 22:1406–1420. https://doi.org/10.1111/gcb.13139

Baccini A, Asner GP (2013) Improving pantropical forest carbon maps with airborne LiDAR sampling. Carbon Manag 4:591–600

Baccini A, Goetz SJ, Walker WS et al (2012) Estimated carbon dioxide emissions from tropical deforestation improved by carbon-density maps. Nat Clim Change 2:182–185. https://doi.org/10.1038/nclimate1354

Baker TR, Phillips OL, Malhi Y et al (2004) Variation in wood density determines spatial patterns in Amazonian forest biomass. Glob Change Biol 10:545–562

Banin L, Feldpausch TR, Phillips OL et al (2012) What controls tropical forest architecture? Testing environmental, structural and floristic drivers. Glob Ecol Biogeogr 21:1179–1190. https://doi.org/10.1111/j.1466-8238.2012.00778.x

Barbier N, Couteron P (2015) Attenuating the bidirectional texture variation of satellite images of tropical forest canopies. Remote Sens Environ 171:245–260

Barbier N, Proisy C, Véga C et al (2011) Bidirectional texture function of high resolution optical images of tropical forest: an approach using LiDAR hillshade simulations. Remote Sens Environ 115:167–179

Bastin J-F, Barbier N, Couteron P et al (2014) Aboveground biomass mapping of African forest mosaics using canopy texture analysis: toward a regional approach. Ecol Appl 24:1984–2001. https://doi.org/10.1890/13-1574.1

Bastin J-F, Fayolle A, Tarelkin Y et al (2015a) Wood specific gravity variations and biomass of central african tree species: the simple choice of the outer wood. PLoS ONE 10:e0142146

Bastin J-F, Barbier N, Réjou-Méchain M et al (2015b) Seeing Central African forests through their largest trees. Sci Rep 5:13156

Bauwens S, Bartholomeus H, Calders K, Lejeune P (2016) Forest inventory with terrestrial LiDAR: a comparison of static and hand-held mobile laser scanning. Forests 7:127

Béland M, Baldocchi DD, Widlowski J-L et al (2014) On seeing the wood from the leaves and the role of voxel size in determining leaf area distribution of forests with terrestrial LiDAR. Agric For Meteorol 184:82–97

Blanchard E, Birnbaum P, Proisy C et al (2015) Prédire la structure des forêts tropicales humides calédoniennes: analyse texturale de la canopée sur des images Pléiades. Rev Fr Photogrammétrie Télédétection 209:141–147

Bouvet A, Mermoz S, Le Toan T et al (2018) An above-ground biomass map of African savannahs and woodlands at 25 m resolution derived from ALOS PALSAR. Remote Sens Environ 206:156–173

Bouvier M, Durrieu S, Fournier RA, Renaud J-P (2015) Generalizing predictive models of forest inventory attributes using an area-based approach with airborne LiDAR data. Remote Sens Environ 156:322–334

Brede B, Lau A, Bartholomeus HM, Kooistra L (2017) Comparing RIEGL RiCOPTER UAV LiDAR derived canopy height and DBH with terrestrial LiDAR. Sensors 17:2371

Bustamante MMC, Roitman I, Aide TM et al (2016) Toward an integrated monitoring framework to assess the effects of tropical forest degradation and recovery on carbon stocks and biodiversity. Glob Change Biol 22:92–109. https://doi.org/10.1111/gcb.13087

Calders K, Newnham G, Burt A et al (2014) Nondestructive estimates of above-ground biomass using terrestrial laser scanning. Methods Ecol Evol. https://doi.org/10.1111/2041-210x.12301

Calders K, Origo N, Burt A et al (2018) Realistic forest stand reconstruction from terrestrial LiDAR for radiative transfer modelling. Remote Sens 10:933

Cescatti A (1997) Modelling the radiative transfer in discontinuous canopies of asymmetric crowns. I. Model structure and algorithms. Ecol Model 101:263–274

Chambers JQ, Negron-Juarez RI, Marra DM et al (2013) The steady-state mosaic of disturbance and succession across an old-growth Central Amazon forest landscape. Proc Natl Acad Sci 110:3949–3954. https://doi.org/10.1073/pnas.1202894110

Chanthorn W, Hartig F, Brockelman WY (2017) Structure and community composition in a tropical forest suggest a change of ecological processes during stand development. For Ecol Manag 404:100–107. https://doi.org/10.1016/j.foreco.2017.08.001

Chave J, Condit R, Aguilar S et al (2004) Error propagation and scaling for tropical forest biomass estimates. Philos Trans R Soc Lond Ser B-Biol Sci 359:409–420

Chave J, Andalo C, Brown S et al (2005) Tree allometry and improved estimation of carbon stocks and balance in tropical forests. Oecologia 145:87–99. https://doi.org/10.1007/s00442-005-0100-x

Chave J, Coomes D, Jansen S et al (2009) Towards a worldwide wood economics spectrum. Ecol Lett 12:351–366
Chave J, Réjou-Méchain M, Búrquez A et al (2014) Improved allometric models to estimate the aboveground biomass of tropical trees. Glob Change Biol 20:3177–3190. https://doi.org/10.1111/gcb.12629
Chen Q, Laurin GV, Valentini R (2015) Uncertainty of remotely sensed aboveground biomass over an African tropical forest: propagating errors from trees to plots to pixels. Remote Sens Environ 160:134–143
Clark DA (2002) Are tropical forests an important carbon sink? Reanalysis of the long-term plot data. Ecol Appl 12:3–7. https://doi.org/10.1890/1051-0761(2002)012%5b0003:atfaic%5d2.0.co;2
Clark D, Clark D (2000) Landscape-scale variation in forest structure and biomass in a tropical rain forest. For Ecol Manag 137:185–198. https://doi.org/10.1016/s0378-1127(99)00327-8
Clark DB, Kellner JR (2012) Tropical forest biomass estimation and the fallacy of misplaced concreteness. J Veg Sci 23:1191–1196. https://doi.org/10.1111/j.1654-1103.2012.01471.x
Condit R (1998) Tropical forest census plots: methods and results from Barro Colorado Island, Panama and a comparison with other plots. Springer, Berlin
Condit R, Ashton PS, Baker P et al (2000) Spatial patterns in the distribution of tropical tree species. Science 288(5470):1414–1418
Condit R, Lao S, Singh A et al (2014) Data and database standards for permanent forest plots in a global network. For Ecol Manag 316:21–31
Côté J-F, Fournier RA, Egli R (2011) An architectural model of trees to estimate forest structural attributes using terrestrial LiDAR. Environ Model Softw 26:761–777. https://doi.org/10.1016/j.envsoft.2010.12.008
Couteron P, Pelissier R, Nicolini EA, Paget D (2005) Predicting tropical forest stand structure parameters from Fourier transform of very high-resolution remotely sensed canopy images. J Appl Ecol 42:1121–1128
Dauzat J, Rapidel B, Berger A (2001) Simulation of leaf transpiration and sap flow in virtual plants: model description and application to a coffee plantation in Costa Rica. Agric For Meteorol 109:143–160
de Castilho CV, Magnusson WE, de Araújo RNO et al (2006) Variation in aboveground tree live biomass in a central Amazonian forest: effects of soil and topography. For Ecol Manag 234:85–96. https://doi.org/10.1016/j.foreco.2006.06.024
de Moura YM, Hilker T, Goncalves FG et al (2016) Scaling estimates of vegetation structure in Amazonian tropical forests using multi-angle MODIS observations. Int J Appl Earth Obs Geoinf 52:580–590
De Reffye P, Houllier F, Blaise F et al (1995) A model simulating above-and below-ground tree architecture with agroforestry applications. Agrofor Syst 30:175–197
de Souza Pereira FR, Kampel M, Gomes Soares ML et al (2018) Reducing uncertainty in mapping of mangrove aboveground biomass using airborne discrete return LiDAR data. Remote Sens 10:637
Detto M, Muller-Landau HC, Mascaro J, Asner GP (2013) Hydrological networks and associated topographic variation as templates for the spatial organization of tropical forest vegetation. PLoS ONE 8:e76296. https://doi.org/10.1371/journal.pone.0076296
Dickinson TA, Tanner EVJ (1978) Exploitation of hollow trunks by tropical trees. Biotropica 10:231–233. https://doi.org/10.2307/2387908
Disney M (2018) Terrestrial LiDAR: a 3D revolution in how we look at trees. New Phytol. https://doi.org/10.1111/nph.15517
Egbert DD (1977) A practical method for correcting bidirectional reflectance variations. In: LARS symposia, p 203
Emilio T, Quesada CA, Costa FRC et al (2013) Soil physical conditions limit palm and tree basal area in Amazonian forests. Plant Ecol Divers 10:1. https://doi.org/10.1080/17550874.2013.772257
ESA (2012) Report for mission selection: biomass, ESA SP-1324/1 (3 volume series). European Space Agency Noordwijk, The Netherlands
Fayad I, Baghdadi N, Guitet S et al (2016) Aboveground biomass mapping in French Guiana by combining remote sensing, forest inventories and environmental data. Int J Appl Earth Obs Geoinf 52:502–514
Fayolle A, Doucet J-L, Gillet J-F et al (2013) Tree allometry in Central Africa: testing the validity of pantropical multi-species allometric equations for estimating biomass and carbon stocks. For Ecol Manag 305:29–37. https://doi.org/10.1016/j.foreco.2013.05.036
Feldpausch TR, Banin L, Phillips OL et al (2011) Height–diameter allometry of tropical forest trees. Biogeosciences 8:1081–1106
Feldpausch TR, Lloyd J, Lewis SL et al (2012) Tree height integrated into pantropical forest biomass estimates. Biogeosciences 9:3381–3403. https://doi.org/10.5194/bg-9-3381-2012
Féret J-B, Asner GP (2014) Mapping tropical forest canopy diversity using high-fidelity imaging spectroscopy. Ecol Appl 24:1289–1296

Ferraz A, Saatchi S, Mallet C, Meyer V (2016) LiDAR detection of individual tree size in tropical forests. Remote Sens Environ 183:318–333

Féret JB, Gitelson AA, Noble SD, Jacquemoud S (2017) PROSPECT-D: towards modeling leaf optical properties through a complete lifecycle. Remote Sens Environ 193:204–215

Flores O, Coomes DA (2011) Estimating the wood density of species for carbon stock assessments. Methods Ecol Evol 2:214–220. https://doi.org/10.1111/j.2041-210x.2010.00068.x

Frazer GW, Wulder MA, Niemann KO (2005) Simulation and quantification of the fine-scale spatial pattern and heterogeneity of forest canopy structure: a lacunarity-based method designed for analysis of continuous canopy heights. For Ecol Manag 214:65–90

Frazer GW, Magnussen S, Wulder MA, Niemann KO (2011) Simulated impact of sample plot size and co-registration error on the accuracy and uncertainty of LiDAR-derived estimates of forest stand biomass. Remote Sens Environ 115:636–649

Fuller WA (1987) Measurement error models. Wiley, New York

Gao S, Wang X, Wiemann MC et al (2017) A critical analysis of methods for rapid and nondestructive determination of wood density in standing trees. Ann For Sci 74:27

Gastellu-Etchegorry J-P, Demarez V, Pinel V, Zagolski F (1996) Modeling radiative transfer in heterogeneous 3-D vegetation canopies. Remote Sens Environ 58:131–156

Gastellu-Etchegorry J-P, Yin T, Lauret N et al (2015) Discrete anisotropic radiative transfer (DART 5) for modeling airborne and satellite spectroradiometer and LiDAR acquisitions of natural and urban landscapes. Remote Sens 7:1667–1701

Gobakken T, Naesset E (2009) Assessing effects of positioning errors and sample plot size on biophysical stand properties derived from airborne laser scanner data. Can J For Res 39:1036–1052

Gomes ACS, Andrade A, Barreto-Silva JS et al (2013) Local plant species delimitation in a highly diverse Amazonian forest: do we all see the same species? J Veg Sci 24:70–79. https://doi.org/10.1111/j.1654-1103.2012.01441.x

Gonzalez de Tanago J, Lau A, Bartholomeus H et al (2018) Estimation of above-ground biomass of large tropical trees with terrestrial LiDAR. Methods Ecol Evol 9:223–234

Goodman RC, Phillips OL, Baker TR (2014) The importance of crown dimensions to improve tropical tree biomass estimates. Ecol Appl 24:680–698. https://doi.org/10.1890/13-0070.1

Gourlet-Fleury S, Rossi V, Réjou-Méchain M et al (2011) Environmental filtering of dense-wooded species controls above-ground biomass stored in African moist forests. J Ecol 99:981–990. https://doi.org/10.1111/j.1365-2745.2011.01829.x

Grau E, Durrieu S, Fournier R et al (2017) Estimation of 3D vegetation density with terrestrial laser scanning data using voxels. A sensitivity analysis of influencing parameters. Remote Sens Environ 191:373–388

Gregoire TG, Næsset E, McRoberts RE et al (2016) Statistical rigor in LiDAR-assisted estimation of aboveground forest biomass. Remote Sens Environ 173:98–108

Guitet S, Pélissier R, Brunaux O et al (2015) Geomorphological landscape features explain floristic patterns in French Guiana rainforest. Biodivers Conserv 24:1215–1237

Guitet S, Sabatier D, Brunaux O et al (2018) Disturbance regimes drive the diversity of regional floristic pools across Guianan rainforest landscapes. Sci Rep 8:3872

Hajj ME, Baghdadi N, Fayad I et al (2017) Interest of integrating spaceborne LiDAR data to improve the estimation of biomass in high biomass forested areas. Remote Sens 9:213

Hansen MC, Potapov PV, Moore R et al (2013) High-resolution global maps of 21st-century forest cover change. Science 342:850–853

Henry M, Besnard A, Asante WA et al (2010) Wood density, phytomass variations within and among trees, and allometric equations in a tropical rainforest of Africa. For Ecol Manag 260:1375–1388

Herold M, Carter S, Avitabile V et al (2019) The role and need for space-based forest biomass-related measurements in environmental management and policy. Surv Geophys. https://doi.org/10.1007/s10712-019-09510-6

Huang W, Swatantran A, Johnson K et al (2015) Local discrepancies in continental scale biomass maps: a case study over forested and non-forested landscapes in Maryland, USA. Carbon Balance Manag 10:19

Hunter MO, Keller M, Victoria D, Morton DC (2013) Tree height and tropical forest biomass estimation. Biogeosciences 10:8385–8399

Inglada J, Vadon H (2005) Fine registration of SPOT5 and Envisat/ASAR images and ortho-image production: a fully automatic approach. In: Proceedings 2005 IEEE international geoscience and remote sensing symposium, 2005. IGARSS'05. IEEE, Vol. 5, pp 3510–3512

Ishimaru A (1978) Wave propagation and scattering in random media, vol 2. Academic press, New York, pp 336–393

Johnson CE, Barton CC (2004) Where in the world are my field plots? Using GPS effectively in environmental field studies. Front Ecol Environ 2:475–482. https://doi.org/10.1890/1540-9295(2004)002%5b0475:witwam%5d2.0.co;2

Jonckheere I, Nackaerts K, Muys B et al (2006) A fractal dimension-based modelling approach for studying the effect of leaf distribution on LAI retrieval in forest canopies. Ecol Model 197:179–195

Jucker T, Asner GP, Dalponte M et al (2017a) A regional model for estimating the aboveground carbon density of Borneo's tropical forests from airborne laser scanning. arXiv Prepr arXiv170509242

Jucker T, Caspersen J, Chave J et al (2017b) Allometric equations for integrating remote sensing imagery into forest monitoring programmes. Glob Change Biol 23:177–190

Jucker T, Asner GP, Dalponte M et al (2018a) Estimating aboveground carbon density and its uncertainty in Borneo's structurally complex tropical forests using airborne laser scanning. Biogeosciences 15:3811–3830

Jucker T, Bongalov B, Burslem DF et al (2018b) Topography shapes the structure, composition and function of tropical forest landscapes. Ecol Lett 21:989–1000

Justice CO, Giglio L, Korontzi S et al (2002) The MODIS fire products. Remote Sens Environ 83:244–262

Kearsley E, De Haulleville T, Hufkens K et al (2013) Conventional tree height–diameter relationships significantly overestimate aboveground carbon stocks in the Central Congo Basin. Nat Commun 4:2269

Kellner JR, Asner GP (2009) Convergent structural responses of tropical forests to diverse disturbance regimes. Ecol Lett 12:887–897

Kennedy RE, Yang Z, Cohen WB (2010) Detecting trends in forest disturbance and recovery using yearly Landsat time series: 1. LandTrendr—temporal segmentation algorithms. Remote Sens Environ 114:2897–2910

Ketterings QM, Coe R, van Noordwijk M et al (2001) Reducing uncertainty in the use of allometric biomass equations for predicting above-ground tree biomass in mixed secondary forests. For Ecol Manag 146:199–209. https://doi.org/10.1016/s0378-1127(00)00460-6

Kleinn C (2017) The renaissance of National Forest Inventories (NFIs) in the context of the international conventions—a discussion paper on context, background and justification of NFIs. Pesqui Florest Bras 37:369–379

Kükenbrink D, Schneider FD, Leiterer R et al (2017) Quantification of hidden canopy volume of airborne laser scanning data using a voxel traversal algorithm. Remote Sens Environ 194:424–436. https://doi.org/10.1016/j.rse.2016.10.023

Labriere N, Tao S, Chave J et al (2018) In situ reference datasets from the TropiSAR and AfriSAR campaigns in support of upcoming spaceborne biomass missions. IEEE J Sel Top Appl Earth Obs Remote Sens 99:1–11

Lagomasino D, Fatoyinbo T, Lee S-K, Simard M (2015) High-resolution forest canopy height estimation in an African blue carbon ecosystem. Remote Sens Ecol Conserv 1:51–60. https://doi.org/10.1002/rse2.3

Larjavaara M, Muller-Landau HC (2013) Measuring tree height: a quantitative comparison of two common field methods in a moist tropical forest. Methods Ecol Evol 4:793–801. https://doi.org/10.1111/2041-210x.12071

Lau A, Bentley LP, Martius C et al (2018) Quantifying branch architecture of tropical trees using terrestrial LiDAR and 3D modelling. Trees 32(5):1219–1231

Le Toan T, Quegan S, Davidson MWJ et al (2011) The BIOMASS mission: mapping global forest biomass to better understand the terrestrial carbon cycle. Remote Sens Environ 115:2850–2860. https://doi.org/10.1016/j.rse.2011.03.020

Lefsky MA, Cohen WB, Parker GG, Harding DJ (2002) LiDAR remote sensing for ecosystem studies LiDAR, an emerging remote sensing technology that directly measures the three-dimensional distribution of plant canopies, can accurately estimate vegetation structural attributes and should be of particular interest to forest, landscape, and global ecologists. Bioscience 52:19–30

Leitold V, Morton DC, Longo M et al (2018) El Niño drought increased canopy turnover in Amazon forests. New Phytol 219:959–971

Li X, Strahler AH (1992) Geometric-optical bidirectional reflectance modeling of the discrete crown vegetation canopy: effect of crown shape and mutual shadowing. IEEE Trans Geosci Remote Sens 30:276–292

Lindenmayer DB, Cunningham RB, Tanton MT et al (1991) Characteristics of hollow-bearing trees occupied by arboreal marsupials in the montane ash forests of the Central Highlands of Victoria, southeast Australia. For Ecol Manag 40:289–308

Liu J-Y, Zheng Z, Xu X et al (2018) Abundance and distribution of cavity trees and the effect of topography on cavity presence in a tropical rainforest, southwestern China. Can J For Res 48:1058–1066

Longo M, Keller M, dos-Santos MN et al (2016) Aboveground biomass variability across intact and degraded forests in the Brazilian Amazon. Glob Biogeochem Cycles 30:1639–1660
Lopez-Gonzalez G, Lewis SL, Burkitt M, Phillips OL (2011) ForestPlots.net: a web application and research tool to manage and analyse tropical forest plot data. J Veg Sci 22:610–613
Lyapustin A, Martonchik J, Wang Y et al (2011) Multiangle implementation of atmospheric correction (MAIAC): 1. Radiative transfer basis and look-up tables. J Geophys Res Atmos 116:1–9
Ma L, Zheng G, Eitel JU et al (2016) Improved salient feature-based approach for automatically separating photosynthetic and nonphotosynthetic components within terrestrial LiDAR point cloud data of forest canopies. IEEE Trans Geosci Remote Sens 54:679–696
Malenovskỳ Z, Martin E, Homolová L et al (2008) Influence of woody elements of a Norway spruce canopy on nadir reflectance simulated by the DART model at very high spatial resolution. Remote Sens Environ 112:1–18
Marra RE, Brazee NJ, Fraver S (2018) Estimating carbon loss due to internal decay in living trees using tomography: implications for forest carbon budgets. Environ Res Lett. https://doi.org/10.1088/1748-9326/aae2bf
Marvin DC, Asner GP, Knapp DE et al (2014) Amazonian landscapes and the bias in field studies of forest structure and biomass. Proc Natl Acad Sci 111:E5224–E5232. https://doi.org/10.1073/pnas.1412999111
Mascaro J, Detto M, Asner GP, Muller-Landau HC (2011) Evaluating uncertainty in mapping forest carbon with airborne LiDAR. Remote Sens Environ 115:3770–3774. https://doi.org/10.1016/j.rse.2011.07.019
McEwan RW, Lin Y-C, Sun I-F et al (2011) Topographic and biotic regulation of aboveground carbon storage in subtropical broad-leaved forests of Taiwan. For Ecol Manag 262:1817–1825. https://doi.org/10.1016/j.foreco.2011.07.028
McRoberts RE, Westfall JA (2013) Effects of uncertainty in model predictions of individual tree volume on large area volume estimates. For Sci 60(1):34–42
Mermoz S, Le Toan T, Villard L et al (2014) Biomass assessment in the Cameroon savanna using ALOS PALSAR data. Remote Sens Environ 155:109–119. https://doi.org/10.1016/j.rse.2014.01.029
Mermoz S, Réjou-Méchain M, Villard L et al (2015) Decrease of L-band SAR backscatter with biomass of dense forests. Remote Sens Environ 15:307–317. https://doi.org/10.1016/j.rse.2014.12.019
Minh DHT, Le Toan T, Rocca F et al (2014) Relating P-band synthetic aperture radar tomography to tropical forest biomass. IEEE Trans Geosci Remote Sens 52:967–979
Minh DHT, Le Toan T, Rocca F et al (2016) SAR tomography for the retrieval of forest biomass and height: cross-validation at two tropical forest sites in French Guiana. Remote Sens Environ 175:138–147
Mitchard ETA (2018) The tropical forest carbon cycle and climate change. Nature 559:527–534. https://doi.org/10.1038/s41586-018-0300-2
Mitchard ET, Saatchi SS, Baccini A et al (2013) Uncertainty in the spatial distribution of tropical forest biomass: a comparison of pan-tropical maps. Carbon Balance Manage 8:10
Mitchard ETA, Feldpausch TR, Brienen RJW et al (2014) Markedly divergent estimates of Amazon forest carbon density from ground plots and satellites. Glob Ecol Biogeogr 23:935–946. https://doi.org/10.1111/geb.12168
Molto Q, Rossi V, Blanc L (2013) Error propagation in biomass estimation in tropical forests. Methods Ecol Evol 4:175–183. https://doi.org/10.1111/j.2041-210x.2012.00266.x
Momo Takoudjou S, Ploton P, Sonké B et al (2018) Using terrestrial laser scanning data to estimate large tropical trees biomass and calibrate allometric models: a comparison with traditional destructive approach. Methods Ecol Evol 9:905–916
Morsdorf F, Eck C, Zgraggen C et al (2017) UAV-based LiDAR acquisition for the derivation of high-resolution forest and ground information. Lead Edge 36:566–570
Morton DC, Nagol J, Carabajal CC et al (2014) Amazon forests maintain consistent canopy structure and greenness during the dry season. Nature 506:221–224. https://doi.org/10.1038/nature13006
Moundounga Mavouroulou Q, Ngomanda A, Engone Obiang NL et al (2014) How to improve allometric equations to estimate forest biomass stocks? Some hints from a central African forest. Can J For Res 44:685–691
Myneni RB (1991) Modeling radiative transfer and photosynthesis in three-dimensional vegetation canopies. Agric For Meteorol 55:323–344
Myneni RB, Ross J, Asrar G (1989) A review on the theory of photon transport in leaf canopies. Agric For Meteorol 45:1–153
Ni W, Li X, Woodcock CE et al (1999) An analytical hybrid GORT model for bidirectional reflectance over discontinuous plant canopies. IEEE Trans Geosci Remote Sens 37:987–999

Nogueira EM, Nelson BW, Fearnside PM (2006) Volume and biomass of trees in central Amazonia: influence of irregularly shaped and hollow trunks. For Ecol Manag 227:14–21. https://doi.org/10.1016/j.foreco.2006.02.004

North PR (1996) Three-dimensional forest light interaction model using a Monte Carlo method. IEEE Trans Geosci Remote Sens 34:946–956

Pargal S, Fararoda R, Rajashekar G et al (2017) Inverting aboveground biomass–canopy texture relationships in a landscape of Forest mosaic in the Western Ghats of India using very high resolution Cartosat imagery. Remote Sens 9:228

Pearson TR, Brown S, Murray L, Sidman G (2017) Greenhouse gas emissions from tropical forest degradation: an underestimated source. Carbon Balance Manag 12:3

Phillips OL, Baker TR, Brienen R, Feldpausch TR (2009) Field manual for plot establishment and remeasurement. https://www.forestplots.net/upload/ManualsEnglish/RAINFOR_field_manual_EN.pdf

Ploton P, Pélissier R, Proisy C et al (2012) Assessing aboveground tropical forest biomass using Google Earth canopy images. Ecol Appl 22:993–1003

Ploton P, Pélissier R, Barbier N et al (2013) Canopy texture analysis for large-scale assessments of tropical forest stand structure and biomass. In: Devy S, Ganesh T, Lowman MD (eds) Treetops at risk. Springer, Berlin, pp 237–245

Ploton P, Barbier N, Momo ST et al (2016) Closing a gap in tropical forest biomass estimation: taking crown mass variation into account in pantropical allometries. Biogeosciences 13:1571–1585

Ploton P, Barbier N, Couteron P et al (2017) Toward a general tropical forest biomass prediction model from very high resolution optical satellite images. Remote Sens Environ 200:140–153

Proisy C, Couteron P, Fromard F (2007) Predicting and mapping mangrove biomass from canopy grain analysis using Fourier-based textural ordination of IKONOS images. Remote Sens Environ 109:379–392. https://doi.org/10.1016/j.rse.2007.01.009

Puliti S, Ørka HO, Gobakken T, Næsset E (2015) Inventory of small forest areas using an unmanned aerial system. Remote Sens 7:9632–9654

Raumonen P, Kaasalainen M, Åkerblom M et al (2013) Fast automatic precision tree models from terrestrial laser scanner data. Remote Sens 5:491–520

Réjou-Méchain M, Muller-Landau HC, Detto M et al (2014) Local spatial structure of forest biomass and its consequences for remote sensing of carbon stocks. Biogeosciences 11:6827–6840

Réjou-Méchain M, Tymen B, Blanc L et al (2015) Using repeated small-footprint LiDAR maps to infer spatial variation and dynamics of a high-biomass neotropical forest. Remote Sens Environ 169:93–101

Réjou-Méchain M, Tanguy A, Piponiot C et al (2017) BIOMASS: an r package for estimating above-ground biomass and its uncertainty in tropical forests. Methods Ecol Evol 8:1163–1167

Robinson C, Saatchi S, Neumann M, Gillespie T (2013) Impacts of spatial variability on aboveground biomass estimation from L-band radar in a temperate forest. Remote Sens 5:1001–1023

Rocchini D, Luque S, Pettorelli N et al (2018) Measuring β-diversity by remote sensing: a challenge for biodiversity monitoring. Methods Ecol Evol 9:1787–1798

Rodrigues WA, Valle RC (1964) Ocorrência de troncos ocos em mata de baixio da regiao de Manaus, 16th edn. Publicacao. Botanica - Instituto Nacional de Pesquisa da Amazonia (Brazil), Manaus

Rodriguez-Veiga P, Wheeler J, Louis V et al (2017) Quantifying forest biomass carbon stocks from space. Curr For Rep 3:1–18

Romijn E, De Sy V, Herold M et al (2018) Independent data for transparent monitoring of greenhouse gas emissions from the land use sector—what do stakeholders think and need? Environ Sci Policy 85:101–112

Roşca S, Suomalainen J, Bartholomeus H, Herold M (2018) Comparing terrestrial laser scanning and unmanned aerial vehicle structure from motion to assess top of canopy structure in tropical forests. Interface Focus 8:20170038

Rosen P, Hensley S, Shaffer S et al (2017) The NASA-ISRO SAR (NISAR) mission dual-band radar instrument preliminary design. In: 2017 IEEE international geoscience and remote sensing symposium (IGARSS), pp 3832–3835

Roujean J-L, Leroy M, Deschamps P-Y (1992) A bidirectional reflectance model of the Earth's surface for the correction of remote sensing data. J Geophys Res Atmos 97:20455–20468

Saatchi SS, Houghton RA, Alvalá DS et al (2007) Distribution of aboveground live biomass in the Amazon basin. Glob Change Biol 13:816–837. https://doi.org/10.1111/j.1365-2486.2007.01323.x

Saatchi S, Marlier M, Chazdon RL et al (2011a) Impact of spatial variability of tropical forest structure on radar estimation of aboveground biomass. Remote Sens Environ 115:2836–2849. https://doi.org/10.1016/j.rse.2010.07.015

Saatchi SS, Harris NL, Brown S et al (2011b) Benchmark map of forest carbon stocks in tropical regions across three continents. Proc Natl Acad Sci 108:9899–9904. https://doi.org/10.1073/pnas.1019576108

Saatchi S, Mascaro J, Xu L et al (2015) Seeing the forest beyond the trees. Glob Ecol Biogeogr 24:606–610

Sagang LBT, Momo ST, Libalah MB et al (2018) Using volume-weighted average wood specific gravity of trees reduces bias in aboveground biomass predictions from forest volume data. For Ecol Manag 424:519–528. https://doi.org/10.1016/j.foreco.2018.04.054

Santoro M, Cartus O, Mermoz S et al (2018) A detailed portrait of the forest aboveground biomass pool for the year 2010 obtained from multiple remote sensing observations. In: EGU general assembly conference abstracts, p 18932

Schlund M, von Poncet F, Kuntz S et al (2015) TanDEM-X data for aboveground biomass retrieval in a tropical peat swamp forest. Remote Sens Environ 158:255–266

Schneider FD, Yin T, Gastellu-Etchegorry J et al (2014) At-sensor radiance simulation for airborne imaging spectroscopy. In: 2014 6th workshop on hyperspectral image and signal processing: evolution in remote sensing (WHISPERS), pp 1–4

Sigrist P, Coppin P, Hermy M (1999) Impact of forest canopy on quality and accuracy of GPS measurements. Int J Remote Sens 20:3595–3610. https://doi.org/10.1080/014311699211228

Simard M, Pinto N, Fisher JB, Baccini A (2011) Mapping forest canopy height globally with spaceborne LiDAR. J Geophys Res Biogeosci 116:1–12

Singh M, Malhi Y, Bhagwat S (2014) Biomass estimation of mixed forest landscape using a Fourier transform texture-based approach on very-high-resolution optical satellite imagery. Int J Remote Sens 35:3331–3349

Sitch S, Huntingford C, Gedney N et al (2008) Evaluation of the terrestrial carbon cycle, future plant geography and climate-carbon cycle feedbacks using five dynamic global vegetation models (DGVMs). Glob Change Biol 14:2015–2039

Solberg S, May J, Bogren W et al (2018) Interferometric SAR DEMs for forest change in Uganda 2000–2012. Remote Sens 10:228

Steininger MK (2000) Satellite estimation of tropical secondary forest above-ground biomass: data from Brazil and Bolivia. Int J Remote Sens 21:1139–1157

St-Onge B, Vega C, Fournier RA, Hu Y (2008) Mapping canopy height using a combination of digital stereo-photogrammetry and LiDAR. Int J Remote Sens 29:3343–3364

Sullivan MJ, Lewis SL, Hubau W et al (2018) Field methods for sampling tree height for tropical forest biomass estimation. Methods Ecol Evol 9:1179–1189

Sun G, Ranson KJ (2000) Modeling LiDAR returns from forest canopies. IEEE Trans Geosci Remote Sens 38:2617–2626

Swenson NG, Enquist BJ (2008) The relationship between stem and branch wood specific gravity and the ability of each measure to predict leaf area. Am J Bot 95:516–519

Tarelkin Y, Hufkens K, Hahn S et al (2019) Wood anatomy variability under contrasted environmental conditions of common deciduous and evergreen species from central African forests. Trees Struct Funct 33:893–909. https://doi.org/10.1007/s00468-019-01826-5

Trochta J, Krůček M, Vrška T, Král K (2017) 3D Forest: an application for descriptions of three-dimensional forest structures using terrestrial LiDAR. PLoS ONE 12:e0176871

Tymen B, Vincent G, Courtois EA et al (2017) Quantifying micro-environmental variation in tropical rainforest understory at landscape scale by combining airborne LiDAR scanning and a sensor network. Ann For Sci 74:32

Verhoef W (1985) Earth observation modeling based on layer scattering matrices. Remote Sens Environ 17:165–178

Vieilledent G, Vaudry R, Andriamanohisoa SF et al (2012) A universal approach to estimate biomass and carbon stock in tropical forests using generic allometric models. Ecol Appl 22:572–583

Villard L (2009) Forward and inverse modeling of synthetic aperture radar in the bistatic configuration: applications in forest remote sensing. Ph.D. thesis, ONERAISAE-Universite Paul Sabatier

Villard L, Le Toan T (2015) Relating P-band SAR intensity to biomass for tropical dense forests in hilly terrain: γ^0 or t^0? IEEE J Sel Top Appl Earth Obs Remote Sens 8:214–223

Vincent G, Caron F, Sabatier D, Blanc L (2012a) LiDAR shows that higher forests have more slender trees. Bois For Trop 314:51–56

Vincent G, Sabatier D, Blanc L et al (2012b) Accuracy of small footprint airborne LiDAR in its predictions of tropical moist forest stand structure. Remote Sens Environ 125:23–33. https://doi.org/10.1016/j.rse.2012.06.019

Vincent G, Sabatier D, Rutishauser E (2014) Revisiting a universal airborne light detection and ranging approach for tropical forest carbon mapping: scaling-up from tree to stand to landscape. Oecologia 175:439–443

Vincent G, Antin C, Laurans M et al (2017) Mapping plant area index of tropical evergreen forest by airborne laser scanning. A cross-validation study using LAI2200 optical sensor. Remote Sens Environ 198:254–266

Wassenberg M, Chiu H-S, Guo W, Spiecker H (2015) Analysis of wood density profiles of tree stems: incorporating vertical variations to optimize wood sampling strategies for density and biomass estimations. Trees 29:551–561

Widlowski J-L, Pinty B, Lopatka M et al (2013) The fourth radiation transfer model intercomparison (RAMI-IV): proficiency testing of canopy reflectance models with ISO-13528. J Geophys Res Atmos 118:6869–6890. https://doi.org/10.1002/jgrd.50497

Williamson GB, Wiemann MC (2010) Measuring wood specific gravity… correctly. Am J Bot 97:519–524

Wu X, Liu H, Li X et al (2018) Differentiating drought legacy effects on vegetation growth over the temperate Northern Hemisphere. Glob Change Biol 24:504–516

Xu L, Saatchi SS, Yang Y et al (2016) Performance of non-parametric algorithms for spatial mapping of tropical forest structure. Carbon Balance Manag 11:18

Xu L, Saatchi SS, Shapiro A et al (2017) Spatial distribution of carbon stored in forests of the Democratic Republic of Congo. Sci Rep 7:15030

Zanne AE, Lopez-Gonzalez G, Coomes DA, Ilic J, Jansen S, Lewis SL, Miller RB, Swenson NG, Wiemann MC, Chave J (2009) Data from: towards a worldwide wood economics spectrum. Dryad Digit Repos. https://doi.org/10.5061/dryad.234

Zolkos SG, Goetz SJ, Dubayah R (2013) A meta-analysis of terrestrial aboveground biomass estimation using LiDAR remote sensing. Remote Sens Environ 128:289–298. https://doi.org/10.1016/j.rse.2012.10.017

Publisher's Note Springer Nature remains neutral with regard to jurisdictional claims in published maps and institutional affiliations.

Affiliations

Maxime Réjou-Méchain[1] · Nicolas Barbier[1] · Pierre Couteron[1] · Pierre Ploton[1] · Grégoire Vincent[1] · Martin Herold[2] · Stéphane Mermoz[3,8] · Sassan Saatchi[4] · Jérôme Chave[5] · Florian de Boissieu[6] · Jean-Baptiste Féret[6] · Stéphane Momo Takoudjou[1,7] · Raphaël Pélissier[1]

[1] AMAP, IRD, CNRS, CIRAD, INRA, Univ Montpellier, Montpellier Cedex 05, France

[2] Laboratory of Geo-Information Science and Remote Sensing, Wageningen University and Research, Droevendaalsesteeg 3, 6708 PB Wageningen, The Netherlands

[3] CESBIO, CNES/CNRS, IRD/UPS, Université de Toulouse, Toulouse, France

[4] Jet Propulsion Laboratory, California Institute of Technology, Pasadena, CA 91109, USA

[5] CNRS, ENFA; UMR5174 EDB (Laboratoire Evolution et Diversité Biologique), Université Paul Sabatier, 118 Route de Narbonne, 31062 Toulouse, France

[6] TETIS, Irstea, AgroParisTech, CIRAD, CNRS, University of Montpellier, 34000 Montpellier, France

[7] Plant Systematic and Ecology Laboratory, Higher Teacher's Training College, University of Yaoundé I, P.O. Box 047, Yaoundé, Cameroon

[8] GlobEO, Avenue Saint-Exupery, Toulouse, France

Article

Unveiling African rainforest composition and vulnerability to global change

https://doi.org/10.1038/s41586-021-03483-6

Received: 29 October 2019

Accepted: 22 March 2021

Published online: 21 April 2021

Check for updates

Maxime Réjou-Méchain[1]✉, Frédéric Mortier[2,3], Jean-François Bastin[1,2,3,4], Guillaume Cornu[2,3], Nicolas Barbier[1], Nicolas Bayol[5], Fabrice Bénédet[2,3], Xavier Bry[6], Gilles Dauby[1], Vincent Deblauwe[7,8], Jean-Louis Doucet[4], Charles Doumenge[2,3], Adeline Fayolle[4], Claude Garcia[2,3,9], Jean-Paul Kibambe Lubamba[10,11], Jean-Joël Loumeto[12], Alfred Ngomanda[13], Pierre Ploton[1], Bonaventure Sonké[14], Catherine Trottier[6,15], Ruppert Vimal[16], Olga Yongo[17], Raphaël Pélissier[1] & Sylvie Gourlet-Fleury[2,3]

Africa is forecasted to experience large and rapid climate change[1] and population growth[2] during the twenty-first century, which threatens the world's second largest rainforest. Protecting and sustainably managing these African forests requires an increased understanding of their compositional heterogeneity, the environmental drivers of forest composition and their vulnerability to ongoing changes. Here, using a very large dataset of 6 million trees in more than 180,000 field plots, we jointly model the distribution in abundance of the most dominant tree taxa in central Africa, and produce continuous maps of the floristic and functional composition of central African forests. Our results show that the uncertainty in taxon-specific distributions averages out at the community level, and reveal highly deterministic assemblages. We uncover contrasting floristic and functional compositions across climates, soil types and anthropogenic gradients, with functional convergence among types of forest that are floristically dissimilar. Combining these spatial predictions with scenarios of climatic and anthropogenic global change suggests a high vulnerability of the northern and southern forest margins, the Atlantic forests and most forests in the Democratic Republic of the Congo, where both climate and anthropogenic threats are expected to increase sharply by 2085. These results constitute key quantitative benchmarks for scientists and policymakers to shape transnational conservation and management strategies that aim to provide a sustainable future for central African forests.

Concomitant increases in climate stress, human population needs and resource extraction in central Africa raise environmental concerns[3–5]. These threats may have considerable impacts on the carbon budget[6], climate[7] and biodiversity of central African forests[8], which shelter some of the world's most iconic wildlife species and which are already experiencing a much drier and seasonal climate than other tropical forests[9]. However, the current composition of central African forests and its determinants at regional scale are still poorly known, often being studied in limited areas[10–12] and datasets[13] or at a very coarse grain with heterogeneous occurrence records[14]. Vast regions of central African forests remain poorly explored scientifically[15], and most space-borne systems of Earth observation provide very limited information on forest composition[16]. This hinders our ability to understand how the composition and functions of forests vary regionally, to forecast how these forests will face upcoming global changes and, ultimately, to anticipate—on scientific bases—how to protect and manage them beyond national boundaries.

In this study, we used an extensive dataset of forest inventories to (1) model the main floristic and functional gradients over central African forests; and (2) assess their expected vulnerability under forecasted conditions of global (climatic and anthropogenic) change. We compiled the abundance distributions of 193 dominant tree taxa in 185,665 field plots (around 90,000 ha) from commercial forest inventories spread over the 5 main forested countries in central Africa (Cameroon, Central African Republic, Democratic Republic of the Congo, Gabon and Republic of the Congo) (Extended Data Fig. 1). We modelled the joint distributions of taxon abundances at 10-km resolution using supervised component generalized linear regression (SCGLR)[17],

[1]AMAP, Univ. Montpellier, IRD, CNRS, CIRAD, INRAE, Montpellier, France. [2]CIRAD, Forêts et Sociétés, Montpellier, France. [3]Forêts et Sociétés, Univ. Montpellier, CIRAD, Montpellier, France. [4]TERRA Teaching and Research Centre, Gembloux Agro-Bio Tech, University of Liège, Gembloux, Belgium. [5]FRM Ingénierie, Mauguio, France. [6]IMAG, CNRS, Univ. Montpellier, Montpellier, France. [7]Center for Tropical Research, Institute of the Environment and Sustainability, University of California, Los Angeles, Los Angeles, CA, USA. [8]International Institute of Tropical Agriculture, Yaoundé, Cameroon. [9]Forest Management and Development Team, Department of Environmental System Science, Institute of Integrative Biology, ETH Zürich, Zürich, Switzerland. [10]Faculté des Sciences Agronomiques, Département de Gestion des Ressources Naturelles, Université de Kinshasa, Kinshasa, Democratic Republic of the Congo. [11]Wildlife Conservation Society, Kinshasa, Democratic Republic of the Congo. [12]Faculté des Sciences et Techniques, Université Marien Ngouabi, Brazzaville, Congo. [13]Institut de Recherche en Écologie Tropicale (IRET/CENAREST), Libreville, Gabon. [14]Plant Systematic and Ecology Laboratory, Higher Teacher's Training College, University of Yaoundé I, Yaoundé, Cameroon. [15]AMIS, Univ. Paul Valéry Montpellier 3, Montpellier, France. [16]GEODE UMR 5602, CNRS, Université Jean-Jaurès, Toulouse, France. [17]Laboratoire de Biodiversité Végétale et Fongique, Faculté des Sciences, Université de Bangui, Bangui, Central African Republic. ✉e-mail: maxime.rejou@ird.fr

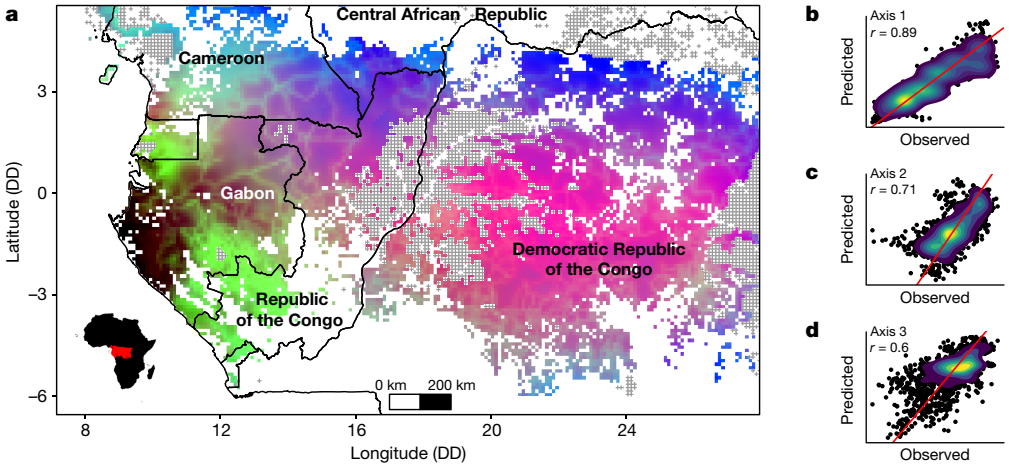

Fig. 1 | Floristic composition of central African forests. a, Spatialized RGB composition of the three first axes of a correspondence analysis (CA) performed on jointly predicted taxon abundances at 10-km resolution ($n = 193$ taxa; axis 1, blue; axis 2, red; axis 3, green). Grey crosses represent forested areas outside the calibration domain, including permanently flooded forests, and country boundaries are represented in black. DD, decimal degrees. **b**–**d**, Cross-validation results comparing the observed and predicted CA gradients for axis 1 (**b**), axis 2 (**c**) and axis 3 (**d**). The 1:1 line is displayed in red. Taxon CA planes 1–2 and 1–3 are provided in Extended Data Fig. 2.

a modelling method that extends partial least-squares regression to the multivariate generalized linear framework. SCGLR models a set of responses (here the abundances of taxa) from synthetic orthogonal explanatory components derived from 24 climatic variables (hereafter, climatic components, CCs) and additional soil type (here, sand versus clay) and anthropogenic pressure covariates. We developed for this study an index, based on population density and road networks, that is specifically designed and calibrated to predict the intensity of recent human-induced forest disturbances in central Africa (see Methods). Finally, thanks to the very large size of the dataset, the predicted floristic and functional gradients were cross-validated with spatially independent observations using Spearman correlation coefficients, ρ_{CV}.

Floristic composition in central Africa

Our model predicted individual taxon abundances with an overall median correlation ρ_{CV} of 0.48 (range of −0.11 to 0.83). This median value was still as high as 0.45 when unoccupied sites were removed, showing that, beyond presence and absence, our model also captured variations in abundance within a taxon's distributional range. A correspondence analysis (CA) performed on the predicted taxon abundances revealed major regional floristic gradients (Fig. 1, Extended Data Figs. 2, 3) that were highly correlated with the observed gradients ($\rho_{CV} = 0.89$, 0.71 and 0.6 for CA axes 1, 2 and 3, respectively; Fig. 1b–d). Contrary to Amazonian and Southeast Asian forests, in which soil was shown to be the primary large-scale driver of tree community composition[18,19], the most prominent floristic gradient predicted here (CA axis 1) was highly related to climate, and in particular to the first predictive CC (Pearson's $r = 0.98$), contrasting areas with a cool and light-deficient[20] dry season (coastal Gabon) and areas with high evapotranspiration rates (northern limit of the central African forests; Extended Data Fig. 4). The second predicted floristic gradient (CA axis 2) was highly correlated with the two other CCs ($r = -0.86$ and -0.72 for CC2 and CC3, respectively) related to seasonality and maximum temperature, thus contrasting equatorial areas with a low water deficit and areas with a high water deficit towards the limits of the tropics. Climate seasonality was also found to be a major driver of tree community composition in Amazonia[18], and maximum temperature has recently been identified as the most important pantropical driver of forest biomass, affecting woody productivity[21]. The third predicted floristic gradient (CA axis 3) revealed floristic variations that are more local and that highlighted human-disturbed forests ($r = 0.67$ with our index of human-induced forest-disturbance intensity).

As already shown in previous studies[22,23], the association between taxon distributions and climate patterns may appear by chance because both are spatially autocorrelated at the regional scale. We thus used a spatially explicit null model that randomized the predictive CCs while preserving their spatial (co)structures. When keeping the soil type and human impact on forests unchanged, the null model predicted abundances with a similar predictive power to the model based on the original CCs for 67% of the taxa ($P > 0.1$). This suggests that variation in taxon abundances directly depends on climate for a minimum of only one-third of the taxa, whereas for most of them, abundance may correlate with climate by chance only. By contrast, the association between climate and the main gradients of floristic assemblages was robust to autocorrelation artefacts ($P = 0.028$, 0.006 and 0.06 for CA1, CA2 and CA3, respectively). This result confirms that extrapolating assemblages from climate variables is more reliable than extrapolating individual taxon abundances[24]. Indeed, individual taxon abundances are likely to be less predictable on the basis of only current drivers as they are also affected by unknown past human disturbances[25], biotic interactions and biogeographical history[26], the idiosyncratic effects of which tend to average out at the community level.

Functional composition in central Africa

From the predicted floristic assemblages, we computed the community weighted mean[27] of three functional traits that are known to have a central role in ecosystem processes: wood density, deciduousness and maximum diameter (Fig. 2). The predicted functional composition was consistent with the observations ($\rho_{CV} = 0.47$, 0.75 and 0.45 for the three traits, respectively; Extended Data Fig. 5). As in Amazonia[18], community wood density varied with soil type, with the highest values found for sandy soils that are located at the boundaries of Cameroon, the Republic of the Congo and the Central African Republic, and where tree species with conservative resource-use strategies predominate[11]. However, larger-scale variations in wood density were primarily driven by human-induced forest disturbances; community wood density was lower in human-disturbed forests, indicating that they are mostly composed of fast-growing taxa[28]. Notably, these areas also contain a high proportion of trees that can potentially reach a large diameter. These two results indicate that human-disturbed forests tend to be

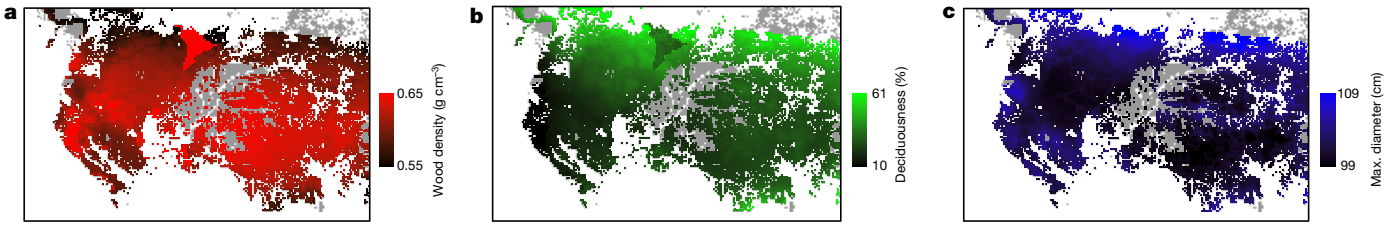

Fig. 2 | Predicted functional composition of central African forests. a–c, Predicted community weighted functional trait values (wood density (**a**), deciduousness (**b**) and maximum diameter (**c**)) at 10-km resolution.

dominated by long-lived pioneer taxa, which are characterized by a low wood density but a large potential stature and thus offer a fast and relatively long-lasting carbon sink potential in the absence of disturbances[29]. Finally, a marked deciduousness gradient ran from the highly evergreen forests of coastal Gabon to the northern limit of the central African forests with, again, a well-known exception on the northern sandy soil plateau[11,30].

A reference map of forest types

To ease practical applications, we performed hierarchical clustering of the predicted floristic gradients (pixel scores on the first five CA axes), which are continuous by nature, and identified ten major types of forest (Fig. 3; Extended Data Table 1). The strongest floristic dissimilarity appeared between Atlantic forests (types 1–3) and the other forest types (4–10), within which semi-deciduous seasonal forests were clearly distinguished (types 4–6). We also observed functional convergences among floristically dissimilar types of forest and vice versa. For example, despite having a regional species pool similar to deciduous forests (types 4 and 6), sandstone forests (type 5) have a functional composition that is closer to remote forest groups (for example, types 2, 3, 7 and 8), with a high wood density and low deciduousness. Soil filtering modifies the relative abundance of species (rather than their presence or absence[31]), favouring suitable functional attributes in poor sandy soils[11]. By contrast, although Atlantic forests (types 1–3) have little taxonomic affinity with the east–central and southern forests (types 7 and 8), they show a similar functional composition owing to climate conditions that are more similar, as represented on the first predictive CC (Extended Data Table 1). This confirms that although taxonomic composition has an important biogeographical component, the functional composition of tree communities can converge in similar environmental conditions.

Vulnerability to global change

For the 10 forest types, most climate models predict current climate conditions either to virtually disappear from central Africa (for example, types 2 and 5; Extended Data Fig. 6), or to move at spatial and temporal scales that are incommensurate with tree dispersal ability (for example, types 4 and 6). This suggests that current forest communities will not be able to track their present climate envelopes and will face the emergence of novel climates, making the prediction of taxon distributions under future climate projection highly risky[32]. We thus assessed the vulnerability of central African forests to climate change through their sensitivity, exposure and adaptive capacity, following the recommendation of the Intergovernmental Panel on Climate Change (IPCC)[33].

We quantified sensitivity at the community level using the inverse of the current climate niche breadth of taxa (Fig. 4c) and assuming that assemblages dominated by taxa with narrow environmental tolerances will be more vulnerable to upcoming changes[34]. Sensitivity appeared to be high in coastal Gabon (type 2), where a high level of species endemism exists[35], and in the driest northern margin of central African forests. Recent studies consistently showed that drier tropical forests exhibited larger functional changes than wetter forests in response to a long-term

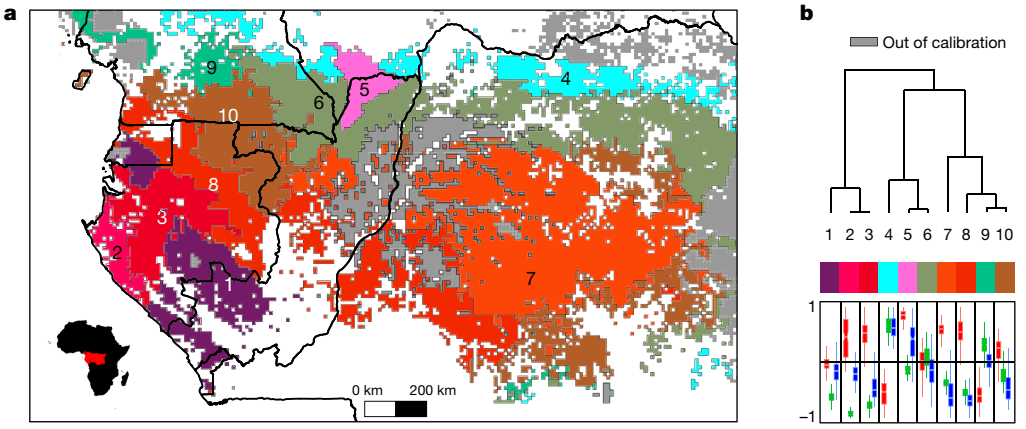

Fig. 3 | Main forest types across central Africa and their functional composition. a, Forest-type classification obtained by hierarchical clustering of the predicted floristic gradients. Colours represent an RGB composite of the mean values of the three functional traits per forest type (see Fig. 2); that is, wood density (red), deciduousness (green) and maximum diameter (blue). Thus, similar colours illustrate a similar functional composition. **b**, Taxonomic relationships among the forest types illustrated by a clustering dendrogram (top) and a box plot of the standardized predicted functional composition over the 12,295 grid cells (bottom), with wood density in red, deciduousness in green and maximum diameter in blue (median is reported at the centre, the lower and upper hinges correspond to the first and third quartiles and the two whiskers extend from these two quartiles to the largest and smallest values, at most 1.5 times the interquartile range from the hinge). Forest-type names and additional information are provided in Extended Data Table 1. Clustering uncertainty is reported in Supplementary Fig. 1.

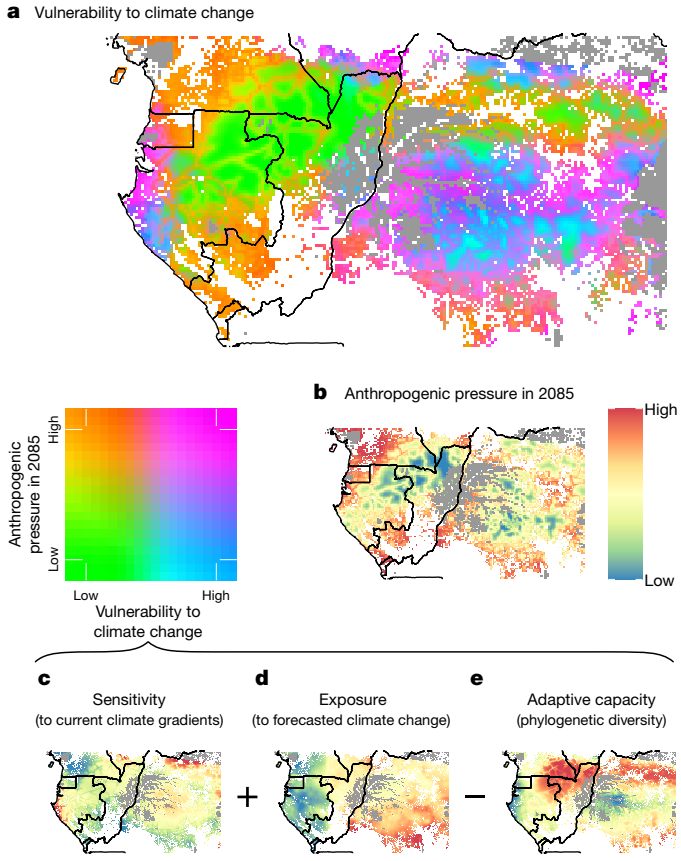

Fig. 4 | Predicted vulnerability of central African tree communities to global changes. a, Composite map of the vulnerability to climate change and of the forecasted human-induced forest-disturbance intensity by 2085. Areas in magenta are predicted to be the most vulnerable to both climate change and anthropogenic pressure; areas in green are predicted to be to the least vulnerable to both climate change and anthropogenic pressure; areas in blue are predicted to be the most vulnerable to climate change but the least vulnerable to anthropogenic pressure; and areas in orange are predicted to be the least vulnerable to climate change but the most vulnerable to anthropogenic pressure. **b**, Projected human-induced forest-disturbance intensity in 2085. **c**–**e**, Vulnerability to climate change was estimated as the sensitivity to current climate (**c**) plus the exposure to forecasted climate changes by 2085 (under the RCP 4.5 scenario) (**d**) minus the adaptive capacity of tree communities using phylogenetic diversity as a proxy (**e**).

drought in west Africa[36] and are likely to be more sensitive to global warming[21]. By contrast, forests from northwest Cameroon showed a relatively low sensitivity to current climate conditions, probably because these forests are dominated by widespread tree taxa that are adapted to anthropogenic pressure (Fig. 2). Long-lived pioneer taxa—typical of these human-disturbed forests—are also expected to be favoured by a possible acceleration in forest dynamics induced by global change[37,38].

Exposure to climate change was quantified as the extent to which the current climate determinants (CC1–CC3) are expected to change by 2085, using 18 unique bias-corrected climate model combinations (under the IPCC Assessment Report 5 (AR5) RCP 4.5 scenario; see Extended Data Fig. 7 for other scenarios). We found that exposure to climate change was mostly driven by an increase in drought stress and maximum temperature[4,39] (Supplementary Fig. 2). The central and east part of central African forests are predicted to be the most exposed, particularly in the south of the Democratic Republic of the Congo (Fig. 4d). Note, however, that climate-change predictions in central Africa are uncertain because meteorological data for model validation are lacking[4] (Supplementary Fig. 3).

Finally, we assessed the adaptive capacity of tree communities through their evolutionary potential. We first found highly significant niche conservatism along the first two climate components ($P < 0.002$). This indicates that closely related taxa tend to share similar climate niche spaces at the regional scale, and suggests that they could be affected similarly by future climate change. We therefore assumed that higher local phylogenetic diversity provides a wider range of potential responses to novel climate conditions[40], in a similar manner to the insurance hypothesis[41]. We thus used the phylogenetic diversity of predicted tree assemblages as a proxy of their adaptive capacity to climate change. Undisturbed semi-deciduous and transitional forests (types 6 and 10 in Fig. 3) appeared phylogenetically more diverse than evergreen forests (Fig. 4e). A recent study in Amazonia[42] also found a peak of phylogenetic diversity at an intermediate level of precipitation, at which dry- and wet-adapted lineages are mixing. As expected[43], we also found that human-disturbed areas tended to have a low phylogenetic diversity.

The resulting vulnerability of tree communities to climate change did not correlate with the expected human impact on forests in 2085 ($\rho = -0.08$), which was assessed here by using country-specific projections of human population growth (Fig. 4a, Extended Data Fig. 8). Vulnerability to climate change is expected to be higher for communities that are dominated by hard-wooded taxa ($\rho = 0.46$ with wood density, Supplementary Table 1). By contrast, the forecasted human impact on forests is predicted to be higher in already disturbed communities; that is, those that are dominated by light-wooded taxa with a large potential size ($\rho = -0.4$ and 0.43 for wood density and maximum size, respectively). However, because we did not account for the appearance of new roads by 2085, we may have underestimated the effect of future anthropogenic activities in remote, currently undisturbed forests. Vulnerability to both climate change and anthropogenic activities (pink colour in Fig. 4a) is predicted to be high for forests of coastal Gabon, in large areas of forests from Democratic Republic of the Congo, and in the northern margin of the forest domain. Forests from Cameroon and in the south of the Republic of the Congo mostly appear vulnerable owing to the high expected human impact on forests by 2085 (orange patches in Fig. 4a). By contrast, the tri-national Sangha transboundary forest complex and the northeastern part of Gabon appeared to be the least vulnerable area in the region (large green patch in Fig. 4a). Globally, the Democratic Republic of the Congo, where most of the central African forests are located, mainly contains forests that are predicted to be vulnerable to climate change and/or to anthropogenic pressure (blue to pink patches in Fig. 4a).

Conclusions and perspectives

Although some country-specific vegetation patterns were already suggested by phytogeographers (for example, refs. [44,45]), here we provide what is to our knowledge the first synoptic view of central African forest composition at a fine resolution, based on a vast amount of quantitative data. Unveiling the functional composition of central African forests provides key insights into their functioning, dynamics and carbon uptake potential, and the ways in which they could respond to global change. Accounting for the functional characteristics of forests can considerably reduce uncertainty in large-scale models of vegetation[46] or improve remote sensing approaches; for example, by assimilating large-scale variation in wood density into forest carbon maps[47]. Our maps may also help scientists to design representative sampling to better understand the long-term impact of climate change on tree species and stand dynamics; for example, monitoring underrepresented forest types or areas that are highly vulnerable to climate change.

The forest types and vulnerability maps should guide the development of new land-use plans that preserve the full range of evolutionary and functional potential of today's forests—or, at least, that maintain their connectivity—to attenuate the threats related

to expected changes. In central Africa, protected areas and logging concessions, which together cover almost half of the forest domain (14.9% and 32.2%, respectively; Extended Data Fig. 9), are important to consider in such plans. Protected areas do not equally cover the 10 identified types of forest (4–54%; Extended Data Table 1) and should therefore be extended to reach a better representativity. How estimated vulnerability should be accounted for when designing protected areas, for example, by extending the network in vulnerable areas to minimize the loss of biodiversity, or in areas with low anthropogenic pressure to improve their protection, is subject to debate[48]. Logging concessions can also contribute to the maintenance of forest cover and functions, providing that they are well managed[49,50], and are likely to act as biodiversity corridors between protected areas at present[51]. However, this will only prove effective in the long term if they strictly comply with legislation and, ideally, with standard certification requirements. These good practices are especially important in forests that are dominated by evergreen taxa with a high wood density, in which disturbances may have a higher impact on community composition. In areas that are expected to be under high anthropogenic pressure, forest connectivity could be preserved by promoting agroforestry and restoration programmes, strictly controlling access to logging roads and stabilizing shifting agriculture[52]. Across central Africa, the highest uncertainties for the future of forests remain in the Democratic Republic of the Congo, where substantial areas that belong to the state are not yet attributed to any land-use category and should warrant particular attention owing to their high vulnerability (Fig. 4).

Online content

Any methods, additional references, Nature Research reporting summaries, source data, extended data, supplementary information, acknowledgements, peer review information; details of author contributions and competing interests; and statements of data and code availability are available at https://doi.org/10.1038/s41586-021-03483-6.

1. Diffenbaugh, N. S. & Giorgi, F. Climate change hotspots in the CMIP5 global climate model ensemble. *Clim. Change* **114**, 813–822 (2012).
2. United Nations, Department of Economic and Social Affairs, Population Division. *World Population Prospects: The 2017 Revision, Key Findings and Advance Table*s. Working Paper No. ESA/P/WP/248 (2017).
3. Malhi, Y., Adu-Bredu, S., Asare, R. A., Lewis, S. L. & Mayaux, P. African rainforests: past, present and future. *Phil. Trans. R. Soc. B* **368**, 20120312 (2013).
4. James, R., Washington, R. & Rowell, D. P. Implications of global warming for the climate of African rainforests. *Phil. Trans. R. Soc. B* **368**, 20120298 (2013).
5. Abernethy, K., Maisels, F. & White, L. J. Environmental issues in Central Africa. *Annu. Rev. Environ. Resour*. **41**, 1–33 (2016).
6. Hubau, W. et al. Asynchronous carbon sink saturation in African and Amazonian tropical forests. *Nature* **579**, 80–87 (2020).
7. De Wasseige, C., Tadoum, M., Atyi, E. & Doumenge, C. *The Forests of the Congo Basin: Forests and Climate Change* (Weyrich, 2015).
8. Stévart, T. et al. A third of the tropical African flora is potentially threatened with extinction. *Sci. Adv*. **5**, eaax9444 (2019).
9. Parmentier, I. et al. The odd man out? Might climate explain the lower tree α-diversity of African rain forests relative to Amazonian rain forests? *J. Ecol*. **95**, 1058–1071 (2007).
10. Réjou-Méchain, M. et al. Regional variation in tropical forest tree species composition in the Central African Republic: an assessment based on inventories by forest companies. *J. Trop. Ecol*. **24**, 663–674 (2008).
11. Réjou-Méchain, M. et al. Tropical tree assembly depends on the interactions between successional and soil filtering processes. *Glob. Ecol. Biogeogr*. **23**, 1440–1449 (2014).
12. Fayolle, A. et al. Geological substrates shape tree species and trait distributions in African moist forests. *PLoS One* **7**, e42381 (2012).
13. Fayolle, A. et al. Patterns of tree species composition across tropical African forests. *J. Biogeogr*. **41**, 2320–2331 (2014).
14. Droissart, V. et al. Beyond trees: biogeographical regionalization of tropical Africa. *J. Biogeogr*. **45**, 1153–1167 (2018).
15. Sosef, M. S. et al. Exploring the floristic diversity of tropical Africa. *BMC Biol*. **15**, 15 (2017).
16. Parmentier, I. et al. Predicting alpha diversity of African rain forests: models based on climate and satellite-derived data do not perform better than a purely spatial model. *J. Biogeogr*. **38**, 1164–1176 (2011).
17. Bry, X., Trottier, C., Verron, T. & Mortier, F. Supervised component generalized linear regression using a PLS-extension of the fisher scoring algorithm. *J. Multivariate Anal*. **119**, 47–60 (2013).
18. ter Steege, H. et al. Continental-scale patterns of canopy tree composition and function across Amazonia. *Nature* **443**, 444–447 (2006).
19. Slik, J. W. et al. Soils on exposed Sunda shelf shaped biogeographic patterns in the equatorial forests of Southeast Asia. *Proc. Natl Acad. Sci. USA* **108**, 12343–12347 (2011).
20. Philippon, N. et al. The light-deficient climates of western Central African evergreen forests. *Environ. Res. Lett*. **14**, 034007 (2019).
21. Sullivan, M. J. P. et al. Long-term thermal sensitivity of Earth's tropical forests. *Science* **368**, 869–874 (2020).
22. Beale, C. M., Lennon, J. J. & Gimona, A. Opening the climate envelope reveals no macroscale associations with climate in European birds. *Proc. Natl Acad. Sci. USA* **105**, 14908–14912 (2008).
23. Deblauwe, V. et al. Remotely sensed temperature and precipitation data improve species distribution modelling in the tropics. *Glob. Ecol. Biogeogr*. **25**, 443–454 (2016).
24. Maguire, K. C. et al. Controlled comparison of species- and community-level models across novel climates and communities. *Proc. R. Soc. B* **283**, 20152817 (2016).
25. Morin-Rivat, J. et al. Present-day central African forest is a legacy of the 19th century human history. *eLife* **6**, e20343 (2017).
26. Ricklefs, R. E. Intrinsic dynamics of the regional community. *Ecol. Lett*. **18**, 497–503 (2015).
27. Violle, C. et al. Let the concept of trait be functional! *Oikos* **116**, 882–892 (2007).
28. Díaz, S. et al. The global spectrum of plant form and function. *Nature* **529**, 167–171 (2016).
29. Rüger, N. et al. Demographic trade-offs predict tropical forest dynamics. *Science* **368**, 165–168 (2020).
30. Ouédraogo, D.-Y. et al. The determinants of tropical forest deciduousness: disentangling the effects of rainfall and geology in central Africa. *J. Ecol*. **104**, 924–935 (2016).
31. Shipley, B. *From Plant Traits to Vegetation Structure: Chance and Selection in the Assembly of Ecological Communities* (Cambridge University Press, 2010).
32. Feeley, K. J. & Silman, M. R. Biotic attrition from tropical forests correcting for truncated temperature niches. *Glob. Change Biol*. **16**, 1830–1836 (2010).
33. Parry, M. et al. *Climate Change 2007 – Impacts, Adaptation, and Vulnerability: Contribution of Working Group II to the Fourth Assessment Report of the IPCC* (Cambridge University Press, 2007).
34. Foden, W. B. et al. Identifying the world's most climate change vulnerable species: a systematic trait-based assessment of all birds, amphibians and corals. *PLoS One* **8**, e65427 (2013).
35. Lachenaud, O., Stévart, T., Ikabanga, D., Ndjabounda, E. C. N. & Walters, G. The littoral forests of the Libreville area (Gabon) and their importance for conservation: description of a new endemic species (Rubiaceae). *Plant Ecol. Evol*. **146**, 68–74 (2013).
36. Aguirre-Gutiérrez, J. et al. Drier tropical forests are susceptible to functional changes in response to a long-term drought. *Ecol. Lett*. **22**, 855–865 (2019).
37. Claeys, F. et al. Climate change would lead to a sharp acceleration of Central African forests dynamics by the end of the century. *Environ. Res. Lett*. **14**, 044002 (2019).
38. McDowell, N. G. et al. Pervasive shifts in forest dynamics in a changing world. *Science* **368**, eaaz9463 (2020).
39. Zhou, L. et al. Widespread decline of Congo rainforest greenness in the past decade. *Nature* **509**, 86–90 (2014).
40. Purvis, A. Phylogenetic approaches to the study of extinction. *Annu. Rev. Ecol. Evol. Syst*. **39**, 301–319 (2008).
41. Yachi, S. & Loreau, M. Biodiversity and ecosystem productivity in a fluctuating environment: the insurance hypothesis. *Proc. Natl Acad. Sci. USA* **96**, 1463–1468 (1999).
42. Neves, D. M. et al. Evolutionary diversity in tropical tree communities peaks at intermediate precipitation. *Sci. Rep*. **10**, 1188 (2020).
43. Letcher, S. G. Phylogenetic structure of angiosperm communities during tropical forest succession. *Proc. R. Soc. B* **277**, 97–104 (2010).
44. Letouzey, R. Notice de la carte phytogéographique du Cameroun au 1:500000 (Institut de la Carte Internationale de la végétation Toulouse-France et Institut de la recherche agronomique (Herbier National) Yaoundé-Cameroun, 1985).
45. Boulvert, Y. Carte phytogéographique de la République Centrafricaine (feuille oust–feuille est) à 1 000 000 (Editions de l'ORSTOM, 1986).
46. Fyllas, N. M., Quesada, C. A. & Lloyd, J. Deriving plant functional types for Amazonian forests for use in vegetation dynamics models. *Perspect. Plant Ecol. Evol. Syst*. **14**, 97–110 (2012).
47. Mitchard, E. T. A. et al. Markedly divergent estimates of Amazon forest carbon density from ground plots and satellites. *Glob. Ecol. Biogeogr*. **23**, 935–946 (2014).
48. Visconti, P., Pressey, R. L., Bode, M. & Segan, D. B. Habitat vulnerability in conservation planning—when it matters and how much. *Conserv. Lett*. **3**, 404–414 (2010).
49. Putz, F. E. et al. Sustaining conservation values in selectively logged tropical forests: the attained and the attainable. *Conserv. Lett*. **5**, 296–303 (2012).
50. Gourlet-Fleury, S. et al. Tropical forest recovery from logging: a 24 year silvicultural experiment from Central Africa. *Phil. Trans. R. Soc. B* **368**, 20120302 (2013).
51. Clark, C. J., Poulsen, J. R., Malonga, R. & Elkan, P. W. Jr. Logging concessions can extend the conservation estate for Central African tropical forests. *Conserv. Biol*. **23**, 1281–1293 (2009).
52. Curtis, P. G., Slay, C. M., Harris, N. L., Tyukavina, A. & Hansen, M. C. Classifying drivers of global forest loss. *Science* **361**, 1108–1111 (2018).

Publisher's note Springer Nature remains neutral with regard to jurisdictional claims in published maps and institutional affiliations.

© The Author(s), under exclusive licence to Springer Nature Limited 2021

Methods

Data reporting

No statistical methods were used to predetermine sample size. The experiments were not randomized and the investigators were not blinded to allocation during experiments and outcome assessment.

Floristic and functional trait data

Forestry data were extracted from management forest inventories conducted in 105 logging concessions covering around 1.6×10^5 km^2 (Extended Data Fig. 1). Most companies followed a standardized inventory protocol similar to that described previously[53]. In most cases, it consisted of continuous and parallel transects 20 m or 25 m wide, often 2–3 km apart, and subdivided into rectangular 0.4- or 0.5-ha plots. Overall, the full dataset had a total of 192,972 plots. Within each plot, trees with a diameter at breast height (DBH) ≥ 30 cm were allocated into 10-cm wide diameter classes and identified at the species or genus level whenever possible through either commercial or local names[53]. Independent analyses performed on 298 scientific plots (≥1 ha in size) showed that the floristic gradients obtained with large trees are representative of the ones obtained with trees ≥10 cm in diameter (Pearson $r > 0.94$; Supplementary Fig. 4). Overall, around 7×10^6 trees were recorded. Taxonomy was revised and homogenized using the African Flowering Plants Database[54] and the Angiosperm Phylogeny Group III for orders and families[55]. A total of 1,092 taxa were recorded in the original dataset. Extensive botanical controls demonstrated that the patterns of both intra (α)- and inter (β)- plot diversity extracted from these data were highly reliable[53].

For the purpose of the present paper, we conducted an additional assessment according to botanical experts and by comparing the distributional range of our taxa with that in other datasets[54,56] to select a set of species and genera deemed to be reliably identified over the whole study area ($n = 195$). The abundances of these taxa were aggregated in 10×10-km^2 grid cells across the study area, but we only kept the taxa occurring in at least 5% of the cells to discard taxa that cannot be studied at the regional scale ($n = 2$). For the statistical analyses, we kept the 10×10-km^2 grid cells having a field plot sampling area ≥10 ha and where the selected taxa represented at least 75% of the total number of individuals originally inventoried to ensure that our dataset was representative of the within-cell tree community composition. The final dataset contains 6.1×10^6 tree individuals belonging to 193 taxa, of which 96 were analysed at the species and 97 at the genus levels (Supplementary Table 2), recorded in 185,665 plots aggregated in 1,571 10×10-km^2 grid cells. Overall, the selected taxa represented 90% of the total number of individuals originally inventoried in the selected grid cells.

For each taxon, we compiled information on three functional traits. First, we extracted an average wood density using the global wood density database[57,58] as well as other wood density data[59]. Wood density is an integrative trait that reflects a trade-off between tree growth potential and mortality risk[28] and is thus highly informative on community dynamics[60]. It ultimately directly affects the amount of carbon that can be stored in the vegetation[61]. Second, we extracted the leaf phenology (deciduous or evergreen) of all taxa from the large unpublished CoForTraits database[62]. This database compiles information on more than 1,000 species from central Africa with values extracted from the literature (mostly from local floras, academic papers and unpublished theses). When several values were available for a given species from different sources, we attributed the one with the maximum of occurrences (ambiguities were left as unknown). At the genus level, we first computed this step for all species belonging to the genus and then attributed the phenology with the maximum of occurrences at the species level to the genus so that all congeneric species have the same weight in the phenology attribution. This approach relies on the assumption that leaf phenological traits are highly phylogenetically conserved[63]. For a few taxa ($n = 5$), the phenology information was obtained from Ouédraogo et al.[30] and following these authors we considered *Lophira alata* Banks ex C. F. Gaertn. and *Musanga cecropioides* R. Br. as leaf exchangers; that is, with a trait value of 0.5, intermediate between evergreen (0) and deciduous (1). Leaf phenology is one of the few traits considered in dynamic global vegetation models as it affects the dynamics of forest productivity[64]. In particular, deciduousness indicates that tree photosynthetic activity, and thus growth, is seasonally depressed, which has a direct effect on carbon, water and nutrient cycling[65]. Deciduousness has often been interpreted as a strategy to avoid water stress and is thus expected to depend on climate and soil conditions[30,66]. Finally, we used the original inventory data to calculate the maximum diameter as the 95th percentile value of the diameter distribution for each taxon. Maximum potential diameter, which is often used as a proxy of maximum height[67], informs both on tree competitive ability for light and on the carbon sequestration potential. At the community level, it is expected to vary along gradients of productivity and disturbance[68]. Leaf phenology was successfully assigned to 89% of the taxa (98% of the individuals), wood density to 91% of the taxa (96% of the individuals) and maximum diameter to all taxa.

Climate and soil data

We considered 24 climatic predictors derived from the open Climatic Research Unit (CRU) dataset[69] (Extended Data Table 2). We decided to rely on the CRU dataset as other datasets, such as WorldClim[70], contain erroneous observations for some climatic stations (for example, Ngoundi in Cameroon) that severely affected our model. Furthermore, our cross-validation approach showed that the CRU database led to higher correlations between observed and predicted taxa abundances, correspondence analyses scores and community weighted trait values than the WorldClim[70] and CHIRPS[71] databases (results not shown).

Soil maps have been published at the country scale in central Africa and their homogenization is very challenging. We thus relied on a global dataset, the Harmonized World Soil Database (HWSD)[72], to attribute a soil type to each grid cell. A cross-validation analysis of our joint distribution model revealed that soil significantly improved predictions, mostly due to the contrast between Arenic Acrisols and the other soil types (Supplementary Fig. 5). To keep the model parsimonious and maximize its robustness, we thus merged all soil categories but the Arenic Acrisols soils into a single category and discarded the permanently flooded areas as mapped in the open European Space Agency Climate Change Initiative (ESA-CCI) landcover product (v.1.6), where no tree inventory data were available.

Human-induced forest-disturbance intensity

Many studies have attempted to spatialize human impacts on the environment at a large scale. In most cases, these human footprint maps have consisted of cumulative threat maps, assuming, for instance, population density and infrastructure effects[73–75]. Moreover, most of these maps relied on population statistics obtained at the level of administrative entities, resulting in human footprint indices with sharp changes at administrative boundaries[76]. We thus developed a statistical model to link the probability for a forest pixel i to be affected by anthropogenic activities depending on human population density and road proximity through nonlinear relationships. This resulted in a spatially continuous index representing human-induced forest-disturbance intensity that can be projected in space and/or time following predefined scenarios of human population dynamics (Extended Data Fig. 8).

We calibrated this index with the 'Settlement Points' dataset produced under the Global Rural Urban Mapping Project (Grumpv1). This dataset provides estimates of human population (counts, in number of people (individuals)) for the year 2000 using a proportional allocation gridding algorithm (1-km^2 grid) based on more than 1,000,000 national and subnational geographic units. Focusing on central Africa, we compared this product with the Natural Earth Populated Places product (v.3.0.0; http://www.naturalearthdata.com/downloads/

10m-cultural-vectors/10m-populated-places/; last accessed 7 October 2018) derived from the LandScan (https://earthworks.stanford.edu/catalog/stanford-yj715rc4110#iso-metadata-reference-info) dataset (pixels with fewer than 200 individuals per km^2 were discarded). The total number of populated points in central Africa (longitude 5.6 to 39.8, latitude −9.8 to 7.5 in decimal degrees) was 807 and 376 for the Grumpv1 and Natural Earth products, respectively. We thus performed a random manual check of the populated places present in Grumpv1 and absent from Natural Earth (the reverse rarely occurred) using Google Earth images and found that in all cases Grumpv1 was correct. We finally used the Grumpv1 dataset, which mostly provides information on populated places with more than around 1,000 people. Because smaller populations may have a substantial impact on forests, we added to this dataset the populated locations of the category 'towns' from OpenStreetMap (https://data.maptiler.com/downloads/planet/#1.59/-17.3/19.7; last accessed 2 October 2018), assuming by default that they all contained 500 people (OpenStreetMap does not provide systematic information on population size).

The road network was extracted from the Global Roads Open Access Data Set, v.1 (https://sedac.ciesin.columbia.edu/data/set/groads-global-roads-open-access-v1; last accessed 14 September 2018), a dataset combining road data by country. Note that logging roads are not fully represented in this dataset, so we may underestimate their effect in this study. A few roads from the northern Republic of the Congo were corrected using data from OpenStreetMap. Preliminary analyses revealed that further accounting for the railway and river networks did not improve predictions of tree taxon and community distributions.

Our index was thus calculated as followed. Let z_i, $i = 1,\ldots, n$ be n random variables indicating the disturbance status of pixel i: 0 if the pixel is undisturbed and 1 if disturbed. We assumed that z_i is distributed as a Bernoulli variable:

$$z_i = \mathrm{Bern}(p_i), \text{ with } p_i = \frac{\mathrm{IP}_i(\theta)}{\mathrm{IP}_i(\theta) + \mathrm{IR}_i^r},$$

where $\mathrm{IP}_i(\theta)$ is a synthetic index describing the influence of the population density of all populated places on pixel i (see below), θ is an unknown parameter to be inferred, and IR_i^r expresses the road influence on pixel i, defined as the normalized square root distance of pixel i to the nearest road r:

$$\mathrm{IR}_i^r = \frac{\min_{r\in R}\sqrt{\mathrm{DR}_i^r}}{\max_{i=1,\ldots,n}\left(\min_{r\in R}\sqrt{\mathrm{DR}_i^r}\right)}$$

where DR denotes the distance to the nearest road in the study area and R denotes all roads in the study area.

Population influence, IP_i^θ, is defined as the normalized square root of the weighted sum of the population size of place j. Note that the weight depends on both the distance between pixel i and populated place j, δ_{ij}, and on the population size N_j:

$$\mathrm{IP}_i^\theta = \frac{\sqrt{\sum_j^n N_j e^{-\frac{\delta_{ij}}{\log(N_j)^\theta}} + 1}}{\max\sqrt{\sum_j^n N_j e^{-\frac{\delta_{ij}}{\log(N_j)^\theta}} + 1}}$$

We finally calibrated the θ parameter using two reference areas of around 190,000 km^2 (Supplementary Fig. 6). These two areas were chosen because they cover contrasting conditions, are well known by our team and were found to be little influenced by atmospheric pollution in the MODIS data. Degraded versus intact forests were identified from a recently published MODIS-based regional vegetation map[20]. Using a likelihood optimization approach in these two areas, we obtained $\theta = 1.27$ and 1.71 in calibration areas 1 and 2, respectively, indicating that under a similar anthropogenic context, forests tend to be disturbed at a greater distance from sources of anthropogenic disturbance in the second calibration area. The final human-induced forest-disturbance intensity index was thus calculated with $\theta = 1.49$, the average estimate for the two calibration areas, over the whole central African forest domain, thus avoiding the risk of artefacts related to atmospheric pollution, from which satellite products suffer, especially over Gabon.

This index, built independently from our floristic dataset, outperformed previously published indices to predict floristic composition in our study area. Using a simple linear model, with individual anthropogenic indices as single predictors, the mean wood density of tree communities was better predicted with our new index ($r = 0.33$) than with the WorldPop[77] ($r = 0.30$), LandScan ($r = 0.15$) and Venter[74] ($r = 0.23$) indices. Similarly, using a simple generalized linear model with a Poisson distribution to predict the abundance of *Musanga cecropioides*—the most widespread and abundant short-lived pioneer taxon over central African forests—revealed a better performance of our index ($r = 0.35$) compared to previous indices ($r = 0.31$, 0.11 and 0.26 for WorldPop, LandScan and Venter, respectively).

Statistical model

To predict the joint taxa distributions we relied on a recently developed methodology called supervised component generalized linear regression (SCGLR)[17], which identifies the most predictive dimensions among a large set of potentially multicollinear predictors. SCGLR is an extension of partial least-squares regression (PLSR) to the uni- and multivariate generalized linear framework. PLSR is particularly well suited for analysing a large array of correlated predictor variables, and many studies have demonstrated its ability for prediction in various biological fields, such as genetics[78] and ecology[79]. Although PLSR is well adapted for continuous variables, SCGLR is suited for non-Gaussian outcomes and noncontinuous covariates. It is a model-based approach that extends PLSR[80], principal component analysis (PCA) on instrumental variables[81], canonical correspondence analysis[82] and other related empirical methods by maximizing a trade-off between goodness of fit of the model and the quantity of information that the components capture from the climatic variables. This information is measured through an indicator of 'structural relevance' (SR)[83], which uses bundles of highly correlated variables to attract components to rich and robust informational dimensions.

The components are sought as K linear combinations of environmental variables common to all species with coefficient vectors denoted $u = u_1,\ldots,u_K$ (under norm and orthogonality constraints). SCGLR also estimates the corresponding $q \times K$ (number of species by number of components) matrix of unknown parameters γ to maximize the following convex sum:

$$s\ \log\psi(u,\gamma) + (1-s)\log\phi_l(u)$$

where ψ is the likelihood and φ_l is the SR. s and l are tuning parameters. s is related to the trade-off between goodness of fit and structural relevance. l is a non-negative scalar related to the narrowness of the bundles of climatic variables the components are wanted to align with. The K climatic components (CCs) are then equal to $\mathrm{CC}_k = Xu_k$, $k = 1,\ldots,K$ and can be understood as the main environmental directions predicting all species simultaneously, whereas γ_j, $j = 1\ldots, q$ are the magnitude of the effects of the K components on the abundances of each species. Then, the species abundances of each taxon $j = 1,\ldots, 193$ on the grid cell $i = 1,\ldots, 1{,}571$ are modelled using a generalized linear Poisson regression such that:

$$y_{ij} \sim P\left(S_i\lambda_{ij}\right)$$

$$\log\left(\lambda_{ij}\right) = X_i\beta_j + T_i\alpha_j = X_iu\gamma_j + T_i\alpha_j = \mathrm{CC}_i\gamma_j + T_i\alpha_j$$

where X denotes climatic variables (Extended Data Table 2), S_i is an offset corresponding to the number of plots within each grid cell, and T is a set of covariates known to affect species abundances: here, the soil type and the human-induced forest-disturbance intensity index, as well as its logarithm to account for nonlinear responses.

The number of components (K) as well as the tuning parameters (l and s) must appropriately be chosen. This was done with a 10% cross-validation procedure in which the criterion used was the harmonic mean of the mean square prediction error (MSPE) across the 194 taxa. A dedicated R package, SCGLR[84], is available (see also https://github.com/SCnext/SCGLR).

To assess the predictive power of our model, we performed a leave-one-block-out cross-validation in which our dataset was divided into 40 spatial clusters identified with a Ward's hierarchical clustering[85] of plot coordinates[86] (Supplementary Fig. 7). All clusters but one were used for training the model (that is, calibration dataset) and the remaining cluster was used for validating the model. We repeated this procedure 40 times such that all clusters were used once in the validation dataset and participated in the model assessment. Model validation was performed through the use of nonparametric Spearman's rank correlation coefficients between observations and predictions. For individual taxon abundances, correlations were estimated using observed and predicted abundance per taxon. For taxon assemblages, a correspondence analysis (CA) was performed on the grid cell × observed species abundance matrix, providing the observed CA axes. The predicted site scores on each CA axis were then obtained by projecting the grid cell × predicted species abundance matrix in the observed CA planes. Correlations were computed on the observed and predicted site scores (that is, loadings) enabling us to assess the ability of our model to predict the main floristic gradients across our area. Finally, for the three functional traits, correlations were estimated on the grid-cell-based community weighted mean (CWM) traits[27] calculated on observed and predicted taxon assemblages.

Taxon abundances and community composition were predicted across the entire study area in a regular 10-km grid. To predict the floristic composition of the existing forests, we first used the ESA-CCI landcover product (v.1.6) to only keep grid cells that are likely to be forested (that is, category 'broadleaved evergreen'). Then, we only selected grid cells that had a combination of predictor values similar to those in the calibration dataset. To do this, we used a three-dimensional (3D) convex hull algorithm on the three climatic components to exclude all the grid cells that had a combination of predictors different from that represented in the calibration dataset. This resulted in 12,295 grid cells, representing 85% of the central African forests; that is, an area of around 1,230,000 km^2.

We finally used the Ward's hierarchical clustering method to classify the predicted floristic composition into broad floristic types. Group classification was done on the first five axes of a CA performed on predicted taxon abundances, accounting for 77% of the total inertia. The number of retained types was chosen based on our expert knowledge. The uncertainty associated with this classification was then assessed through Gaussian finite mixture models[87] (repeated 500 times) using a spherical, equal volume model (EII).

Spatially explicit null models

Whenever predictors and observations are spatially structured, model errors of type I (false positive associations) are inflated[88], hindering our capacity to extrapolate predictions in space or time[22]. We thus built a spatialized null model to test the degree to which the successfulness of our predictions resulted from an actual relationship with climatic variables or was simply due to spatial costructures between taxon distributions and climatic gradients that arose by chance. We used the RGeostats R package[89] to simulate sets of SCGLR CCs having similar spatial properties to those of the observed CCs as well as similar spatial costructures between them. This step consisted of fitting theoretical variograms and covariograms to empirical ones to simulate random realizations that can be then used as 'null' spatialized predictors (Supplementary Figs. 8, 9). We simulated 500 sets of 'null' spatialized predictors and used them as predictors in our GLMs using the leave-one-block-out cross-validation described above. The resulting correlations between observed and predicted taxon abundances, and axes scores (for taxon assemblages) were finally compared with the correlations obtained when observed climatic predictors were considered. The resulting P values were calculated as the number of times a simulated correlation was higher than the observed one, divided by the total number of realizations (n = 501).

Forest vulnerability to global change

Vulnerability to climate change, as assessed through the IPCC framework, is composed of three components: (1) sensitivity, (2) exposure and (3) adaptive capacity to climate change.

Sensitivity to climate change, Sensitivity$_{clim}$, was first estimated at the taxon level in a similar way to that described previously[34]. For each taxon, we calculated the mean of the weighted standard deviation (SDw) of the three climatic components (CCs) at the present time, using locally observed taxon abundances as weights. SDw thus represents the width of the climatic niche currently occupied by the taxa. Taxon-specific climate sensitivity was then measured as $1/\overline{\mathrm{SDw}}$ (it increases as niche width decreases). To upscale tree sensitivity to climate change at the community level and over our study area, sensitivity was measured as the CWM of taxon-specific climate-sensitivity scores, using predicted taxon assemblages.

Exposure to climate change, Exposure$_{clim}$, was assessed using projected changes in climate from 18 unique climate model combinations provided by the AFRICLIM v3.0 dataset[90] (last accessed 3 February 2020). These models corresponded to pairwise combinations of five regional climate models (RCMs) driven by 10 general circulation models (GCMs), with an unequal number of GCMs models per RCM (10 models for the Swedish Meteorological and Hydrological (SMHI) RCM, four for the Climate Limited-area Modelling Community (CLMCOM) RCM, two for the Royal Netherlands Meteorological Institute (KNMI) RCM, one for the Canadian Centre for Climate Modelling (CCCMA) RCM and one for the Danish Meteorological Institute (DMI) RCM). These models were generated using change-factor downscaling approaches to model spatial variation at local scales while correcting for differences between observed and simulated baseline climates (see ref. [90] for more details). We here concentrated on one representative concentration pathway of the IPCC AR5 (RCP 4.5) for the late 21st century (2071–2100; hereafter named 2085) and reconstructed the three SCGLR selected CCs from the climatic predictions as follows: let $X_{\mathrm{rcp4.5}}$ be the predicted future climatic conditions and let $m = \overline{X}$ and S = sd(X) be the mean and standard deviation matrices of the current climatic conditions. The predictive climatic components under future scenarios are then equal to $f_{\mathrm{rcp4.5}} = (X_{\mathrm{rcp4.5}} - m)S\hat{u}$, where $\hat{u}$ represents SCGLR CCs. We then calculated the Euclidean distance between the 3 current and the 3 predicted CCs for each of the 18 models and then estimated the exposure to climate change as the mean distance over the 18 models.

Adaptive capacity to climate change, Adaptive$_{clim}$, was assessed through the phylogenetic diversity of predicted assemblages at the genus level. We used a recently published dated phylogeny[91], covering 167 out of our 180 genera (representing 94% of predicted individuals). We first tested if the studied taxa exhibited a significant conservatism in their climate niches using Abouheif's permutation tests[92] on the taxa-specific score (γ) values on the three SCGLR climate components (γ represents the influence of a CC on a given taxa distribution; see above). We then measured the phylogenetic diversity (PD) of predicted assemblages at the genera level using the Chao's PD index with an order q of 1 (equivalent to the Shannon index)[93] that we used as a proxy of adaptive capacity.

Vulnerability to climate change, $\text{Vulnerability}_{\text{clim}}$, was finally estimated as the sum of the three standardized (st) (0 to 1) components:

$$\text{Vulnerability}_{\text{clim}} = \left(\text{Sensitivity}^{\text{st}}_{\text{clim}} + \text{Exposure}^{\text{st}}_{\text{clim}} - \text{Adaptive}^{\text{st}}_{\text{clim}}\right).$$

$\text{Vulnerability}_{\text{clim}}$ theoretically ranges from −1 (low vulnerability) to 2 (high vulnerability) and, owing to the standardization of its three components, it expresses a relative vulnerability over the study area and is thus little affected by the IPCC scenario chosen (RCP 4.5 or 8.5) because different scenarios predict different amplitudes of changes but similar spatial patterns (Extended Data Fig. 7).

Forecasted human impact on forests in 2085 was assessed using our human-induced forest-disturbance intensity index combined with country-specific projections of human populations in 2085. We assigned to each current town a country-specific relative population increase drawn from the United Nations World Population Prospects[2] and rebuilt our index based on this modified dataset. This approach did not account for new roads that might be established by 2085, and thus tended to underestimate the increase in anthropogenic pressure.

Software and packages

All analyses were performed and figures were created with R[94], mostly using the ade4[95], alphashape3d[96], ggplot2[97], raster[98], RGeostats[89], entropart[99] and SCGLR[84] (https://github.com/SCnext/SCGLR/) packages. Data are archived in a public repository (https://doi.org/10.18167/DVN1/UCNCA7).

Reporting summary

Further information on research design is available in the Nature Research Reporting Summary linked to this paper.

Data availability

All maps and data used for this article are accessible online in a public repository at https://doi.org/10.18167/DVN1/UCNCA7. Raw floristic data are, however, archived in a private data repository, owing to the highly sensitive nature of commercial inventory data, and access may be granted for research purposes using the form provided in the public repository.

Code availability

R scripts are available at https://github.com/MaximeRM/ScriptNature.

53. Réjou-Méchain, M. et al. Detecting large-scale diversity patterns in tropical trees: can we trust commercial forest inventories? *For. Ecol. Manage.* **261**, 187–194 (2011).
54. African Plant Database v.3.4.0 (Conservatoire et Jardin Botaniques de la Ville de Genève and South African National Biodiversity Institute, Pretoria, accessed 10 February 2017).
55. The Angiosperm Phylogeny Group. An update of the Angiosperm Phylogeny Group classification for the orders and families of flowering plants: APG III. *Bot. J. Linn. Soc.* **161**, 105–121 (2009).
56. Dauby, G. et al. RAINBIO: a mega-database of tropical African vascular plants distributions. *PhytoKeys* **74**, 1–18 (2016).
57. Chave, J. et al. Towards a worldwide wood economics spectrum. *Ecol. Lett.* **12**, 351–366 (2009).
58. Zanne, A. E. et al. Data from: towards a worldwide wood economic spectrum. *Dryad* https://doi.org/10.5061/dryad.234 (2009).
59. Gourlet-Fleury, S. et al. Environmental filtering of dense-wooded species controls above-ground biomass stored in African moist forests. *J. Ecol.* **99**, 981–990 (2011).
60. Westoby, M. & Wright, I. J. Land-plant ecology on the basis of functional traits. *Trends Ecol. Evol.* **21**, 261–268 (2006).
61. Chave, J. et al. Improved allometric models to estimate the aboveground biomass of tropical trees. *Glob. Change Biol.* **20**, 3177–3190 (2014).
62. Bénédet, F. et al. CoForTraits, African plant traits information database v.1.0, https://doi.org/10.18167/DVN1/Y2BIZK (2013).
63. Davies, T. J. et al. Phylogenetic conservatism in plant phenology. *J. Ecol.* **101**, 1520–1530 (2013).
64. Cramer, W. et al. Global response of terrestrial ecosystem structure and function to CO_2 and climate change: Results from six dynamic global vegetation models. *Glob. Change Biol.* **7**, 357–373 (2001).
65. Menzel, A. Phenology: its importance to the global change community. *Clim. Change* **54**, 379 (2002).
66. Borchert, R., Rivera, G. & Hagnauer, W. Modification of vegetative phenology in a tropical semi-deciduous forest by abnormal drought and rain. *Biotropica* **34**, 27–39 (2002).
67. Kraft, N. J. B., Valencia, R. & Ackerly, D. D. Functional traits and niche-based tree community assembly in an Amazonian forest. *Science* **322**, 580–582 (2008).
68. Schamp, B. S. & Aarssen, L. W. The assembly of forest communities according to maximum species height along resource and disturbance gradients. *Oikos* **118**, 564–572 (2009).
69. New, M., Lister, D., Hulme, M. & Makin, I. A high-resolution data set of surface climate over global land areas. *Clim. Res.* **21**, 1–25 (2002).
70. Hijmans, R. J., Cameron, S. E., Parra, J. L., Jones, P. G. & Jarvis, A. Very high resolution interpolated climate surface for global land areas. *Int. J. Climatol.* **25**, 1965–1978 (2005).
71. Funk, C. et al. The climate hazards infrared precipitation with stations—a new environmental record for monitoring extremes. *Sci. Data* **2**, 150066 (2015).
72. Nachtergaele, F. et al. The harmonized world soil database. In *Proc. 19th World Congress of Soil Science, Soil Solutions for a Changing World* (eds Gilkes, R. & Prakongkep, N.) 34–37 (International Union of Soil Sciences, 2010).
73. Woolmer, G. et al. Rescaling the human footprint: a tool for conservation planning at an ecoregional scale. *Landsc. Urban Plan.* **87**, 42–53 (2008).
74. Venter, O. et al. Sixteen years of change in the global terrestrial human footprint and implications for biodiversity conservation. *Nat. Commun.* **7**, 12558 (2016).
75. Geldmann, J., Joppa, L. N. & Burgess, N. D. Mapping change in human pressure globally on land and within protected areas. *Conserv. Biol.* **28**, 1604–1616 (2014).
76. Linard, C., Gilbert, M., Snow, R. W., Noor, A. M. & Tatem, A. J. Population distribution, settlement patterns and accessibility across Africa in 2010. *PLoS One* **7**, e31743 (2012).
77. Lloyd, C. T. et al. Global spatio-temporally harmonised datasets for producing high-resolution gridded population distribution datasets. *Big Earth Data* **3**, 108–139 (2019).
78. Boulesteix, A.-L. & Strimmer, K. Partial least squares: a versatile tool for the analysis of high-dimensional genomic data. *Brief. Bioinform.* **8**, 32–44 (2007).
79. Carrascal, L. M., Galván, I. & Gordo, O. Partial least squares regression as an alternative to current regression methods used in ecology. *Oikos* **118**, 681–690 (2009).
80. Tenenhaus, M. *La Régression PLS: Théorie et Pratique* (Editions Technip, 1998).
81. Sabatier, R., Lebreton, J. D. & Chessel, D. in *Multiway Data Analysis* (eds Coppi, R. & Bolasco, S.) 341–352 (1989).
82. Ter Braak, C. J. F. in *Theory and Models In Vegetation Science* (eds Prentice, I. C. & van der Maarel, E.) 69–77 (Springer, 1987).
83. Bry, X. & Verron, T. THEME: THEmatic model exploration through multiple co-structure maximization. *J. Chemometr.* **29**, 637–647 (2015).
84. Cornu, G., Mortier, F., Trottier, C. & Bry, X. SCGLR: supervised component generalized linear regression. R version 3.0 https://cran.r-project.org/web/packages/SCGLR/index.html (2016).
85. Ward, J. H. Jr. Hierarchical grouping to optimize an objective function. *J. Am. Stat. Assoc.* **58**, 236–244 (1963).
86. Ploton, P. et al. Spatial validation reveals poor predictive performance of large-scale ecological mapping models. *Nat. Commun.* **11**, 4540 (2020).
87. Scrucca, L., Fop, M., Murphy, T. B. & Raftery, A. E. mclust 5: clustering, classification and density estimation using gGussian finite mixture models. *R J.* **8**, 289–317 (2016).
88. Dormann, C. F. et al. Methods to account for spatial autocorrelation in the analysis of species distributional data: A review. *Ecography* **30**, 609–628 (2007).
89. Renard, D. et al. RGeostats: the geostatistical package v.11.0. 1 http://rgeostats.free.fr/ (MINES ParisTech, 2014).
90. Platts, P. J., Omeny, P. A. & Marchant, R. AFRICLIM: high-resolution climate projections for ecological applications in Africa. *Afr. J. Ecol.* **53**, 103–108 (2015).
91. Janssens, S. B. et al. A large-scale species level dated angiosperm phylogeny for evolutionary and ecological analyses. *Biodivers. Data J.* **8**, e39677 (2020).
92. Abouheif, E. A method for testing the assumption of phylogenetic independence in comparative data. *Evol. Ecol. Res.* **1**, 895–909 (1999).
93. Chao, A., Chiu, C.-H. & Jost, L. Phylogenetic diversity measures based on Hill numbers. *Phil. Trans. R. Soc. B* **365**, 3599–3609 (2010).
94. R Core Team. *R: a language and environment for statistical computing*. (R Foundation for Statistical Computing, 2017).
95. Chessel, D., Dufour, A. B. & Thioulouse, J. The ade4 package – I: one-table methods. *R News* **4**, 5–10 (2004).
96. Lafarge, T. & Pateiro-Lopez, B. alphashape3d: implementation of the 3D alpha-shape for the reconstruction of 3D sets from a point cloud. R version 1.3.1 https://cran.r-project.org/web/packages/alphashape3d/index.html (2017).
97. Wickham, H. *ggplot2: Elegant Graphics for Data Analysis* (Springer-Verlag, 2016).
98. Hijmans, R. J. raster: geographic data analysis and modelling. R version 3.4-5 https://cran.r-project.org/web/packages/raster/index.html (2017).
99. Marcon, E. & Hérault, B. entropart: An R package to measure and partition diversity. *J. Stat. Softw.* **67**, 1–26 (2015).
100. Dufrêne, M. & Legendre, P. Species assemblages and indicator species: the need for a flexible asymmetrical approach. *Ecol. Monogr.* **67**, 345–366 (1997).

Acknowledgements We thank the 105 forest companies that provided access, albeit restricted, to their inventory data for research purposes and members of the central African plot network (https://central-african-plot-network.netlify.app/), Y. Yalibanda, F. Allah-Barem, F. Baya, F. Boyemba, M. Mbasi Mbula, P. Berenger, M. Mazengue, V. Istace, I. Zombo, E. Forni, Nature+ and the CEB-Precious Woods company for giving access to the scientific inventories described in Supplementary Fig. 4, some of which were funded by the AFD and the FFEM (for example, DynAfFor and P3FAC projects). We thank J. Chave, P. Couteron, S. Lewis and M. Tadesse for their comments and discussions on previous versions, B. Sultan for useful discussions on climate projections, O. J. Hardy for advice on phylogenetical analyses, B. Locatelli for advice on vulnerability analyses, G. Vieilledent for discussions on the human-induced forest-disturbance intensity index and A. Stokes for English editing. This work was supported by the CoForTips project (ANR-12-EBID-0002) funded by the ERA-NET BiodivERsA, with the national funders ANR, BELSPO and FWF, as part of the 2012

BiodivERsA call for research proposals, the GAMBAS project funded by the French National Research Agency (ANR-18-CE02-0025) and the project 3DForMod funded by the UE FACCE ERA-GAS consortium (ANR-17-EGAS-0002-01). This study is a contribution to the research program of LMI DYCOFAC (Dynamique des écosystèmes continentaux d'Afrique Centrale en contexte de changements globaux).

Author contributions Conceptualization: M.R.-M., F.M., R.P. and S.G.-F.; data curation: G.C. and F.B.; formal analysis: M.R.-M. and F.M.; project administration: C.G.; writing (original draft): M.R.-M., F.M., R.P. and S.G.-F.; writing (review and editing): all authors.

Competing interests The authors declare no competing interests.

Additional information

Supplementary information The online version contains supplementary material available at https://doi.org/10.1038/s41586-021-03483-6.

Correspondence and requests for materials should be addressed to M.R.-M.

Peer review information *Nature* thanks Jonas Geldmann, Marion Pfeifer, Philip Platts and the other, anonymous, reviewer(s) for their contribution to the peer review of this work.

Reprints and permissions information is available at http://www.nature.com/reprints.